frontiers | Research Topics

Physio-logging in marine animals: recent advances and future directions

Edited by
Kagari Aoki, J. Chris McKnight and Takashi Kitagawa

Published in
Frontiers in Physiology

ISSN 1664-8714
ISBN 978-2-8325-6852-1
DOI 10.3389/978-2-8325-6852-1

Generative AI statement
Any alternative text (Alt text) provided alongside figures in the articles in this ebook has been generated by Frontiers with the support of artificial intelligence and reasonable efforts have been made to ensure accuracy, including review by the authors wherever possible. If you identify any issues, please contact us.

About Frontiers

Frontiers is more than just an open access publisher of scholarly articles: it is a pioneering approach to the world of academia, radically improving the way scholarly research is managed. The grand vision of Frontiers is a world where all people have an equal opportunity to seek, share and generate knowledge. Frontiers provides immediate and permanent online open access to all its publications, but this alone is not enough to realize our grand goals.

Frontiers journal series

The Frontiers journal series is a multi-tier and interdisciplinary set of open-access, online journals, promising a paradigm shift from the current review, selection and dissemination processes in academic publishing. All Frontiers journals are driven by researchers for researchers; therefore, they constitute a service to the scholarly community. At the same time, the *Frontiers journal series* operates on a revolutionary invention, the tiered publishing system, initially addressing specific communities of scholars, and gradually climbing up to broader public understanding, thus serving the interests of the lay society, too.

Dedication to quality

Each Frontiers article is a landmark of the highest quality, thanks to genuinely collaborative interactions between authors and review editors, who include some of the world's best academicians. Research must be certified by peers before entering a stream of knowledge that may eventually reach the public - and shape society; therefore, Frontiers only applies the most rigorous and unbiased reviews. Frontiers revolutionizes research publishing by freely delivering the most outstanding research, evaluated with no bias from both the academic and social point of view. By applying the most advanced information technologies, Frontiers is catapulting scholarly publishing into a new generation.

What are Frontiers Research Topics?

Frontiers Research Topics are very popular trademarks of the *Frontiers journals series*: they are collections of at least ten articles, all centered on a particular subject. With their unique mix of varied contributions from Original Research to Review Articles, Frontiers Research Topics unify the most influential researchers, the latest key findings and historical advances in a hot research area.

Find out more on how to host your own Frontiers Research Topic or contribute to one as an author by contacting the Frontiers editorial office: frontiersin.org/about/contact

Physio-logging in marine animals: recent advances and future directions

Topic editors

Kagari Aoki — Teikyo University of Science, Japan

J. Chris McKnight — University of St. Andrews, United Kingdom

Takashi Kitagawa — The University of Tokyo, Japan

Citation

Aoki, K., McKnight, J. C., Kitagawa, T., eds. (2025). *Physio-logging in marine animals: recent advances and future directions*. Lausanne: Frontiers Media SA. doi: 10.3389/978-2-8325-6852-1

Table of contents

frontiers | Frontiers in Physiology

TYPE Editorial
PUBLISHED 28 August 2025
DOI 10.3389/fphys.2025.1675117

OPEN ACCESS

EDITED AND REVIEWED BY
Colin K. Drummond,
Case Western Reserve University,
United States

*CORRESPONDENCE
Kagari Aoki,
aokikagari@ntu.ac.jp

RECEIVED 28 July 2025
ACCEPTED 05 August 2025
PUBLISHED 28 August 2025

CITATION
Aoki K, McKnight JC and Kitagawa T (2025) Editorial: Physio-logging in marine animals: recent advances and future directions. *Front. Physiol.* 16:1675117. doi: 10.3389/fphys.2025.1675117

Editorial: Physio-logging in marine animals: recent advances and future directions

Kagari Aoki[1]*, J. Chris McKnight[2] and Takashi Kitagawa[3]

[1]Faculty of Life and Environmental Sciences, Teikyo University of Science, Uenohara, Japan, [2]Sea Mammal Research Unit, School of Biology, Faculty of Science, University of St Andrews, St. Andrews, United Kingdom, [3]Graduate School of Frontier Sciences, The University of Tokyo, Kashiwa, Japan

KEYWORDS

physio-logging, bio-logging, electrocardiograms (ECGs), thermal adaptation, oxidative stress, neurologgers

Editorial on the Research Topic
Physio-logging in marine animals: recent advances and future directions

Integrating physiological data, such as heart rate, respiration, body temperature, and stress hormone levels with specific behavioral data, allows us to unravel the underlying mechanisms that may directly or indirectly limit, drive, and/or affect certain actions. These insights contribute to our understanding of the process of adaptive evolution and provide vital information for interpreting how behavior and population dynamics interact with extrinsic *and* intrinsic factors. Building upon the foundations of traditional bio-logging and its capacity to remotely measure and understand behavior and distribution, as well as environmental characteristics, physio-logging enables researchers to investigate physiological processes. This linkage between behavior, distribution, environment, and intrinsic physiology is crucial for the fields of ecology and conservation physiology (Cooke et al., 2021; Fahlman et al., 2021).

Physio-logging has provided valuable insight into how animals respond to various environmental factors, such as the behavioral thermal adaptation of Pacific bluefin tuna *Thunnus thynnus orientalis* (e.g., Kitagawa et al., 2000; Kitagawa et al., 2022) and the behavioral response of homing chum salmon *Oncorhynchus keta* to varying ambient temperature structures (Kitagawa et al., 2016). Physio-logging can also provide the necessary tools for conservation management, which will contribute toward reducing the impacts of anthropogenic disturbances on species. For example, assessment of stress levels, such as measuring corticosterone, cortisol or heart rate, may help evaluate the impact of anthropogenic disturbance (e.g., Thompson et al., 2014; Lyamin et al., 2016). This potential has been demonstrated in recent studies across taxa: for example, tissue perfusion and behavioral conflict have been documented in grey seals *Halichoerus grypus* using physio-logging tools (McKnight et al., 2019). Similarly, Ponganis 2021 applied heart rate loggers to air-breathing animals such as a blue whale *Balaenoptera musculus* and emperor penguins *Aptenodytes forsteri* to monitor physiological effort during deep dives, revealing thresholds in oxygen management relevant to survival limits under environmental stress. Near-infrared spectroscopy has also been proposed by Ruesch et al. (2022) as a non-invasive tool to assess blood oxygenation in marine mammals, thereby opening new avenues for evaluating stress and health status under conditions of human care or environmental disturbance

(Fahlman et al., 2021; Ruesch et al., 2022). This emerging era of physio-logging will enable long-term studies aimed at improving our understanding of fundamental physiological function, health, welfare or wellbeing of animals (e.g., Abe et al.; Naveed Yousaf et al., 2022) and humans, as well as their responses to environmental and/or anthropogenic changes. The current Research Topic, "Physio-logging in Marine Animals: Recent Advances and Future Directions", introduces diverse application examples in the field of physio-logging.

In this Research Topic, physio-logging techniques are applied to diverse taxa, including sea turtles, seabirds and teleost fish. For instance, Saito et al. introduced non-invasive methods to measure electrocardiograms (ECGs), which provide heart rate data in green sea turtles—an important step toward understanding their physiological adaptations to the environment. Narazaki et al. and Makiguchi et al. extended these approaches to reproductive context in loggerhead turtles *Caretta caretta* and chum salmon, respectively, and provided insights into autonomic nervous system activity through variations in heart rate during spawning events. Abe et al. and Aoki et al. explored how thermal physiology shapes the behavior and thermoregulatory capacity of tunas. They emphasized the importance of both heat retention and production in thermal adaptation, offering insight into how tunas cope with environmental variability through physiological and behavioral mechanisms. Koyama et al. and Mizutani et al. investigated how foraging behavior and oxidative stress reflect the physiological condition and adaptive strategies in seabirds. Their work highlights the importance of integrating behavioral, oxidative stress, and environmental data to understand energy allocation, reproductive trade-offs, and species responses to ecological pressures. The other paper summarized findings from studies applying neurologgers to teleost fish, revealing various spatial-cognition cells in regions of the telencephalon analogous to the mammalian hippocampus that are deeply involved in spatial navigation (Takahashi et al.). These contributions demonstrate the transformative capacity of physio-logging to uncover physiological correlates of behavior across a variety of taxa and life-history stages.

In the future, as new sensors such as brain wave sensors are developed and big data recording and analysis technologies evolve, physio-logging will continue to evolve as a tool for measuring the physiological functions of marine organisms and will contribute to our understanding of the ecology of organisms on Earth, including ourselves.

Author contributions

KA: Writing – original draft, Writing – review and editing. JM: Writing – original draft, Writing – review and editing. TK: Writing – original draft, Writing – review and editing.

Funding

The author(s) declare that no financial support was received for the research and/or publication of this article.

Conflict of interest

The authors declare that the research was conducted in the absence of any commercial or financial relationships that could be construed as a potential conflict of interest.

The author(s) declared that they were an editorial board member of Frontiers, at the time of submission. This had no impact on the peer review process and the final decision.

Generative AI statement

The author(s) declare that no Generative AI was used in the creation of this manuscript.

Any alternative text (alt text) provided alongside figures in this article has been generated by Frontiers with the support of artificial intelligence and reasonable efforts have been made to ensure accuracy, including review by the authors wherever possible. If you identify any issues, please contact us.

Publisher's note

References

Cooke, S. J., Bergman, J. N., Madliger, C. L., Cramp, R. L., Beardall, J., Burness, G., et al. (2021). One hundred research questions in conservation physiology for generating actionable evidence to inform conservation policy and practice. *Conserv. Physiol.* 9 (1), coab009. doi:10.1093/conphys/coab009

Fahlman, A., Aoki, K., Bale, G., Brijs, J., Chon, K. H., Drummond, C. K., et al. (2021). The new era of physio-logging and their grand challenges. *Front. Physiol.* 12, 669158. doi:10.3389/fphys.2021.669158

Kitagawa, T., Abe, T. K., Kubo, K., Fujioka, K., Fukuda, H., and Tanaka, Y. (2022). Rapid endothermal development of juvenile pacific bluefin tuna. *Front. Physiol.* 13, 968468. doi:10.3389/fphys.2022.968468

Kitagawa, T., Hyodo, S., and Sato, K. (2016). Atmospheric depression-mediated water temperature changes affect the vertical movement of chum salmon *Oncorhynchus keta*. *Mar. Environ. Res.* 119, 72–78. doi:10.1016/j.marenvres.2016.05.016

Kitagawa, T., Nakata, H., Kimura, S., Itoh, T., Tsuji, S., and Nitta, A. (2000). Effect of ambient temperature on the vertical distribution and movement of Pacific bluefin tuna (*Thunnus thynnus orientalis*). *Mar. Ecol. Prog. Ser.* 206, 251–260. doi:10.3354/meps20625

Lyamin, O. I., Ostras, D. A., Mukhametov, L. M., and Rozhnov, V. V. (2016). Cardiac response to high frequency and ship noise in belugas. *Proceedings of Meetings on Acoustics* 27, 050002. doi:10.1121/2.0000368

McKnight, J. C., Bennett, K. A., Bronkhorst, M., Russell, D. J. F., Balfour, S., Milne, R., et al. (2019). Shining new light on mammalian diving physiology using wearable near-infrared spectroscopy. *PLoS Biol* 17 (6), e3000306. doi:10.1371/journal.pbio.3000306

Naveed Yousaf, M., Røn, Ø, Hagen, P. P., and McGurk, C. (2022). Monitoring fish welfare using heart rate bio-loggers in farmed Atlantic salmon (*Salmo salar* L.): An insight into the surgical recovery. *Aquaculture* 555, 738211. doi:10.1016/j.aquaculture.2022.738211

Ruesch, A., McKnight, J. C., Fahlman, A., Shinn-Cunningham, B. G., and Kainerstorfer, J. M. (2022). Near-Infrared spectroscopy as a tool for marine mammal research and care. *Front. Physiol.* 12, 816701. doi:10.3389/fphys.2021.816701

Thompson, L. A., Spoon, T. R., Goertz, C. E. C., Hobbs, R. C., and Romano, T. A. (2014). Blow collection as a non-invasive method for measuring cortisol in the beluga (*Delphinapterus leucas*). *PLoS ONE* 9 (12), e114062. doi:10.1371/journal.pone.0114062

frontiers | Frontiers in Physiology

TYPE Mini Review
PUBLISHED 06 November 2024
DOI 10.3389/fphys.2024.1499058

OPEN ACCESS

EDITED BY
Tereza Manousaki,
Hellenic Centre for Marine Research (HCMR), Greece

REVIEWED BY
Todd Streelman,
Georgia Institute of Technology, United States

*CORRESPONDENCE
Susumu Takahashi,
stakahas@mail.doshisha.ac.jp

RECEIVED 20 September 2024
ACCEPTED 28 October 2024
PUBLISHED 06 November 2024

CITATION
Takahashi S, Sawatani F, Ide K, Abe TK, Kitagawa T and Makiguchi Y (2024) Mapping spatial memory in teleosts: a new Frontier in neural logging techniques.
Front. Physiol. 15:1499058.
doi: 10.3389/fphys.2024.1499058

Mapping spatial memory in teleosts: a new Frontier in neural logging techniques

Susumu Takahashi[1]*, Fumiya Sawatani[1], Kaoru Ide[1], Takaaki K. Abe[2], Takashi Kitagawa[3] and Yuya Makiguchi[2]

[1]Laboratory of Cognitive and Behavioral Neuroscience, Graduate School of Brain Science, Doshisha University, Kyotanabe, Japan, [2]College of Bioresource Science, Nihon University, Fujisawa, Kanagawa, Japan, [3]Graduate School of Frontier Sciences, The University of Tokyo, Chiba, Japan

Recent advancements in microelectromechanical system technology have significantly enhanced our ability to monitor neuronal activity in free-swimming fish without disrupting their natural movement, thereby greatly improving the capabilities of neural logging using "neurologger" technology. In this review, we compiled the findings from studies applying neurologgers to teleost fish, emphasizing the discovery of various spatial-cognition cells in regions of the telencephalon analogous to the mammalian hippocampus that are deeply involved in spatial navigation. We detailed how different fish species, such as goldfish and salmonids, correlate their neural activity with environmental boundaries, head direction, speed, and other navigational cues for spatial memory and navigation strategies. We critically analyzed the similarities and differences in these mechanisms to provide insights into the evolutionary aspects of spatial cognition. We also identified gaps in current methodologies and suggest directions for future research, emphasizing the need for further exploration of spatial encoding in aquatic environments. The insights gained herein suggest the existence of a complex and evolutionarily conserved substrate for navigation and memory in vertebrates, highlighting the potential of neurologgers to expand our understanding of spatial cognition.

KEYWORDS

spatial memory, neural logging, teleosts, neurologgers, telencephalon

1 Introduction

The study of spatial cognition in teleost fish has seen substantial advancements due to the development of cutting-edge technologies using microelectromechanical systems (Ide and Takahashi, 2022). These technologies, referred to as "neurologgers," enable researchers to record neuronal activity in free-swimming fish, providing a more accurate representation of their natural behavior. Zebrafish, a commonly used model organism among teleosts (Lieschke and Currie, 2007), offers various advantages for experimental manipulation, such as genetic tractability and transparency during the larval stage, which cannot yet be applied to them owing to their small size. Understanding spatial cognition in teleosts is crucial, as it sheds light on the fundamental neural mechanisms that support navigation and memory in vertebrates, a topic of significant interest in neurobiology. Recent studies have focused on the telencephalon of teleost fish, particularly in species like goldfish and salmonids (Vinepinsky et al., 2020; Takahashi et al., 2021), and have revealed the presence of various space-responsive cells. These include cells analogous to the mammalian head-direction

and border cells, indicating a sophisticated system for spatial navigation. Previous research has highlighted the role of these cells in encoding spatial information; however, questions remain regarding the differences in spatial information representation across species and the impact of environmental factors.

This review aimed to synthesize findings from recent studies on space-responsive cells in the telencephalons of goldfish and salmonids. It sought to compare the similarities and differences in spatial information processing between species, exploring how these species use different environmental cues for navigation. This review also examined the evolutionary implications of these findings, particularly concerning the conservation of spatial cognition mechanisms across vertebrates. We focused on the recent research conducted using advanced neurologgers. Although the review provides a comprehensive overview of the neuronal substrates involved in spatial cognition, its scope was limited to goldfish and salmonids; it did not cover other teleost species or vertebrates in detail, acknowledging the need for further research to generalize these findings across a broader range of species. The central hypothesis of this review was that the neural mechanisms underlying spatial cognition in teleosts are evolutionarily conserved as well as highly adaptable, reflecting the specific ecological needs and environmental contexts of different species.

Understanding spatial cognition in teleosts has broader implications for the field of neurobiology, particularly in understanding how complex cognitive functions have evolved across vertebrates. Insights gained from studying these fish can improve our understanding of neuronal processes in other animal species. Furthermore, the methodological advancements discussed in this review, such as the use of neurologgers, have the potential to revolutionize the study of neuronal activity in freely behaving animals, offering new avenues for research in various fields of biology and neuroscience.

2 Neural substrates of spatial cognition in teleosts

The telencephalon of teleosts, particularly in species like goldfish and salmonids, has been identified as a crucial region for spatial navigation, as evidenced by studies linking brain lesions to impaired behavior (Rodriguez et al., 2002). This area contains a variety of space-responsive cells, including those resembling mammalian head-direction cells (Vinepinsky et al., 2020; Cohen et al., 2023). These findings underscore the complexity and sophistication of the spatial navigation systems in teleosts, similar to those found in mammals.

Extensive studies have demonstrated the presence of neurons that respond to specific environmental boundaries and head directions in goldfish. These neurons are believed to be critical for the cognitive map, allowing fish to orient themselves in their environment. For instance, head-direction cells in the lateral pallium of goldfish consistently fire when the head is oriented in a specific direction (Vinepinsky et al., 2020). This is akin to the function of the head-direction cells in mammals, which are essential for maintaining spatial orientation during navigation. Additionally, goldfish possess edge-encoding cells that become active when the fish are near environmental boundaries, such as the walls of a tank, similar to the border cells and boundary vector cells found in mammalian brains (Vinepinsky et al., 2020; Cohen et al., 2023). These cells likely provide a reference frame for spatial orientation, helping the fish navigate by maintaining an awareness of their position relative to environmental boundaries. Interestingly, some neurons in the goldfish pallium encode speed and velocity-vector cells that show increased firing rates correlated with the fish's swimming speed and vector along the swimming direction, respectively (Vinepinsky et al., 2020). These cells integrate information about head direction and speed, which are crucial for calculating the fish's trajectory and planning navigational strategies. Such integration indicates a complex neural network capable of supporting advanced navigational behaviors, including homing and exploration.

A notable study on free-swimming salmonids used wireless neurologgers to record neuronal activity in the telencephalon. This study revealed that these fish also possess head-direction cells that exhibit neuronal responses similar to those observed in goldfish and rodents (Takahashi et al., 2021). These findings suggest a conserved mechanism of heading orientation signals for spatial navigation across vertebrates. Recording neuronal activity using biotelemetry in naturalistic settings provides a more comprehensive understanding of how teleosts process spatial information. This approach allows researchers to observe neuronal activity in real-world environments, thereby providing more accurate insights into the neural mechanisms underlying spatial navigation.

A comparative analysis of goldfish and salmonids highlighted both similarities and differences in their spatial navigation mechanisms. Although both species share head-direction cells, the specific environmental cues they use may vary. This variation reflects adaptations to their respective habitats, with goldfish often relying more on visual cues (Broglio et al., 2003) and salmonids potentially using geomagnetic information for long-distance migration (Putman et al., 2013) (Figure 1). The absence of border cells in the pallium of salmonids may be due to their ethological needs and living environment. In studies on salmonids, the number of recorded cells and environmental variables are limited (Takahashi et al., 2021), which may be crucial for supporting or refuting this hypothesis in future research. In particular, because goldfish do not engage in long-distance migration, their response to changes in magnetic fields is a critical area for empirical study.

Despite these advancements, several challenges remain in the study of spatial cognition in teleosts. Most studies have been conducted in controlled laboratory environments, which may not fully capture the complexities of natural habitats. Future studies should explore how different environmental factors, such as water currents, salinity, changes in lighting, or underwater topography, affect the neural processing of spatial information. Additionally, understanding how teleosts encode three-dimensional space remains a significant challenge because their aquatic environments add complexity to spatial navigation. As goldfish are entirely freshwater fish and salmonids migrate between saltwater and freshwater, it is important to investigate, in the future, fish that exclusively inhabit oceanic environments, as we still do not fully understand what cues they use for spatial cognition. The continued development of wireless neurologgers

10.3389/fphys.2024.1499058

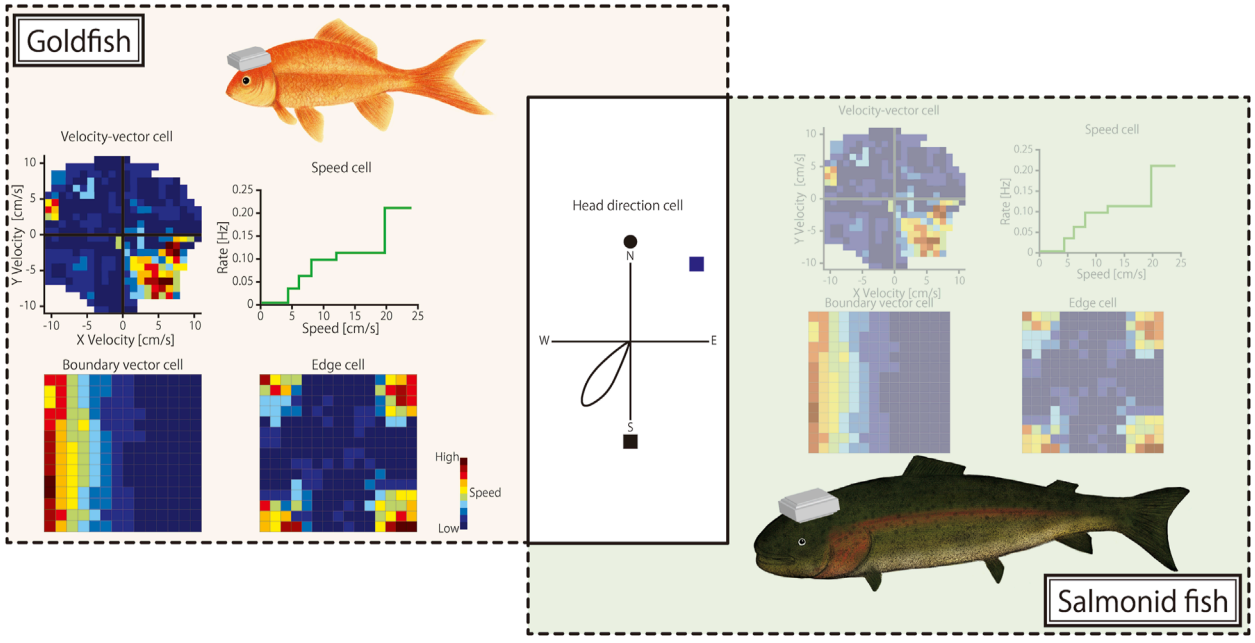

FIGURE 1
Spatial cognition cell types found in goldfish and salmonid fish. On the left, neural representations of spatial cognition cell types found in the telencephalon of goldfish are illustrated: (top left) velocity-vector cells that encode swimming velocity in two dimensions; (top right) speed cells with firing rates correlated with swimming speed; (bottom left) boundary-vector cells responding to environmental boundaries; and (bottom right) edge cells encoding edges of the environment. The central diagram shows a head-direction cell that fires when the fish's head is oriented in a specific direction, a cell type found in both goldfish and salmonids. On the right, neuronal activity in the telencephalon of salmonid fish remains unclear for other spatial cognition cell types (denoted by shaded illustration), with only head-direction cells confirmed to be common between the two species.

and biotelemetry technologies is crucial for overcoming these challenges and enabling more detailed and extended studies in diverse and challenging environments. Overall, the exploration of space-responsive cells in teleosts has provided valuable insights into the neural substrates of spatial cognition, highlighting both the evolutionary conservation and adaptability of these systems across vertebrates.

3 Comparative analysis and evolutionary considerations

Comparative studies have highlighted similarities and differences between the spatial navigation systems of teleosts and mammals. For instance, while the hippocampal formation in mammals has been well-documented for its role in spatial memory (Wilson and McNaughton, 1993; Dickerson and Eichenbaum, 2010), homologous structures in teleosts, such as the lateral pallium, also play a significant role in spatial learning and memory. For example, the lateral pallium in goldfish has been implicated in the encoding of allocentric spatial strategies akin to the function of the hippocampus in mammals. Research involving lesion studies in goldfish has shown that damage to the lateral pallium impairs their ability to navigate using an allocentric strategy (Rodriguez et al., 2002), indicating its critical role in spatial cognition. Recent single-cell studies in teleost fish, particularly in goldfish and cichlids, provide additional evidence that the neuronal mechanisms supporting spatial navigation may be evolutionarily conserved. For example, mapping of the goldfish telencephalon using single-cell RNA sequencing and spatial transcriptomics revealed a hippocampal marker NEUROD6 expression scattered across the dorsolateral and dorsomedial regions (Tibi et al., 2023). Similarly, neurons in the subdivision of the dorsolateral pallium of cichlid fish share transcriptional profiling and neuroanatomy with mammalian hippocampus (Hegarty et al., 2024), offering further support for the hypothesis that spatial navigation mechanisms are conserved across vertebrates.

In mammals, spatial navigation relies heavily on the hippocampus and associated structures in which place cells (O'Keefe and Dostrovsky, 1971), grid cells (Hafting et al., 2005), border cells (Solstad et al., 2008), speed cells (Kropff et al., 2015) and head-direction cells (Taube et al., 1990) reside. These cells encode information regarding the animal's location, direction, and distance traveled. Similarly, teleosts such as goldfish and zebrafish possess analogous neurons that respond to spatial cues, including edge-encoding cells that are activated near boundaries, and head-direction cells that maintain stable activity relative to the fish's heading. Notably, recent research has identified place cells in the telencephalon of zebrafish (Yang et al., 2024), suggesting that teleosts share similar neural mechanisms for spatial cognition as mammals. These findings suggest that while the specific types of neurons and their functions can vary between species, the fundamental neural mechanisms supporting spatial navigation have been conserved across vertebrate evolution.

The use of geomagnetic cues in navigation is another area wherein significant differences emerge between aquatic and

terrestrial vertebrates. For example, salmonids use geomagnetic cues for long-distance migration, a mechanism less prevalent in terrestrial mammals, which typically rely on visual and olfactory cues for navigation. This adaptation reflects the distinct environmental challenges faced by these species. The reliance on different sensory modalities for navigation in various environments underscores the versatility and adaptability of the spatial navigation systems in different taxa.

Furthermore, a comparative approach revealed that teleosts, such as goldfish, may lack certain features seen in mammalian spatial systems, such as theta oscillations (Cohen et al., 2023). These oscillations are prominent in mammalian hippocampal activity and are associated with navigation and memory encoding (Buzsáki, 2002). The absence of such rhythms in teleosts suggests that while the overall architecture of spatial cognition may be conserved, the specific neural dynamics can differ significantly from those in bats (Eliav et al., 2018).

Overall, these findings suggest that the neural mechanisms underlying spatial cognition have been conserved to some extent across vertebrate evolution. However, the specificity of how different species process spatial information varies, reflecting their adaptations to their respective environments. This comparative perspective not only highlights the evolutionary conservation of spatial navigation mechanisms, but also emphasizes the unique adaptations that different species have developed to navigate their specific ecological niches.

4 Methodological advances and future directions

The emergence of neurologgers has contributed significantly toward uncovering the neural bases of spatial cognition in teleosts. These tools enable high-resolution recording of neuronal activity in freely behaving animals and provide valuable insights into how these fish navigate complex environments. Methodological improvements are needed to overcome the current technological limitations. Although neurologgers have been revolutionary, challenges remain, such as the need for more robust waterproofing and longer battery life for extended recordings in underwater conditions. Moreover, developing smaller devices will allow researchers to study smaller species and younger individuals, broadening the scope of research on neural mechanisms in teleosts. Overall, these methodological advances and future directions highlight the potential for further discoveries regarding spatial cognition in teleosts. As we continue to refine our techniques and expand our understanding, we expect to gain deeper insights into the neural underpinnings of navigation and memory, not only in fish but also across the entire vertebrate lineage.

5 Discussion

Studies on spatial memory and navigation in teleosts highlight the remarkable complexity and sophistication of their neural systems. This body of research reveals that teleosts possess advanced spatial-cognition mechanisms, including space-responsive cells, such as head-direction cells, which are analogous to those found in mammals. These discoveries underscore the significant evolutionary conservation of spatial-cognition mechanisms across vertebrate lineages, suggesting that the ability to navigate and form an internal compass is a fundamental trait that may have evolved early in vertebrate history.

Teleosts, such as goldfish and salmonids, can use various environmental cues, including visual landmarks and geomagnetic fields, to navigate their environments. The presence of specialized neurons that respond to these cues indicates a highly developed neural substrate capable of processing complex spatial information. For instance, the discovery of head-direction cells in both goldfish and salmonids and their functional similarities to those in mammals points to a conserved neural architecture that supports spatial orientation and navigation across different species and ecological niches.

As research in this field advances, it is expected to further uncover the neural mechanisms that enable fish to navigate their aquatic habitats. This includes understanding how different types of space-responsive cells interact within broader neural networks, and how these networks integrate sensory information to support behaviors such as migration, homing, and exploration. The study of these systems in teleosts not only enhances our understanding of fish neurobiology, but also provides valuable insights into the evolution of cognitive functions in vertebrates.

The continued development and refinement of neurologgers is crucial for driving these discoveries. These tools have enabled researchers to record the neuronal activity in freely behaving animals, thereby offering a more accurate representation of how fish process spatial information in naturalistic settings. Future technological advancements may include more robust waterproofing, longer battery life, and device miniaturization, which will allow for extended and more detailed studies on smaller and younger fish.

Furthermore, future research should explore the neural encoding of three-dimensional space, given the unique challenges posed by the aquatic environments in which teleosts live. Understanding how these fish encode vertical and horizontal spatial information will provide deeper insights into the neural basis of three-dimensional navigation. The integration of neurologgers with other devices, such as depth sensors and accelerometers, in biotelemetry systems (Korpela et al., 2020; Otsuka et al., 2024; Tanigaki et al., 2024) may offer solutions to these challenges. Moreover, manipulating environmental variables, such as geomagnetic fields, in experimental settings can shed light on the specific neural circuits involved in processing these cues, further elucidating the mechanisms of spatial cognition, as the head-direction cells in the pallium of migratory birds prefer geomagnetic north (Takahashi et al., 2022).

In summary, research on spatial memory and navigation in teleost fish not only advances our knowledge of these fascinating animals, but also contributes to a broader understanding of the evolution of cognitive functions in vertebrates. As we continue to refine our methodologies and explore new technologies, we are likely to uncover new dimensions of the neural processes underlying spatial cognition. These findings have the potential to revolutionize our understanding of neurobiology and cognition across the animal kingdom, highlighting the shared and unique aspects of neural

architecture and function that have evolved to support life in diverse environments.

Author contributions

ST: Conceptualization, Writing–original draft, Writing–review and editing. FS: Conceptualization, Writing–review and editing. KI: Visualization, Writing–review and editing. TA: Conceptualization, Writing–review and editing. TK: Conceptualization, Writing–review and editing. YM: Conceptualization, Writing–review and editing.

Funding

The author(s) declare that financial support was received for the research, authorship, and/or publication of this article. This work was supported by Kakenhi grants from the Japan Society for the Promotion of Science (21H05296 and 23H00502 to ST) and by the Core Research for Evolutional Science and Technology (CREST) program of the Japan Science and Technology (JST) Agency (JPMJCR23P2 to ST).

Acknowledgments

The authors acknowledge Kakenhi grants and JST CREST for supporting the study. In the preparation of this manuscript, the authors used ChatGPT-4o, a generative AI language model developed by OpenAI, to improve readability and language. Following the initial edits, the authors thoroughly reviewed and adjusted the content to ensure its accuracy and integrity. The authors take full responsibility for the final version of the manuscript.

Conflict of interest

The authors declare that the research was conducted in the absence of any commercial or financial relationships that could be construed as a potential conflict of interest.

The author(s) declared that they were an editorial board member of Frontiers, at the time of submission. This had no impact on the peer review process and the final decision.

Publisher's note

References

Broglio, C., Rodríguez, F., and Salas, C. (2003). Spatial cognition and its neural basis in teleost fishes. *Fish Fish.* 4, 247–255. doi:10.1046/j.1467-2979.2003.00128.x

Buzsáki, G. (2002). Theta oscillations in the Hippocampus. *Neuron* 33, 325–340. doi:10.1016/S0896-6273(02)00586-X

Cohen, L., Vinepinsky, E., Donchin, O., and Segev, R. (2023). Boundary vector cells in the goldfish central telencephalon encode spatial information. *PLOS Biol.* 21, e3001747. doi:10.1371/journal.pbio.3001747

Dickerson, B. C., and Eichenbaum, H. (2010). The episodic memory system: neurocircuitry and disorders. *Neuropsychopharmacol* 35, 86–104. doi:10.1038/npp.2009.126

Eliav, T., Geva-Sagiv, M., Yartsev, M. M., Finkelstein, A., Rubin, A., Las, L., et al. (2018). Nonoscillatory phase coding and synchronization in the bat hippocampal formation. *Cell* 175, 1119–1130. doi:10.1016/j.cell.2018.09.017

Hafting, T., Fyhn, M., Molden, S., Moser, M.-B., and Moser, E. I. (2005). Microstructure of a spatial map in the entorhinal cortex. *Nature* 436, 801–806. doi:10.1038/nature03721

Hegarty, B. E., Gruenhagen, G. W., Johnson, Z. V., Baker, C. M., and Streelman, J. T. (2024). Spatially resolved cell atlas of the teleost telencephalon and deep homology of the vertebrate forebrain. *Commun. Biol.* 7, 612–616. doi:10.1038/s42003-024-06315-1

Ide, K., and Takahashi, S. (2022). A review of neurologgers for extracellular recording of neuronal activity in the brain of freely behaving wild animals. *Micromachines* 13, 1529. doi:10.3390/mi13091529

Korpela, J., Suzuki, H., Matsumoto, S., Mizutani, Y., Samejima, M., Maekawa, T., et al. (2020). Machine learning enables improved runtime and precision for bio-loggers on seabirds. *Commun. Biol.* 3, 633–639. doi:10.1038/s42003-020-01356-8

Kropff, E., Carmichael, J. E., Moser, M.-B., and Moser, E. I. (2015). Speed cells in the medial entorhinal cortex. *Nature* 523, 419–424. doi:10.1038/nature14622

Lieschke, G. J., and Currie, P. D. (2007). Animal models of human disease: zebrafish swim into view. *Nat. Rev. Genet.* 8, 353–367. doi:10.1038/nrg2091

O'Keefe, J., and Dostrovsky, J. (1971). The hippocampus as a spatial map. Preliminary evidence from unit activity in the freely-moving rat. *Brain Res.* 34, 171–175. doi:10.1016/0006-8993(71)90358-1

Otsuka, R., Yoshimura, N., Tanigaki, K., Koyama, S., Mizutani, Y., Yoda, K., et al. (2024). Exploring deep learning techniques for wild animal behaviour classification using animal-borne accelerometers. *Methods Ecol. Evol.* 15, 716–731. doi:10.1111/2041-210X.14294

Putman, N. F., Lohmann, K. J., Putman, E. M., Quinn, T. P., Klimley, A. P., and Noakes, D. L. G. (2013). Evidence for geomagnetic imprinting as a homing mechanism in pacific salmon. *Curr. Biol.* 23, 312–316. doi:10.1016/j.cub.2012.12.041

Rodriguez, F., López, J. C., Vargas, J. P., Gómez, Y., Broglio, C., and Salas, C. (2002). Conservation of spatial memory function in the pallial forebrain of reptiles and ray-finned fishes. *J. Neurosci.* 22, 2894–2903. doi:10.1523/JNEUROSCI.22-07-02894.2002

Solstad, T., Boccara, C. N., Kropff, E., Moser, M.-B., and Moser, E. I. (2008). Representation of geometric borders in the entorhinal cortex. *Science* 322, 1865–1868. doi:10.1126/science.1166466

Takahashi, S., Hombe, T., Matsumoto, S., Ide, K., and Yoda, K. (2022). Head direction cells in a migratory bird prefer north. *Sci. Adv.* 8, eabl6848. doi:10.1126/sciadv.abl6848

Takahashi, S., Hombe, T., Takahashi, R., Ide, K., Okamoto, S., Yoda, K., et al. (2021). Wireless logging of extracellular neuronal activity in the telencephalon of free-swimming salmonids. *Anim. Biotelemetry* 9, 9. doi:10.1186/s40317-021-00232-4

Tanigaki, K., Otsuka, R., Li, A., Hatano, Y., Wei, Y., Koyama, S., et al. (2024). Automatic recording of rare behaviors of wild animals using video bio-loggers with on-board light-weight outlier detector. *PNAS Nexus* 3, pgad447. doi:10.1093/pnasnexus/pgad447

Taube, J., Muller, R., and Ranck, J. (1990). Head-direction cells recorded from the postsubiculum in freely moving rats. I. Description and quantitative analysis. *J. Neurosci.* 10, 420–435. doi:10.1523/JNEUROSCI.10-02-00420.1990

Tibi, M., Biton Hayun, S., Hochgerner, H., Lin, Z., Givon, S., Ophir, O., et al. (2023). A telencephalon cell type atlas for goldfish reveals diversity in the evolution of spatial structure and cell types. *Sci. Adv.* 9, eadh7693. doi:10.1126/sciadv.adh7693

Vinepinsky, E., Cohen, L., Perchik, S., Ben-Shahar, O., Donchin, O., and Segev, R. (2020). Representation of edges, head direction, and swimming kinematics in the brain of freely-navigating fish. *Sci. Rep.* 10, 14762. doi:10.1038/s41598-020-71217-1

Wilson, M. A., and McNaughton, B. L. (1993). Dynamics of the hippocampal ensemble code for space. *Science* 261, 1055–1058. doi:10.1126/science.8351520

Yang, C., Mammen, L., Kim, B., Li, M., Robson, D. N., and Li, J. M. (2024). A population code for spatial representation in the zebrafish telencephalon. *Nature* 634, 397–406. doi:10.1038/s41586-024-07867-2

frontiers | Frontiers in Physiology

TYPE Methods
PUBLISHED 14 January 2025
DOI 10.3389/fphys.2024.1511443

OPEN ACCESS

EDITED BY
Takashi Kitagawa,
The University of Tokyo, Japan

REVIEWED BY
Amanda Williard,
University of North Carolina Wilmington, United States
Yuya Makiguchi,
Nihon University, Japan

*CORRESPONDENCE
Ayaka Saito,
saito-ayaka97@g.ecc.u-tokyo.ac.jp

RECEIVED 15 October 2024
ACCEPTED 27 December 2024
PUBLISHED 14 January 2025

CITATION
Saito A, Sakai K, Kawai M, Lyu L, Kameda K, Kudo H, Sato K and Sakamoto KQ (2025) Development of a non-invasive heart rate measurement method for sea turtles with dense keratinous scutes through effective electrode placement.
Front. Physiol. 15:1511443.
doi: 10.3389/fphys.2024.1511443

Development of a non-invasive heart rate measurement method for sea turtles with dense keratinous scutes through effective electrode placement

Ayaka Saito[1]*, Kino Sakai[1], Megumi Kawai[1], Lyu Lyu[1], Kazunari Kameda[2], Hiromi Kudo[3], Katsufumi Sato[1] and Kentaro Q. Sakamoto[1]

[1]Atmosphere and Ocean Research Institute, The University of Tokyo, Kashiwa, Japan, [2]Kuroshima Research Station, Sea Turtle Association of Japan, Taketomi, Japan, [3]Center for Research and Education of Wildlife, Kyoto City Zoo, Kyoto, Japan

Measuring the heart rate of sea turtles is important for understanding their physiological adaptations to the environment. Non-invasive methods to measure the electrocardiogram (ECG) of sea turtles have been developed by attaching electrodes to their carapace. However, this method has only been applicable to sea turtles with sparse keratin on their shell surfaces, such as loggerhead turtles, and it is difficult to detect heartbeats in sea turtles with dense keratinous scutes, including green sea turtles. Here, we explored the electrode placements on the plastron that can be applied to ECG measurement in green turtles. ECG signals were checked using a handheld ECG monitor at three sets of electrode placement on the plastron. When ECG signals could be detected, they were measured in the water tanks for several days to confirm the clarity of the ECG signals. Of the 29 green turtles, when the negative electrode was placed near the neck area of the plastron, clear ECG signals were obtained in nine individuals (39.1%), whereas ECG signals were not detected at any placements in four individuals (17.4%). Furthermore, in the water tank experiments, continuous ECG signals were successfully recorded by attaching a negative electrode near the neck: almost noiseless clear ECG signals even during moving in seven out of ten individuals and slightly weak and noisy signals in other individuals. The measured heart rate of ten individuals during resting was 8.6 $\pm$ 2.9 (means $\pm$ s.d.) beats min^{-1} and that during moving was 12.2 $\pm$ 4.7 beats min^{-1}, similar to those reported in a previous study involving the insertion of electrodes inside the body. Therefore, for measuring the ECG of green turtles, the negative electrode should be placed closer to the neck, and the positive and earth electrodes should be placed to the lower left of the plastron. Although the selection of suitable individuals for measurements is required, this heart rate measurement method will contribute to a better understanding of the physiological status of sea turtles with dense keratinous scutes, including green turtles.

KEYWORDS

heart rate, sea turtle, non-in vasive method, biologging, electrocardiogram

1 Introduction

Sea turtles are diving reptiles specialized in the marine environments. Despite being air-breathing animals, they have outstanding abilities for deep (e.g., 1,186 m in leatherback turtles, López-Mendilaharsu et al., 2009; 340 m in loggerhead turtles, Narazaki et al., 2015) and long dives (e.g., 614 min in loggerhead turtles, Broderick et al., 2007; 330 min in green turtles, Fukuoka et al., 2015) among marine reptiles. Moreover, they spend most of their life at sea, except for nesting and hatching on land (Lutcavage et al., 1987; Hochscheid et al., 2010). To understand the physiological adaptations of sea turtles to the marine environment, many studies have been conducted to measure their cardiovascular adjustments using an electrocardiogram (ECG). From the ECG records of free-ranging animals, the number of heartbeats per minute, i.e., the heart rate, can be calculated, which reflects the cardiovascular status at that time. As sea turtles have hard shells, it is difficult to measure ECG by attaching electrodes to their body surfaces, as in terrestrial animals. Therefore, ECG measurements in turtles have been conducted by inserting electrodes inside the body (Southwood et al., 1999, 2003; Williams et al., 2019; Okuyama et al., 2020). Recently, an ECG measurement method has been developed by attaching electrode patches to the surface of the carapace in several species of hard-shelled sea turtles (Sakamoto et al., 2021). However, these non-invasive methods have only been applicable in loggerhead (*Caretta caretta*), black (black morphotypes of the eastern Pacific *Chelonia mydas*; Álvarez-Varas et al., 2021), and olive ridley turtles (*Lepidochelys olivacea*). In some species, such as green (*C. mydas*) and hawksbill turtles (*Eretmochelys imbricata*), ECG signals were hardly detected even when the electrodes were attached to the same positions reported for loggerhead turtles on the carapace. Sakamoto et al. (2021) suggested that the lack of detection may be due to the dense keratinous scutes of these species, making it difficult to transmit biopotentials.

Although non-invasive heart rate measurement methods have been difficult to apply to sea turtle species with dense keratinous scutes, there has been great interest in studying their physiological status. Green turtles, for example, are distributed from temperate to tropical areas and are listed as "Endangered" on the International Union for Conservation of Nature and Natural Resources Red List (Seminoff, 2023). However, conflicts with fishermen have become problematic because of bycatch in set nets and the modification of coastal marine ecosystems associated with seaweed feeding. Heart rate is regulated according to diving behavior under natural environments (Ponganis, 2015). Cardiovascular adjustment including such heart rate regulation is related to the use of oxygen store and is essential for diving ability (Ponganis, 2015). A more sophisticated understanding of sea turtle physiology based on heart rate may provide key insights into solving the issues in sea turtles. Therefore, it is desirable to develop a non-invasive ECG measurement method for sea turtles with dense keratinous scutes. In loggerhead turtles, clear ECG waves could be obtained by changing the electrode placements from the carapace to the plastron, closer to the heart (Kinoshita et al., 2022a). Therefore, we tested whether ECG signals could be obtained by placing the electrodes in different placements from those used in previous studies.

In this study, we explored the effective electrode placement for ECG measurement in green turtles by attaching electrodes to their plastron. First, the quality of the ECG signals obtained from three different electrode placements was evaluated using a handheld ECG monitor. Next, when ECG signals were confirmed, animal-borne recorders were used to check whether ECG signals could be measured continuously for several days in the water tanks. We report that a high percentage of clear ECG signals can be obtained by placing the electrodes closer to the necks of green turtles.

2 Materials and Equipment

2.1 Animals and study sites

Juvenile green turtles, *C. mydas*, were collected from two regions: the Sanriku coastal area and Kuroshima Island, Japan (Table 1). The Sanriku coastal area of Japan is located in the temperate region of the western North Pacific and is a summer-restricted foraging ground for green turtles (Fukuoka et al., 2015). Fifteen turtles were incidentally captured by commercial set nets between June and August of 2020–2023. Once safely rescued, the turtles were promptly transferred to the marine station of the University of Tokyo (Otsuchi Coastal Research Center, Atmosphere and Ocean Research Institute, The University of Tokyo; 39°21′05″N, 141°56′04″E). Kuroshima Island, on the Yaeyama Islands, located in a subtropical area in southern Japan, provides a year-round foraging habitat for green turtles (Kameda et al., 2017, 2023). Fourteen turtles were captured using an entanglement net (200 m length × 2 m height, mesh size = 40 cm) in February 2023. The net was set in the inner reef area

TABLE 1 Summary of data for green sea turtles in 2 study sites.

Study site	No. of turtles	*BM* (kg)	*SCL* (cm)
Kuroshima Island	14	15.7 ± 6.7	48.2 ± 6.2
		(6.4–32.1)	(37.0–61.4)
Sanriku coastal area	15	15.6 ± 7.2	46.7 ± 6.7
		(8.0–35.9)	(39.2–64.6)
Total	29	15.6 ± 6.8	47.4 ± 6.4
		(6.4–35.9)	(37.0–64.6)

BM, body mass; *SCL*, straight carapace length. Means are reported ± s.d. Numbers in parentheses indicate maximum and minimum values.

10.3389/fphys.2024.1511443

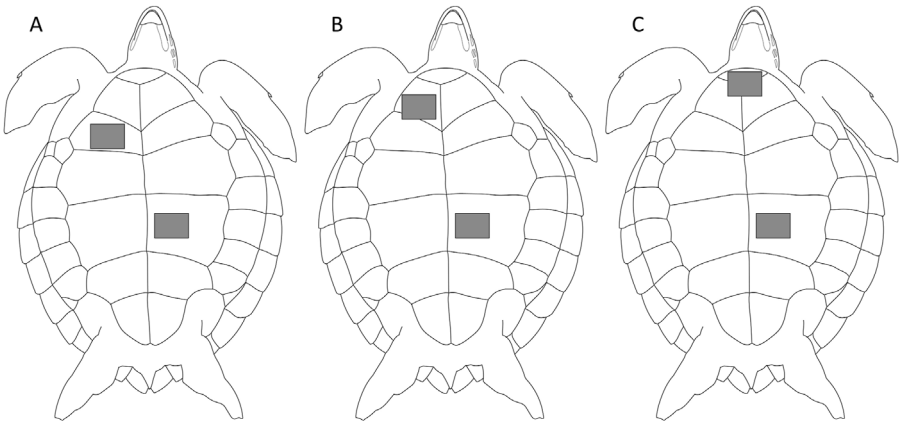

FIGURE 1
Three positions of electrodes of green sea turtles. Two electrodes were attached to the plastron; the negative electrode was attached to **(A)** humeral scute, the same position reported for loggerhead turtles (Kinoshita et al., 2022a), **(B)** gular scute, or **(C)** intergular scute, and positive and earth electrodes were attached to abdominal scute.

at two sites, the northeast and south sides of Kuroshima Island, and was carefully checked by snorkelers to avoid the risk of mortality of the turtles. Once a turtle was captured, the turtle was promptly transferred to the Kuroshima Research Station, Sea Turtle Association of Japan (24°14′24.0″N, 123°59′36.4″E).

After the turtles were transferred to each marine station, the straight carapace length (*SCL*) and body mass (*BM*) were measured. The *BM* and *SCL* of the turtles were 15.6 ± 6.8 (means ± s.d.) kg and 47.4 ± 6.4 cm, respectively (Table 1). The sex of all turtles was not determined. After morphological measurements, they were kept in outdoor flow-through seawater tanks for 1—2 months at most. After the experiments, all the turtles were released into the sea around where they were caught. This study was conducted as a part of a "tag and release" program. All turtles were tagged with metal or plastic ID tags. All experimental procedures were approved by the Animal Ethics Committee of the Atmosphere and Ocean Research Institute at the University of Tokyo (approval numbers P20-11, P21-13, P22-12, P22-21, and P23-21). The study in Kuroshima Island was approved by the Marine Fisheries Coordinating Committee of Okinawa Prefecture, Japan (approval numbers: Oki-cho K4-16).

2.2 Electrocardiogram and behavioral recorders

The experiment involved two steps. Firstly, a handheld ECG monitor (Checkme ECG; San-ei Medisys, Kyoto, Japan) was used to confirm the ECG signals for a short period on land. Secondly, if ECG signals were detected by the monitor, animal-borne ECG recorders were used to verify whether ECG signals could be measured for up to 4 days in water tanks. ECG was recorded at 250 Hz using an ECG recorder (ECG400-DT; Little Leonardo, Tokyo, Japan; cuboid shape: 21 mm wide, 64 mm long, 23 mm high, 60 g mass in air; ECG400-D3GT; Little Leonardo; cuboid shape: 31 mm wide, 67 mm long, 17 mm high, 61 g mass in air). Turtle behavior was recorded using an accelerometer (M190L-D2GT; Little Leonardo; cylindrical shape; 15 mm diameter, 53 mm length, 18 g mass in air). The accelerometer and ECG recorder were attached to the turtles along the longitudinal axis of their carapaces. The longitudinal acceleration was recorded at 16 Hz or 50 Hz, and temperature, and depth were recorded at 1 Hz, and 1 Hz, respectively.

3 Methods

3.1 Confirmation of ECG signals in a short time

The R wave (depolarization of the ventricles) shows the most drastic change in voltage among the ECG signals and is used to detect heartbeats (Sakamoto et al., 2021). To measure clear R waves, it is suitable to attach the negative electrode to the upper right and both the positive and earth electrodes to the lower left of the plastron for loggerhead turtles (Kinoshita et al., 2022a; Figure 1A). Therefore, these electrodes were attached to different placements of the plastron of green turtles, and the amplitudes and stability of the ECG signals were confirmed by using the handheld monitor. The signals were confirmed on land after the turtles were removed from the tank. For conformation, we used 15 turtles from the Sanriku coastal area and 14 turtles from Kuroshima Island.

Three positions were tested for the negative electrode: humeral scute (Position A; Figure 1A), the same position reported for loggerhead turtles (Kinoshita et al., 2022a), gular scute (Position B; Figure 1B), and intergular scute (Position C; Figure 1C). Positive and earth electrodes were attached to the abdominal scute. Preliminary experiments showed that the detectability of the signal changed depending on the position of the negative electrode, and ECG signals were more likely to be confirmed when the electrode was placed close to the neck. Therefore, we selected Position C, the conventional position (Position A), and Position B, which is in between the two, as the position of the negative electrode. A conductive adhesive tape (KNZ-ST50 shield cloth tape; Kyowa Harmonet Ltd., Kyoto, Japan) was cut into squares (1 cm × 2.5 cm) to make the small electrodes. Small electrodes were attached at each position and connected to a handheld

ECG monitor by clipping the electrodes with alligator clips. The handheld ECG monitor displayed ECG signals in real-time. We checked whether the signals could be detected for 30 s to several minutes at each position.

3.2 Confirmation of ECG signals in a long time

ECG data may not be applicable for analysis if the ECG contains noise produced by muscle contractions, particularly when the turtle is moving. To confirm whether a qualified ECG could be measured continuously for up to 4 days, animal-borne recorders were attached to 14 turtles (six in the Sanriku coastal area and eight on Kuroshima Island) after confirming successful detection from the handheld ECG monitor.

The ECG signals of the turtles were recorded using a previously described non-invasive method that involved attaching two-electrode patches to the carapace of the turtles (Sakamoto et al., 2021) with some modifications (Kinoshita et al., 2022a). The ECG electrodes were made by cutting conductive adhesive tape into squares (4 cm × 5 cm). A lead wire was attached to the ends of the electrodes using the same adhesive tape. Two electrodes were attached to the plastron where the ECG signals were confirmed by using the handheld monitor in each turtle. In the water tank experiments, the specific electrode placements for each individual were as follows: G2015 at Position A; G2262, G2263, and G2268 at Position B; and other individuals at Position C. After attaching the electrodes, a conductive cream (ECG cream; Suzuken, Aichi, Japan) was applied to the surfaces to allow the electrical signals to pass. As seawater intrusion into the electrodes causes electrical noise in the ECG, the water droplets around the electrodes were carefully removed using acetone. Thereafter, the electrodes were waterproofed with waterproof adhesive plasters (BAND-AID Brand Hydroseal XL bandages; Johnson & Johnson, NJ, United States), and the edges of the adhesive plasters were glued using an instant adhesive (Aron Alpha Jelly Extra; Konishi, Osaka, Japan). Waterproof films (FC waterproof free-cut; Hakujuji, Tokyo, Japan) were used to cover the electrodes completely. To ensure that the electrodes were waterproof, they were thinly coated with an epoxy (Bond Quick 5; Konishi). The lead wires of the electrodes were arranged from the plastron along the side of the body to the carapace and fixed with adhesive tape and instant adhesive. These wires were connected to the lead wires extending from the ECG recorder and sealed with a heat-shrinkable tube. Finally, the ECG recorder and accelerometer were placed on a waterproof adhesive plaster pasted on the carapace using an instant adhesive. The attachment of the instruments was completed within approximately 1 h. After the electrodes were attached, the turtles were returned to their tanks (1 m × 2 m × 1 m).

3.3 Analysis

The ECG signals were evaluated based on their amplitudes and stability as "undetectable" when they were visually detectable for less than 30% of the measurement period, "unclear" when they were 30%–70%, and "clear" when they were more than 70%. To analyze ECG, longitudinal acceleration, and temperature data obtained by animal-borne recorders, IGOR Pro version 8.04 (Wavemetrics, Portland, OR, United States) was used with the Ethographer program package (Sakamoto et al., 2009). Data within a 12-h period after returning to the water tank was excluded to eliminate handling effects from the instrument attachments. In the case of turtle G2356, only the ECG and longitudinal acceleration data were analyzed because the temperature data were lost owing to a device error. Small R waves may be partially offset by the noise produced by muscle contractions when the turtle is moving, preventing the accurate detection of R waves. Therefore, the behavior of the turtles was classified into resting or moving phases based on longitudinal acceleration data to calculate the heart rate during each phase (Kinoshita et al., 2022a). The degree of activity of sea turtles can be reflected by the values of the standard deviation of longitudinal acceleration. We defined 0.5 m s^{-2} as the threshold to distinguish between resting and moving phases (sea turtles were hardly moving when the value was below 0.5 m s^{-2}). The standard deviation of the longitudinal acceleration was calculated every minute; values lower than 0.5 m s^{-2} were regarded as representing resting status, otherwise as moving status. Only the same status that continued for at least 2 min was defined as the corresponding phase. The ECG data were processed using the ECGtoHR package (Sakamoto et al., 2021), which runs on IGOR Pro. After band-pass filtering, the R waves were detected. For each turtle, the heart rate during each phase (resting and moving) was calculated by dividing the total number of R-waves per period by the duration of each period. These values were averaged to obtain the grand mean value for each phase. The values are expressed as means ± s.d.

TABLE 2 Summary of evaluations for 3 sets of electrode placements using handheld ECG monitor.

Evaluation	Electrode placement					
	Position A		Position B		Position C	
Undetectable	4	(16.7%)	4	(14.3%)	4	(17.4%)
Unclear	20	(83.3%)	20	(71.4%)	10	(43.5%)
Clear	0	(0%)	4	(14.3%)	9	(39.1%)
Total	24		28		23	

4 Results

The ECG signals of the 29 green turtles were checked for three sets of electrode placements on the plastron using a handheld ECG monitor (Table 2). By attaching electrodes at Position A, the same position reported for loggerhead turtles, no signal was detected in any individual. On the other hand, clear ECG signals were detected when the negative electrode was attached closer to the neck with signals detected from four individuals (14.3%) at Position B and nine individuals (39.1%) at Position C. When unclear ECG signals were detected at Position A, the same individual showed clear signals by attaching the electrodes at Position C, the placement closest to the neck (nine individuals, 31.0%; Supplementary Table S1). However, no matter where the electrodes were placed, ECG signals were unclear from ten individuals (34.5%) and undetectable from four individuals (17.4%). Among the individuals used in this study, the

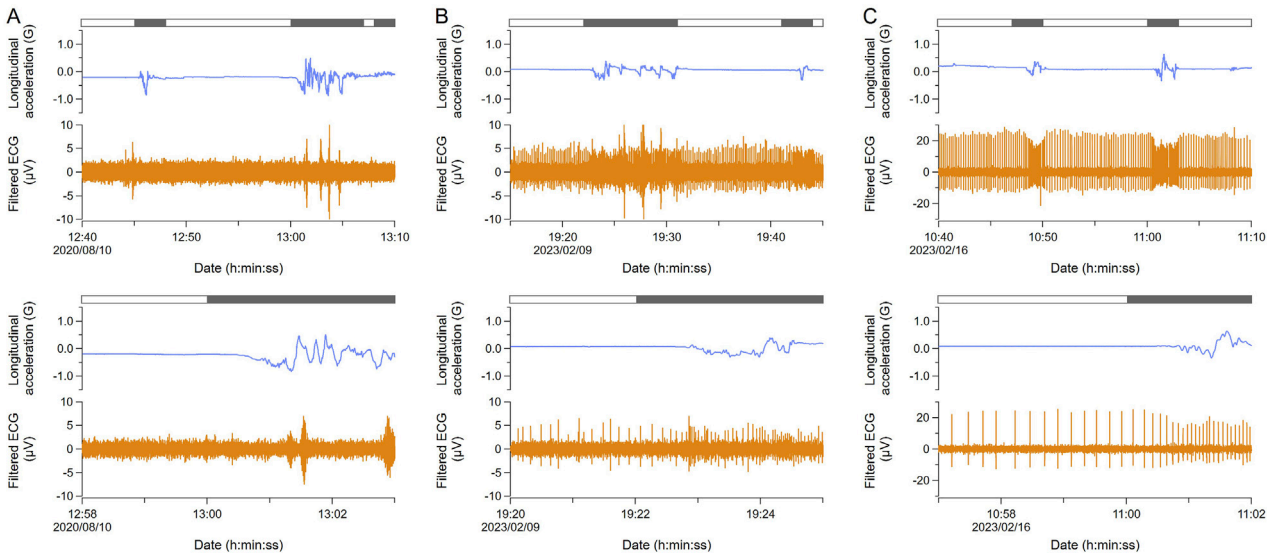

FIGURE 2
Comparison of ECG signals measured with animal-borne recorders. In each section, the top figure shows the data for 30 min and the bottom one is the enlarged data. Blue and orange lines indicate longitudinal acceleration and filtered ECG, respectively. The bar above indicates moving (black) and resting (white) phases. **(A)** ECG signals were undetectable (G2015; Position A). **(B)** ECG signals were unclear. ECG waves contained some noises produced by muscle contraction, especially during moving (KG2308; Position C). **(C)** ECG signals were clear (KG2310; Position C). Therefore, placing the electrode at position C is recommended. Note that the range of the *Y* axis in ECG is different from others.

body size and habitat did not have any obvious effects on the clarity of the ECG signal of ECG measurements (Supplementary Table S1).

After the ECG signals were confirmed using a handheld ECG monitor, the ECG and behavior of 14 turtles were measured for 2–4 days using animal-borne recorders (Supplementary Table S1). In one individual with electrodes placed at Position A, ECG signals were undetectable (Figure 2A). Three individuals with electrodes placed at Position B showed clear ECG signals even during the moving phases, although they were not tested at Position C using a handheld ECG monitor (Supplementary Table S1). For the ten individuals with electrodes placed at Position C, closest to the neck, the signals were continuously confirmed. While three of them showed unclear ECG signals, specifically during the moving phases (Figure 2B), seven of them showed clear ECG signals with almost no noise even during moving phases (Figure 2C). The mean heart rate of ten individuals was 8.6 ± 2.9 beats min^{-1} (n = 2,520) during resting phases and 12.2 ± 4.7 beats min^{-1} (n = 1991) during moving phases. The average water temperature during the experiments was 23.4°C ± 1.1°C (the Sanriku coastal area; 24.3°C ± 0.2°C, Kuroshima Island; 23.3°C ± 1.2°C).

5 Discussion

In green turtles, clear ECG signals could be obtained from a higher percentage of individuals by placing the negative electrode closer to the neck on the plastron. Both the positive and earth electrodes were placed to the lower left as shown in Kinoshita et al. (2022a), whereas the negative electrode should be placed close to the neck. The variations in the quality of the signals within individuals may be due to differences in electrical conductivity among the positions of the plastron for some reasons. For example, the scapula (shoulder blade) is under the humeral scute (Wyneken, 2001), and the bones do not transmit electricity. In addition, the border of the scutes near the neck may allow biopotentials to easily transmit. Therefore, factors such as the position of bone, the thickness of the plastron, and the amount of muscle and fat may affect the electro-conductivity of the body. Necropsy data such as the presence of bones and tissues under various scutes and the composition of plastron will guide the optimal electrode placement for future heart rate measurements in sea turtles. Moreover, body size had no obvious effect on the position of the electrodes and the clarity of the ECG signals among the individuals used in this study. However, the effect of larger body size and growth stage have not been confirmed in green turtles. Further study is needed to determine whether body size affects the percentage of individuals available for heart rate measurements. At that time, it will be effective to adjust the electrode placements using a handheld ECG monitor, as in this study.

In a previous study that measured ECG by inserting electrodes inside the body, the heart rate of juvenile green turtles (*BM*; 19.4 ± 1.5 kg, *SCL*; 53.8 ± 1.4 cm) was reported to be 11.1 ± 0.4 beats min^{-1} during resting dives and 15.0 ± 0.5 beats min^{-1} during active dives (Okuyama et al., 2020). The values in this study are slightly lower than those in the previous study, possibly due to the lower water temperature (this study; 23.4°C ± 1.1°C, Okuyama et al., 2020; 29.0°C ± 0.0°C). Therefore, the heart rate measured in this study was similar to that obtained by inserting electrodes into the body, suggesting that this method allowed us to obtain a highly accurate ECG of green turtles. The amplitude of the ECG signal in this study was approximately one-tenth of the signal obtained using the conventional approach; however considering band-pass filter processing, this amplitude is sufficient to detect R waves.

Our method is minimally stressful for sea turtles and can be applied to monitor the health of captive individuals in aquariums. It

can also be used to measure the heart rate of sea turtles in the field without recapturing them by using an automated tag release system for removing the electrodes and recorders (Saito et al., 2024). This helps us to understand the physiological status of sea turtles under natural conditions. By using our method, ECG of green turtles could be measured stably for at least 4 days. This was the limit of the battery in the recorder, but the electrodes remained attached to the plastron in the water tank for about a week. In the future, ECG might be measured for longer periods by improving the wires and electrodes. The non-invasive ECG measurement method is now applicable to sea turtles, which was previously unavailable. Diving ability, such as dive duration and depth varies among species; therefore, a comparison of heart rates among sea turtle species may reveal the physiological functions underlying differences in diving ability. Heart rate is used as a proxy for indirectly estimating field metabolic rates on a fine time scale (Kinoshita et al., 2022b). In addition, when sea turtles are entangled in fishing nets, their heart rates will increase due to higher activity levels, potentially causing gas emboli and rapid oxygen depletion (Williams et al., 2019). Studying heart rate of sea turtles during diving and various levels of activity can lead to a better understanding of energetics under natural environments and the physiological effects of interrupting natural diving patterns. Such knowledge will be fundamental to assessing the potential impacts of the issues in sea turtles, including bycatch and the modification of coastal marine ecosystems.

This study successfully identified an effective electrode placement for heart rate measurement in green turtles. The negative electrode should be placed closer to the neck, and both the positive and earth electrodes should be placed to the lower left of the plastron. While the ECG signals in some individuals were less distinct or undetectable regardless of placement, the use of a handheld monitor, as demonstrated in this study, offers a practical approach for selecting suitable individuals, especially for turtles with dense keratinous scutes, such as green turtles. Green and hawksbill turtles, which face extinction, primarily use coastal areas after growing up and are closely related to human activities through bycatch and feeding damage. To coexist with sea turtles, it is important not only to understand their ecology but also to closely examine their physiological status such as their heart rate. Our method contributes to a better understanding of the physiological status of free-ranging sea turtles.

Data availability statement

The original contributions presented in the study are included in the article/Supplementary Material, further inquiries can be directed to the corresponding author.

Ethics statement

The animal study was approved by the Animal Ethics Committee of the Atmosphere and Ocean Research Institute at the University of Tokyo and the Marine Fisheries Coordinating Committee of Okinawa Prefecture, Japan. The study was conducted in accordance with the local legislation and institutional requirements.

Author contributions

AS: Conceptualization, Formal Analysis, Investigation, Methodology, Writing–original draft, Writing–review and editing, Funding acquisition. KiS: Conceptualization, Investigation, Methodology, Writing–review and editing. MK: Investigation, Writing–review and editing. LL: Investigation, Writing–review and editing. KK: Supervision, Writing–review and editing. HK: Methodology, Writing–review and editing. KaS: Supervision, Writing–review and editing. KeS: Conceptualization, Supervision, Writing–review and editing, Funding acquisition.

Funding

The author(s) declare that financial support was received for the research, authorship, and/or publication of this article. This work was supported by JST SPRING, Grant Number JPMJSP2108, JSPS KAKENHI Grant Number 20K21362, 22H05648, and 22K21355.

Acknowledgments

We are grateful to all volunteers from the Fisheries Cooperative Association of Funakoshi Bay, Shin-Otsuchi, Sanriku-Yamada, and Yamaichi, who provided us with wild-caught sea turtles in the Sanriku coastal area. We also thank T. Fukuoka, C. Kinoshita, M. Miyayama, R. Murakami, T. Tajima, and Y. Nakanishi who assisted this research. We are grateful to the editor and two reviewers for their constructive comments on the manuscript.

Conflict of interest

The authors declare that the research was conducted in the absence of any commercial or financial relationships that could be construed as a potential conflict of interest.

The handing editor TK declared a shared affiliation with the authors AS, KiS, MK, LL, KaS and KeS at the time of review.

Generative AI statement

The author(s) declare that no Generative AI was used in the creation of this manuscript.

Publisher's note

Supplementary material

The Supplementary Material for this article can be found online at: https://www.frontiersin.org/articles/10.3389/fphys.2024.1511443/full#supplementary-material

References

Álvarez-Varas, R., Rojas-Hernández, N., Heidemeyer, M., Riginos, C., Benítez, H. A., Araya-Donoso, R., et al. (2021). Green, yellow or black? Genetic differentiation and adaptation signatures in a highly migratory marine turtle. *Proc. Biol. Sci.* 288 (1954), 20210754. doi:10.1098/rspb.2021.0754

Broderick, A. C., Coyne, M. S., Fuller, W. J., Glen, F., and Godley, B. J. (2007). Fidelity and over-wintering of sea turtles. *Proc. Natl. Acad. Sci. U. S. A.* 274, 1533–1538. doi:10.1098/rspb.2007.0211

Fukuoka, T., Narazaki, T., and Sato, K. (2015). Summer-restricted migration of green turtles *Chelonia mydas* to a temperate habitat of the northwest Pacific Ocean. *Endanger. Species Res.* 28, 1–10. doi:10.3354/esr00671

Hochscheid, S., Bentivegna, F., Hamza, A., and Hays, G. C. (2010). When surfacers do not dive: multiple significance of extended surface times in marine turtles. *J. Exp. Biol.* 213, 1328–1337. doi:10.1242/jeb.037184

Kameda, K., Wakatsuki, M., Kuroyanagi, K., Iwase, F., Shima, T., Kondo, T., et al. (2017). Change in population structure, growth and mortality rate of juvenile green turtle (*Chelonia mydas*) after the decline of the sea turtle fishery in Yaeyama Islands, Ryukyu Archipelago. *Mar. Biol.* 164 (6), 143. doi:10.1007/s00227-017-3171-4

Kameda, K., Wakatsuki, M., Takase, M., Nakanishi, Y., and Kamezaki, N. (2023). Apparent survival probability and abundance of juvenile green turtles in the foraging ground at Kuroshima Island, Ryukyu Archipelago. *Endanger. Species Res.* 50, 209–215. doi:10.3354/esr01228

Kinoshita, C., Saito, A., Kawai, M., Sato, K., and Sakamoto, K. Q. (2022a). A non-invasive heart rate measurement method is improved by placing the electrodes on the ventral side rather than the dorsal in loggerhead turtles. *Front. Physiol.* 13, 811947–811949. doi:10.3389/fphys.2022.811947

Kinoshita, C., Saito, A., Sakamoto, K. Q., Niizuma, Y., and Sato, K. (2022b). Heart rate as a proxy for estimating oxygen consumption rates in loggerhead turtles (*Caretta caretta*). *Biol. Open* 11, bio058952. doi:10.1242/bio.058952

López-Mendilaharsu, M., Rocha, C. F., Domingo, A., Wallace, B. P., and Miller, P. (2009). Prolonged deep dives by the leatherback turtle *Dermochelys coriacea*: pushing their aerobic dive limits. *Mar. Biodivers. Rec.* 2, e35. doi:10.1017/S1755267208000390

Lutcavage, M. E., Lutz, P. L., and Baier, H. (1987). Gas exchange in the loggerhead sea turtle *Caretta Caretta*. *J. Exp. Biol.* 131, 365–372. doi:10.1242/jeb.131.1.365

Narazaki, T., Sato, K., and Miyazaki, N. (2015). Summer migration to temperate foraging habitats and active winter diving of juvenile loggerhead turtles *Caretta caretta* in the western North Pacific. *Mar. Biol.* 162, 1251–1263. doi:10.1007/s00227-015-2666-0

Okuyama, J., Shiozawa, M., and Shiode, D. (2020). Heart rate and cardiac response to exercise during voluntary dives in captive sea turtles (*Cheloniidae*). *Biol. Open* 9, bio049247. doi:10.1242/bio.049247

Ponganis, P. J. (2015). *Diving physiology of marine mammals and seabirds*. Cambridge, UK: University Press.

Saito, A., Kinoshita, C., Sakai, K., Sato, K., and Sakamoto, K. Q. (2024). Heart rate reduction during voluntary deep diving in free-ranging loggerhead sea turtles. *J. Exp. Biol.* 227, jeb246334. doi:10.1242/jeb.246334

Sakamoto, K. Q., Miyayama, M., Kinoshita, C., Fukuoka, T., Ishihara, T., and Sato, K. (2021). A non-invasive system to measure heart rate in hard-shelled sea turtles: potential for field applications. *Philos. Trans. R. Soc. B Biol. Sci.* 376, 20200222. doi:10.1098/rstb.2020.0222

Sakamoto, K. Q., Sato, K., Ishizuka, M., Watanuki, Y., Takahashi, A., Daunt, F., et al. (2009). Can ethograms be automatically generated using body acceleration data from free-ranging birds? *PLoS ONE* 4, e5379. doi:10.1371/journal.pone.0005379

Seminoff, J. A. (2023). "*Chelonia mydas* (amended version of 2004 assessment)," in The IUCN Red List of Threatened Species *2023: e.T4615A247654386*. doi:10.2305/IUCN.UK.2023-1.RLTS.T4615A247654386.en

Southwood, A. L., Andrews, R. D., Lutcavage, M. E., Paladino, F. V., West, N. H., George, R. H., et al. (1999). Heart rates and diving behavior of leatherback sea turtles in the eastern pacific ocean. *J. Exp. Biol.* 202, 1115–1125. doi:10.1242/jeb.202.9.1115

Southwood, A. L., Darveau, C. A., and Jones, D. R. (2003). Metabolic and cardiovascular adjustments of juvenile green turtles to seasonal changes in temperature and photoperiod. *J. Exp. Biol.* 206 (24), 4521–4531. doi:10.1242/jeb.00689

Williams, C. L., Sato, K., and Ponganis, P. J. (2019). Activity, not submergence, explains diving heart rates of captive loggerhead sea turtles. *J. Exp. Biol.* 222, jeb200824. doi:10.1242/jeb.200824

Wyneken, J. (2001). *The anatomy of sea turtles*. Miami: U.S. Department of Commerce NOAA Technical Memorandum.

frontiers | Frontiers in Physiology

TYPE Original Research
PUBLISHED 31 January 2025
DOI 10.3389/fphys.2025.1462940

OPEN ACCESS

EDITED BY
Martin C. Arostegui,
Woods Hole Oceanographic Institution,
United States

REVIEWED BY
Itsumi Nakamura,
Nagasaki University, Japan
Ken Yoda,
Nagoya University, Japan

*CORRESPONDENCE
Yoshinori Aoki,
aoki_yoshinori04@fra.go.jp

RECEIVED 10 July 2024
ACCEPTED 07 January 2025
PUBLISHED 31 January 2025

CITATION
Aoki Y, Kitagawa T and Kiyofuji H (2025) Surfacing and diving behavior associated with thermal physiology in oceanic habitats of skipjack tuna (*Katsuwonus pelamis*) in the western north Pacific Ocean.
Front. Physiol. 16:1462940.
doi: 10.3389/fphys.2025.1462940

Surfacing and diving behavior associated with thermal physiology in oceanic habitats of skipjack tuna (*Katsuwonus pelamis*) in the western north Pacific Ocean

Yoshinori Aoki[1]*, Takashi Kitagawa[2] and Hidetada Kiyofuji[1]

[1]Fisheries Resources Institute, Japan Fisheries Research and Education Agency, Yokohama, Kanagawa, Japan, [2]Graduate School of Frontier Sciences, The University of Tokyo, Kashiwa, Chiba, Japan

Introduction: Thermal physiology is a pivotal biotic factor for the ecophysiology of commercially valuable tuna, influencing not only horizontal but also vertical behaviors. We aimed to examine how the thermal physiology of skipjack tuna (*Katsuwonus pelamis*, SKJ) can explain the differences in their vertical behavior, focusing on surfacing and diving, among various thermal environments during their northward migration in the western North Pacific.

Methods: We analyzed archival tag data collected during 2012–2015, with individual time series (Fork length: 38–49 cm, N = 38) of swimming depth, water temperature, and peritoneal body temperature during northward migration from subtropical areas to temperate regions around Japan. We quantified surfacing and diving behavior as an index of vertical behavior and estimated the whole-body heat transfer coefficient (λ) during the cooling and warming phases associated with diving using body and water temperature records as indicators of thermal physiology.

Results: In the southern mixed layer areas, SKJ were widely distributed at a depth layer <200 m, whereas they were restricted to the surface in the strong thermocline areas in the north. The dive duration was significantly shortened with a strong thermal gradient during northward migration. We observed minor to no differences in λ values between the cooling and warming phases in the southern areas, whereas the λ values in temperate areas differed by a factor of 2–3 between the phases.

Discussion: Our findings of changes in λ values between the cooling and warming phases represent the first evidence of thermoregulation in SKJ. Surfacing preference behavior and short dive duration in temperate areas may be an avoidance of prolonged exposure to cold temperatures, a behavior commonly exhibited in other tuna. Moreover, we discussed how the changes in vertical behavior driven by thermal physiology can explain spatial heterogeneity in SKJ fishery grounds in the western Pacific Ocean.

KEYWORDS

skipjack tuna, vertical behavior, archival tag, migration, thermal physiology, thermoregulation

1 Introduction

A core challenge in the ecophysiology of commercially valuable tuna is predicting how species respond to environmental changes, such as global warming, which is essential for interpreting their distribution, population dynamics, fishing strategies, and effective management (Lehodey et al., 2013; Dueri et al., 2014; Bernal et al., 2017; Bell et al., 2021). In particular, the vertical behavior of tuna is crucial for fishing activities, particularly regarding the overlap in depths and time between target species and gear settings by humans (Post et al., 2008; Lennox et al., 2017; Wright et al., 2021; Matsubara et al., 2024). Surface-oriented behavior renders tuna more vulnerable to surface fisheries than the behavior that keeps them at deep depth for a long time (Matsubara et al., 2024). Therefore, changes in vertical behavior across areas can be a good indicator to explain the spatial heterogeneity of fishery grounds (Forget et al., 2015; Scutt Phillips et al., 2017).

In 2022, Skipjack tuna (*Katsuwonus pelamis*, SKJ) was the third most exploited fish species globally (2.8 million tons), for the 11th consecutive year (FAO, 2022). SKJ catch in the Western and Central Pacific Ocean (WCPO) is predominantly exploited by purse seine (84% of 1,735,500 mt for 2022) and pole-and-line fisheries (8%), along with various "artisanal" gears (8%, Williams, 2023). These fisheries have been mainly operated in tropical and temperate areas (Williams, 2023) and rarely operated in subtropical areas, despite SKJ being widely distributed from tropical to temperate areas (Matsumoto et al., 1984; Wild and Hampton, 1994). Beyond fishery-dependent information, advancements in biologging technologies have improved the study of SKJ migration ecology in the WCPO (Aoki et al., 2017; Kiyofuji et al., 2019). SKJ exhibit long-distance north-southward migration, moving from subtropical areas to foraging temperate foraging grounds off Japan. Throughout the northward migration, the vertical distribution becomes shallower as latitude increases, likely due to the avoidance of lower temperatures (Kiyofuji et al., 2019). These field observations can explain the spatial gap in fishery grounds by improving our knowledge of the depths at which SKJ is distributed during migration. However, we still lack a clear understanding of how and why their depth changes. To address this gap, behavioral differences among thermal habitats should be evaluated in conjunction with the underlying physiological mechanisms.

Inferring thermal physiology is a key field for addressing the underlying reasons behind tuna behavior, as their unexceptionally elevated body temperature has ecological advantages in the expansion of thermal niches (Brill, 1994; Bernal et al., 2017). A key feature contributing to the ability to elevate body temperature above that of ambient water is the axial positioning of the locomotor red muscle, which reduces conductive heat loss to the environment at the body surface (Dickson, 1996; Graham and Dickson, 2000; Korsmeyer and Dewar, 2001). Furthermore, heat generated in the red muscle is effectively conserved by a complex vascular network of counter-current heat exchangers (retia mirabilia), which play a role in minimizing convective heat loss to the gills (Carey and Teal, 1966; Brill, 1994). Owing to their unique anatomy, body temperature during dives can be maintained relatively stable in tuna, a phenomenon known as short-term thermoregulation (Holland et al., 1992; Aoki et al., 2020; Hino et al., 2021). For example, Bigeye tuna (*Thunnus obesus*) inhabiting cool water below the thermocline quickly ascend to warmer surface water to rapidly absorb heat via conduction, as their body temperature approaches the ambient temperature (Holland et al., 1992; Boye et al., 2009; Hino et al., 2021). Subsequently, they immediately descend back below the thermocline while suppressing the decrease in their body temperature. This remarkable thermoregulation is a result of the physiological modulation of thermal conductance during the cooling and warming phases associated with their vertical movements (Evans et al., 2008; Holland et al., 1992; Malte et al., 2007). The degree of physiological modulation, often expressed as the whole-body heat transfer coefficient (λ), exhibits variability across tuna species (Aoki et al., 2020; Kitagawa et al., 2006; Kitagawa et al., 2022). Regarding thermoregulation in SKJ, only laboratory experiments have compared the differences in the λ values between the warming and cooling phases, leading to the conclusion that they do not thermoregulate during the short term (Neill et al., 1976; Don and Neill William, 1979). These studies have mostly focused on the range of the thermal tolerance of SKJ; however, SKJ often dive beyond the thermocline and reach environments outside the critical temperature limits in the wild (Kiyofuji et al., 2019). In addition to physiological thermoregulation, further exploration of the behavioral aspect is required, as the free-ranging environment is completely different from controlled experiments (Brill, 1994). While laboratory studies have established a solid understanding of thermoregulation in SKJ, relatively few studies have comprehensively compared the thermoregulation of SKJ in terms of both behavioral and physiological aspects across their broad thermal range in the wild.

Physio-logging in free-ranging animals is a promising tool for accumulating long-term data, leading to a better understanding of their thermal physiological traits and responses to the natural environment (Fahlman et al., 2021). Accumulation of SKJ biologging data, including records of internal body temperature from previous studies (Aoki et al., 2017; Kiyofuji et al., 2019), allows us to extract new knowledge of their thermal physiology. Moreover, the distinct thermal habitats they encounter during migration (Aoki et al., 2017) enable us to identify specific thermal physiological traits for each thermal habitat. Building on previous tagging and recapture studies by our group, our study focuses on how the thermal physiology of SKJ explains the differences in its vertical behavior, particularly surfacing and diving, across various thermal environments during their northward migration. First, we classified thermal habitats using temperature and swimming depth records in a cluster analysis with newly added tagging data from a previous study (Aoki et al., 2017). Subsequently, we quantified the surfacing and diving behaviors in each thermal habitat, estimated the λ in the cooling and warming phases, and compared the values among thermal habitats to assess whether short-term thermoregulation occurred. Finally, we discussed how SKJ behavior addresses the spatial gap between migration ecology and fisheries in subtropical areas from the viewpoint of thermal physiology.

2 Materials and methods

2.1 Tagging procedure

Our tagging research is a part of a comprehensive tagging project described in previous studies (Aoki et al., 2017; Kiyofuji et al., 2019) and briefly mentioned herein. SKJ were captured by pole-and-line vessels at subtropical areas (20–24 N, 136–141°E) and off the Boso

10.3389/fphys.2025.1462940

TABLE 1 Recaptured tags used for the analysis.

Tag ID	Release				Recapture			
	FL cm	Date	Lat. (°N)	Lon. (°E)	FL (cm)	Date	Lat. (°N)	Lon. (°E)
411	42.5	08 February, 2012	23.40	129.67	Na	15 May 2012	30.41	130.24
476	42.0	15 February, 2012	20.40	136.20	44.0	21 May 2012	35.00	140.23
532	43.0	08 February, 2012	26.65	140.92	46.0	06 April, 2012	24.00	140.00
602	45.0	08 February, 2012	26.65	140.93	46.0	07 May 2012	31.55	139.83
1222	40.0	09 February, 2013	23.18	138.02	43.5	28 April, 2013	30.57	131.23
1316	40.0	16 March, 2013	20.40	136.18	45.0	31 May 2013	34.00	138.83
1328	39.0	10 March, 2013	24.85	141.13	46.0	07 June, 2013	33.33	139.67
1348	40.0	10 March, 2013	24.77	141.18	44.3	07 June, 2013	32.50	144.00
1359	38.0	10 March, 2013	24.85	141.13	44.3	08 June, 2013	33.38	139.22
1883	46.5	27 June, 2013	35.05	141.62	47.0	18 July, 2013	38.50	145.50
1886	48.0	17 June, 2013	34.93	143.93	51.5	07 August, 2013	37.00	147.00
1894	48.0	27 June, 2013	35.05	141.62	48.4	24 July, 2013	38.00	145.00
1897	48.0	01 July, 2013	35.52	145.35	48.0	14 July, 2013	38.72	147.75
1932	49.0	10 July, 2013	36.95	144.33	54.9	11 September, 2013	38.00	148.83
1950	46.0	11 July, 2013	36.18	142.15	47.0	27 August, 2013	40.00	145.00
1974	48.0	01 July, 2013	35.52	145.35	51.3	26 July, 2013	38.88	146.80
2410	47.0	14 March, 2014	20.43	136.02	47.1	6 April, 2014	20.33	136.08
2536	44.0	14 March, 2014	20.43	136.02	42.5	6 April, 2014	20.33	136.08
2601	45.0	28 May 2014	30.73	141.33	Na	01 August, 2014	37.33	147.00
2605	45.0	28 May 2014	30.73	141.33	48.0	25 June, 2014	36.00	148.50
2607	45.0	28 May 2014	30.73	141.33	48.0	16 June, 2014	34.67	144.50
2608	44.0	28 May 2014	30.73	141.33	45.0	21 June, 2014	38.30	141.50
2620	46.0	28 May 2014	30.73	141.33	46.4	24 June, 2014	35.50	147.50
2673	45.0	2 June, 2014	31.58	144.22	Na	25 June, 2014	35.67	147.83
2680	44.0	2 June, 2014	31.58	144.22	49.5	31 July, 2014	33.07	142.95
2746	44.0	2 June, 2014	31.63	143.98	44.2	27 June, 2014	35.03	150.05
2810	46.0	2 June, 2014	31.63	143.98	50.5	30 July, 2014	33.00	142.00
2822	45.0	11 June, 2014	34.33	148.40	Na	02 July, 2014	35.00	151.00
2832	43.0	2 June, 2014	31.59	144.22	46.0	20 July, 2014	34.65	145.87
3136	41.0	10 March, 2015	23.75	141.72	42.1	23 March, 2015	23.63	141.78
3164	39.0	10 March, 2015	23.75	141.72	42.0	20 April, 2015	22.00	140.00
3174	40.0	10 March, 2015	23.75	141.72	42.3	31 March, 2015	23.85	142.83
3230	38.0	12 March, 2015	23.48	141.95	Na	13 April, 2015	23.50	141.93
3417	41.0	10 March, 2015	23.75	141.72	Na	13 April, 2015	23.50	141.93
3690	43.0	21 May 2015	33.60	143.25	48.0	11 June, 2015	36.00	145.00
3735	46.0	2 June, 2015	33.12	149.05	48.0	11 July, 2015	37.00	145.00
3964	49.0	10 June, 2015	37.33	143.40	47.9	16 June, 2015	37.47	144.08
3969	48.0	10 June, 2015	37.33	143.40	52.4	21 June, 2015	38.00	143.52

areas (30–40°N, 141–145 E) during February to March 2012–2015 and May to July 2013–2015, respectively. SKJ individuals with a fork length (FL) of 38–49 cm were selected for investigating the north migration process and were tagged on board with archival tags surgically inserted into the peritoneal cavity. Overall, 1251 tagged individuals were released. The electric tag type, LAT2910 (Length, 26 mm; diameter, 7.8 mm; Lotek Wireless Inc., Newfoundland, Canada), was used in this study, as it has previously been successful in recording behavioral data for SKJ with minimal effects from tag attachments (Kiyofuji et al., 2019). The stalk of the thin, flexible sensor records light intensity and external temperature. The main body, embedded in the peritoneal cavity, also has a sensor for recording internal temperature and pressure. These data are recorded at 30-s intervals, and the tag can continue recording for at least 1 year using an embedded battery. To date, 76 individuals were recaptured, and data were retrieved from 38 of them (Table 1). The others were not used for analysis because of technical issues (e.g., short recapture within 1 day of release or tag deterioration). Daily geolocation estimates based on light intensity for all the recovered tags have been already published in the study by Kiyofuji et al. (2019), and we referred to the literature for the corresponding geolocations.

2.2 Thermal habitat classification

Spatial and temporal changes due to migration make the comparison of behavior and thermal physiologies in the same thermal habitat difficult. To address this, temperature profiles collected with electronic tags were used in a clustering analysis to characterize SKJ thermal habitats. The habitats utilized by SKJ during their northward migration were referenced from a previously reported study (Aoki et al., 2017), with some updates based on the addition of newly recovered tags. Thermal habitats were classified into six clusters using daily thermal profiles, calculated from pairs of swimming depth and ambient temperature records (Figure 1). The daily thermal profile was reproduced using the following procedures. The ambient temperature recorded each day was divided into the following bins based on the swimming depth: (i) 5-m depth (0–10 m), (ii) 10-m depth (10–100 m), and (iii) 25-m depth (100–200 m). As the surfacing behavior of SKJ made data collection at deeper depths difficult, the depth bins were set wider at greater depths. All temperature data within each depth bin was averaged as a representative temperature at the depth, and the average temperatures from 0 to 200 m were combined to reproduce the daily thermal profile. Missing values at each depth were replaced by the environmental data of World Ocean Atlas 13 (0.25° grid). Profiles in coastal areas for which there were no environmental data were removed due to the incomplete data set. Profiles collected on release and recapture days were also removed, as the data length for these days differed from other days at liberty. The complete set of daily thermal profiles was grouped using a hierarchical agglomerative clustering algorithm, which was implemented on a dissimilarity matrix calculated from Euclidean distances using Ward's linkage method. This method was selected because it successfully produces compact groups in highly migrated species (Bestley et al., 2009; Aoki et al., 2017). In this study, we allocated the thermal habitats for the newly added data based on the six known thermal habitats (Aoki et al., 2017), indicating that our update focused on the reallocation of the thermal habitats to the newly added data.

2.3 Vertical behavior in each thermal habitat

A daily surfacing rate is a useful indicator for evaluating the encounter rate between fish and fisheries, particularly as SKJ are vulnerable to surface fishery. To understand the basic features of the surfacing rate in each thermal habitat, a daily surfacing rate during the daytime was examined by assessing the proportion of time spent at the surface (≤10 m). The effect of thermal habitats on the daily surfacing rate was examined via the generalized linear mixed effect model (GLMM) using a binomial distribution with a logit link function in the "glmer" function of the "lme4" package in R software (R Foundation, Vienna, Austria). The purpose of this analysis is to evaluate the effect of thermal habitat on the daily surfacing rate. We modeled the daily surfacing rate as a response variable and the thermal habitat effect (HAB) as a fixed effect of the explanatory variable. The probability (π) of SKG being distributed at depths shallower than 10 m was calculated from the number of data on the surface (Surface) and the number of data during the day (Total), expressed using the following Equation 1:

$$\mathrm{Surface}_{ij} = \mathrm{Bin}\left(\pi_{ij,}, \mathrm{Total}_{\mathrm{ij}}\right) \quad (1)$$

$$logit\left(\pi_{ij}\right) = \beta_k \times HAB_k + z_i + \varepsilon_{ij}, z_i \sim N\left(0, \sigma^2_{TAGID}\right)$$

where $Surface_{ij}$ represents the number of data in the surface (≤10 m) during daytime for observation j in each fish i and β_k represents the effect of HAB_k (k = 1, 2, 3, … 6). As observations were repeated measures collected from the same individuals, we incorporated individual fish as random intercept effect (z_i), assuming them to be normally distributed with mean 0 and variance σ^2_{TAGID}. In the binomial distribution, the variance is automatically determined when the mean is determined, resulting in overdispersion, where the variance of the observed data is larger than the expected one. Therefore, we applied two models for the error structure: (1) a model that only considers the individual effect, and (2) an observation level model that includes both individual effect and the error ε_{ij} at each observation. The choice of the best model was determined based on the Akaike Information Criteria (AIC). In addition, we used the dispersion statistic to assess overdispersion by calculating the sum of squared Pearson residual divided by the number of observations, minus the number of parameters. We then confirmed that the overdispersion was less than 1 (Zuur et al., 2013). We finally selected the observation level model as it exhibited a lower AIC (18156) than the model that considers only individual effects (450111). Dispersion static (0.06) did not indicate overdispersion (Zuur et al., 2013).

2.4 Effect of diving behavior on body temperature

Thermal differences between body and water temperature during dives provide a simple way to assess the effect of diving

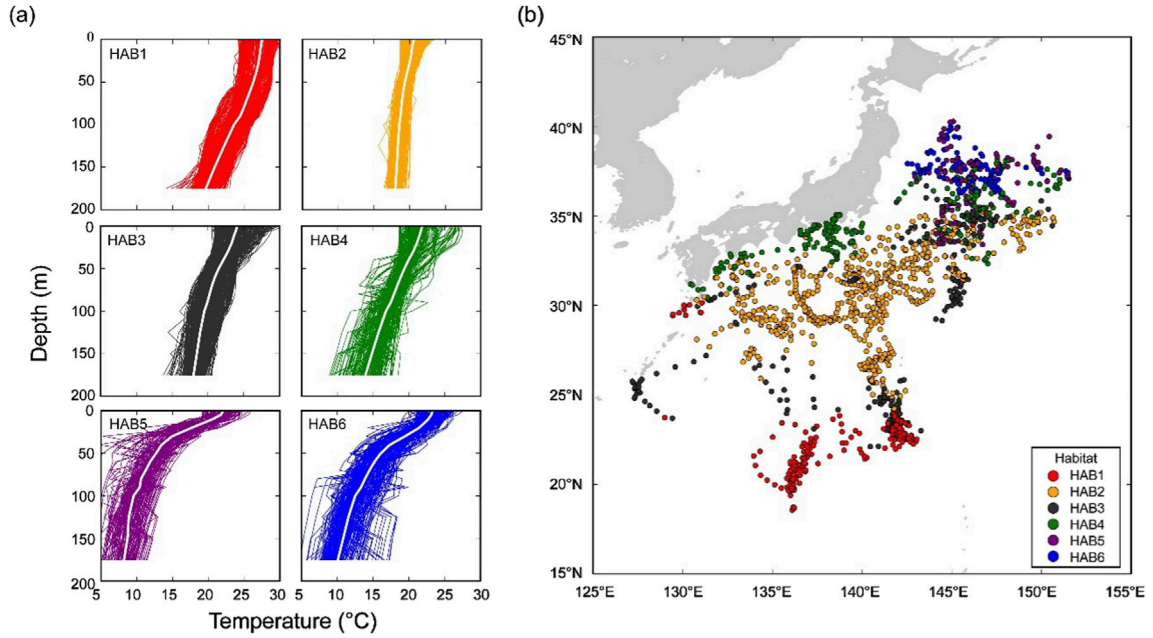

FIGURE 1
Thermal habitat (HAB) classification based on daily thermal profiles (0–200 m). **(A)** Vertical thermal profiles of the identified six habitats. The average temperature-at-depth of the profile is represented by a white line in each thermal habitat. **(B)** Daily geolocations of 38 individuals classified based on the thermal habitats. Each color represents habitat (HAB−-6) grouped by cluster analysis based on thermal profiles. Note that this figure was updated from the original figure in Aoki et al. (2017).

behavior on body temperature (Kitagawa et al., 2007). We examined the thermal difference during dives by averaging the thermal difference and water temperature during dives. Each dive event was extracted from the recorded swimming depth data as follows: The beginning of the dive was defined as the last point where SKJ descended to the depth (>10 m), and the end of the dive was defined as the first point where SKJ ascended back to the depth (<10 m). Data from depths shallower than 100 m during the dive were not used in this analysis, as the purpose of this analysis was to examine the effects of temperature changes during the dive on body temperature, which requires data outside their typical vertical range (Average swimming depth is 99 m; Kiyofuji et al., 2019).

Dive duration is another important variable for surface fisheries because it provides an estimate of the time it takes for SKJ to reappear at the surface after a dive. The particular concern here is how the dive duration changes in association with the thermal gradient in each thermal habitat. Dive duration was calculated as the time elapsed from the beginning to the end of the dive, and the thermal gradient between 0–10 m and 90–100 m was used as an indicator of the thermocline. As the dive duration exhibits a non-linear relationship with the thermal gradient, we applied generalized additive mixed effects models (GAMMs) with normal distribution in the "mgcv" package of R software to evaluate the effect of thermal gradient (*Grad*) on dive durations (*Dive*). We incorporated the thermal gradient as an explanatory variable (fixed effect) and dive duration as the response variable, as presented in the Equation 2 below for each observation j in each fish i.

$$\mathrm{Dive}_{ij} \sim N\left(\mu_{ij}, \sigma^2\right) \tag{2}$$

$$\mu_{ij} = \beta_1 + f\left(\mathrm{Grad}_{ij}\right) + a_i, a_i \sim N\left(0, \sigma^2_{\mathrm{TAGID}}\right)$$

where β_1 is the intercept, and f is the smoothing function of the thermal gradient. Individual effect a_i was incorporated as a random effect, assuming it to follow a normal distribution with mean 0 and variance $\sigma^2_{\mathrm{TAGID}}$. To account for errors in different thermal habitats, the variance in the equation was set to (1) σ2 when constant, and to (2) σ^2_k when the variance changed among thermal habitats (k = 1, 2, … 6). Using AIC and likelihood ratio tests (Table 2), we finally identified the model that accounts for errors in different thermal habitats.

2.5 Thermal physiology

The whole-body heat transfer coefficient (λ) during the cooling and warming phases associated with dives was compared to investigate whether SKJ can thermoregulate during their dive. The coefficient was estimated from the recorded body (T_b) and water (T_a) temperatures using the heat budget model as follows (Holland et al., 1992; Aoki et al., 2017; 2020):

$$\frac{dT_b}{\mathrm{dt}} = \lambda\left(T_a - T_b\right) + \dot{T}_m \tag{3}$$

This model describes that T_b changes depend on T_a, λ, and heat production due to metabolism ($\dot{T}_m$). The magnitude of λ and $\dot{T}_m$ were estimated from the T_b curve during the warming and cooling phases (Aoki et al., 2017) using the method of non-linear least squares optimization. These phases used in the regression were extracted by analyzing whether the differences in the temperature

TABLE 2 Comparisons between two models [one with constant variance σ^2 and the other with variable variance σ_k^2, (k = 1, 2···6)].

Model variance	df	AIC	BIC	logLik	Likelihood ratio	*p*-value
Constant	5	86,915	86,950	−43453	—	714
Variable	10	85,458	85,527	−42719	1,468	<0.0001

data ($T_{b\ t+1}$- T_{bt}) were positive or negative. Consecutive positive and negative data points that last for more than 10 min were selected as warming and cooling curves, respectively. To remove noisy data, T_b changes <1.0°C were excluded from this analysis.

The purpose of this analysis was to evaluate the differences in estimated λ between two the warming and cooling phases, providing evidence for physiological thermoregulation (Holland et al., 1992; Aoki et al., 2020; Hino et al., 2021). As the λ is a positive value, a GLMM with log-normal distribution was applied as follows Equation 4:

$$\lambda_{ij} \sim N\left(\log\left(\mu_{ij}\right), \sigma^2\right) \tag{4}$$
$$\log\left(\mu_{ij}\right) = \text{Phase}_{ij} + a_i,\ a_i \sim N\left(0, \sigma^2_{TAGID}\right)$$

where λ_{ij} represents the λ of individual i at observation j. Two phases of warming and cooling were incorporated as the fixed effect of categorical value ($Phase_{ij}$), and the individual effect was expressed as a_i, assuming it to follow the normal distribution with mean 0 and variance σ^2_{TAGID}. AIC in models with/without the $Phase_{ij}$ was compared to evaluate the effect of the two phases in each HAB.

Estimated λ and $\dot{T}_m$ in each HAB were used to simulate dive durations required for T_b to reach the critical temperature of 18°C (Barkley et al., 1978; Kiyofuji et al., 2019), when SKJ descend from the surface to a depth of 200 m in each HAB. In this simulation, the following equation, based on Equation 3, was used.

$$\frac{T_b(t+\Delta t) - T_b(t)}{\Delta t} = \lambda\left(T_a(t) - T_b(t)\right) + \dot{T}_m \tag{5}$$

The median value of λ and $\dot{T}_m$ in the cooling phase, T_a at 200 m, and T_b in each HAB (Table 3) were incorporated into Equation 5. As the λ and $\dot{T}_m$ can vary depending on the specific temperature range reached during the cooling phase, we adopted the median λ values to estimate the most frequently utilized thermal ranges for each thermal habitat as a representative value of these parameters. T_b was simulated in every interval (Δt) until 200 min. The simulated dive durations were compared with observed dive durations calculated in Section 2.4. (Effect of diving behavior on the body temperature). Note that while the simulated durations considered only the cooling phase, the actual dive durations included both the cooling and warming phases associated with dives.

3 Results

3.1 Thermal habitat classification

The daily geolocations of classified thermal habitats (N = 1385), based on the thermal profile with the updated data, covered the area of the Pacific region around Japan and captured the ocean currents (Figure 1). Overall geographical trends for the updated thermal habitats did not differ from those reported in the study by Aoki et al. (2017). However, our study provided more data for the area around the Boso region (30–35°N, 140–145°E), where spatial coverage was low in the original study, thereby strengthening the robustness of the classification. Looking more specifically at each thermal habitat, HAB1 (N = 213), mainly distributed south of latitude 25°N, had a warm surface temperature (SST: 25.0°C ± 0.8°C) with an isothermal layer extending from 0 to 50 m. Below a depth of 50 m, the temperature gradually decreased with increasing depth. HAB2 (N = 598) was widely spread out from 25°N to 30°N and had the lowest SST (20.5°C ± 1.0°C), with a mixed layer extending from 0 to 150 m. HAB3 (N = 244) was mostly found around the edge of HAB2, and its thermal profile exhibited a gradual decline from 0 to 150 m. Habitat 4 (N = 181) was distributed in coastal areas of the main island, Japan, and appeared close to the areas around HAB5 and 6. Further, the average temperature within depths ranging from 175 to 200 m was 13.8°C, which closely resembled the features of the Kuroshio, where the temperature at a depth of 200 m is 15°C (Stommel and Yoshida, 1972). HAB5 (N = 80) and 6 (N = 69) were found between 35°N and 40°N. Both habitats had strong thermocline, but the difference between the two thermal habitats was that the temperature at depths of 175–200 m in HAB6 was slightly colder than that in Habitat 5.

3.2 Characteristics of vertical distribution in each thermal habitat

A weekly time series of vertical movements in each thermal habitat is presented in Figure 2 as a representative example. Tag ID 476 at HAB1 showed clear diurnal migration, with a daily average depth of 97–152 m deeper than that at night (50–96 m). Tag (1328 HAB2) also exhibited diurnal migration as in HAB1, and widely spread within the mixed layer (i.e., daily average depth: 17–131 m). The daily average depth of Tag ID 411 at HAB3 was 30–74 m, and the individual spent the daytime within the mixed layer. Tag (1316) at HAB4 showed a shallower distribution (daily average, 10–20 m) than the depths reached by HAB1–3, and the individual frequently dove around 79–179 m. It should be noted that the individual reached a depth of 286 m and experienced a water temperature of 8.3°C on 18 May 2013. Tag (1932 HAB5) exhibited a shallow daily average depth of 7–16 m, with a daily average water temperature of 24°C. Further, dive behavior beyond 100 m was frequently observed during daytime, and the individual experienced water temperatures as cool as 8°C. Tag (1950 HAB6) was distributed at a depth of 2–18 m on a daily average, and the individual experienced surface temperatures of 19°C–24°C.

In total, SKJ distributions in HAB1–3 were mainly restricted to the thick mixed layer from 0 to 200 m (Figures 1, 2), and they did not experience drastic temperature changes during their dives. The

10.3389/fphys.2025.1462940

TABLE 3 Parameters used for the dive simulation.

	HAB1	HAB2	HAB3	HAB4	HAB5	HAB6
Body temp. (°C)	24.51	20.58	22.18	22.14	24.2	23.49
Whole-body heat transfer coefficient λ ($10^{-3}s^{-1}$)	0.52	0.62	0.57	0.40	0.31	0.48
Metabolic heat production $\dot{T}_m$ (10^{-3}°C·s^{-1})	1.39	0.70	1.00	0.77	1.29	1.40
Temp. 200 m (°C)	19.21	18.16	18.36	13.75	9.28	6.52
Observed duration (min)	47.0	61.1	45.2	34.2	15.1	5.2
Estimated duration (min)	—	—	—	42.6	46.2	17.2

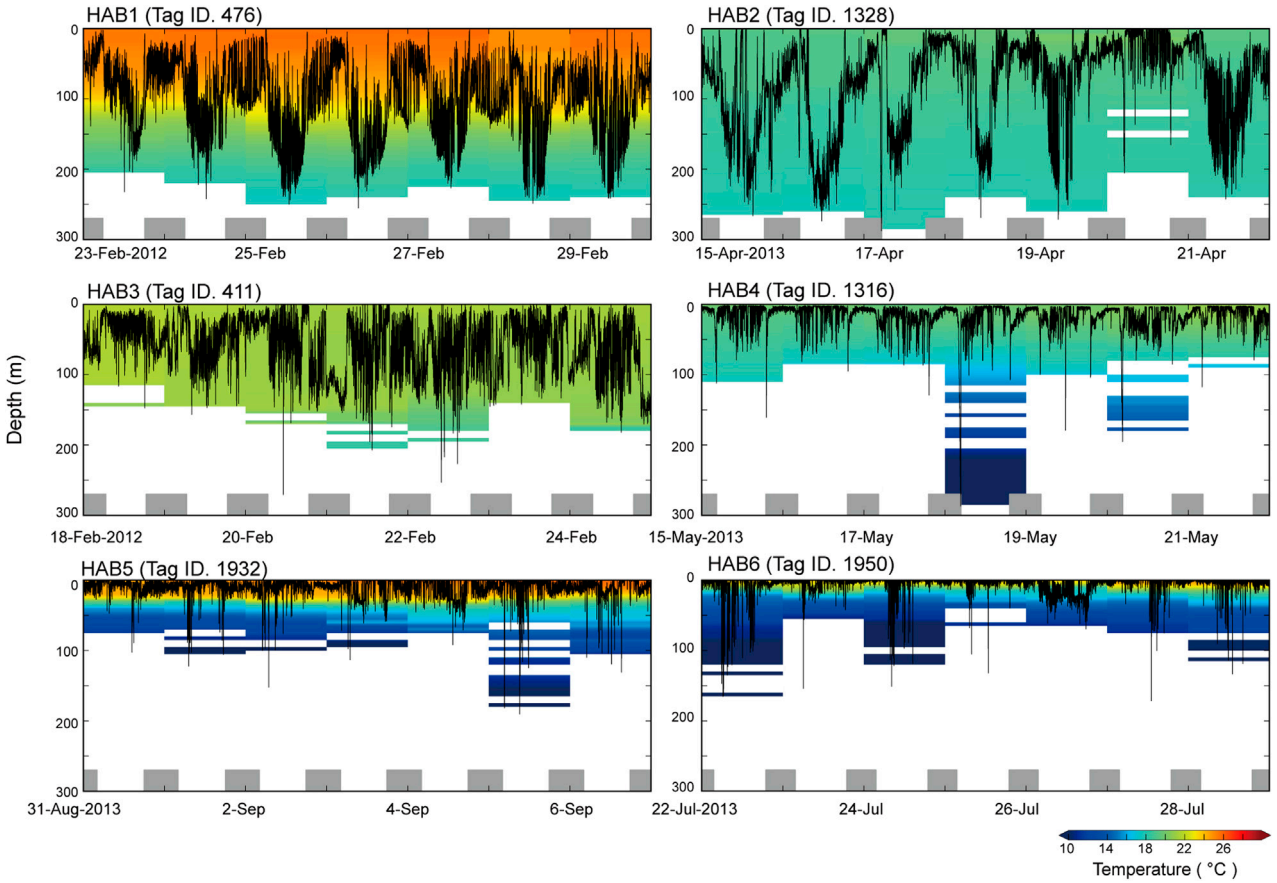

FIGURE 2
Examples (Tag ID 476, 1328, 411, 1316, 1932, 1950) of weekly time series showing vertical movements and daily ambient temperature profiles in thermal habitat (HAB) 1–6. The profiles were calculated from the time series for swimming depth and ambient temperature collected every 30 s. Bottom gray bars represent the night periods.

temperature differences experienced during these dives were not large in HAB1–3. Contrastingly, SKJ in HAB4–6 spent most of their time on the surface, with occasional vertical dives to depths deeper than 100 m during the day. A remarkable change in ambient temperature was noted owing to strong stratification. These distribution trends are also reflected in the significant differences in the probability of being at the surface (>10 m) among thermal habitats (Figure 3; Table 4). Specifically, the lowest average probability was found in the southern area of HAB1 (20%), whereas the highest probability was noted in the northern area of HAB6 (90%).

3.3 Effect of diving behavior on body temperature

The average water temperature and the thermal difference between body and water temperature during dives are presented

10.3389/fphys.2025.1462940

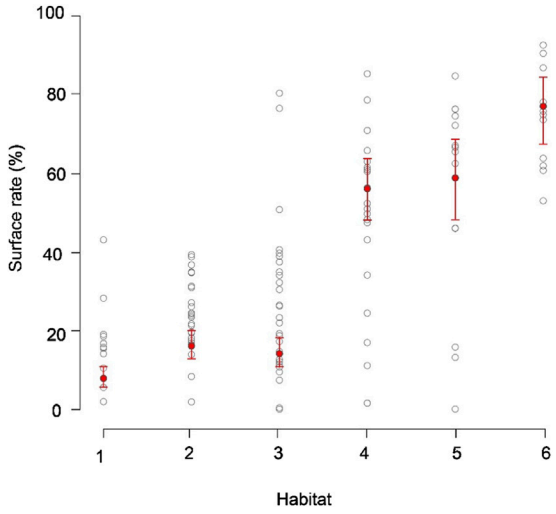

FIGURE 3
Probability of staying on the surface throughout the thermal habitats (HAB1–6). Circles show the average rate of staying on the sea surface (0–10 m) in the daytime of each individual and habitat. Note that daily surface rates were used in the statistical model, but the averages per individual and per thermal habitat are shown for visualization of the results. Red circles and bars indicate the estimated fixed effect and its 95% confidence intervals, respectively. The intervals were calculated by the fitted values plus or minus 1.96 × standard errors.

in Figure 4. The overall body temperature ranged from 17.1°C to 28°C, and the thermal differences were more pronounced in the northern areas of HAB4–6 (0°C–15°C) compared to those in the southern areas of HAB1–3 (0°C–7°C). The minimum temperature during the dive was 6.2°C in HAB6.

The dive duration significantly shortened with a strong thermal gradient (Figure 5; $f(\text{Difference}_{ij}) = 4.024$, F value; 70.35, $p < 0.001$). The average dive durations in HABs with weak thermal gradients (HAB1–3) were 47.0, 61.1, and 45.2 min, respectively. In contrast, the durations in strong thermocline areas (HAB4–6) were 34.2, 15.1, and 5.2 min, respectively.

The frequency distribution of the estimated median value of λ during the descent and ascent phases in each thermal habitat and the AIC values for models with phase effect (M1) and without the effect (M2) are presented in Figure 6 and Table 5, respectively. AIC for M1 showed lower values than those for M2, except in HAB2, and the phase effect was significant (t-static, $p < 0.01$). The estimated median λ in the descent phase was higher than that in the ascent phase (Table 5). The λ difference between the phases in HAB1 and 3 are 1.38 and 1.47, respectively, whereas the difference in HAB4–6 was 1.9–2.9. Focusing solely on the difference in λ among HABs, there was a tendency for a slight decrease in λ along with movements from low-latitude areas (HAB 1) to mid-latitude areas (HAB5–6). Calculating the reciprocal of the heat time constant ($1/\lambda$) provided a more intuitive understanding of the efficacy of their thermal physiology. This constant quantifies the degree of responsiveness to temperature changes and denotes the time required for the body temperature to change to 1/e (approximately 63.2%) of a specific temperature. The thermal constant time in HABs, calculated from λ, was 32, 27, 29, 42, 54, and 35 min for HAB1–6, respectively.

In addition to this intuitive interpretation, we performed a more practical simulation for body cooling time specific to each thermal habitat. We calculated the time required for the body temperature to be cooled to 18°C when an SKJ individual dives to a depth of 200 m. The simulated dive time in HAB4–6 was 4, 46, and 17, respectively, which was longer than the actual observed dive durations (Figure 7; Table 3). In HAB1–3, the body temperature was not cooled to a critical temperature limit of 18°C, as the water depth at 18°C was deeper than 200 m.

4 Discussion

In the present study, we applied a physio-logging technique to estimate the thermal physiology parameter of λ during the cooling and warming phases associated with diving, based on body temperature records. Our findings provide evidence of thermoregulation in wild SKJ, showing several patterns in the differences in λ values between phases, largely attributable to their surrounding thermal profiles. Our findings on the thermoregulation in SKJ are not surprising, as this species is known as regional endothermy fish, possessing anatomically unique rete mirabilia, a feature commonly found in other tuna species (Carey and Teal, 1966; Brill, 1994). However, the new finding of changes in λ, which has not been reported in previous laboratory experiments (Neill et al., 1976; Stevens and Neill, 1979), further expands the interpretation of their thermoregulation ability specific in free-ranging environments. Identifying thermal physiology in the wild also provides mechanistic insights into why their surfacing

TABLE 4 Result of estimated thermal habitat effect for surface model.

Habitat effect	Estimated β_k	Std. error	z-value	Pr (>|z|)
HAB1	−2.442	0.174	−14.002	<2e-16
HAB2	0.808	0.167	4.837	1.32E-06
HAB3	0.594	0.174	3.423	<0.000619
HAB4	2.755	0.192	14.345	<2e-16
HAB5	2.861	0.252	11.353	<2e-16
HAB6	3.788	0.314	12.055	<2e-16

Z-values are obtained by dividing the estimated regression parameters using the standard errors, and the probability of absolute z-value is calculated by using the Z distribution.

10.3389/fphys.2025.1462940

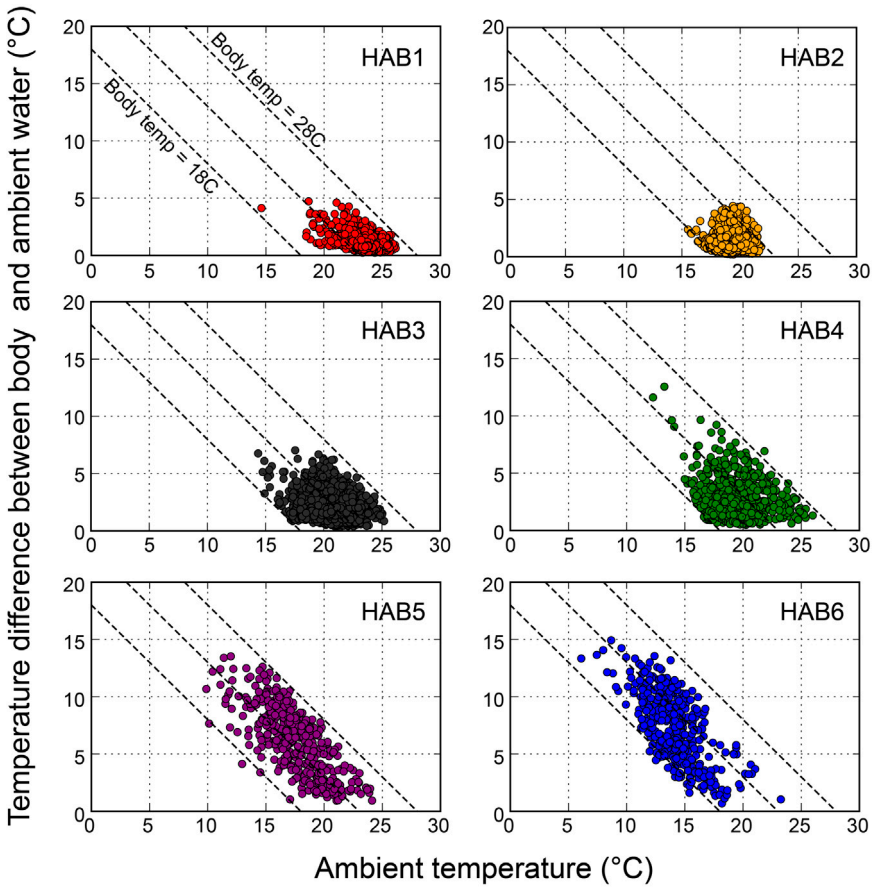

FIGURE 4
Relationships between the ambient temperature and the temperature difference between body (peritoneal cavity) and ambient during dives in habitats (HAB1–6), shown as average temperature values during one dive. Three dashed lines represent body temperatures of 18, 23, and 28°C, respectively.

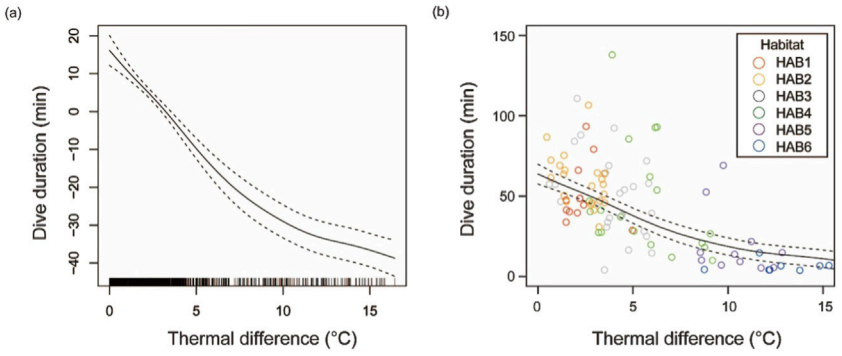

FIGURE 5
Dive durations of skipjack tuna from the surface to a depth beyond 100 m depth according to the strength of the thermal gradient (temperature difference between 0–10 m and 90–100 m layers). **(A)** Smooth function and **(B)** Dive duration (min) vs. thermal difference (°C) estimated using the generalized additive mixed modeling (GAMM). Solid and dashed lines show the fixed effect of the thermal gradient and its 95% confidence interval.

10.3389/fphys.2025.1462940

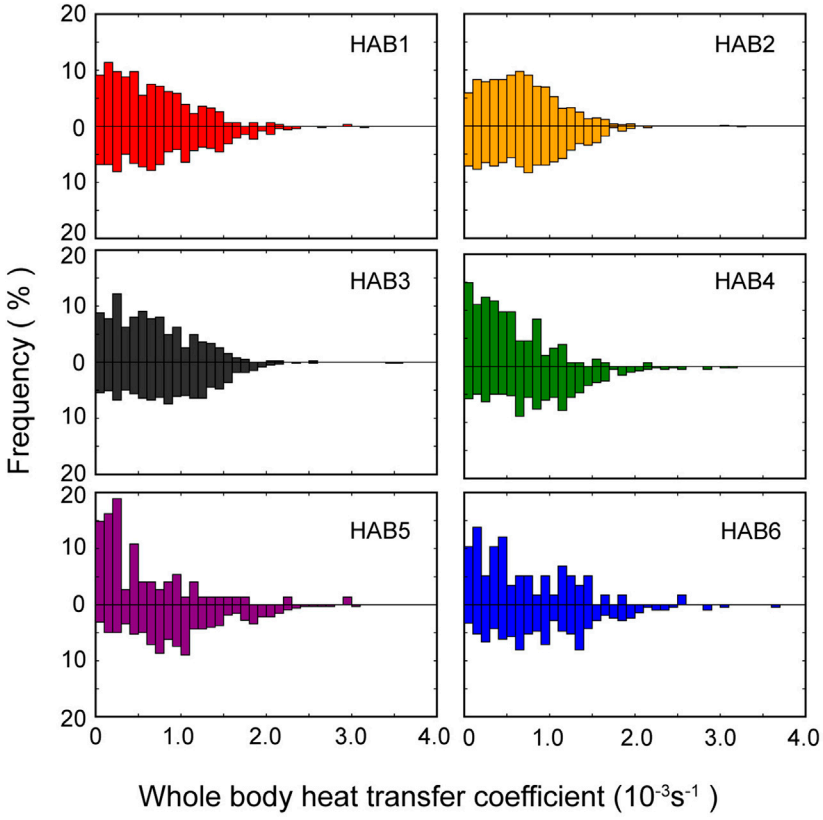

FIGURE 6
Frequency distribution of whole-body heat transfer coefficient in each thermal habitat. Upper and lower parts of each panel present the cooling (descending) and warming (ascending) phases, respectively.

TABLE 5 Median values of whole-body heat transfer coefficient λ ($10^{-3}s^{-1}$) in the warming and cooling phases among thermal habitats and the comparisons between two models.

Habitat	Cooling		Warming		AIC	
	Number	λ ($10^{-3}s^{-1}$)	Number	λ ($10^{-3}s^{-1}$)	M1	M2
HAB1	306	0.52	478	0.72	2206	2221
HAB2	757	0.62	671	0.73	3799	3748
HAB3	384	0.57	600	0.84	2670	2697
HAB4	154	0.40	378	0.84	1481	1532
HAB5	74	0.31	322	0.91	1047	1099
HAB6	58	0.48	208	0.92	714	727

behaviors are unique in each thermal habitat, as well as a quantitative evaluation of how their dive duration is linked to their physiology.

In this section, we evaluated the validity of the classification of thermal habitats in our study and then discussed how thermal physiology differs among thermal habitats, focusing on the short-term thermoregulation, while comparing our results to previous findings from laboratory experiments (Neill et al., 1976; Stevens and Neill, 1979). We also subsequently discussed the links between area-specific thermal physiology and the vertical behavior of surfacing and diving in each thermal habitat. Finally, we described the implications for the spatial heterogeneity of SKJ fishery grounds in the northwestern Pacific Ocean.

4.1 Validity of the classification of thermal habitats

In the present study, habitat classification was based solely on recorded depth and water temperature from tagged SKJ to avoid

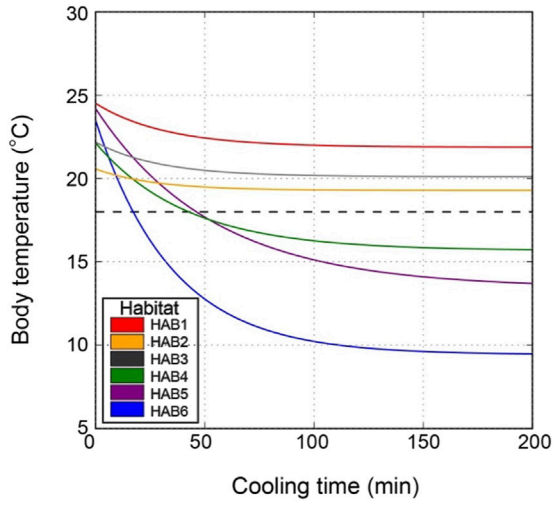

FIGURE 7
Simulation of body temperature change at a dive depth of 200 m in each thermal habitat (HAB). Initial body temperature, water temperature at a depth of 200 m, whole-body heat transfer, and metabolic heat production used in this simulation are presented in Table 3. Dashed horizontal line shows a critical temperature limit of 18°C estimated based on the study by Barkley et al. (1978).

arbitrary spatial and temporal boundaries dependent on position estimates (Bestley et al., 2009; Aoki et al., 2017; Matsubara et al., 2024). This objective approach effectively captures the basin-scale oceanographic structures as a large water mass. Specifically, the thermal profile in HAB1 has a similar feature of the subtropical front around the latitude of 25°N in the western North Pacific (Kobashi et al., 2006), and the strong mixed layer in HAB2 corresponds to that of the subtropical mode water (Suga and Hanawa, 1995; Oka et al., 2023). Moreover, the thermal profile in HAB4 exhibited features similar to those of the Kuroshio, where the temperature at a depth of 200 m is 15°C, with broad overlap with the coastal regions of the Kuroshio current (Stommel and Yoshida, 1972). These consistencies with the description of the oceanic structure support the validity of our classification. However, there are limitations in identifying habitats as a single oceanographic area, leading to difficulty in interpreting the SKJ habitat-specific behavior, particularly in HAB3 and 4. Although the thermal profile is consistent within each HAB, the sparse locations of HAB3 (found north and south of HAB2) and HAB4 (found around HAB5 and 6) should be carefully considered when evaluating behavior in these thermal habitats. There is considerable variation in the surface rate in HAB3 and 4. However, given that these data points are relatively few, we assumed that their effects would be minimized when using average trends.

4.2 Characteristics of SKJ thermal physiology

The large thermal differences between body and water temperature during dives in low-latitude (HAB 1) areas compared to those in mid-latitude (HAB5–6) areas offer an intuitive understanding of the differences in their thermal physiology depending on the thermal habitats. High body temperature during dives can be explained by the change in the λ between the cooling and warming phases (Holland et al., 1992; Kitagawa et al., 2007; Aoki et al., 2020). Our observations of slight or little difference in λ in HAB1–3 are consistent with the results of Neill et al. (1976) and Stevens and Neill (1979) in SKJ (0.4–3.5 kg body weight) tested at water temperatures above 18°C, suggesting that this species was not physiologically able to regulate its body temperature. The minimal difference in λ observed in these areas is reasonable, as the water temperature at 200 m depth in these HABs was higher than the critical temperature limit of 18°C (Barkley et al., 1978). The agreement between the laboratory studies and our findings in the wild suggests that SKJ are not severely required to thermoregulate in the short term to maintain their body temperature within environments that fall within their thermal tolerance range.

In contrast, the λ in HAB4–6 differed by a factor of 2–3 between descent and ascent, indicating that SKJ physiologically regulated their body temperature during their diving behavior. Tropical tuna species, such as bigeye and yellowfin tuna, thermoregulate both behaviorally and physiologically by reducing λ during descent to prevent heat release from the body and increasing λ during ascent to absorb heat from the warmer water, allowing them and recover body temperature in a short period (Holland et al., 1992; Aoki et al., 2020). While the difference in λ for SKJ was not as pronounced as in bigeye tuna (with a 12-fold difference between phases), it was still slightly higher than that of yellowfin tuna (two-fold difference). This physiological thermoregulation in strong thermocline areas suggests that such mechanisms are common in tropical tuna and are vital for accessing depths below the thermocline that exceed their thermal tolerance in the wild.

The change in the λ between the cooling and warming phases is likely due to changes in blood flow during dives. Heat exchange in fish can be mainly divided into the effect of body inertia and internal body effects such as blood flow (Kitagawa and Kimura, 2006; Aoki et al., 2020). Although thermal inertia does not change in a short period such as diving behavior, changes in the blood flow can occur. According to a study that examined the relationship between blood circulation and respiration (Brill Richard and Bushnell Peter, 2001), the volume of blood output from the heart of SKJ remains constant, but changes in heart rate can alter the volume of blood output per unit time. As heat exchange occurs between arterial and venous blood in the counter-current heat exchanger developed in tuna (Carey et al., 1971), changes in heart rate are believed to alter heat exchange efficiency in the rete mirabile.

In addition to short-term thermoregulation, long-term thermoconservation, driven by the body bulk effect, contributes to substantial thermal inertia, helping to maintain a high core temperature (Neill et al., 1976). In the Kuroshio–Oyashio transition area, only SKJ with an FL of >45 cm and a high-fat condition factor (≥20) are found in the waters north of the Kuroshio front. This suggests that large individuals meeting these criteria can move from relatively warm waters in the 20°C range to cold waters in the 18°C range (Nihira, 1996), a phenomenon called "size-screening". However, the consecutive measurements of the daily average temperature during the northward migration revealed that SKJ (<45 cm FL) already experienced the lowest temperature of 18°C in areas around HAB2, which is further south of the

Kuroshio–Oyashio transition area (Kiyofuji et al., 2019). The direct link between experienced temperature and thermal inertia, previously hypothesized as a size-screening phenomenon, has not been validated in individuals with archival tags in the Kuroshio–Oyashio transition area. However, it is noteworthy that slight decreases in λ during the cooling phase were observed alongside movements from low-latitude areas (HAB 1) to mid-latitude areas (HAB5 and 6). This observation could be interpreted as developments in thermal inertia associated with growth. In HAB5 and 6, the presence of the Oyashio current beneath the upper warm layer offers abundant food resources derived from high productivity (Yasuda, 2003; Sassa et al., 2007). Feeding while reducing the λ in these rich food areas would further contribute to lowering λ by increasing thermal inertia due to additional fat reserves (Aoki et al., 2017). This process could initiate a positive feedback loop, stimulating enhanced exploitation of food resources within this area (Nihira, 1996). The body bulk effect is commonly developed in marine animals as they grow (Nakamura et al., 2020); however, the developmental shift to regional endothermy, associated with unique anatomical features, occurs more rapidly in juvenile tuna (Kitagawa and Fujioka, 2017; Hino et al., 2021; Kitagawa et al., 2022). Although increases in thermal inertia in SKJ were subtle in our study, further investigation targeting individuals with a wide variety of body sizes and fat contents is necessary to capture the drastic shift in their thermos-conservation ability, particularly along the ontogenetic shift.

4.3 Links between thermal physiology and vertical behavior

Surface-oriented behavior and short dive durations in SKJ are likely behaviors to avoid exposure to cold temperatures (Kitagawa et al., 2007; Lawson et al., 2010; Matsumoto et al., 2013; Matsubara et al., 2024). As high energy demand species, tuna must meet high oxygen demands (Brill Richard and Bushnell Peter, 2001; Bernal et al., 2017; Humphries et al., 2024). Prolonged exposure to cold temperatures would reduce oxygen supply and cardiac output, resulting in an increased risk of hypoxia (Bushnell et al., 1990; Shiels et al., 2015). Although SKJ possess the physiological ability to thermoregulate in the short term to maintain stable body temperature, as mentioned above, this ability is not sustainable beyond a certain duration. Our comparison of the body cooling stimulation with actual dive duration provided field evidence of how dive duration in SKJ is determined based on thermal physiology. An observed dive duration shorter than the simulated cooling time indicates that SKJ returned to the surface before their body temperature decreased to the critical level of 18°C (Barkley et al., 1978), which can be interpreted as behavioral thermoregulation (Kitagawa et al., 2007). During northward migration, the shallower the depth at which the 18°C threshold is reached (Kiyofuji et al., 2019), the more frequent the surfacing behavior and the shorter the dive duration. Therefore, areas with shallow depths, where this lower thermal tolerance is present, such as the temperate areas, would result in the vertical distribution of SKJ being near the surface with occasional short dives. In contrast, the relatively few restrictions posed by low thermal tolerance in subtropical areas allow SKJ to spend most of the daytime throughout a wide range of water columns.

The diving behavior of tuna offers advantages in encountering food resources and is particularly essential in areas where surface prey is scarce (Kitagawa et al., 2004; Walli et al., 2009; Bauer et al., 2017). Successful foraging associated with diving is related to both access to prey depths and long dive duration, which maximize prey encounters (Josse et al., 1998; Kitagawa et al., 2007; Walli et al., 2009). Prolonging the dive duration in subtropical areas, which are poor prey environments for SKJ (Aoki et al., 2017), is reasonable as it enables them to forage for long periods across a wider range of the water column. Although SKJ in subtropical areas expend three times more energy on feeding than they do in temperate areas, their estimated food intake is still only half of what is observed in temperate areas (Aoki et al., 2017). In contrast, the strong thermocline in temperate areas restricts the diving period of SKJ (Kitagawa et al., 2007; Lawson et al., 2010), which increases the risk of unsuccessful foraging. However, the rich prey environment in temperate areas (Aoki et al., 2017; Fujioka et al., 2018; Muhling et al., 2022) allows them to meet their high energy demands, even within the short foraging period.

4.4 Implications for SKJ surface fishery

The concept of prey-predator encounter based on the overlap of depths and times within vertical habitats is extendable to fishing activities between prey (SKJ) and predator (human) (Post et al., 2008; Lennox et al., 2017). Given that SKJ is mainly exploited by the purse seine and pole-and-line fisheries, which rely on visually locating schools swimming at the surface (Gaertner et al., 1999; Matsubara et al., 2022), changes in the vertical behavior among habitats would explain the spatial heterogeneity of scarce catch being reported in subtropical areas. The comprehensive behavioral dataset obtained from subtropical and temperate areas in this study, combined with previous literature from tropical regions, provides a valuable opportunity to compare and evaluate changes in vertical behavior. Our findings of non-surfacing behavior and long dive duration in subtropical areas may serve as a plausible explanation for the decrease in the encounter rate by surface fisheries. Nevertheless, a slight catch can be observed in subtropical areas (Williams, 2023), probably due to the increased chances of encounter during the limited time of dawn and dusk periods when SKJ distribution shifts between day and night. Notably, the habitat in subtropical areas would not be optimal for surface fisheries in terms of efficiency when searching schools on the surface. On the contrary, the surface-oriented behavior and shorter dive durations observed in temperate areas would facilitate the discovery of schools and subsequent catches by fisheries (Matsubara et al., 2024). While surface rates for individuals in tropical areas are unavailable, research on SKJ (53–73 cm FL) in tropical areas, both associated and unassociated with floating aggregate devices (FADs), indicates shallower depths (10.4 and 44 m during the day, respectively) (Schaefer and Fuller, 2007) than those observed in subtropical areas (HAB1, 97–152 m) in our study. In addition, SKJ unassociated with FADs showed surface-oriented behavior (less than 10 m below the surface for periods >10 min), ranging from 5 to 23 events in a day, each lasting 10–214 min per event (Schaefer and Fuller, 2007). The

primary drivers of the surface-oriented behavior and relatively shallow depths in tropical areas remain unclear. However, it is plausible that this behavior enhances encounter rates for surface fisheries in tropical areas compared to those in subtropical areas. Therefore, integrating our findings on the shift in vertical behavior driven by thermal physiology in subtropical and temperate areas with previous literature from tropical areas explains why SKJ fishery grounds predominantly thrive in tropical and temperate regions (HAB4–6) in the western Pacific Ocean, consequently resulting in a spatial gap in subtropical areas.

Finally, this study established a link between the vertical distribution of SKJ and their vulnerability to fisheries by adding a novel component: the response of this species to thermal environments in the wild. A better understanding of the physiological mechanisms controlling vertical habitat use in the water column would offer ecologists a more mechanistic understanding of depth-related habitat, helping them predict the hotspots associated with changes in thermal profiles driven by ocean environmental variations. The predicted decline in the thickness of STMW in HAB2 (Oka et al., 2023) and the shoaling of the mixed layer in the Kuroshio Extension area (Zhang et al., 2016) in HAB5 and 6 highlight the importance of exploring thermal physiological responses. This knowledge is essential for predicting the redistribution of hot and cool spots for SKJ fisheries under these future climate change scenarios (Sunday et al., 2012). Such evaluations would reduce the uncertainty in future stock management and bring us closer to achieving sustainable fisheries (Lehodey et al., 2013).

5 Summary

This study investigated the vertical behavior and thermal physiology of skipjack (SKJ) during their northward migration from subtropical to temperate areas in the western Pacific Ocean using a physio-logging technique. We quantified the surfacing rate on the surface and dive duration and estimated the whole-body heat transfer coefficient (λ) based on body temperature records as an index of their thermal physiology. SKJ exhibited non-surface-oriented behavior with extended dive duration in the southern mixed layer areas, whereas they demonstrated surface-restricted behavior with occasional short dives in northern areas with strong thermocline. Notably, SKJ in northern areas exhibited greater thermoregulation (with differences in λ of 2–3-fold between the warming and cooling phases associated with diving) than those in southern areas (minor differences in λ between the phases). This provides new field evidence of short-term thermoregulation during dives in SKJ, which exhibit distinct patterns across the thermal habitats. This adjustment in λ during the phases in the northern areas allows SKJ to minimize heat release from the body by reducing λ during the cooling phase in descent and to absorb heat from the warm water near the warm surface and quickly recover body temperature by increasing λ during warming phase in ascent. Non-surface-oriented behavior with a long dive duration in warm subtropical areas would enable SKJ to forage efficiently in poor prey environments without requiring thermoregulation. The surfacing behavior, with occasional short dives in temperate areas, can be interpreted as a consequence of thermoregulation, avoiding exposure to cold temperatures beyond the thermocline while foraging in rich prey environments. The spatial difference in thermal habitat suitability would explain why SKJ exploitation by surface fisheries does not thrive in subtropical areas from the viewpoint of encounter rate by fisheries, which rely on the overlapping depth and time at the surface. Our findings of SKJ thermal physiology and its implications for vertical behavior and fishery vulnerability underscore the importance of considering thermal physiology in predicting species responses to ocean environmental changes, thus providing more plausible future stock estimates.

Data availability statement

The raw data supporting the conclusions of this article will be made available by the authors, without undue reservation.

Ethics statement

The studies involving animals were reviewed and approved by the Animal Experimental Council in fisheries resources institute, Japan Fisheries Research and Education Agency.

Author contributions

YA: Conceptualization, Data curation, Formal Analysis, Investigation, Methodology, Visualization, Writing–original draft, Writing–review and editing. TK: Conceptualization, Data curation, Funding acquisition, Writing–original draft, Writing–review and editing. HK: Conceptualization, Data curation, Investigation, Writing–original draft, Writing–review and editing.

Funding

The author(s) declare that financial support was received for the research, authorship, and/or publication of this article. This research was supported by a grant from the Japan Fisheries Agency, partially supported by JST, CREST Grant Numbers JPMJCR13A5 and JPMJCR23P2, Japan, and by a grant-in-aid for Scientific Research (B) from the Japan Society for the Promotion of Science (No 24350104) to Takashi Kitagawa.

Acknowledgments

We are grateful to the captains and crewmembers of the pole-and-line fishing vessel, No. 8 Nissho-Maru (Skipper: K. Nakata and Captain: S. Okamoto), R/V Miyazaki-Maru of the Miyazaki prefecture. We would like to thank Y. Watanabe and T. Kawamura of the University of Tokyo for their helpful comments on an early version of the manuscript.

Conflict of interest

The authors declare that the research was conducted in the absence of any commercial or financial relationships that could be construed as a potential conflict of interest.

The author(s) declared that they were an editorial board member of Frontiers, at the time of submission. This had no impact on the peer review process and the final decision.

Publisher's note

References

Aoki, Y., Aoki, A., Ohta, I., and Kitagawa, T. (2020). Physiological and behavioural thermoregulation of juvenile yellowfin tuna Thunnus albacares in subtropical waters. *March Biol.* 167, 71. doi:10.1007/s00227-020-03679-w

Aoki, Y., Kitagawa, T., Kiyofuji, H., Okamoto, S., and Kawamura, T. (2017). Changes in energy intake and cost of transport by skipjack tuna (*Katsuwonus pelamis*) during northward migration in the northwestern Pacific Ocean. *Deep Sea Res. II* 140, 83–93. doi:10.1016/j.dsr2.2016.05.012

Barkley, R. A., Neill, W. H., and Gooding, R. M. (1978). Skipjack tuna, Katsuwonus-pelamis, habitat based on temperature and oxygen requirements. *Fish. Bull.* 76, 653–662.

Bauer, R. K., Fromentin, J. M., Demarcq, H., and Bonhommeau, S. (2017). Habitat use, vertical and horizontal behaviour of Atlantic bluefin tuna (Thunnus thynnus) in the northwestern Mediterranean Sea in relation to oceanographic conditions. *Deep Sea Res. II* 141, 248–261. doi:10.1016/j.dsr2.2017.04.006

Bell, J. D., Senina, I., Adams, T., Aumont, O., Calmettes, B., Clark, S., et al. (2021). Pathways to sustaining tuna-dependent Pacific Island economies during climate change. *Nat. Sustain.* 4, 900–910. doi:10.1038/s41893-021-00745-z

Bernal, D., Brill, R. W., Dickson, K. A., and Shiels, H. A. (2017). Sharing the water column: physiological mechanisms underlying species-specific habitat use in tunas. *Rev. Fish. Biol. Fish.* 27, 843–880. doi:10.1007/s11160-017-9497-7

Bestley, S., Gunn, J. S., and Hindell, M. A. (2009). Plasticity in vertical behaviour of migrating juvenile southern bluefin tuna (*Thunnus maccoyii*) in relation to oceanography of the south Indian Ocean. *Fish. Oceanogr.* 18, 237–254. doi:10.1111/j.1365-2419.2009.00509.x

Boye, J., Musyl, M., Brill, R., and Malte, H. (2009). Transectional heat transfer in thermoregulating bigeye tuna (Thunnus obesus) – a 2D heat flux model. *J. Exp. Biol.* 212, 3708–3718. doi:10.1242/jeb.031427

Brill, R. W. (1994). A review of temperature and oxygen tolerance studies of tunas pertinent to fisheries oceanography, movement models and stock assessments. *Fish. Oceanogr.* 3, 204–216. doi:10.1111/j.1365-2419.1994.tb00098.x

Brill Richard, W., and Bushnell Peter, G. (2001). "The cardiovascular system of tunas," in *Fish physiology, book volume 19*. Editors B. Barbara and E. Stevens (Academic Press).

Bushnell, P. G., Brill, R. W., and Bourke, R. E. (1990). Cardiorespiratory responses of skipjack tuna (Katsuwonus pelamis), yellowfin tuna (Thunnus albacares), and bigeye tuna (Thunnus obesus) to acute reductions of ambient oxygen. *Can. J. Zool.* 68, 1857–1865. doi:10.1139/z90-265

Carey, F. G., and Teal, J. M. (1966). Heat conservation in tuna fish muscle. *Proc. Natl. Acad. Sci. U. S. A.* 56, 1464–1469. doi:10.1073/pnas.56.5.1464

Carey, F. G., Teal, J. M., Kanwisher, J. W., Lawson, K. D., and Beckett, J. S. (1971). Warm-bodied fish. *Am. Zool.* 11, 137–143. doi:10.1093/icb/11.1.137

Dickson, K. A. (1996). Locomotor muscle of high-performance fishes: what do comparisons of tunas with ectothermic sister taxa reveal? *Comp. Biochem. Physiol. A* 113, 39–49. doi:10.1016/0300-9629(95)02056-X

Don, S. E., and Neill William, H. (1979). "5 body temperature relations of tunas, especially skipjack," in *Fish physiology, book volume 7*. Editors W. S. Hoar and D. J. Randall (Academic Press).

Dueri, S., Bopp, L., and Maury, O. (2014). Projecting the impacts of climate change on skipjack tuna abundance and spatial distribution. *Glob. Change Biol.* 20, 742–753. doi:10.1111/gcb.12460

Evans, K., Langley, A., Clear, N. P., Williams, P., Patterson, T., Sibert, J., et al. (2008). Behaviour and habitat preferences of bigeye tuna (*Thunnus obesus*) and their influence on longline fishery catches in the western Coral Sea. *Can. J. Fish. Aquat. Sci.* 65, 2427–2443. doi:10.1139/F08-148

Fahlman, A., Aoki, K., Bale, G., Brijs, J., Chon, K. H., Drummond, C. K., et al. (2021). The new era of physio-logging and their grand challenges. *Front. Physiol.* 12, 669158. doi:10.3389/fphys.2021.669158

FAO. (2022). Towards blue transformation. State World Fish. Aquacult. (Rome: Food and Agriculture Organization).

Forget, F. G., Capello, M., Filmalter, J. D., Govinden, R., Soria, M., Cowley, P. D., et al. (2015). Behaviour and vulnerability of target and non-target species at drifting fish aggregating devices (FADs) in the tropical tuna purse seine fishery determined by acoustic telemetry. *Can. J. Fish. Aquat. Sci.* 72, 1398–1405. doi:10.1139/cjfas-2014-0458

Fujioka, K., Fukuda, H., Tei, Y., Okamoto, S., Kiyofuji, H., Furukawa, S., et al. (2018). Spatial and temporal variability in the trans-Pacific migration of Pacific bluefin tuna (Thunnus orientalis) revealed by archival tags. *Prog. Oceanogr.* 162, 52–65. doi:10.1016/j.pocean.2018.02.010

Gaertner, D., Pagavino, M., and Marcano, J. (1999). Influence of Fishers' behaviour on the catchability of surface tuna schools in the Venezuelan purse-seiner fishery in the Caribbean Sea. *Can. J. Fish. Aquat. Sci.* 56, 394–406. doi:10.1139/f98-191

Graham, J. B., and Dickson, K. A. (2000). The evolution of thunniform locomotion and heat conservation in scombrid fishes: new insights based on the morphology of *Allothunnus fallai*. *Zool. J. Linn. Soc.* 129, 419–466. doi:10.1111/j.1096-3642.2000.tb00612.x

Hino, H., Kitagawa, T., Matsumoto, T., Aoki, Y., and Kimura, S. (2021). Development of behavioral and physiological thermoregulatory mechanisms with body size in juvenile bigeye tuna Thunnus obesus. *Fish. Oceanogr.* 30, 219–231. doi:10.1111/fog.12515

Holland, K. N., Brill, R. W., Chang, R. K., Sibert, J. R., and Fournier, D. A. (1992). Physiological and behavioural thermoregulation in bigeye tuna (*Thunnus obesus*). *Nature* 358, 410–412. doi:10.1038/358410a0

Humphries, N. E., Fuller, D. W., Schaefer, K. M., and Sims, D. W. (2024). Highly active fish in low oxygen environments: vertical movements and behavioural responses of bigeye and yellowfin tunas to oxygen minimum zones in the eastern Pacific Ocean. *March Biol.* 171, 55. doi:10.1007/s00227-023-04366-2

Josse, E., Bach, P., and Dagorn, L. (1998). Simultaneous observations of tuna movements and their prey by sonic tracking and acoustic surveys. *Hydrobiologia* 371, 61–69. doi:10.1007/978-94-011-5090-3_8

Kitagawa, T., Abe, T. K., Kubo, K., Fujioka, K., Fukuda, H., and Tanaka, Y. (2022). Rapid endothermal development of juvenile pacific bluefin tuna. *Front. Physiol.* 13, 968468. doi:10.3389/fphys.2022.968468

Kitagawa, T., and Fujioka, K. (2017). Rapid ontogenetic shift in juvenile Pacific bluefin tuna diet. *March Ecol. Prog. Ser.* 571, 253–257. doi:10.3354/meps12129

Kitagawa, T., Kimura, S., Nakata, H., and Yamada, H. (2004). Diving behavior of immature, feeding Pacific bluefin tuna (Thunnus thynnus orientalis) in relation to season and area: the East China Sea and the Kuroshio–Oyashio transition region. *Fish. Oceanogr.* 13, 161–180. doi:10.1111/j.1365-2419.2004.00282.x

Kitagawa, T., and Kimura, S. (2006). An alternative heat-budget model relevant to heat transfer in fishes and its practical use for detecting their physiological thermoregulation. *Zool. Sci.* 23 (12), 1065–1071.

Kitagawa, T., Kimura, S., Nakata, H., and Yamada, H. (2006). Thermal adaptation of Pacific bluefin tuna *Thunnus orientalis* to temperate waters. *Fish. Sci.* 72, 149–156. doi:10.1111/j.1444-2906.2006.01129.x

Kitagawa, T., Kimura, S., Nakata, H., and Yamada, H. (2007). Why do young Pacific bluefin tuna repeatedly dive to depths through the thermocline? *Fish. Sci.* 73, 98–106. doi:10.1111/j.1444-2906.2007.01307.x

Kiyofuji, H., Aoki, Y., Kinoshita, J., Okamoto, S., Masujima, M., Matsumoto, T., et al. (2019). Northward migration dynamics of skipjack tuna (*Katsuwonus pelamis*) associated with the lower thermal limit in the western Pacific Ocean. *Prog. Oceanogr.* 175, 55–67. doi:10.1016/j.pocean.2019.03.006

Kobashi, F., Mitsudera, H., and Xie, S. P. (2006). Three subtropical fronts in the North Pacific: observational evidence for mode water-induced subsurface frontogenesis. *J. Geophys. Res.* 111. doi:10.1029/2006JC003479

Korsmeyer, K., and Dewar, H. (2001). "Tuna metabolism and energetics,"*E. D. Stevens Fish. Physiol. Tunas Physiol.* Editor B. A. Block, 19, 35–78. doi:10.1016/S1546-5098(01)19003-5

Lawson, G. L., Castleton, M. R., and Block, B. A. (2010). Movements and diving behavior of Atlantic bluefin tuna Thunnus thynnus in relation to water column

structure in the northwestern Atlantic. *March Ecol. Prog. Ser.* 400, 245–265. doi:10.3354/meps08394

Lehodey, P., Senina, I., Calmettes, B., Hampton, J., and Nicol, S. (2013). Modelling the impact of climate change on Pacific skipjack tuna population and fisheries. *Clim. Change.* 119, 95–109. doi:10.1007/s10584-012-0595-1

Lennox, R. J., Alós, J., Arlinghaus, R., Horodysky, A., Klefoth, T., Monk, C. T., et al. (2017). What makes fish vulnerable to capture by hooks? A conceptual framework and a review of key determinants. *Fish. Fish.* 18, 986–1010. doi:10.1111/faf.12219

Malte, H., Larsen, C., Musyl, M., and Brill, R. (2007). Differential heating and cooling rates in bigeye tuna (*Thunnus obesus* Lowe): a model of non-steady state heat exchange. *J. Exp. Biol.* 210, 2618–2626. doi:10.1242/jeb.003855

Matsubara, N., Aoki, Y., Aoki, A., and Kiyofuji, H. (2024). Lower thermal tolerance restricts vertical distributions for juvenile albacore tuna (Thunnus alalunga) in the northern limit of their habitats. *Front. March Sci.* 11. doi:10.3389/fmars.2024.1353918

Matsubara, N., Aoki, Y., and Tsuda, Y. (2022). Historical developments of fishing devices in Japanese pole-and-line fishery. Online meeting: the Commission for the conservation and management of highly migratory fish stocks in the western and central Pacific Ocean. *Sci. Comm. EighteenthRegular Sess. (WCPFC)*. WCPFC-SC18–2022/SA-IP-16.

Matsumoto, T., Kitagawa, T., and Kimura, S. (2013). Vertical behavior of juvenile yellowfin tuna Thunnus albacares in the southwestern part of Japan based on archival tagging. *Fish. Sci.* 79, 417–424. doi:10.1007/s12562-013-0614-9

Matsumoto, W. M., Skillman, R. A., and Dizon, A. E. (1984). Synopsis of biological data on skipjack tuna, *Katsuwonus pelamis*. *Natl. Ocean. Atmos. Adm. Tech. Rep. NMFS Circular* 451, 92.

Muhling, B. A., Snyder, S., Hazen, E. L., Whitlock, R. E., Dewar, H., Park, J. Y., et al. (2022). Risk and reward in foraging migrations of North Pacific albacore determined from estimates of energy intake and movement costs. *Front. March Sci.* 9, 730428. doi:10.3389/fmars.2022.730428

Nakamura, I., Matsumoto, R., and Sato, K. (2020). Body temperature stability in the whale shark, the world's largest fish. *J. Exp. Biol.* 223, jeb210286. doi:10.1242/jeb.210286

Neill, W. H., Chang, R. K. C., and Dizon, A. E. (1976). Magnitude and ecological implications of thermal inertia in skipjack tuna,Katsuwonus pelamis (Linnaeus). *Environ. Biol. Fishes.* 1, 61–80. doi:10.1007/BF00761729

Nihira, A. (1996). Studies on the behavioral ecology and physiology of migratory fish schools of skipjack tuna (*Katsuwonus pelamis*) in the oceanic frontal area. *Bol. Tohokunatl.Fish.Res.Inst.* 58, 137–233.

Oka, E., Sugimoto, S., Kobashi, F., Nishikawa, H., Kanada, S., Nasuno, T., et al. (2023). Subtropical Mode Water south of Japan impacts typhoon intensity. *Sci. Adv.* 9, eadi2793. doi:10.1126/sciadv.adi2793

Post, J. R., Persson, L., Parkinson, E. A., and van Kooten, T. (2008). Angler numerical response across landscapes and the collapse of freshwater fisheries. *Ecol. Appl.* 18, 1038–1049. doi:10.1890/07-0465.1

Sassa, C., Kawaguchi, K., and Taki, K. (2007). Larval mesopelagic fish assemblages in the Kuroshio–Oyashio transition region of the western North Pacific. *March Biol.* 150, 1403–1415. doi:10.1007/s00227-006-0434-x

Schaefer, K. M., and Fuller, D. W. (2007). "Vertical movement patterns of skipjack tuna (Katsuwonus pelamis) in the eastern equatorial Pacific Ocean," in *As revealed with archival tags*.

Scutt Phillips, J., Pilling, G. M., Leroy, B., Evans, K., Usu, T., Lam, C. H., et al. (2017). Revisiting the vulnerability of juvenile bigeye (Thunnus obesus) and yellowfin (*T. albacares*) tuna caught by purse-seine fisheries while associating with surface waters and floating objects. *PLOS One* 12, e0179045. doi:10.1371/journal.pone.0179045

Shiels, H. A., Galli, G. L. J., and Block, B. A. (2015). Cardiac function in an endothermic fish: cellular mechanisms for overcoming acute thermal challenges during diving. *Proc. Biol. Sci.* 282, 20141989. doi:10.1098/rspb.2014.1989

Stevens, E. D., and Neill, W. H. (1979). "Body temperature relations of tunas, especially skipjack,". *Fish physiology: locomotion*. Editors W. S. Hoar and D. J. Randall (Academic Press), 7, 316–360.

Stommel, H., and Yoshida, K. (1972). Kuroshio: physical aspects of the Japan current.

Suga, T., and Hanawa, K. (1995). The subtropical mode water circulation in the North Pacific. *J. Phys. Oceanogr.* 25 (5), 958–970. doi:10.1175/1520-0485(1995)025<0958:tsmwci>2.0.co;2

Sunday, J. M., Bates, A. E., and Dulvy, N. K. (2012). Thermal tolerance and the global redistribution of animals. *Nat. Clim. Change* 2, 686–690. doi:10.1038/NCLIMATE1539

Walli, A., Teo, S. L. H., Boustany, A., Farwell, C. J., Williams, T., Dewar, H., et al. (2009). Seasonal movements, aggregations and diving behavior of Atlantic bluefin tuna (*Thunnus thynnus*) revealed with archival tags. *PLOS One* 4, e6151. doi:10.1371/journal.pone.0006151

Wild, A., and Hampton, J. (1994). "A review of the biology and fisheries for skipjack tuna, *Katsuwonus pelamis*, in the Pacific Ocean," in *Interactions of pacific tuna fisheries proceedings of the first FAO expert consultation on interactions of pacific tuna fisheries book 336. FAO fisheries*. Editors R. S. Shomura, J. Majkowski, and S. Langi (Tech).

Williams, R. (2023). Overview of tuna fisheries in the western and central Pacific Ocean, including economic conditions – 2022. WCPFC-SC19-2023/GN WP-1 (Scientific Committee) 19th Regular Session. *Koror, Palau, 16 –24 August*, 2023.

Wright, S. R., Righton, D., Naulaerts, J., Schallert, R. J., Griffiths, C. A., Chapple, T., et al. (2021). Yellowfin tuna behavioural ecology and catchability in the South Atlantic: the right place at the right time (and depth). *Front. March Sci.* 8, 664593. doi:10.3389/fmars.2021.664593

Yasuda, I. (2003). Hydrographic structure and variability in the Kuroshio-Oyashio transition area. *J. Oceanogr.* 59, 389–402. doi:10.1023/A:1025580313836

Zhang, R., Xie, S. P., Xu, L., and Liu, Q. (2016). Changes in mixed layer depth and spring bloom in the Kuroshio extension under global warming. *Adv. Atmos. Sci.* 33, 452–461. doi:10.1007/s00376-015-5113-8

Zuur, A. F., Hilbe, J. M., and Ieno, E. N. (2013). *A beginner's guide to glm and GLMM with R. A frequentist and bayesian perspective for ecologists*. Newburgh UK: Highland Statistics Ltd.

frontiers | Frontiers in Physiology

TYPE Original Research
PUBLISHED 31 January 2025
DOI 10.3389/fphys.2025.1519701

OPEN ACCESS

EDITED BY
Takashi Kitagawa,
The University of Tokyo, Japan

REVIEWED BY
Motohiro Ito,
Toyo University, Japan
Akinori Takahashi,
National Institute of Polar Research, Japan
Nobuhiko Sato,
Japan Fisheries Research and Education Agency (FRA), Japan

*CORRESPONDENCE
Yuichi Mizutani,
mizutani.yuichi.g0@f.mail.nagoya-u.ac.jp

RECEIVED 30 October 2024
ACCEPTED 08 January 2025
PUBLISHED 31 January 2025

CITATION
Mizutani Y, Goto Y, Shoji A and Yoda K (2025) Effects of nest locations on foraging behavior and physiological responses in seabird colony. *Front. Physiol.* 16:1519701.
doi: 10.3389/fphys.2025.1519701

Effects of nest locations on foraging behavior and physiological responses in seabird colony

Yuichi Mizutani *, Yusuke Goto , Akiko Shoji and Ken Yoda

Graduate School of Environmental Studies, Nagoya University, Nagoya, Japan

Breeding success and survival in colonial seabirds are influenced by nest location, physical surroundings, and external disturbances. Nest location may also directly or indirectly affect individual foraging behavior and physiological conditions, shaping reproductive success and survival. Despite these influences, few studies have integrated the analysis of nest location, behavior, and physiological status. In this study, we analyzed 20 black-tailed gulls (*Larus crassirostris*) nesting in the center of a colony within a protected area (Central Group, CG) and five gulls on the periphery outside the protected area, where human disturbance is frequent (Peripheral Group, PG). Using GPS movement trajectories and physiological indicators, we found that although clutch sizes were similar between the CG and PG, the PG exhibited shorter foraging trip durations, maximum distances from the nest, and a lower daily frequency of foraging trips. Antioxidant capacity did not differ between the groups; however, oxidation levels were lower in the PG. These behavioral and physiological differences associated with nest location may partly result from the incubation period influenced by human activity. The PG individuals remained in the peripheral group for at least 2 years (some for over 15 years), with all reproductive attempts failing, suggesting consistently low reproductive success. However, reduced foraging activity and lower oxidative stress levels reflect an energy-saving strategy that may mitigate the costs of repeated breeding failures. These findings suggest a potential life-history trade-off, in which individuals prioritize survival over reproductive success. This highlights how external disturbances and nest location can shape energy allocation strategies within a colony's peripheral-central distribution.

KEYWORDS

seabird, colony, reproductive cost, antioxidants, pro-oxidant, BAP, d-ROMs, GPS

1 Introduction

In colony-forming seabirds, individuals nesting at the center of a colony generally exhibit higher parental survival and reproductive success than those nesting at the periphery, a pattern known as the peripheral-central distribution (Coulson, 1968; Tenaza, 1971; Aebischer and Coulson, 1990; Piro and Schmitz Ornés, 2021). Variations in fitness-related traits across nesting locations may be influenced by internal parental factors, such as age (Aubry et al., 2009), breeding experience (Vergara and Aguirre, 2006), and foraging ability (Spurr, 1975), as well as external factors, including predation risk (Vine,

1971; Brodin, 2001; Brown and Kotler, 2004; Piro and Schmitz Ornés, 2021), physical environmental conditions (Montevecchi, 1978; Rounds et al., 2004; Minias, 2014; Pagenaud et al., 2022), and social interaction levels (Birkhead, 1977; Kokko et al., 2004).

Seabirds may select nesting sites according to these factors, often shifting from subcolonies or peripheral areas to more significant central sites (Serrano and Tella, 2007). As a result, older, more experienced, and reproductively successful individuals are more likely to occupy the central regions, whereas less experienced individuals tend to nest peripherally (Aebischer and Coulson, 1990; Bosch and Sol, 1998; Kim and Monaghan, 2005; Indykiewicz et al., 2019). However, some seabird species exhibit strong nesting site fidelity, returning to the same location in each breeding season (Pearce, 2007; Piro and Schmitz Ornés, 2021), potentially because of their genetic preferences for specific habitats (Rodway and Regehr, 1999).

Although colony position and associated factors can influence reproductive outcomes (but not always; see Ryder and Ryder (1981), Shaw (1985)), the long-term strategies of iteroparous seabirds may buffer against the negative impacts of occasional breeding failures. Temporary breeding failures in peripheral nests may not substantially reduce overall fitness because skipping a breeding attempt allows individuals to conserve resources, including physiological conditions, that can be allocated to future breeding opportunities. To further clarify the peripheral-central nest-site distribution, comparing the physiological loads of parental seabirds, in conjunction with their behavior, between the peripheral and central nests is essential.

One promising approach involves examining oxidative stress, which has become a key indicator of the physiological costs associated with wildlife behavior (Koyama et al., 2021). It arises from an imbalance between pro-oxidants, particularly reactive oxygen species (ROS), and antioxidant defenses (Monaghan et al., 2008). While ROS plays a crucial role in pathogen elimination, their excessive accumulation can damage DNA, proteins, and lipids, leading to fatigue due to impaired mitochondrial function and a shift toward anaerobic metabolism. Conversely, antioxidants mitigate oxidative damage through endogenous enzymes and dietary compounds (Dröge, 2002). Elevated ROS levels are generally associated with physiological strains, whereas antioxidant levels indicate the capacity for recovery and resilience (Ahmadi et al., 2006). In avian studies, female European starlings (*Sturnus vulgaris*) experimentally subjected to increased breeding costs exhibit reduced physiological functions, including increased oxidative stress (Fowler and Williams, 2017). Furthermore, individuals may adjust their antioxidant mechanisms in response to anticipated conditions, potentially balancing endogenous and dietary antioxidant activities based on past environmental experiences and expected intake (Noguera et al., 2015). Oxidative stress has also been observed to exert delayed effects on life-history traits linked to survival (Noguera et al., 2012) and is often positively correlated with reproductive effort (Christe et al., 2012; Fletcher et al., 2013); however, some studies have reported no such correlation (Nussey et al., 2009; Markó et al., 2011).

In this study, we compared the physiological loads and foraging movements of black-tailed gulls (*Larus crassirostris*) incubating on Kabushima Island, where a fenced, sea-surrounded protected center (Central Group, CG) was contrasted with a more exposed periphery accessible to humans and predators (Peripheral Group, PG) (Figure 1). Although defining clear boundaries between the central and peripheral areas is challenging, the fenced structure of this colony allowed us to identify distinct groups consistent with the peripheral-central distribution. We recorded foraging movements using biologging and measured physiological loads based on oxidation levels and antioxidant capacity. Given that sexual differences in foraging behavior (Kazama et al., 2018) and/or antioxidant capacity (Lin et al., 2022) may reflect differences in breeding investment or physical condition, we also compared clutch size and body size, traits often correlated with and indicative of reproductive effort, between the CG and PG. Clutch size, which represents reproductive demand, may also influence oxidative stress because it is related to the heat requirements of seabirds (Biebach, 1984; Moreno et al., 1991; Moreno and Sanz, 1994), including black-tailed gulls (Niizuma et al., 2005). Because black-tailed gulls on Kabushima Island are known to exhibit strong nest site fidelity (Narita and Narita, 2004), we hypothesized that PG individuals may consistently experience lower reproductive success due to interrupted breeding or reduced reproductive investment while simultaneously gaining physiological benefits that enhance self-maintenance and future breeding potential.

2 Methods

2.1 Ethical note

All fieldwork was conducted by highly skilled personnel who had completed comprehensive training in animal experimentation ethics as required by the Animal Experimental Committee of Nagoya University. All procedures used in this study were approved by the Animal Experimental Committee of Nagoya University (V230001-003). Additionally, protocols for capturing birds on Kabushima Island, a national natural monument, were approved by the Hachinohe City Board of Education (permit number 2023-294) and the Aomori Prefectural Government (permit number 2023-3045) under the Ministry of the Environment approval for equipment installation (2404111).

2.2 Field work

This study was conducted at the black-tailed gull breeding site on Kabushima Island, Japan (40°32′20°N, 141°33′26 E) from April to June 2023, coinciding with the breeding season of the species. Intermittent marking surveys have been conducted at the site since 1922. Since 1973, approximately 2,000 chicks have been banded annually with metal rings by the Ministry of the Environment before fledging (Narita and Narita, 2004), allowing for precise age determination and individual identification of many parent birds in the colony. Kabushima Island has been designated a protected natural monument since 1922 and was connected to the mainland in 1943 through land reclamation. The island's perimeter, shrine precincts, and approach roads are open to visitors. In contrast, the remaining areas, from the midsection to the coast, are fenced and designated as protected zones inaccessible to the

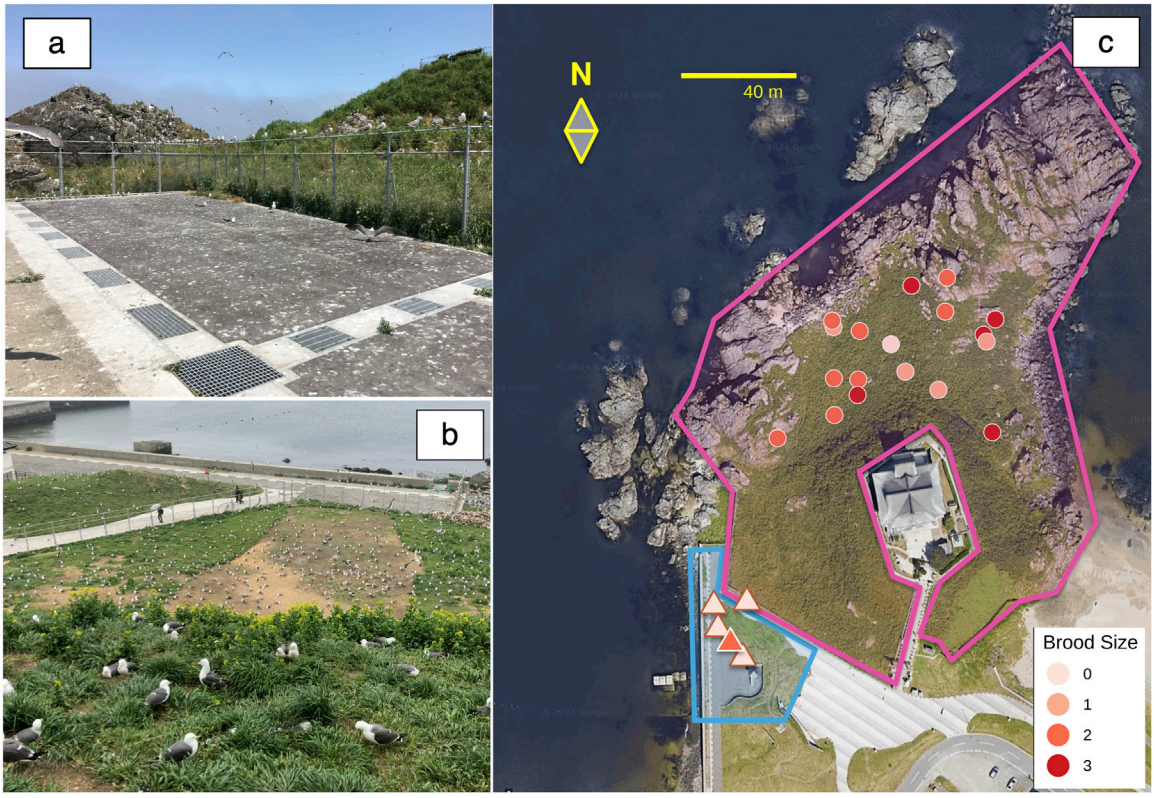

FIGURE 1
Photographs of Kabushima Island and its surroundings **(A, B)** and an aerial view **(C)** (modified from the "Kabushima Island Black-tailed Gull Breeding Ground" Natural Monument Environmental Survey Report). **(A)** The nesting area is located directly outside the fence and is accessible to visitors. **(B)** View from Kabushima Shrine at the island's summit (located on the right hill in (a)), showing the protected zone in the foreground and the unprotected area beyond the fence in the background. **(C)** The pink-outlined area marks the protected zone, fenced on the land side and facing the sea, while the blue-outlined area indicates the accessible, unfenced zone used for the peripheral group survey. The nesting locations within the protected area (Central Group, CG) are shown as circles based on GPS-measured coordinates. In contrast, those outside the protected area (Peripheral Group, PG) are shown as triangles, mapped relative to the fence and fence posts. GPS data were unavailable for one CG individual, and one pair was included, resulting in 18 nests displayed for CG.

public (Figure 1). Approximately 30,000 black-tailed gulls inhabit protected and unprotected areas on and around the island (Biodiversity Center of Japan, 2019). In May 2023, 52 dead individuals were found on and around Kabushima Island. The cause of death was unknown in 50 cases; one case was attributed to predation by a cat, and the other to predation by a bird (FY2024 Kabushima black-tailed gull monitoring report).

The Peripheral Group (PG) consisted of five adult birds marked with metal or numbered plastic rings in 2007 and 2008, nested in unfenced areas or immediately below the fenced region. Individuals were selected based on their rings to ensure a history of consistent nesting in the area. In recent years, no chicks have survived in these areas, and no successful nestlings have been recorded since 2021 (Figure 1C). Observations began during the pre-nesting period, and egg-laying dates, egg measurements, and clutch sizes were recorded upon confirmation of nesting. Parent birds were captured manually during the incubation period. Daily patrols were conducted until all eggs were hatched or 5 days after the expected hatching date. Unhatched eggs were recorded for each nest, and nests with dead chicks or eggshells following the anticipated hatching date were classified as unsuccessful. In 2023, breeding began approximately 2 weeks earlier than in previous years, complicating the determination of exact egg-laying dates for some individuals. For eggs with uncertain laying dates, the incubation periods were estimated based on data from the 2021 and 2022 surveys, in which the laying and hatching dates were confirmed. The incubation period for the first egg was calculated as 28.6 days and standardized to 29 days, whereas that for the second and third eggs was calculated as 26.9 days and standardized to 27 days.

Captured adult birds were weighed, and morphometric measurements were collected. Approximately 700 μL of blood was drawn from the brachial vein, with the area disinfected using a cotton pad soaked in 70% ethanol. Blood was collected using a 25G or 29G syringe (NIPRO, Japan) preloaded with liquid heparin (5,000˚units/5 mL; Mochida Pharmaceutical Co., Ltd., Tokyo, Japan) and stored in microtubes for transport to the laboratory. Subsequent experimental procedures were conducted after ensuring hemostasis at the puncture site. Previous studies have indicated that the volume of blood collected has negligible effects on the behavior, reproductive success, and survival of adult black-tailed gulls (Mizutani et al., 2013).

After blood collection, FLEX II Max devices (15.5 g, Druid Technology, China) were attached to the birds using the harness method (Thaxter et al., 2014; Koyama et al., 2024). A Teflon ribbon

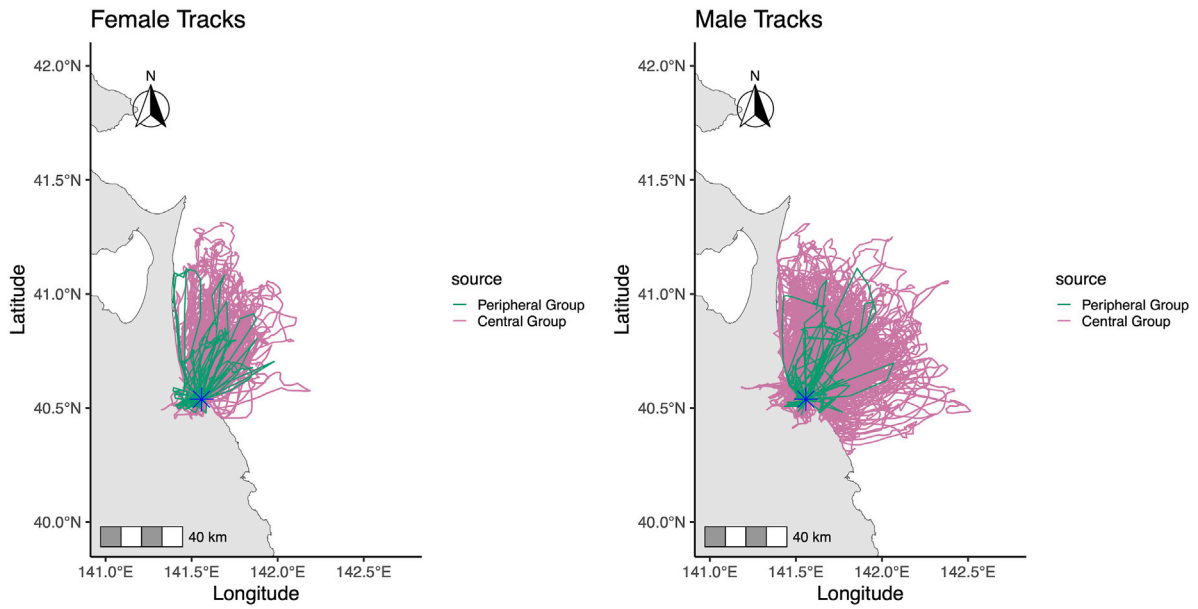

FIGURE 2
Foraging trip tracks of black-tailed gulls on Kabushima Island during the incubation period. Tracks for the Central Group (red; 20 birds: 5 females, 15 males) and the Peripheral Group (green; 5 birds: 3 females, 2 males) are shown. The asterisk marks the location of Kabushima Island.

(TH-25; 6 mm width; BallyRibbonMills, Bally, PA, United States) secured the device on the bird's back. This method, previously employed in black-tailed gulls at this site, has been shown to have minimal effects on survival, reproduction, and behavior over periods exceeding 1 year (Hibiki Sugiyama *in prep.*).

The FLEX II device, powered by solar energy, transmits data via mobile radio, eliminating the need for recapture. Behavioral data were collected continuously, even after breeding efforts ceased. The device was set to the standard mode with a GNSS positioning interval of one point per hour and a communication interval of 8 hours. For comparison, the same behavioral and physiological surveys were conducted on 20 black-tailed gulls nested in a protected area (CG), with blood samples collected for oxidative stress analysis. For the CG birds, a VHF/GPS logger (PinPoint VHF/GPS with solar panels, 82 mm × 25 mm × 27 mm, 18 g; Lotek Wireless Inc., Canada) was used for biologging using the harness method. GPS data for the CG were collected at 5-minute intervals, allowing for detailed multi-year tracking of individual behavior. Because birds that lose their eggs often abandon their nests, communication devices are attached to PG birds to ensure continuous data collection. For the CG birds, we used individuals equipped with a VHF/GPS logger that our research group had deployed for long-term monitoring over multiple years.

2.3 Laboratory procedures: blood processing and oxidative stress assays

The blood samples were transported from the study site to the laboratory in light-protected containers. Within a few hours of collection, samples were centrifuged to separate plasma and hemocyte fractions, which were then stored at −20°C for later oxidative stress assays. DNA was extracted from blood cells obtained after centrifugation using the DNeasy Kit, and sex was determined using a PCR-based method (Fridolfsson and Ellegren, 2000; Mizutani et al., 2016). For oxidative stress measurements, plasma samples were thawed for 1 h before analysis and centrifuged at 14,000 rpm at 4°C for 10 min. A middle plasma layer was used to avoid the contamination of the upper and lower layers. Oxidative stress levels were measured using the Free Carrio Duo system (Diacron International, Grosseto, Italy) with d-ROMs and BAP test reagents, following established protocols to assess oxidative status (d-ROMs in U. CARR) and antioxidant capacity (BAP in μM) (Koyama et al., 2021). To maintain sample integrity, all assays were conducted with samples kept below 10°C. Plasma samples that appeared turbid during measurement were excluded from subsequent analyses and treated as missing values. This affected four individuals in the CG (d-ROM and BAP measurements) and one in the PG (BAP only).

2.4 Laboratory procedures: analysis of biologging data

All behavioral and statistical analyses were conducted using R version 4.3.2 (R Development Core Team, 2023). Only high-accuracy biologging data (GNSS accuracy below 7 HDOP or VDOP) were retained for analysis, and missing values were removed. Because two different devices were used, movement data from the FLEX II and VHF/GPS loggers were standardized and resampled at 30-minute intervals using the adehabitatLT package (version 0.3.28; Calenge, 2006). Data points with speeds exceeding 90 km/h, considered errors, were removed using the ddfilter function of the SDLfilter package (version 2.3.3; Shimada, 2023).

As black-tailed gulls engage in central-place foraging during the breeding season, a foraging trip (hereafter "trip") was defined as any excursion of at least 500 m from the nest that lasted 30 min or more. We defined the distance as the straight-line path between the GPS positioning points recorded by the device and the border between the colony and a nearby location (fishing port) where the birds were expected to stay. The duration, maximum distance from the breeding site, and total distance traveled were calculated as the primary trip parameters for each trip. To ensure consistency within the incubation period, analyses were limited to data collected from May 1st or the device deployment date. This allowed for a more extended period, until the emergence of the first hatchling. As a result, the average analysis periods were 25.4 days (range: 18–31 days) for CG and 21 days (range: 19–23 days) for PG (see supplementary materials).

This study examined whether behavioral and physiological variables differed by nest location and investigated the influence of behavioral parameters (trip duration, maximum distance from the colony, and total trip distance as indicators of foraging effort) and clutch size on oxidative stress markers (d-ROMs and BAP). However, the maximum distance from the colony and the total distance were highly correlated (Pearson correlation coefficients: trip duration and maximum distance, $r = -0.214$; trip duration and total distance, $r = 0.373$; maximum distance and total distance, $r = 0.747$). Because of the wide sampling interval (1 point per 30 min) even after interpolation, the maximum distance from the colony was used as the primary trip distance indicator in subsequent analyses. Bayesian *t*-test was used to evaluate the impact of each variable on oxidative stress levels (d-ROM and BAP). To examine group differences in oxidative stress markers, foraging behaviors during the incubation period (trip duration, maximum reach, total distance, total number of trips during the period, number of days measured, and average number of trips per day based on these figures), and clutch size between the PG and CG, we used Bayes Factor analysis with the BayesFactor package in R (version 0.9.12–4.7; Morey et al., 2024). A Bayes Factor (BF) value greater than one supports the alternative hypothesis, indicating a difference between groups, whereas a value less than one is evidence for the null hypothesis, indicating no difference. In addition, we used BF to confirm the absence of differences between the CG and PG in terms of body mass, and each external measurement was analyzed separately for males and females (see supplementary materials). Moreover, the relationship between clutch size and female body mass was evaluated using a Bayesian linear model, which did not detect a significant relationship between these variables (detailed methods and results are provided in the Supplementary Materials).

3 Results

The average clutch size for the five PG gulls (3 females and 2 males) was 2.4 ± 0.54 SD (range: 2–3). No chicks hatched in four of these nests, whereas in one nest, two chicks hatched; however, the first chick disappeared at 5 days post-hatching, and the second chick died at 4 days of age. Although PG parents remained near the nest after these losses, no additional eggs were laid. For the CG, 20 gulls (5 females and 15 males) were caught during the incubation period, with an average clutch size of 2.25 ± 0.79 SD (range: 1–4), an average of 1.86 ± 0.91 SD (range: 0–3) hatched chicks per clutch, and an average of 1.00 ± 0.77 SD (range: 0–3) fledglings (chicks that survived to 30 days of age). In two CG nests, all eggs failed to hatch.

The PG birds were at least 10 years old, including one born in 2006 and another in 2013 (both identified by metal rings). The other three were captured in 2007 and 2008 and identified using plastic rings. The age of the CG birds ranged from 5 to 24.

The average trip duration and maximum distance traveled were 1.48 ± 3.20 h and 15.72 ± 15.70 km for PG, and 3.26 ± 2.89 h and 24.28 ± 18.89 km for CG (Figures 2, 3). The mean number of daily foraging trips was 3.79 ± 1.24 for CG and 2.75 ± 1.18 for PG, respectively. The mean oxidation levels (d-ROMs) and antioxidant capacity (BAP) were 41.8 ± 25.7 U. CARR and 1,431.0 ± 435.0 μM for PG, and 69.6 ± 25.2 U. CARR and 1,293.0 ± 326.0 μM for CG (Figure 3). In addition, behavioral and oxidative stress measurements of the two CG gulls whose eggs failed to hatch did not deviate from the range observed in the CG group.

The Bayesian *t*-test results showed significant differences in trip duration between the PG and CG, with a Bayes Factor (BF) of 20.97, indicating a strong effect. BF = 4.60 suggested a moderate difference between the groups for the maximum distance traveled. The oxidation level showed weak evidence for a difference with BF = 1.82, whereas the antioxidant capacity (BF = 0.54) showed no difference between the groups. The clutch size also showed no evidence for a difference, with a BF of 0.45. Additionally, the Bayesian *t*-test results for the number of measurement days, the total number of trips, and the average number of trips per day yielded the following BF values: 2.52 for the number of measurement days, providing weak evidence for a difference between the groups, 148.30 for the total number of trips, providing strong evidence for a difference; and 21.90 for the average number of trips per day, also providing strong evidence for a difference.

4 Discussion

The PGs could not raise chicks because of several factors, including non-hatching, egg loss, and chick mortality, a pattern similar to that observed in previous years for most parents in peripheral areas. It is unclear whether non-hatching results from unfertilized eggs or inadequate embryonic development. This is because the PG area was easily accessible to tourists and feral cats, frequent disturbances caused parents to leave their nests. These disturbances are likely to reduce hatching success, either through direct nest attacks or lowered nest temperatures linked to shortened incubation periods (Di Giovanni et al., 2022; Clemencin et al., 2024), as well as increased stress resulting from proximity to disturbances (Ellenberg et al., 2007).

Regardless of hatching success, the antioxidant capacity was similar between the PG and CG, indicating that the intra-species variation in antioxidant capacity was slight. This finding suggests that black-tailed gulls maintain comparable levels of non-enzymatic endogenous antioxidants (e.g., vitamins A and E, uric acid; Sharma et al., 2018) and exogenous antioxidants (e.g., coenzyme Q10; Zozina et al., 2018) and carotenoids (Milani et al., 2017). In contrast, differences in foraging movements and oxidative stress levels suggest that the primary defense against oxidative stress during the breeding season likely

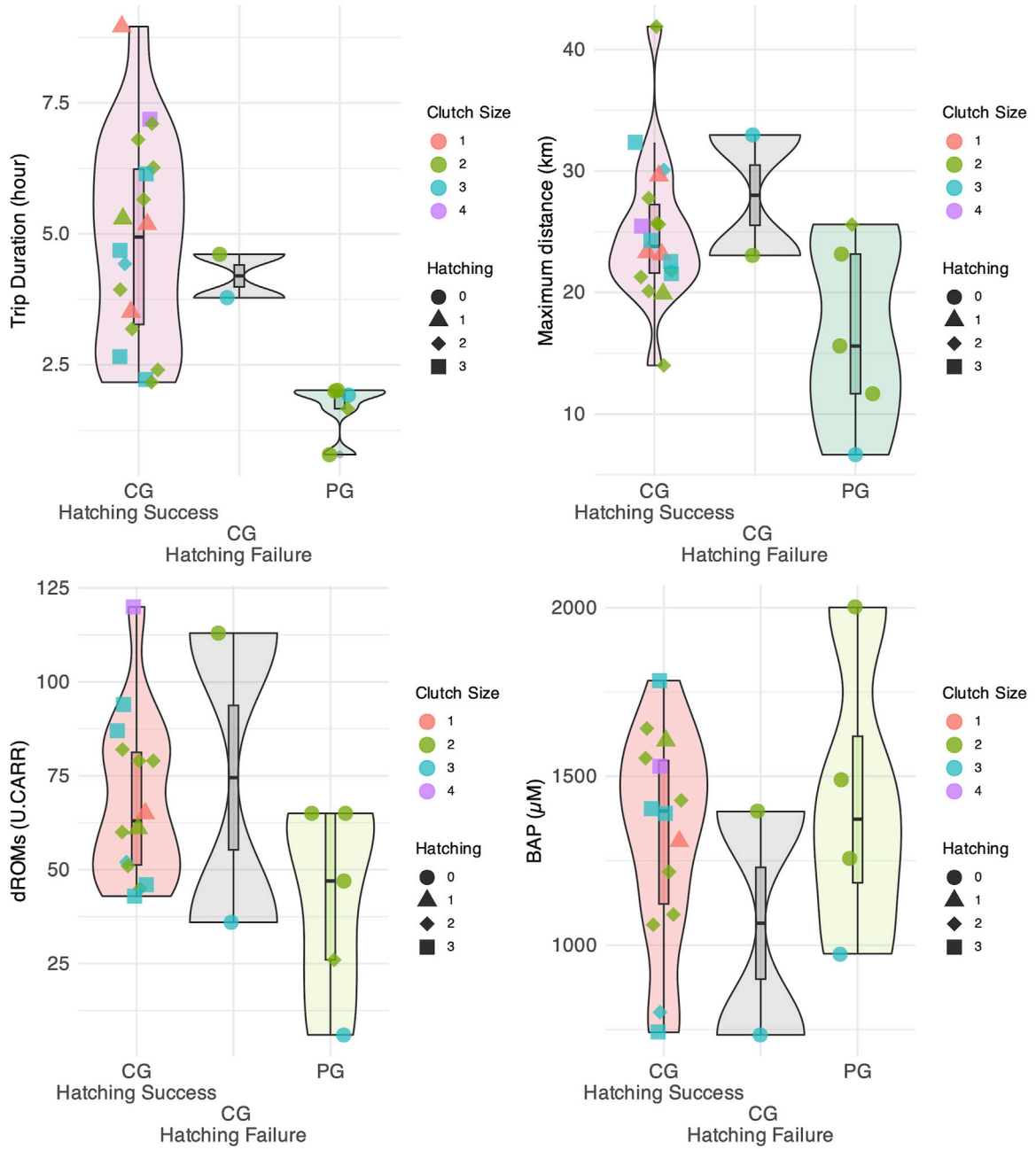

FIGURE 3
Distribution of trip duration, maximum distance reached from the colony, oxidation levels, and antioxidant capacity for the Peripheral Group (PG) and Central Group (CG). The CG is further divided into groups based on whether egg hatching was successful or not.

depends on endogenous enzymes such as glutathione peroxidase. Similar to other bird species (McWilliams et al., 2021), glutathione peroxidase may serve as the first line of defense against ROS. Consequently, if the observed levels of foraging and breeding efforts remain within the capacity of endogenous enzymatic systems, the immediate need for additional exogenous antioxidants may be minimal.

Compared to the CG, the PG exhibited significantly shorter trip durations, a smaller maximum distance reached (strongly correlated with the total distance), and a lower frequency of foraging trips. Black-tailed gulls on Kabushima Island utilize a variety of feeding grounds and consume a broad diet beyond fish and shellfish (Yoda et al., 2012; Mizutani et al., 2021). Their regurgitated food items include freshwater fish and insects (Narita and Narita, 2004). Although the exact types and quantities of food consumed in this study remain unknown, the foraging range of PG overlapped substantially with that of CG, and no differences in antioxidant levels were observed between the groups. This suggests that both the PG and CG consumed similar types and amounts of food. However, the observed differences in foraging behavior likely influenced

energy expenditure, leading to slight differences in ROS production and oxidation levels.

Although antioxidant levels were similar between individuals, PG exhibited lower oxidation levels, possibly due to nearby, shorter foraging trips and a lower daily foraging frequency. Gull species spend much of their flying time flapping their wings, a highly energy-intensive activity (Bishop, 2005; Mizrahy-Rewald et al., 2022) that likely increases energy consumption and ROS production. Additionally, the incubation period imposes significant physiological costs on the parent birds. For example, in common eiders (*Somateria mollissima*), high incubation demands lead to weight loss and decreased immune function due to reduced food intake, resulting in decreased fertility in the following year and long-term fitness costs (Hanssen et al., 2005). In contrast, the failed hatching observed in PG suggests inadequate incubation, which would have led to lower incubation costs. Although breeding costs are generally buffered during the non-breeding season (Senner et al., 2014; Briedis et al., 2018; Gow et al., 2019), consistently reduced breeding investment may minimize negative carryover effects in subsequent seasons.

PG individuals experienced consistently low reproductive success over multiple years; however, it is intriguing that they do not change their nesting locations. They may lack the competitive ability to secure favorable nest sites. Instead, the low oxidative stress associated with less demanding foraging trips may offset the high reproductive costs borne by CG individuals, reflecting an underlying life-history trade-off. Our results indicate that a peripheral-central distribution generates heterogeneity in reproductive success within a colony. However, the peripheral groups may gain fitness benefits by occasionally foregoing reproduction. Future research should investigate behavioral differences during the incubation, chick-rearing, and non-breeding periods, as well as their long-term physiological costs. Such investigations would enable a more comprehensive evaluation of rearing costs within the broader framework of life-history trade-offs. From a conservation perspective, completely fencing off all black-tailed gull nesting areas to protect PG groups from predators and human disturbances may be impractical. Instead, phased measures, such as deterrents against easily accessible small terrestrial mammals and visitor restrictions, combined with countermeasures such as fencing, which are considered critical to success, are expected to improve the hatching success rate of PGs.

One limitation of this study is the absence of continuously recorded physiological data. Blood, a vital biomarker source, is widely used in diagnostics and research (Toner and Irimia, 2005), underscoring the significant demand for real-time blood sampling loggers. Wearable automatic blood-sampling devices designed to minimize pain and distress are being developed for use in captivity settings (Li et al., 2009; Li et al., 2015; Hopper, 2016). While the long-term collection of blood from wild flying animals remains challenging, advances in non-invasive techniques, such as continuous glucose monitoring via interstitial fluid (Mathew et al., 2024), offer promising alternatives. Deploying such technologies in seabirds could revolutionize biologging, enabling researchers to explore how species balance reproduction and survival, respond to environmental disturbances, and allocate energy across life-history stages.

Data availability statement

The raw data supporting the conclusions of this article will be made available by the authors, without undue reservation.

Ethics statement

The animal study was approved by the Animal Experimental Committee of Nagoya University (GSES2023) the Hachinohe City Board of Education (permit number 2023-3045) the Aomori Prefectural Government (permit number 2023-3045) the Ministry of the Environment approval for equipment installation (V230001-003, V230005-003). The study was conducted in accordance with the local legislation and institutional requirements.

Author contributions

YM: Conceptualization, Data curation, Formal Analysis, Funding acquisition, Investigation, Methodology, Project administration, Resources, Validation, Visualization, Writing–original draft, Writing–review and editing. YG: Formal Analysis, Validation, Writing–original draft, Writing–review and editing. AS: Validation, Writing–original draft, Writing–review and editing. KY: Funding acquisition, Supervision, Validation, Writing–original draft, Writing–review and editing.

Funding

The author(s) declare that financial support was received for the research, authorship, and/or publication of this article. This study was supported by Grants-in-Aid for Scientific Research from the Japan Society for the Promotion of Science (Grant numbers 18K14788, 23K05918, and 21H05294) and CREST, Japan Science and Technology Agency (Grant number JPMJCR23P2).

Acknowledgments

We are grateful to A. Narita, the staff at the observation post on Kabushima Island, and our colleagues for their help in conducting the experiments. We would like to thank Editage (www.editage.jp) for English language editing.

Conflict of interest

The authors declare that the research was conducted in the absence of any commercial or financial relationships that could be construed as a potential conflict of interest.

Generative AI statement

The author(s) declare that Generative AI was used in the creation of this manuscript. We used the AI-assisted

technologies, ChatGPT and Claude, in preparing this article to correct grammar and translate it into English. After using this tool, we reviewed and edited the content as necessary. We take full responsibility for the content of this study.

Publisher's note

Supplementary material

The Supplementary Material for this article can be found online at: https://www.frontiersin.org/articles/10.3389/fphys.2025.1519701/full#supplementary-material

References

Aebischer, N. J., and Coulson, J. C. (1990). Survival of the kittiwake in relation to sex, year, breeding experience and position in the colony. *J. Anim. Ecol.* 59, 1063–1071. doi:10.2307/5031

Ahmadi, M. R., Bazyar, A. A., Safi, S., Ytrestøyl, T., and Bjerkeng, B. (2006). Effects of dietary astaxanthin supplementation on reproductive characteristics of rainbow trout (*Oncorhynchus mykiss*). *J. Appl. Ichthyol.* 22, 388–394. doi:10.1111/j.1439-0426.2006.00770.x

Aubry, L. M., Cam, E., and Monnat, J.-Y. (2009). "Habitat selection, age-specific recruitment and reproductive success in a long-lived seabird," in *Modeling demographic processes in marked populations*. Editors D. L. Thomson, E. G. Cooch, and M. J. Conroy (Boston, MA: Springer US), 365–392. doi:10.1007/978-0-387-78151-8_16

Biebach, H. (1984). Effect of clutch size and time of day on the energy expenditure of incubating starlings (*Sturnus vulgaris*). *Physiol. Zool.* 57, 26–31. doi:10.1086/physzool.57.1.30155963

Biodiversity Center of Japan (2019). Monitoring sites 1000 seabird survey report. Preprint at 2019. *Ministry Environ.* Available at: https://www.biodic.go.jp/moni1000/findings/reports/pdf/2019_seabirds.pdf (Accessed December 7, 2023).

Birkhead, T. R. (1977). The effect of habitat and density on breeding success in the common guillemot (*Uria aalge*). *J. Anim. Ecol.* 46, 751–764. doi:10.2307/3638

Bishop, C. M. (2005). Circulatory variables and the flight performance of birds. *J. Exp. Biol.* 208, 1695–1708. doi:10.1242/jeb.01576

Bosch, M., and Sol, D. (1998). Habitat selection and breeding success in Yellow-legged Gulls *Larus cachinnans*. *Ibis* 140, 415–421. doi:10.1111/j.1474-919X.1998.tb04602.x

Briedis, M., Krist, M., Král, M., Voigt, C. C., and Adamík, P. (2018). Linking events throughout the annual cycle in a migratory bird—non-breeding period buffers accumulation of carry-over effects. *Behav. Ecol. Sociobiol.* 72, 93. doi:10.1007/s00265-018-2509-3

Brodin, A. (2001). Mass-dependent predation and metabolic expenditure in wintering birds: is there a trade-off between different forms of predation? *Anim. Behav.* 62, 993–999. doi:10.1006/anbe.2001.1844

Brown, J. S., and Kotler, B. P. (2004). Hazardous duty pay and the foraging cost of predation: foraging cost of predation. *Ecol. Lett.* 7, 999–1014. doi:10.1111/j.1461-0248.2004.00661.x

Calenge, C. (2006). The package adehabitat for the R software: a tool for the analysis of space and habitat use by animals. *Compr. R. Arch. Netw. (CRAN)* 197, 516–519. doi:10.1016/j.ecolmodel.2006.03.017

Christe, P., Glaizot, O., Strepparava, N., Devevey, G., and Fumagalli, L. (2012). Twofold cost of reproduction: an increase in parental effort leads to higher malarial parasitaemia and to a decrease in resistance to oxidative stress. *Proc. Biol. Sci.* 279, 1142–1149. doi:10.1098/rspb.2011.1546

Clemencin, L., Barba, E., and Diez-Méndez, D. (2024). Research disturbance negatively impacts incubation behaviour of female great tits. *Behav. Ecol. Sociobiol.* 78, 99. doi:10.1007/s00265-024-03514-y

Coulson, J. C. (1968). Differences in the quality of birds nesting in the centre and on the edges of a colony. *Nature* 217, 478–479. doi:10.1038/217478a0

Di Giovanni, A. J., Miller, M. J., Jones, T. M., Benson, T. J., and Ward, M. P. (2022). Hatching failure is greater in altricial bird species with cavity nests and large clutches. *Auk* 140, ukac048. doi:10.1093/ornithology/ukac048

Dröge, W. (2002). Free radicals in the physiological control of cell function. *Physiol. Rev.* 82, 47–95. doi:10.1152/physrev.00018.2001

Ellenberg, U., Setiawan, A. N., Cree, A., Houston, D. M., and Seddon, P. J. (2007). Elevated hormonal stress response and reduced reproductive output in Yellow-eyed penguins exposed to unregulated tourism. *Gen. Comp. Endocrinol.* 152, 54–63. doi:10.1016/j.ygcen.2007.02.022

Fletcher, Q. E., Selman, C., Boutin, S., McAdam, A. G., Woods, S. B., Seo, A. Y., et al. (2013). Oxidative damage increases with reproductive energy expenditure and is reduced by food-supplementation. *Evolution* 67, 1527–1536. doi:10.1111/evo.12014

Fowler, M. A., and Williams, T. D. (2017). A physiological signature of the cost of reproduction associated with parental care. *Am. Nat.* 190, 762–773. doi:10.1086/694123

Fridolfsson, A. K., and Ellegren, H. (2000). Molecular evolution of the avian CHD1 genes on the Z and W sex chromosomes. *Genetics* 155, 1903–1912. doi:10.1093/genetics/155.4.1903

Gow, E. A., Burke, L., Winkler, D. W., Knight, S. M., Bradley, D. W., Clark, R. G., et al. (2019). A range-wide domino effect and resetting of the annual cycle in a migratory songbird. *Proc. Biol. Sci.* 286, 20181916. doi:10.1098/rspb.2018.1916

Hanssen, S. A., Hasselquist, D., Folstad, I., and Erikstad, K. E. (2005). Cost of reproduction in a long-lived bird: incubation effort reduces immune function and future reproduction. *Proc. Biol. Sci.* 272, 1039–1046. doi:10.1098/rspb.2005.3057

Hopper, L. D. (2016). Automated microsampling technologies and enhancements in the 3Rs. *ILAR J.* 57, 166–177. doi:10.1093/ilar/ilw020

Indykiewicz, P., Podlaszczuk, P., Kamiński, M., Włodarczyk, R., and Minias, P. (2019). Central–periphery gradient of individual quality within a colony of Black-headed Gulls. *Ibis* 161, 744–758. doi:10.1111/ibi.12689

Kazama, K., Nishizawa, B., Tsukamoto, S., Gonzalez, J. E., Kazama, M. T., and Watanuki, Y. (2018). Male and female Black-tailed Gulls *Larus crassirostris* feed on the same prey species but use different feeding habitats. *J. Ornithol.* 159, 923–934. doi:10.1007/s10336-018-1565-9

Kim, S.-Y., and Monaghan, P. (2005). Effects of vegetation on nest microclimate and breeding performance of lesser black-backed gulls (*Larus fuscus*). *J. Ornithol.* 146, 176–183. doi:10.1007/s10336-005-0077-6

Kokko, H., Harris, M. P., and Wanless, S. (2004). Competition for breeding sites and site-dependent population regulation in a highly colonial seabird, the common guillemot *Uria aalge*. *J. Anim. Ecol.* 73, 367–376. doi:10.1111/j.0021-8790.2004.00813.x

Koyama, S., Mizutani, Y., Matsumoto, S., and Yoda, K. (2024). Interannual linkages between oceanographic condition, seabird behaviour and chick growth from a decadal biologging study. *Anim. Behav.* 209, 63–81. doi:10.1016/j.anbehav.2023.12.012

Koyama, S., Mizutani, Y., and Yoda, K. (2021). Exhausted with foraging: foraging behavior is related to oxidative stress in chick-rearing seabirds. *Comp. Biochem. Physiol. A* 258, 110984. doi:10.1016/j.cbpa.2021.110984

Li, C. G., Dangol, M., Lee, C. Y., Jang, M., and Jung, H. (2015). A self-powered one-touch blood extraction system: a novel polymer-capped hollow microneedle integrated with a pre-vacuum actuator. *Lab. Chip* 15, 382–390. doi:10.1039/c4lc00937a

Li, T., Barnett, A., Rogers, K. L., and Gianchandani, Y. B. (2009). A blood sampling microsystem for pharmacokinetic applications: design, fabrication, and initial results. *Lab. Chip* 9, 3495–3503. doi:10.1039/b910508e

Lin, Y., Patterson, A., Jimenez, A. G., and Elliott, K. (2022). Altered oxidative status as a cost of reproduction in a seabird with high reproductive costs. *Physiol. Biochem. Zool.* 95, 35–53. doi:10.1086/717916

Markó, G., Costantini, D., Michl, G., and Török, J. (2011). Oxidative damage and plasma antioxidant capacity in relation to body size, age, male sexual traits and female reproductive performance in the collared flycatcher (*Ficedula albicollis*). *J. Comp. Physiol. B* 181, 73–81. doi:10.1007/s00360-010-0502-x

Mathew, T. K., Zubair, M., and Tadi, P. (2024). "Blood glucose monitoring," in *StatPearls* (Treasure Island, FL: StatPearls Publishing). Available at: https://europepmc.org/article/NBK/nbk555976 (Accessed November 29, 2024).

McWilliams, S., Carter, W., Cooper-Mullin, C., DeMoranville, K., Frawley, A., Pierce, B., et al. (2021). How birds during migration maintain (oxidative) balance. *Front. Ecol. Evol.* 9, 742642. doi:10.3389/fevo.2021.742642

Milani, A., Basirnejad, M., Shahbazi, S., and Bolhassani, A. (2017). Carotenoids: biochemistry, pharmacology and treatment. *Br. J. Pharmacol.* 174, 1290–1324. doi:10.1111/bph.13625

Minias, P. (2014). Evolution of within-colony distribution patterns of birds in response to habitat structure. *Behav. Ecol. Sociobiol.* 68, 851–859. doi:10.1007/s00265-014-1697-8

Mizrahy-Rewald, O., Perinot, E., Fritz, J., Vyssotski, A. L., Fusani, L., Voelkl, B., et al. (2022). Empirical evidence for energy efficiency using intermittent gliding flight in Northern Bald Ibises. *Front. Ecol. Evol.* 10, 891079. doi:10.3389/fevo.2022.891079

Mizutani, Y., Niizuma, Y., and Yoda, K. (2016). How do growth and sibling competition affect telomere dynamics in the first month of life of long-lived seabird? *PLoS One* 11, 01672611–e167314. doi:10.1371/journal.pone.0167261

Mizutani, Y., Suzuki, H., Maekawa, T., Korpela, J., Miyatake, T., Koshiyama, Y., et al. (2021). Capture of flying insects by Black-tailed Gulls *Larus crassirostris* over inland and offshore areas. *Jpn. J. Ornithol.* 70, 53–60. doi:10.3838/jjo.70.53

Mizutani, Y., Tomita, N., Niizuma, Y., and Yoda, K. (2013). Environmental perturbations influence telomere dynamics in long-lived birds in their natural habitat. *Biol. Lett.* 9, 20130511. doi:10.1098/rsbl.2013.0511

Monaghan, P., Metcalfe, N. B., and Torres, R. (2008). Oxidative stress as a mediator of life history trade-offs: mechanisms, measurements and interpretation. *Biol. Lett.* 12, 75–92. doi:10.1111/j.1461-0248.2008.01258.x

Montevecchi, W. A. (1978). Nest site selection and its survival value among laughing gulls. *Behav. Ecol. Sociobiol.* 4, 143–161. doi:10.1007/bf00354977

Moreno, J., Gustafsson, L., Carlson, A., and Pärt, T. (1991). The cost of incubation in relation to clutch-size in the Collared Flycatcher *Ficedula albicollis*. *Ibis* 133, 186–193. doi:10.1111/j.1474-919x.1991.tb04830.x

Moreno, J., and Sanz, J. J. (1994). The relationship between the energy expenditure during incubation and clutch size in the pied flycatcher ficedula hypoleuca. *J. Avian Biol.* 25, 125. doi:10.2307/3677030

Morey, R. D., Rouder, J. N., Jamil, T., Urbanek, S., Forner, K., and Ly, A. (2024). Computation of Bayes factors for common designs [R package BayesFactor version 0.9.12-4.7]. *Compr. R. Arch. Netw. (CRAN)*. Available at: https://CRAN.R-project.org/package=BayesFactor (Accessed October 1, 2024).

Narita, K., and Narita, A. (2004). Observation reports of black-tailed gull: Kabushima-Island Hachinohe city (in Japanese). *Hachinohe Kimura-Shoten*.

Niizuma, Y., Takagi, M., Senda, M., Chochi, M., and Watanuki, Y. (2005). Incubation capacity limits maximum clutch size in black-tailed gulls *Larus crassirostris*. *J. Avian Biol.* 36, 421–427. doi:10.1111/j.0908-8857.2005.03252.x

Noguera, J. C., Kim, S. Y., and Velando, A. (2012). Pre-fledgling oxidative damage predicts recruitment in a long-lived bird. *Biol. Lett.* 8, 61–63. doi:10.1098/rsbl.2011.0756

Noguera, J. C., Monaghan, P., and Metcalfe, N. B. (2015). Interactive effects of early and later nutritional conditions on the adult antioxidant defence system in zebra finches. *J. Exp. Biol.* 218, 2211–2217. doi:10.1242/jeb.120956

Nussey, D., Pemberton, J., Pilkington, J., and Blount, J. D. (2009). Life history correlates of oxidative damage in a free-living mammal population. *Funct. Ecol.* 23, 809–817. doi:10.1111/J.1365-2435.2009.01555.X

Pagenaud, A., Ravache, A., Bourgeois, K., Mathivet, M., Bourguet, É., Vidal, É., et al. (2022). Nest-site selection and its influence on breeding success in a poorly-known and declining seabird: the Tahiti petrel Pseudobulweria rostrata. *PLoS One* 17, e0267408. doi:10.1371/journal.pone.0267408

Pearce, J. M. (2007). Philopatry: a return to origins. *Auk* 124, 1085–1087. doi:10.1093/auk/124.3.1085

Piro, S., and Schmitz Ornés, A. (2021). Nest site tenacity and mate fidelity in the Black-headed Gull (*Chroicocephalus ridibundus*). *Avian Res.* 12, 63–67. doi:10.1186/s40657-021-00300-6

R Development Core Team (2023). A language and environment for statistical computing. *R Found. Stat. Comput.* Available at: https://www.r-project.org/ (Accessed October 28, 2024).

Rodway, M. S., and Regehr, H. M. (1999). Habitat selection and reproductive performance of food-stressed herring gulls. *Condor* 101, 566–576. doi:10.2307/1370186

Rounds, R. A., Erwin, R. M., and Porter, J. H. (2004). Nest-site selection and hatching success of waterbirds in coastal Virginia: some results of habitat manipulation. *J. Field Ornithol.* 75, 317–329. doi:10.1648/0273-8570-75.4.317

Ryder, P. L., and Ryder, J. P. (1981). Reproductive performance of ring-billed gulls in relation to nest location. *Condor* 83, 57. doi:10.2307/1367603

Senner, N. R., Hochachka, W. M., Fox, J. W., and Afanasyev, V. (2014). An exception to the rule: carry-over effects do not accumulate in a long-distance migratory bird. *PLoS One* 9, e86588. doi:10.1371/journal.pone.0086588

Serrano, D., and Tella, J. L. (2007). The role of despotism and heritability in determining settlement patterns in the colonial lesser kestrel. *Am. Nat.* 169, E53–E67. doi:10.1086/510598

Sharma, G. N., Gupta, G., and Sharma, P. (2018). A comprehensive review of free radicals, antioxidants, and their relationship with human ailments. *Crit. Rev. Eukaryot. Gene Expr.* 28, 139–154. doi:10.1615/CritRevEukaryotGeneExpr.2018022258

Shaw, P. (1985). Age-differences within breeding pairs of Blue-eyed Shags *Phalacrocorax atriceps*. *Ibis* 127, 537–543. doi:10.1111/j.1474-919x.1985.tb04849.x

Shimada, T. (2023). SDLfilter: an R package for filtering and assessing the sample size of tracking data. *Github*. Available at: https://github.com/TakahiroShimada/SDLfilter/tree/master (Accessed September 26, 2024).

Spurr, E. B. (1975). Breeding of the adélie penguin pygoscelis adeliae at cape bird. *Ibis* 117, 324–338. doi:10.1111/j.1474-919X.1975.tb04220.x

Tenaza, R. (1971). Behavior and nesting success relative to nest location in Adelie penguins (*Pygoscelis adeliae*). *Condor* 73, 81–92. doi:10.2307/1366127

Thaxter, C. B., Ross-Smith, V. H., Clark, J. A., Clark, N. A., Conway, G. J., Marsh, M., et al. (2014). A trial of three harness attachment methods and their suitability for long-term use on Lesser Black-backed Gulls and Great Skuas. *Ringing Migr.* 29, 65–76. doi:10.1080/03078698.2014.995546

Toner, M., and Irimia, D. (2005). Blood-on-a-chip. *Annu. Rev. Biomed. Eng.* 7, 77–103. doi:10.1146/annurev.bioeng.7.011205.135108

Vergara, P., and Aguirre, J. I. (2006). Age and breeding success related to nest position in a White stork *Ciconia ciconia* colony. *Acta oecol. (Montrouge)* 30, 414–418. doi:10.1016/j.actao.2006.05.008

Vine, I. (1971). Risk of visual detection and pursuit by a predator and the selective advantage of flocking behaviour. *J. Theor. Biol.* 30, 405–422. doi:10.1016/0022-5193(71)90061-0

Yoda, K., Tomita, N., Mizutani, Y., Narita, A., and Niizuma, Y. (2012). Spatio-temporal responses of black-tailed gulls to natural and anthropogenic food resources. *Mar. Ecol. Prog. Ser.* 466, 249–259. doi:10.3354/meps09939

Zozina, V. I., Covantev, S., Goroshko, O. A., Krasnykh, L. M., and Kukes, V. G. (2018). Coenzyme Q10 in cardiovascular and metabolic diseases: current state of the problem. *Curr. Cardiol. Rev.* 14, 164–174. doi:10.2174/1573403X14666180416115428

frontiers | Frontiers in Physiology

TYPE Original Research
PUBLISHED 19 March 2025
DOI 10.3389/fphys.2025.1509511

OPEN ACCESS

EDITED BY
J. Chris McKnight,
University of St Andrews, United Kingdom

REVIEWED BY
Kentaro Q. Sakamoto,
The University of Tokyo, Japan
Yuya Makiguchi,
Nihon University, Japan

*CORRESPONDENCE
Shiho Koyama,
koyama.shiho.f0@a.mail.nagoya-u.ac.jp

RECEIVED 11 October 2024
ACCEPTED 25 February 2025
PUBLISHED 19 March 2025

CITATION
Koyama S, Mizutani Y, Goto Y and Yoda K (2025) Species-specific physiological status in seabirds: insights from integrating oxidative stress measurements and biologging. *Front. Physiol.* 16:1509511. doi: 10.3389/fphys.2025.1509511

Species-specific physiological status in seabirds: insights from integrating oxidative stress measurements and biologging

Shiho Koyama *, Yuichi Mizutani , Yusuke Goto and Ken Yoda

Graduate School of Environmental Studies, Nagoya University, Nagoya, Japan

Understanding the relationship between behavior and physiological state, as well as species differences in physiological responses, is key to identifying the behavioral and physiological adaptations necessary for wild animals to avoid physiological deterioration, thereby enhancing their survival and fitness. A commonly used measure of physiological condition is oxidative stress, which results from an imbalance between oxidative damage—often exacerbated by respiration during exercise and indicative of physical harm—and antioxidant capacity, which reflects the organism's ability to recover from such damage. Despite its importance, oxidative stress has rarely been linked to behavior, such as foraging, leaving this relationship underexplored. In this study, we focused on two seabird species, black-tailed gulls (*Larus crassirostris*) and streaked shearwaters (*Calonectris leucomelas*), which are similar in body size and primarily forage on the same prey species but differ in traits such as habitat, flight style, and physiological function. We recorded the trajectories of these birds for approximately 1 week using biologging and measured their plasma oxidative stress. We found that oxidative stress in black-tailed gulls was higher than that in streaked shearwaters, suggesting that species differences in life histories, habitats, and physiological function may be related to long-term oxidative stress. However, over a 1-week timescale, there were no significant species differences in changes in oxidative stress, suggesting that behavioral differences between the two species might not necessarily lead to species-specific oxidative stress responses in the short term. Additionally, no consistent relationship was found between changes in oxidative stress of the two species and their behavioral metrics in most years, suggesting that this relationship may vary depending on yearly environmental fluctuations. Based on our findings, we encourage future studies that would explore and integrate the interactions between marine environments, behavior, and oxidative stress of different bird species to clarify the contribution of specific foraging behaviors to either the deterioration or recovery of physiological conditions, and the varying effect of environmental conditions on these relationships.

KEYWORDS

marine animals, antioxidants, pro-oxidant, gulls, shearwaters, BAP, d-ROMs, GPS

1 Introduction

Wild animals attempt to minimize physiological deterioration, such as reduction in nutrition (Bishop et al., 2009) and immunity (Cabezas et al., 2011) and increase in stress hormones (Kitaysky et al., 2007; Romero and Wikelski, 2010; Wey et al., 2015) and oxidative stress (Noguera et al., 2012; Costantini and Dell'Omo, 2015), that can reduce their survival and fitness. In particular, long-lived animals with multiple breeding opportunities are likely to behave efficiently to minimize physiological deterioration and successfully raise offspring during the breeding period to ensure both current and future reproductive success by adjusting their foraging and provisioning behaviors, such as locomotion style, time spent foraging, and the distance to the foraging site (Killen et al., 2013; Cooke et al., 2014; Crino et al., 2017). These behavioral adaptations can vary significantly among species based on their life history and habitat, leading to differences in how foraging and provisioning behaviors impact physiological conditions across species. To understand species-specific behavioral adaptation, it is necessary to assess which foraging and provisioning behaviors contribute to either the deterioration or recovery of physiological conditions and how these differ between species.

In addition to individual-level responses, wild animals are expected to develop species-specific tolerance to physiological deterioration depending on their habitat and life history (McCue, 2010; Bozinovic et al., 2011). Laboratory experiments have demonstrated species differences in physiological conditions and survival under stressors such as starvation, drugs, and parasites (Haley, 2003; Matzkin et al., 2009; Rohr et al., 2010). Evaluating species differences in tolerance of wild animals may lead to a deeper understanding of their physiological adaptations to habitats and life histories (Hermes-Lima and Zenteno-Savín, 2002; Kroeger et al., 2019).

Oxidative stress, an indicator of physiological condition, results from an imbalance between oxidative damage, such as reactive oxygen species (ROS) generated by respiration, and antioxidant capacity (Sies, 1997; Urso and Clarkson, 2003). While ROS can eliminate pathogens in body tissues, excessive accumulation damages biomolecules such as DNA, proteins, and lipids, leading to physiological deterioration (Filomeni et al., 2015; Sies et al., 2017). This deterioration reduces the efficiency of energy metabolism mainly by interfering with mitochondrial function (Pan et al., 2008) and causing physical fatigue. Antioxidant capacity comprises both endogenous antioxidants produced within the body and exogenous antioxidants obtained from food, which removes ROS and oxidized biomolecules, facilitating recovery from oxidative damage (Shahidi, 2000; Pisoschi and Pop, 2015). Thus, oxidized biomolecules indicate physiological deterioration, whereas exogenous antioxidant capacity obtained through foraging reflects tolerance to oxidative damage.

In wild birds, oxidative stress is linked to fitness factors such as individual resistance probability (Saino et al., 2011; Noguera et al., 2012; Costantini and Dell'Omo, 2015), reproductive decisions (Costantini et al., 2020), reproductive success (Losdat et al., 2013; Costantini et al., 2015), behavioral traits like migration (Larcombe et al., 2008; Alan and McWilliams, 2013) and foraging behavior (Koyama et al., 2021), as well as external factors such as urbanization, environmental pollution (Espín et al., 2016; Isaksson et al., 2017; Salmón et al., 2018), and pathogens (Costantini and Dell'Omo, 2006; Isaksson et al., 2013; Sebastiano et al., 2017). Therefore, measuring oxidative damage and antioxidant capacity, which may be associated with behavior and fitness, is ideal for quantifying the physiological deterioration and resilience of wild birds. However, few studies have combined detailed measurements of foraging and movement behavior with oxidative stress data in wild animals, and the combination of oxidative stress measurements with precise behavioral tracking enabled by biologging remains particularly rare. As a result, our understanding of the relationship between behavior and oxidative stress remains limited.

Here, we focused on two seabirds, black-tailed gull (*Larus crassirostris*) and streaked shearwater (*Calonectris leucomelas*), which are similar in body size (Chochi et al., 2002; Shirai et al., 2013) and primarily feed on small fish such as anchovies (Narita and Narita, 2004; Kurasawa et al., 2012; Matsumoto et al., 2012; Yoda et al., 2012; Kazama et al., 2018; De Alwis et al., 2025). During the breeding season, we recorded the behavior of these birds for approximately 1 week by using GPS loggers attached to them. Additionally, we measured changes in oxidative stress at the beginning and end of the behavioral recording. Species differences in oxidative stress levels were used as an indicator of chronic physiological stress that is expected to be linked to their habitat, life history, and physiological function. During the breeding season, black-tailed gulls, which often inhabit urban areas (Yoda et al., 2012), typically lay two to three eggs (Tomita and Narita, 2021), whereas the streaked shearwaters found in rural areas lay one egg (Oka et al., 2002; Oka, 2004; Koyama et al., 2024b). During the non-breeding season, black-tailed gulls move around the Japanese Archipelago (Tomita et al., 2015), whereas streaked shearwaters migrate to tropical regions near the equator (Yamamoto et al., 2010). These reproductive or migratory differences may cause differences in oxidative stress levels. The species differences in the changes in oxidative stress levels were also used as a reflection of the accumulation of physiological deterioration or recovery due to the recorded behavior. During the breeding season, black-tailed gulls take round trips from the colony to the foraging site (foraging trip) several times per day and forage in coastal and land areas relatively close to their breeding sites (Yoda et al., 2012; Kazama et al., 2018; Park et al., 2024). In contrast, streaked shearwaters undertake foraging trips lasting from one to 14 days and forage around the colony and in the open ocean (Yoda et al., 2014; Matsumoto et al., 2017; Koyama et al., 2024b). Differences in foraging behavior may lead to species-specific changes in oxidative stress over a weekly timescale. Finally, we examined the relationship between foraging behavior and changes in oxidative stress to evaluate the types of behaviors that affect oxidative stress. For example, increasing the foraging time, during which individuals obtain food, is expected to decrease oxidative stress. Additionally, the influence of foraging and provisioning behaviors on oxidative stress may vary depending on the species. For instance, streaked shearwaters, which adopt energy-saving flight called dynamic soaring (Mir et al., 2018), may not generate ROS compared to black-tailed gulls, which adopt flapping flight, due to differences in heart rate increases associated with these flight styles (Ropert-Coudert et al., 2006; Sakamoto et al., 2013). Thus, it is expected that increasing flight distance would elevate

oxidative stress in flapping black-tailed gulls but does not have a significant effect on soaring streaked shearwaters.

2 Method

2.1 Fieldwork and data collection

Fieldwork was conducted on egg-laying black-tailed gulls in Kabushima Island (40° 32′N, 141° 33′E), during May in 2018, 2019, and 2021 and on chick-rearing streaked shearwaters in Awashima Island (38° 28′N, 139° 14′E), from mid-August to late September from 2018 to 2023. Birds were captured, their blood samples were collected, and GPS loggers were attached to them. Blood samples were collected from the wing veins of the gulls and the lower limb veins of the shearwaters using a needle and syringe prefilled with a small amount of the anticoagulant heparin sodium (5000 units 5 mL^{-1}; Mochida Pharmaceutical Co., Ltd., Tokyo, Japan). The volume of collected blood samples was less than 1 mL, corresponding to less than 1% of the body mass of the birds. Blood samples were centrifuged at 2,680 g for 10 min at room temperature, divided into blood cells and plasma, and frozen. Blood sampling did not significantly affect the behavioral parameters (detailed in Supplementary Material, Supplementary Table S1). Body masses of the birds were measured in 5 g units using a spring scale (Pesola LightLine Metric 11,000, ±0.3%; PESOLA AG, Baar, Switzerland) before logger attachment (Supplementary Material, Supplementary Tables S2, S3).

Animal-borne GPS loggers (Axy-Trek with resin 55 × 25 × 11 mm, 25 g; Technosmart, Roma, Italy) were attached on the birds' back using waterproof tape (Tesa®; Beiersdorf AG, Hamburg, Germany) and cyanoacrylate glue (Henkel Loctite Adhesives Ltd., Hatfield, UK). The Axy-Trek without resin was housed in waterproof heat-shrink tubing (less than 25 g) and attached to the bird's back using a Teflon ribbon (TH-25; width, 6 mm; Bally Ribbon Mills, Bally, PA, U.S.A.). Another type of GPS logger (PinPoint VHF with solar panels, body size excluding antenna 82 × 25 × 27 mm, 18 g; Lotek Wireless Inc., Newmarket, Ontario, Canada) were attached to the back of the bird using a Teflon ribbon. The PinPoint VHF and Axy-Trek loggers were attached to different individuals. The GPS sampling intervals were set to either 1 point per minute or 1 point every 5 min. The attachment of the same or similarly sized loggers did not significantly affect reproduction (Yoda et al., 2012) or reproduction, behavior, and subsequent survival of the shearwaters (Shiomi et al., 2012; Yoda et al., 2014; Koyama et al., 2024b).

On the day of logger attachment and day after, the birds were recaptured, and additional blood samples were taken and measured body mass after the loggers were retrieved. Individuals with PinPoint VHF loggers were released to record their migration.

The sexes of the birds were determined based on their body size for the gulls (males being larger than females; Chochi et al., 2002), and on their vocalizations for the shearwaters (males had higher-pitched calls than females; Arima et al., 2014). Based on a previous study (Koyama et al., 2021), we included in the analysis individuals that could be recaptured; a second blood sample was collected from these individuals within 17 days after logger attachment and from the date of first blood sampling.

2.2 Oxidative stress measurement

Plasma pro-oxidant levels (derivatives of reactive oxygen metabolites; d-ROMs) and plasma antioxidant capacity (biological antioxidant potential; BAP) were measured using a free radical analyzer (FREE Carrio Duo; Diacron International, Grosseto, Italy). The d-ROMs, expressed in Carratelli units (U. CARR = 0.08 mg H_2O_2 dL^{-1}), reflect plasma concentrations of hydroperoxides (R-OOH) while BAP represents both the endogenous organic compounds and external substances acquired from food. The measurements were conducted according to the experimental protocol described by Koyama et al. (2021). The values of BAP for the gulls in 2018 were measured twice, and the average value was used in the subsequent analysis. Changes in the d-ROMs and BAP levels were calculated by subtracting the levels of the first blood sample (at the time of logger deployment) from those of the second blood sample (at the time of logger retrieval).

2.3 Data analysis

Data analyses were conducted using R version 4.2.1 (R Development Core Team, 2020). The duration between the first and second blood sampling did not influence the changes in d-ROMs or BAP (Supplementary Material, Supplementary Table S4). Therefore, the duration of blood sampling was not taken into account in the subsequent analysis. To evaluate the species-based difference in changes in oxidative stress using linear regression models, we used the 'lm' function in R, with species as the explanatory variable and changes in d-ROMs or changes in BAP values as the response variables. To examine species differences in d-ROMs and BAP values, we used Tobit models implemented with the 'vglm' function in the VGAM package (Yee, 2025). Species was set as the explanatory variable, and d-ROMs and BAP values were set as the response variables. Tobit models are appropriate for modeling response variables with range restrictions. For this analysis, the accurate detection limits of the analyzer, 40 to 1,000 for d-ROMs and 500 to 6,000 for BAP, were set as the detection ranges.

We analyzed the effect of handling time (ranging from 1 to 9 min for black-tailed gulls and 1–32 min for streaked shearwaters in our study) from capture to the completion of blood sampling. Handling times of 10 min or less, which encompassed all samples of black-tailed gulls and 96.8% (179 out of 185) samples of streaked shearwaters, did not significantly affect d-ROMs or BAP values (detailed in the Supplementary Material; Supplementary Tables S5, S6; Supplementary Figure S1). While blood collection is generally recommended to be completed within 3 min, particularly for measuring baseline hormone levels, which are highly sensitive to short-term handling (Kitaysky et al., 1999), previous studies have reported no significant effects on oxidative stress variation in birds even with handling times of 30 min or longer (Costantini et al., 2007; Fowler et al., 2023). Given these findings, the handling times in our study likely had minimal impact on oxidative stress.

The GPS data recorded by the loggers were extracted to match the period between the first and second blood samples. From this dataset, we removed GPS points with ground speeds exceeding 90 km h^{-1} using "ddfilter" function of SDLfilter package (Shimada,

2023) in R. Foraging trip was defined as an extended trip of more than 1 km from the colony and more than 1 h for the gulls (Yoda et al., 2012) and more than 3 km from the colony and more than 6 h (Koyama et al., 2021) for the shearwaters. Foraging trip parameters, such as total flight distance, maximum distance from the colony, and number of takeoffs, were calculated for each foraging trip. To calculate number of takeoffs, flight state was defined as ground speed more than 15 km h^{-1} calculated from GPS points (Shiomi et al., 2012; Yoda et al., 2012). The number of takeoffs was calculated as the number of times the birds switched from the stationary phase (less than 15 km h^{-1}) to the flight phase (greater than 15 km h^{-1}). We then calculated the average frequency of takeoffs by dividing the number of takeoffs by the trip duration for each foraging trip.

To calculate the foraging duration, we applied hidden Markov models (HMM) to classify bird behavior into three states: resting, foraging, and flight. These states are commonly used to describe the behavior of seabirds that forage exclusively in the ocean, such as shearwaters (Clay et al., 2020; Darby et al., 2022). First, intervals of GPS points were resampled to 10 min intervals using "redisltraj" function in adehabitatLT package (Clement et al., 2024) of R because in previous studies that classified seabird behavior into three states using HMMs, GPS data with 5–30 min intervals were often used (Clay et al., 2020; Darby et al., 2022; Clay et al., 2023; Gillies et al., 2023a; 2023b). Each GPS point was classified into three states based on the step length and turning angle between GPS points using "momentuHMM" function in momentuHMM package (McClintock and Michelot 2022) of R. Step lengths were calculated as the net distance between two consecutive GPS points. Turning angles, representing changes in direction, were calculated as the angles between two consecutive step vectors constructed from successive GPS points. We defined the resting, foraging, and flight states as GPS points with small step lengths and turning angles, medium step lengths and large turning angles, and having large step lengths and small turning angles, respectively. We defined the continuous GPS points classified as a foraging state of more than two as the foraging phase. The foraging duration was calculated by summing the time differences between the first and last GPS points of each foraging phase.

To calculate the foraging parameters for individuals, the total flight distance and number of takeoffs were calculated by summing the values across all foraging trips for each individual. The average maximum distance was calculated by dividing the total maximum distance from the colony, which was calculated by adding the values of each trip, by the number of trips. The average frequency of takeoffs for each individual was calculated by averaging the average frequency of takeoffs for each foraging trips. The percentage of foraging duration was calculated by dividing the foraging duration by the logger-recorded duration. For the gulls that use urban areas to forage, insects, and food derived from human activities on land (Yoda et al., 2012; Mizutani et al., 2021), utilization percentage of the land per individual was calculated. Because GPS points may tend to be missing in urban areas than over the ocean, GPS points were resampled to 1 min intervals using "approx.irts" function in tseries package (Trapletti et al., 2024). We counted GPS points corresponding to flight states, defined as ground speeds greater than 15 km h^{-1} (Shiomi et al., 2012; Yoda et al., 2012), during foraging trips and calculated the utilization percentage of the land divided by all resampled GPS points during foraging trips for individuals.

We established Bayesian regression models using "brms" function in "brms" package (Bürkner et al., 2024) for each year and species to evaluate the relationships between behavioral metrics and oxidative stress. The relationship between changes in oxidative stress and foraging behavior may vary depending on food availability in the surrounding environment (Koyama et al., 2021; Lin et al., 2022), and these relationships were evaluated separately for each year. We used the total flight distance, number of takeoffs, average maximum distance, average frequency of takeoffs, foraging duration, percentage of foraging duration, utilization percentage of the land for the gulls, and sex as explanatory variables. To avoid multicollinearity, variance inflation factors (VIF) were calculated using "vif" function in car package (Fox et al., 2024). The parameters with the highest VIF were removed until the VIF values of all the parameters were less than three (Zuur et al., 2010; Supplementary Table S7). Changes in d-ROMs and BAP were used as response variables. Gaussian distributions were used in this analysis. The relationship between changes in oxidative stress and behavioral parameters was evaluated based on the calculated 95% Bayesian credible interval (CI). A CI greater than zero was considered a positive relationship, and *vice versa*.

3 Results

We obtained the oxidative and behavioral data for 41 black-tailed gulls (17, 9, and 15 gulls for 2018, 2019, and 2021, respectively) and 101 streaked shearwaters (11, 20, 18, 17, 23, and 12 shearwaters for 2018, 2019, 2020, 2021, 2022, and 2023, respectively). The average duration between the first and second blood samples was 7.51 days (range, 4–14 days) for the gulls and 5.74 days (range, 1–17 days) for the shearwaters. Because all d-ROMs values of streaked shearwaters in 2022 (range, 3–39 U. CARR) and 2023 (range, 5–33 U. CARR) were lower than the accurate detection limit of the analyzer, 40 U. CARR, we excluded them from the following analysis.

We recorded 400 and 337 foraging trips for the gulls (Figure 1A) and the shearwaters (Figure 1B), respectively. At the individual scale, for the gulls, total trip duration was 71.21 ± 31.99 (h), total flight distance was 923.48 ± 454.31 (km), average maximum distance from the colony was 33.8 ± 13.54 (km), average frequency of takeoffs was 0.81 ± 0.32 (times h^{-1}), foraging duration was 43.84 ± 22.35 (h), percentage of foraging duration was 23.84 ± 8.78 (%), and utilization percentage of the land was 11.02 ± 13.62 (%). For the shearwaters, total trip duration was 121.06 ± 98.69 (h), total flight distance was 1,651.49 ± 1,496.27 (km), average maximum distance from the colony was 221.63 ± 201.39 (km), average frequency of takeoffs was 2.08 ± 0.69 (times h^{-1}), foraging duration was 45.36 ± 36.74 (h), and percentage of foraging duration for individuals was 37.87 ± 11.87 (%).

For black-tailed gulls, the average d-ROMs, BAP, changes in d-ROMs, changes in BAP were 131.52 ± 76.52 (U. CARR) (average ±standard deviation), 1,437.51 ± 416.73 (μM/L), −10.67 ± 71.27, and 44.87 ± 498.76, respectively (Supplementary Table S8A). For streaked shearwaters, the average d-ROMs, BAP, changes in d-ROMs, changes in BAP were 59.61 ± 36.59 (U. CARR), 1706 ± 352.85 (μM/L), −6.37 ± 39.92, −97.88 ± 365.04, respectively

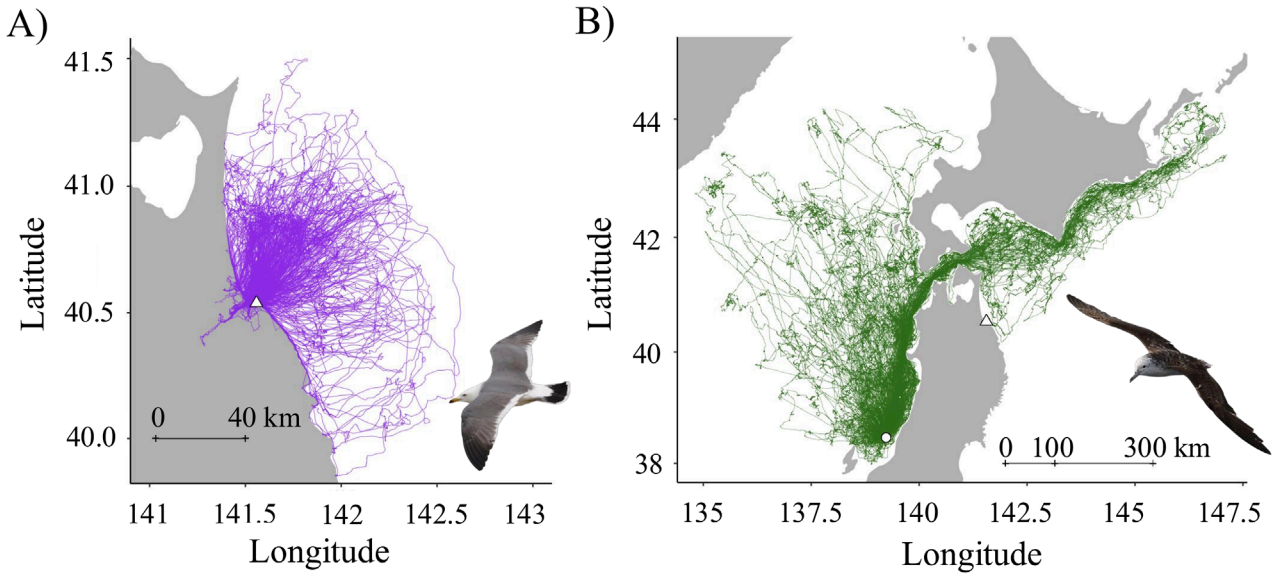

FIGURE 1
Trajectories of black-tailed gulls **(A)** and streaked shearwaters **(B)**. Purple lines represent the flight trajectories of black-tailed gulls, whereas green lines represent those of streaked shearwaters. Triangle and circle marks indicate the breeding site of black-tailed gulls, Kabushima Island, and that of streaked shearwaters, Awashima Island, respectively. The copyrights of the seabird photos in Figures 1A, B belong to Yuichi Mizutani and Yusuke Goto, respectively, who are authors of this paper.

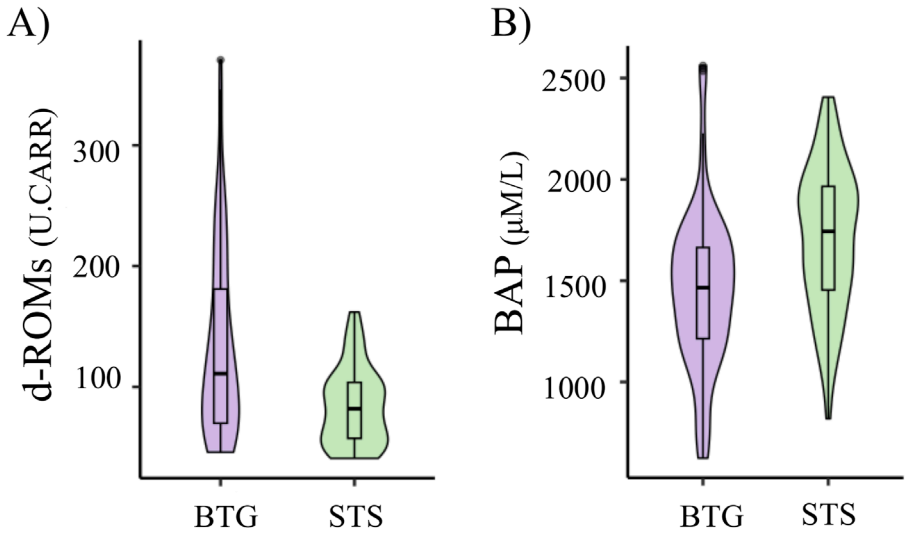

FIGURE 2
Species differences in d-ROMs **(A)** and BAP **(B)**. The values of black-tailed gulls (BTG) are represented by the purple violin plot, whereas those of streaked shearwaters (STS) are represented by the green violin plot. The d-ROMs values are expressed in Carratelli units (U. CARR = 0.08 mg H_2O_2 dL^{-1}).

(Supplementary Table S8B). d-ROMs was significantly larger in gulls than in shearwaters (estimate = −49.01; P < 0.01, Figure 2A). BAP was significantly lower in gulls than in shearwaters (estimate = −252, P < 0.01; Figure 2B). There were no significant differences between the changes in d-ROMs (estimate = 4.30, P = 0.69) and BAP (estimate = −142.74, P = 0.093) for gulls and shearwaters.

Using the brms, we evaluated the relationship between behavioral parameters and changes in oxidative stress each year. For the gulls, changes in d-ROMs were negatively related to the percentage of foraging duration (−14.48 [95% CI −27.08, −2.00]) and the utilization percentage of the land (−5.19 [95% CI −10.02, −0.25]) in 2018, and positively related to the total flight distance (0.06 [95% CI 0.01, 0.12]) in 2021 (Table 1; Supplementary Table S7A). For the shearwaters, changes in BAP were positively related to the foraging duration (5.83 [95% CI 1.69, 9.88]) and negatively related to the average maximum distance (−0.69 [95% CI −1.26, −0.13]) in 2022

10.3389/fphys.2025.1509511

TABLE 1 Relationship between behavioral parameters and the changes in d-ROMs of black-tailed gulls (A) and changes in BAP of streaked shearwaters (B). Only the years with significant relationships are presented. Behavioral parameters removed based on VIF are indicated by blank spaces. N.S. indicates no significant relationship. Positive (+) and negative (–) relationships are shown where applicable.

(A)Year	2018	2021
total flight distance	N.S.	+
average maximum distance	N.S.	N.S.
foraging duration		
percentage of foraging duration	–	N.S.
average frequency of takeoffs	N.S.	
utilization percentage of the land	–	N.S.
sex (male)	N.S.	N.S.
(B)Year	**2022**	**2023**
total flight distance		
average maximum distance	–	
foraging duration	+	N.S.
percentage of foraging duration		N.S.
average frequency of takeoffs	N.S.	–
sex (male)	N.S.	+

and negatively related to the average frequency of takeoffs (−458.47 [95% CI −747.12, −152.72]) in 2023. Sex-based differences in the changes in BAP were observed in 2023; the changes in males were larger than those in females (395.26 [95% CI 146.58, 630.01]) for the shearwaters (Table 1; Supplementary Table S7B). There was no significant relationship between the changes in oxidative stress and behavioral parameters for the gulls in 2019, and for the shearwaters from 2018 to 2021.

4 Discussion

Black-tailed gulls during the egg-laying period exhibit higher oxidative damage and lower antioxidant capacity than streaked shearwaters during the chick-rearing period in terms of chronic oxidative stress. The species differences might be explained by differences in their habitat, species-specific physiological functions, and reproductive stages. As environmental pollution (Espín et al., 2016; Isaksson et al., 2017; Salmón et al., 2018) and pathogens (Costantini and Dell'Omo, 2006; Isaksson et al., 2013; Sebastiano et al., 2017) can increase oxidative stress, living in urban areas might increase oxidative stress in black-tailed gulls. Black-tailed gulls, which inhabit a variety of environments, might possess physiological mechanisms that enhance their tolerance to oxidative damage as well as antioxidant capacity, such as autophagy (promoting the degradation of damaged biomolecules) (Yun et al., 2020) and DNA repair pathways (Barzilai and Yamamoto, 2004), preventing oxidative damage from becoming fatal. In contrast, streaked shearwaters exhibit reproductive traits, with their chicks growing slowly and storing fat reserves to withstand starvation (Oka et al., 2002). Previous studies have shown that birds with higher fat content have been found to possess higher antioxidant capacities (Costantini et al., 2007 but see Eikenaar et al., 2020), and it is possible that adult streaked shearwaters, displaying similar traits as their chicks, may also store fat and similarly accumulate antioxidant compounds in their bodies, enhancing their tolerance to oxidative damage. In 2022 and 2023, the oxidative damage to the shearwaters was so low that it fell below the detection limit of the measurement equipment. As shown in other migratory birds, streaked shearwaters, which migrate approximately 3,000 km from Japan to the equator (Takahashi et al., 2008), might accumulate antioxidant capacity in preparation for extended migrations (Skrip and Mcwilliams, 2016; Gutiérrez et al., 2019), or may have evolved mechanisms to upregulate endogenous antioxidant capacity in response to elevated oxidative damage (Costantini, 2008; Jenni-Eiermann et al., 2014; Cooper-Mullin and McWilliams, 2016). Notably, our results did not confirm the existence of these physiological functions in either species. We encourage further studies to clarify species-specific physiological mechanisms and their adaptations to habitat and life histories. Furthermore, the reproductive stage is also a factor that may influence oxidative stress in birds and mammals, including seabirds (Costantini et al., 2014; Montoya et al., 2016; Speakman and Garratt, 2014). As demonstrated in previous studies, incubation might increase oxidative stress in gulls compared to chick-rearing, although the underlying mechanism remains unclear (Colominas-Ciuró et al., 2017; 2022; Kulaszewicz et al., 2018). We recommend that future studies investigate whether reproductive factors, including not only reproductive stage but also egg number, egg size, chick condition, and chick age, are associated with parental oxidative stress, and explore the mechanisms driving these relationships.

Over a weekly timescale, there were no significant species differences in changes in oxidative damage and antioxidant capacity, suggesting that behavioral differences, such as daily short-range coastal foraging *versus* extended oceanic foraging trips lasting up to 2 weeks, might not necessarily lead to species-specific changes in oxidative stress. Our findings indicate that seabirds might possess physiological adaptations to prevent oxidative stress buildup over a weekly timescale, even during the breeding season, which is one of their most energetically demanding periods. These adaptations may include physiological mechanisms such as the upregulation of nuclear factors that modulate antioxidant defenses in response to oxidative damage, similar to those observed in laboratory and domestic animals, as well as humans (Ungvari et al., 2008; Ge et al., 2019; Surai et al., 2019; Castiglione et al., 2020).

There was no consistent trend in the relationship between oxidative stress and behavioral metrics across all years or species, suggesting that the effects of behavior on oxidative stress may vary with environmental differences each year, regardless of species.

The energy requirements for flight may vary with annual wind conditions (Furness and Bryant, 1996; Thorne et al., 2023), and the effect of migration on oxidative stress may fluctuate. Additionally, as shown in black-tailed gulls in 2018 and streaked shearwaters in 2022, a longer foraging duration might decrease oxidative damage or increase antioxidant capacity resulting in decreased oxidative stress in years when food availability is high. However, a longer foraging duration might not result in obtaining food, which decreases oxidative stress, depending on the food species that change from year to year (De Alwis et al., 2025), food availability (Garthe et al., 2011; Horswill et al., 2017), and the presence of competitors (Koyama et al., 2024a). Our results indicate no significant species differences in the changes in oxidative stress, species-related factors such as flight style, reproductive traits, and life history might not influence oxidative stress as strongly as environmental factors.

Comprehensive investigations of behavioral and physiological conditions offer significant insights into how wild animals adapt to their habitats through species-specific functions and provide a foundation for assessing species' vulnerabilities and responses to threats such as urbanization and climate change (Cooke et al., 2014; Andrews and Enstipp, 2016). To date, comprehensive investigations have mainly been conducted on large marine animals, such as seals and turtles, by combining multiple loggers that record their behavioral activity and physiological conditions, such as heart rate (Ropert-Coudert et al., 2006; Clark et al., 2010; Viblanc et al., 2011; McDonald et al., 2018), body temperature (Southwood et al., 2005; Papastamatiou et al., 2015), and brain activity (Kendall-Bar et al., 2023). Unlike logger-based physiological recordings, measurement of oxidative damage allows for a more direct assessment of physiological stress in animals by quantifying the damage to biomolecules. Additionally, antioxidant capacity reflects the quality of an animal's food intake and nutritional status, providing valuable insights into the physiological effects of external factors such as food availability. Thus, we propose combining behavioral biologging with oxidative stress measurement, which is useful for quantifying oxidative damage as physiological deterioration caused by exercise and antioxidant capacity as tolerance to oxidative damage derived from the prey, despite its limitation in providing only instantaneous physiological data. Integrating environmental, behavioral, and oxidative stress data would help identify the environmental factors that cause physiological deterioration or recovery, especially for small- and medium-sized animals, for which attaching multiple loggers is challenging owing to weight limitations (Barron et al., 2010; Portugal and White, 2018). Oxidative stress measurements have been measured in marine animals of various sizes, including seals (Vázquez-Medina et al., 2012), sea turtles (Labrada-Martagón et al., 2011; Perrault and Stacy, 2018), seabirds (Merkling et al., 2017; Kulaszewicz et al., 2018), sharks (Barrera-García et al., 2012; Vélez-Alavez et al., 2013), and fish (Janssens et al., 2000; Bacanskas et al., 2004; Cappello et al., 2016), demonstrating its potential for broad applications across marine species. We encourage future integrated studies on the marine environment, behavior, and oxidative stress of different species and animals to clarify what kind of foraging and provisioning behavior contributes to either the deterioration or recovery of their physiological conditions depending on the surrounding environment.

Data availability statement

The original contributions presented in the study are included in the article/Supplementary Material, further inquiries can be directed to the corresponding author.

Ethics statement

The animal study was approved by This study for black-tailed gulls and streaked shearwaters was approved by the Animal Experimental Committee of Nagoya University (GSES2018–2023), Aomori prefecture (2018-4036, 2019-3033, 2021-3058), Hachinohe City Board of Education (2018-237, 2019-329, 2021-207), the Ministry of the Environment to install the structure (1803201, 1804042, 1903281, 2103303), and Awashimaura Village Office, Niigata Prefecture (2018-2023), Japan. The study was conducted in accordance with the local legislation and institutional requirements.

Author contributions

SK: Conceptualization, Data curation, Formal Analysis, Funding acquisition, Investigation, Methodology, Project administration, Resources, Writing–original draft. YM: Conceptualization, Data curation, Funding acquisition, Investigation, Project administration, Resources, Writing–review and editing. YG: Conceptualization, Data curation, Formal Analysis, Methodology, Validation, Writing–review and editing. KY: Conceptualization, Data curation, Funding acquisition, Resources, Supervision, Writing–review and editing.

Funding

The authors declare that financial support was received for the research and/or publication of this article. This study was supported by the Sasakawa Scientific Research Grant from the Japan Science Society (grant number 2019-5003); the Collaborative Research Program of Wildlife Research Center, Kyoto University (grant numbers 2020-B-2, 2021-A-14); JST SPRING (grant number JPMJSP2125); the Grants-in-Aid for Scientific Research from the Japan Society for the Promotion of Science (grant numbers 18K14788, 21H05294, 21H05299, 22H00569, 22J14219); and CREST, Japan Science and Technology Agency (grant number JPMJCR23P2).

Acknowledgments

We are grateful to A. Narita, the staff of the observation post at Kabushima Island, and all our colleague for their help in conducting the experiments. We thank to all our colleagues and the villagers in Awashima Island helping for their assistance in our fieldwork. We are grateful to Prof. A. Shoji for contributing to the improvement of the manuscript.

Conflict of interest

The authors declare that the research was conducted in the absence of any commercial or financial relationships that could be construed as a potential conflict of interest.

Generative AI statement

The author(s) declare that Generative AI was used in the creation of this manuscript. We have used AI-assisted technologies, ChatGPT and Claude, in preparing this article to correct grammar. After using this tool, we reviewed and edited the content as necessary. We take full responsibility for the content of the publication.

Publisher's note

All claims expressed in this article are solely those of the authors and do not necessarily represent those of their affiliated organizations, or those of the publisher, the editors and the reviewers. Any product that may be evaluated in this article, or claim that may be made by its manufacturer, is not guaranteed or endorsed by the publisher.

Supplementary material

The Supplementary Material for this article can be found online at: https://www.frontiersin.org/articles/10.3389/fphys.2025.1509511/full#supplementary-material

References

Alan, R. R., and McWilliams, S. R. (2013). Oxidative stress, circulating antioxidants, and dietary preferences in songbirds. *Comp. Biochem. Physiology - B Biochem. Mol. Biol.* 164, 185–193. doi:10.1016/j.cbpb.2012.12.005

Andrews, R. D., and Enstipp, M. R. (2016). Diving physiology of seabirds and marine mammals: relevance, challenges and some solutions for field studies. *Comp. Biochem. Physiol. A Mol. Integr. Physiol.* 202, 38–52. doi:10.1016/j.cbpa.2016.07.004

Arima, H., Oka, N., Baba, Y., Sugawa, H., and Ota, T. (2014). Gender identification by calls and body size of the streaked shearwater examined by CHD genes. *Ornithol. Sci.* 13, 9–17. doi:10.2326/osj.13.9

Bacanskas, L. R., Whitaker, J., and Di Giulio, R. T. (2004). Oxidative stress in two populations of killifish (*Fundulus heteroclitus*) with differing contaminant exposure histories. *Mar. Environ. Res.* 58, 597–601. doi:10.1016/j.marenvres.2004.03.048

Barrera-García, A., O'Hara, T., Galván-Magaña, F., Méndez-Rodríguez, L. C., Castellini, J. M., and Zenteno-Savín, T. (2012). Oxidative stress indicators and trace elements in the blue shark (*Prionace glauca*) off the east coast of the Mexican Pacific Ocean. *Comp. Biochem. Physiol. C. Toxicol. Pharmacol.* 156, 59–66. doi:10.1016/j.cbpc.2012.04.003

Barron, D. G., Brawn, J. D., and Weatherhead, P. J. (2010). Meta-analysis of transmitter effects on avian behaviour and ecology: meta-analysis of avian transmitter effects. *Methods Ecol. Evol.* 1, 180–187. doi:10.1111/j.2041-210x.2010.00013.x

Barzilai, A., and Yamamoto, K.-I. (2004). DNA damage responses to oxidative stress. *DNA Repair (Amst.)* 3, 1109–1115. doi:10.1016/j.dnarep.2004.03.002

Bishop, C. J., White, G. C., Freddy, D. J., Watkins, B. E., and Stephenson, T. R. (2009). Effect of enhanced nutrition on mule deer population rate of change. *Wildl. Monogr.* 172, 1–28. doi:10.2193/2008-107

Bozinovic, F., Calosi, P., and Spicer, J. I. (2011). Physiological correlates of geographic range in animals. *Annu. Rev. Ecol. Evol. Syst.* 42, 155–179. doi:10.1146/annurev-ecolsys-102710-145055

Bürkner, P., Gabry, J., Weber, S., Johnson, A., Modrak, M., Badr, H. S., et al.(2024). brms: Bayesian Regression Models using 'Stan'. *R Package Version 2.19.0*. doi:10.32614/CRAN.package.brms

Cabezas, S., Calvete, C., and Moreno, S. (2011). Survival of translocated wild rabbits: importance of habitat, physiological and immune condition. *Anim. Conserv.* 14, 665–675. doi:10.1111/j.1469-1795.2011.00472.x

Calenge, C., Dray, S., and Royer, M. (2024). adehabitatLT: Analysis of Animal Movements. *R Package Version 0.3.25*. doi:10.32614/CRAN.package.adehabitatLT

Cappello, T., Brandão, F., Guilherme, S., Santos, M. A., Maisano, M., Mauceri, A., et al. (2016). Insights into the mechanisms underlying mercury-induced oxidative stress in gills of wild fish (*Liza aurata*) combining ^{1}H NMR metabolomics and conventional biochemical assays. *Sci. Total Environ.* 548–549, 13–24. doi:10.1016/j.scitotenv.2016.01.008

Castiglione, G. M., Xu, Z., Zhou, L., and Duh, E. J. (2020). Adaptation of the master antioxidant response connects metabolism, lifespan and feather development pathways in birds. *Nat. Commun.* 11, 2476. doi:10.1038/s41467-020-16129-4

Chochi, M., Niizuma, Y., and Takagi, M. (2002). Sexual differences in the external measurements of black-tailed gulls breeding on Rishiri Island, Japan. *Ornithol. Sci.* 1, 163–166. doi:10.2326/osj.1.163

Clark, T. D., Sandblom, E., Hinch, S. G., Patterson, D. A., Frappell, P. B., and Farrell, A. P. (2010). Simultaneous biologging of heart rate and acceleration, and their relationships with energy expenditure in free-swimming sockeye salmon (*Oncorhynchus nerka*). *J. Comp. Physiol. B* 180, 673–684. doi:10.1007/s00360-009-0442-5

Clay, T. A., Hodum, P., Hagen, E., and Brooke, M. de L. (2023). Adjustment of foraging trips and flight behaviour to own and partner mass and wind conditions by a far-ranging seabird. *Anim. Behav.* 198, 165–179. doi:10.1016/j.anbehav.2023.02.007

Clay, T. A., Joo, R., Weimerskirch, H., Phillips, R. A., den Ouden, O., Basille, M., et al. (2020). Sex-specific effects of wind on the flight decisions of a sexually dimorphic soaring bird. *J. Anim. Ecol.* 89, 1811–1823. doi:10.1111/1365-2656.13267

Colominas-Ciuró, R., Bertellotti, M., Carabajal, E., D'Amico, V. L., and Barbosa, A. (2017). Incubation increases oxidative imbalance compared to chick rearing in a seabird, the Magellanic penguin (*Spheniscus magellanicus*). *Mar. Biol.* 164, 99–108. doi:10.1007/s00227-017-3139-4

Colominas-Ciuró, R., Cianchetti-Benedetti, M., Michel, L., Dell'Omo, G., and Quillfeldt, P. (2022). Foraging strategies and physiological status of a marine top predator differ during breeding stages. *Comp. Biochem. Physiology -Part A Mol. Integr. Physiology* 263, 111094. doi:10.1016/j.cbpa.2021.111094

Cooke, S. J., Blumstein, D. T., Buchholz, R., Caro, T., Fernández-Juricic, E., Franklin, C. E., et al. (2014). Physiology, behavior, and conservation. *Physiol. Biochem. Zool.* 87, 1–14. doi:10.1086/671165

Cooper-Mullin, C., and McWilliams, S. R. (2016). The role of the antioxidant system during intense endurance exercise: lessons from migrating birds. *J. Exp. Biol.* 219, 3684–3695. doi:10.1242/jeb.123992

Costantini, D. (2008). Oxidative stress in ecology and evolution: lessons from avian studies. *Ecol. Lett.* 11, 1238–1251. doi:10.1111/j.1461-0248.2008.01246.x

Costantini, D., Cardinale, M., and Carere, C. (2007). Oxidative damage and anti-oxidant capacity in two migratory bird species at a stop-over site. *Comp. Biochem. Physiol. C Pharmacol. Toxicol. Endocrinol.* 144, 363–371. doi:10.1016/j.cbpc.2006.11.005

Costantini, D., Casasole, G., Abdelgawad, H., Asard, H., and Eens, M. (2020). *Experimental evidence that oxidative stress influences reproductive decisions*, 1169–1174.

Costantini, D., and Dell'Omo, G. (2006). Effects of T-cell-mediated immune response on avian oxidative stress. *Comp. Biochem. Physiol. A Mol. Integr. Physiol.* 145, 137–142. doi:10.1016/j.cbpa.2006.06.002

Costantini, D., and Dell'Omo, G. (2015). Oxidative stress predicts long-term resight probability and reproductive success in scopoli's shearwater (*Calonectris diomedea*). *Conserv. Physiol.* 3, cov024. doi:10.1093/conphys/cov024

Costantini, D., Goutte, A., Barbraud, C., Faivre, B., Sorci, G., Weimerskirch, H., et al. (2015). Demographic responses to oxidative stress and inflammation in the wandering albatross (*Diomedea exulans*). *PLoS One* 10, e0133967. doi:10.1371/journal.pone.0133967

Costantini, D., Meillère, A., Carravieri, A., Lecomte, V., Sorci, G., Faivre, B., et al. (2014). Oxidative stress in relation to reproduction, contaminants, gender and age in a long-lived seabird. *Oecologia* 175, 1107–1116. doi:10.1007/s00442-014-2975-x

Crino, O. L., Buchanan, K. L., Trompf, L., Mainwaring, M. C., and Griffith, S. C. (2017). Stress reactivity, condition, and foraging behavior in zebra finches: effects on boldness, exploration, and sociality. *Gen. Comp. Endocrinol.* 244, 101–107. doi:10.1016/j.ygcen.2016.01.014

Darby, J., Clairbaux, M., Bennison, A., Quinn, J. L., and Jessopp, M. J. (2022). Underwater visibility constrains the foraging behaviour of a diving pelagic seabird. *Proc. Biol. Sci.* 289, 20220862. doi:10.1098/rspb.2022.0862

De Alwis, C., Yoda, K., Watanuki, Y., Takahashi, A., Imura, S., Watanabe, K., et al. (2025). Inter-annual, seasonal, and sex differences in the diet of a surface feeding seabird, streaked shearwater (*Calonectris leucomelas*), breeding in the Sea of Japan. *Ornithol. Sci.* 24. doi:10.2326/osj.24.99

Eikenaar, C., Winslott, E., Hessler, S., and Isaksson, C. (2020). Oxidative damage to lipids is rapidly reduced during migratory stopovers. *Funct. Ecol.* 34, 1215–1222. doi:10.1111/1365-2435.13540

Espín, S., Martínez-López, E., Jiménez, P., María-Mojica, P., and García-Fernández, A. J. (2016). Interspecific differences in the antioxidant capacity of two Laridae species exposed to metals. *Environ. Res.* 147, 115–124. doi:10.1016/j.envres.2016.01.029

Filomeni, G., De Zio, D., and Cecconi, F. (2015). Oxidative stress and autophagy: the clash between damage and metabolic needs. *Cell Death Differ.* 22, 377–388. doi:10.1038/cdd.2014.150

Fowler, M. A., Wong, J. B., and Harrison, A. L. (2023). Oxidative physiology of two small and highly migratory Arctic seabirds: arctic terns (*Sterna paradisaea*) and long-tailed jaegers (*Stercorarius longicaudus*). *Conserv. Physiol.* 11 (1), coad060. doi:10.1093/conphys/coad060

Fox, J., Weisberg, S., Price, B., Adler, D., Bates, D., Baud-Bovy, G., et al. (2024). car: Companion to Applied Regression. *R Package Version 3.1.0*. doi:10.32614/CRAN.package.car

Furness, R. W., and Bryant, D. M. (1996). Effect of wind on field metabolic rates of breeding northern fulmars. *Ecology* 77, 1181–1188. doi:10.2307/2265587

Garthe, S., Montevecchi, W. A., and Davoren, G. K. (2011). Inter-annual changes in prey fields trigger different foraging tactics in a large marine predator. *Limnol. Oceanogr.* 56, 802–812. doi:10.4319/lo.2011.56.3.0802

Ge, J., Zhang, C., Sun, Y.-C., Zhang, Q., Lv, M.-W., Guo, K., et al. (2019). Cadmium exposure triggers mitochondrial dysfunction and oxidative stress in chicken (*Gallus gallus*) kidney via mitochondrial UPR inhibition and Nrf2-mediated antioxidant defense activation. *Sci. Total Environ.* 689, 1160–1171. doi:10.1016/j.scitotenv.2019.06.405

Gillies, N., Martín López, L. M., den Ouden, O. F. C., Assink, J. D., Basille, M., Clay, T. A., et al. (2023a). Albatross movement suggests sensitivity to infrasound cues at sea. *Proc. Natl. Acad. Sci. U. S. A.* 120, e2218679120. doi:10.1073/pnas.2218679120

Gillies, N., Weimerskirch, H., Thorley, J., Clay, T. A., Martín López, L. M., Joo, R., et al. (2023b). Boldness predicts plasticity in flight responses to winds. *J. Anim. Ecol.* 92, 1730–1742. doi:10.1111/1365-2656.13968

Gutiérrez, J. S., Sabat, P., Castañeda, L. E., Contreras, C., Navarrete, L., Peña-Villalobos, I., et al. (2019). Oxidative status and metabolic profile in a long-lived bird preparing for extreme endurance migration. 1–11.

Haley, P. J. (2003). Species differences in the structure and function of the immune system. *Toxicology* 188, 49–71. doi:10.1016/s0300-483x(03)00043-x

Hermes-Lima, M., and Zenteno-Savín, T. (2002). Animal response to drastic changes in oxygen availability and physiological oxidative stress. *Comp. Biochem. Physiol. C. Toxicol. Pharmacol.* 133, 537–556. doi:10.1016/s1532-0456(02)00080-7

Horswill, C., Trathan, P. N., and Ratcliffe, N. (2017). Linking extreme interannual changes in prey availability to foraging behaviour and breeding investment in a marine predator, the macaroni penguin. *PLoS One* 12, e0184114. doi:10.1371/journal.pone.0184114

Isaksson, C., Andersson, M. N., Nord, A., von Post, M., and Wang, H.-L. (2017). Species-dependent effects of the urban environment on fatty acid composition and oxidative stress in birds. *Front. Ecol. Evol.* 5. doi:10.3389/fevo.2017.00044

Isaksson, C., Sepil, I., Baramidze, V., and Sheldon, B. C. (2013). Explaining variance of avian malaria infection in the wild: the importance of host density, habitat, individual life-history and oxidative stress. *BMC Ecol.* 13, 15. doi:10.1186/1472-6785-13-15

Janssens, B. J., Childress, J. J., Baguet, F., and Rees, J. F. (2000). Reduced enzymatic antioxidative defense in deep-sea fish. *J. Exp. Biol.* 203, 3717–3725. doi:10.1242/jeb.203.24.3717

Jenni-Eiermann, S., Jenni, L., Smith, S., and Costantini, D. (2014). Oxidative stress in endurance flight: an unconsidered factor in bird migration. *PLoS One* 9, e97650. doi:10.1371/journal.pone.0097650

Kazama, K., Nishizawa, B., Tsukamoto, S., Gonzalez, J. E., Kazama, M. T., and Watanuki, Y. (2018). Male and female black-tailed gulls *Larus crassirostris* feed on the same prey species but use different feeding habitats. *J. Ornithol.* 159, 923–934. doi:10.1007/s10336-018-1565-9

Kendall-Bar, J. M., Williams, T. M., Mukherji, R., Lozano, D. A., Pitman, J. K., Holser, R. R., et al. (2023). Brain activity of diving seals reveals short sleep cycles at depth. *Science* 380, 260–265. doi:10.1126/science.adf0566

Killen, S. S., Marras, S., Metcalfe, N. B., McKenzie, D. J., and Domenici, P. (2013). Environmental stressors alter relationships between physiology and behaviour. *Trends Ecol. Evol.* 28, 651–658. doi:10.1016/j.tree.2013.05.005

Kitaysky, A. S., Piatt, J. F., and Wingfield, J. C. (2007). Stress hormones link food availability and population processes in seabirds. *Mar. Ecol. Prog. Ser.* 352, 245–258. doi:10.3354/meps07074

Kitaysky, A. S., Wingfield, J. C., and Piatt, J. F. (1999). Dynamics of food availability, body condition and physiological stress response in breeding black-legged kittiwakes. *Funct. Ecol.* 13 (5), 577–584. doi:10.1046/j.1365-2435.1999.00352.x

Koyama, S., Goto, Y., Furukawa, S., Maekawa, T., and Yoda, K. (2024a). Hidden rivals: the negative impacts of dolphinfish on seabird foraging behaviour. *Biol. Lett.* 20, 20240223. doi:10.1098/rsbl.2024.0223

Koyama, S., Mizutani, Y., Matsumoto, S., and Yoda, K. (2024b). Interannual linkages between oceanographic condition, seabird behaviour and chick growth from a decadal biologging study. *Anim. Behav.* 209, 63–81. doi:10.1016/j.anbehav.2023.12.012

Koyama, S., Mizutani, Y., and Yoda, K. (2021). Exhausted with foraging: foraging behavior is related to oxidative stress in chick-rearing seabirds. *Comp. Biochem. Physiol. A Mol. Integr. Physiol.* 258, 110984. doi:10.1016/j.cbpa.2021.110984

Kroeger, C., Crocker, D. E., Thompson, D. R., Torres, L. G., Sagar, P., and Shaffer, S. A. (2019). Variation in corticosterone levels in two species of breeding albatrosses with divergent life histories: responses to body condition and drivers of foraging behavior. *Physiol. Biochem. Zool.* 92, 223–238. doi:10.1086/702656

Kulaszewicz, I., Wojczulanis-Jakubas, K., and Jakubas, D. (2018). Breeding phased dependent oxidative balance in a small High Arctic seabird, the little auk. *J. Avian Biol.* 49, 1–11. doi:10.1111/jav.01702

Kurasawa, K., Itabashi, Y., Yamamoto, M., and Watanuki, Y. (2012). Prey of streaked shearwaters during long foraging trips estimated by fatty acid composition of the stomach oil. *Jpn. J. Ornithol.* 61, 137–141. doi:10.3838/jjo.61.137

Labrada-Martagón, V., Rodríguez, P. A. T., Méndez-Rodríguez, L. C., and Zenteno-Savín, T. (2011). Oxidative stress indicators and chemical contaminants in East Pacific green turtles (*Chelonia mydas*) inhabiting two foraging coastal lagoons in the Baja California peninsula. *Comp. Biochem. Physiol. C. Toxicol. Pharmacol.* 154, 65–75. doi:10.1016/j.cbpc.2011.02.006

Larcombe, S. D., Tregaskes, C. A., Coffey, J. S., Stevenson, A. E., Alexander, L., and Arnold, K. E. (2008). The effects of short-term antioxidant supplementation on oxidative stress and flight performance in adult budgerigars *Melopsittacus undulatus*. *J. Exp. Biol.* 211, 2859–2864. doi:10.1242/jeb.017970

Lin, Y., Patterson, A., Jimenez, A. G., and Elliott, K. (2022). Altered oxidative status as a cost of reproduction in a seabird with high reproductive costs. *Physiol. Biochem. Zool.* 95, 35–53. doi:10.1086/717916

Losdat, S., Helfenstein, F., Blount, J. D., Marri, V., Maronde, L., and Richner, H. (2013). Nestling erythrocyte resistance to oxidative stress predicts fledging success but not local recruitment in a wild bird. *Biol. Lett.* 9, 20120888–20120911. doi:10.1098/rsbl.2012.0888

Matsumoto, K., Oka, N., Ochi, D., Muto, F., Satoh, T. P., and Watanuki, Y. (2012). Foraging behavior and diet of streaked shearwaters *Calonectris leucomelas* rearing chicks on Mikura island. *Ornithol. Sci.* 11, 9–19. doi:10.2326/osj.11.9

Matsumoto, S., Yamamoto, T., Yamamoto, M., Zavalaga, C. B., and Yoda, K. (2017). Sex-related differences in the foraging movement of streaked shearwaters *Calonectris leucomelas* breeding on Awashima island in the Sea of Japan. *Ornithol. Sci.* 16, 23–32. doi:10.2326/osj.16.23

Matzkin, L. M., Watts, T., and Markow, T. (2009). Evolution of stress resistance in Drosophila: interspecific variation in tolerance to desiccation and starvation. *Funct. Ecol.* 23, 521–527. doi:10.1111/j.1365-2435.2009.01533.x

McClintock, B., and Michelot, T. (2022). momentuHMM: Maximum Likelihood Analysis of Animal Movement Behavior Using Multivariate Hidden Markov Models. *R Package Version 1.5.5*. doi:10.32614/CRAN.package.momentuHMM

McCue, M. D. (2010). Starvation physiology: reviewing the different strategies animals use to survive a common challenge. *Comp. Biochem. Physiol. A Mol. Integr. Physiol.* 156, 1–18. doi:10.1016/j.cbpa.2010.01.002

McDonald, B. I., Johnson, M., and Madsen, P. T. (2018). Dive heart rate in harbour porpoises is influenced by exercise and expectations. *J. Exp. Biol.* 221, jeb168740. doi:10.1242/jeb.168740

Merkling, T., Blanchard, P., Chastel, O., Glauser, G., Vallat-Michel, A., Hatch, S. A., et al. (2017). Reproductive effort and oxidative stress: effects of offspring sex and number on the physiological state of a long-lived bird. *Funct. Ecol.* 31, 1201–1209. doi:10.1111/1365-2435.12829

Mir, I., Eisa, S. A., and Maqsood, A. (2018). Review of dynamic soaring: technical aspects, nonlinear modeling perspectives and future directions. *Nonlinear Dyn.* 94, 3117–3144. doi:10.1007/s11071-018-4540-3

Mizutani, Y., Suzuki, H., Maekawa, T., Korpela, J., Miyatake, T., Koshiyama, Y., et al. (2021). Capture of flying insects by black-tailed gulls *Larus crassirostris* over inland and offshore areas. *Jpn. J. Ornithol.* 70, 53–60. doi:10.3838/jjo.70.53

Montoya, B., Valverde, M., Rojas, E., and Torres, R. (2016). Oxidative stress during courtship affects male and female reproductive effort differentially in a wild bird with biparental care. *J. Exp. Biol.* 219, 3915–3926. doi:10.1242/jeb.141325

Narita, K., and Narita, A. (2004). *Observation reports of black-tailed gull (in Japanese)*. Hachinohe: Kimura-Shoten.

Noguera, J. C., Kim, S.-Y., Velando, A., Supplement, D., and Noguera, C. (2012). Pre-fledgling oxidative damage predicts recruitment in a long-lived bird. *Biol. Lett.* 8, 61–63. doi:10.1098/rsbl.2011.0756

Oka, N. (2004). The distribution of streaked shearwater colonies, with special attention to population size, area of sea where located and surface water temperature. *J. Yamashina Inst. Ornithol.* 35, 164–188. doi:10.3312/jyio.35.164

Oka, N., Suginome, H., Jida, N., and Maruyama, N. (2002). Chick growth and fledgling performance of streaked shearwaters *Calonectris leucomelas* on Mikura island for two breeding seasons. *J. Yamashina Inst. Ornithol.* 34, 39–59. doi:10.3312/jyio1952.34.39

Pan, J.-S., He, S.-Z., Xu, H.-Z., Zhan, X.-J., Yang, X.-N., Xiao, H.-M., et al. (2008). Oxidative stress disturbs energy metabolism of mitochondria in ethanol-induced gastric mucosa injury. *World J. Gastroenterol.* 14, 5857–5867. doi:10.3748/wjg.14.5857

Papastamatiou, Y. P., Watanabe, Y. Y., Bradley, D., Dee, L. E., Weng, K., Lowe, C. G., et al. (2015). Drivers of daily routines in an ectothermic marine predator: hunt warm, rest warmer? *PLoS One* 10, e0127807. doi:10.1371/journal.pone.0127807

Park, J.-H., Jeong, I.-Y., Lee, S.-H., Yoo, J.-C., and Lee, W.-S. (2024). Changes in flight altitude of black-tailed gulls according to temporal and environmental differences. *Anim. (Basel)* 14, 202. doi:10.3390/ani14020202

Perrault, J. R., and Stacy, N. I. (2018). Note on the unique physiologic state of loggerhead sea turtles (*Caretta caretta*) during nesting season as evidenced by a suite of health variables. *Mar. Biol.* 165, 71. doi:10.1007/s00227-018-3331-1

Pisoschi, A. M., and Pop, A. (2015). The role of antioxidants in the chemistry of oxidative stress: a review. *Eur. J. Med. Chem.* 97, 55–74. doi:10.1016/j.ejmech.2015.04.040

Portugal, S. J., and White, C. R. (2018). Miniaturization of biologgers is not alleviating the 5% rule. *Methods Ecol. Evol.* 9, 1662–1666. doi:10.1111/2041-210x.13013

R Development Core Team (2020). *A language and environment for statistical computing*. Vienna, Austria: R Foundation for Statistical Computing. Available online at: https://www.R-project.org/.

Rohr, J. R., Raffel, T. R., and Hall, C. A. (2010). Developmental variation in resistance and tolerance in a multi-host–parasite system: resistance and tolerance across hosts and parasites. *Funct. Ecol.* 24, 1110–1121. doi:10.1111/j.1365-2435.2010.01709.x

Romero, L. M., and Wikelski, M. (2010). Stress physiology as a predictor of survival in Galapagos marine iguanas. *Proc. R. Soc. B* 277, 3157–3162. doi:10.1098/rspb.2010.0678

Ropert-Coudert, Y., Wilson, R. P., Grémillet, D., Kato, A., Lewis, S., and Ryan, P. G. (2006). Electrocardiogram recordings in free-ranging gannets reveal minimum difference in heart rate during flapping versus gliding flight. *Mar. Ecol. Prog. Ser.* 328, 275–284. doi:10.3354/meps328275

Saino, N., Caprioli, M., Romano, M., Boncoraglio, G., Rubolini, D., Ambrosini, R., et al. (2011). Antioxidant defenses predict long-term survival in a passerine bird. *PLoS One* 6, e19593. doi:10.1371/journal.pone.0019593

Sakamoto, K. Q., Takahashi, A., Iwata, T., Yamamoto, T., Yamamoto, M., and Trathan, P. N. (2013). Heart rate and estimated energy expenditure of flapping and gliding in black-browed albatrosses. *J. Exp. Biol.* 216, 3175–3182. doi:10.1242/jeb.079905

Salmón, P., Stroh, E., Herrera-Dueñas, A., von Post, M., and Isaksson, C. (2018). Oxidative stress in birds along a NO_x and urbanisation gradient: an interspecific approach. *Sci. Total Environ.* 622–623, 635–643. doi:10.1016/j.scitotenv.2017.11.354

Sebastiano, M., Eens, M., Elgawad, H. A., Thoisy, B., Lacoste, V., Pineau, K., et al. (2017). Oxidative stress biomarkers are associated with visible clinical signs of a disease in frigatebird nestlings. *Sci. Rep.* 7, 1599. doi:10.1038/s41598-017-01417-9

Shahidi, F. (2000). Antioxidants in food and food antioxidants. *Nahrung* 44, 158–163. doi:10.1002/1521-3803(20000501)44:3<158::AID-FOOD158>3.0.CO;2-L

Shimada, T. (2023). SDLfilter: Filtering and Assessing the Sample Size of Tracking Data. *R Package Version 2.3.3*. doi:10.32614/CRAN.package.SDLfilter

Shiomi, K., Yoda, K., Katsumata, N., and Sato, K. (2012). Temporal tuning of homeward flights in seabirds. *Anim. Behav.* 83, 355–359. doi:10.1016/j.anbehav.2011.11.010

Shirai, M., Niizuma, Y., Tsuchiya, K., Yamamoto, M., and Oka, N. (2013). Sexual size dimorphism in streaked shearwaters *Calonectris leucomelas*. *Ornithol. Sci.* 12, 57–62. doi:10.2326/osj.12.57

Sies, H. (1997). Oxidative stress: oxidants and antioxidants. *Exp. Physiol.* 82, 291–295. doi:10.1113/expphysiol.1997.sp004024

Sies, H., Berndt, C., and Jones, D. P. (2017). Oxidative stress. *Annu. Rev. Biochem.* 86, 715–748. doi:10.1146/annurev-biochem-061516-045037

Skrip, M. M., and Mcwilliams, S. R. (2016). Oxidative balance in birds: an atoms-to-organisms-to-ecology primer for ornithologists. *J. Field Ornithol.* 87, 1–20. doi:10.1111/jofo.12135

Southwood, A. L., Andrews, R. D., Paladino, F. V., and Jones, D. R. (2005). Effects of diving and swimming behavior on body temperatures of Pacific leatherback turtles in tropical seas. *Physiological Biochem. Zoology* 78, 285–297. doi:10.1086/427048

Speakman, J. R., and Garratt, M. (2014). Oxidative stress as a cost of reproduction: beyond the simplistic trade-off model. *Bioessays* 36, 93–106. doi:10.1002/bies.201300108

Surai, P. F., Kochish, I. I., Fisinin, V. I., and Kidd, M. T. (2019). Antioxidant defence systems and oxidative stress in poultry biology: an update. *Antioxidants (Basel)* 8, 235. doi:10.3390/antiox8070235

Takahashi, A., Ochi, D., Watanuki, Y., Deguchi, T., Oka, N., Afanasyev, V., et al. (2008). Post-breeding movement and activities of two streaked shearwaters in the north-western Pacific. *Ornithol. Sci.* 35, 29–35. doi:10.2326/1347-0558(2008)7[29:pmaaot]2.0.co;2

Thorne, L. H., Clay, T. A., Phillips, R. A., Silvers, L. G., and Wakefield, E. D. (2023). Effects of wind on the movement, behavior, energetics, and life history of seabirds. *Mar. Ecol. Prog. Ser.* 723, 73–117. doi:10.3354/meps14417

Tomita, N., Mizutani, Y., Trathan, P., and Niizuma, Y. (2015). Relationship between non-breeding migratory movements and stable isotopes of nitrogen and carbon from primary feathers of black-tailed gull *Larus crassirostris*. *Ornithol. Sci.* 14, 3–11. doi:10.2326/osj.14.3

Tomita, N., and Narita, A. (2021). Monitoring breeding performance of the black-tailed gull *Larus crassirostris* on Kabushima island, Japan, from 2012 to 2020. *Yamashina Choruigaku Zasshi* 53, 39–43. doi:10.3312/jyio.53.39

Trapletti, A., Hornik, K., and LeBaron, B. (2024). tseries: Time Series Analysis and Computational Finance. *R Package Version 0.10-51*. doi:10.32614/CRAN.package.tseries

Ungvari, Z., Parrado-Fernandez, C., Csiszar, A., and de Cabo, R. (2008). Mechanisms underlying caloric restriction and lifespan regulation: implications for vascular aging. *Circ. Res.* 102, 519–528. doi:10.1161/CIRCRESAHA.107.168369

Urso, M. L., and Clarkson, P. M. (2003). Oxidative stress, exercise, and antioxidant supplementation. *Toxicology*, 189. 41, 54. doi:10.1016/S0300-483X(03)00151-3

Vázquez-Medina, J. P., Zenteno-Savín, T., Elsner, R., and Ortiz, R. M. (2012). Coping with physiological oxidative stress: a review of antioxidant strategies in seals. *J. Comp. Physiol. B* 182, 741–750. doi:10.1007/s00360-012-0652-0

Vélez-Alavez, M., Labrada-Martagón, V., Méndez-Rodriguez, L. C., Galván-Magaña, F., and Zenteno-Savín, T. (2013). Oxidative stress indicators and trace element concentrations in tissues of mako shark (*Isurus oxyrinchus*). *Comp. Biochem. Physiol. A Mol. Integr. Physiol.* 165, 508–514. doi:10.1016/j.cbpa.2013.03.006

Viblanc, V. A., Mathien, A., Saraux, C., Viera, V. M., and Groscolas, R. (2011). It costs to be clean and fit: energetics of comfort behavior in breeding-fasting penguins. *PLoS One* 6, e21110. doi:10.1371/journal.pone.0021110

Wey, T. W., Lin, L., Patton, M. L., and Blumstein, D. T. (2015). Stress hormone metabolites predict overwinter survival in yellow-bellied marmots. *Acta Ethol.* 18, 181–185. doi:10.1007/s10211-014-0204-6

Yamamoto, T., Takahashi, A., Katsumata, N., Sato, K., and Trathan, P. N. (2010). At-sea distribution and behavior of streaked shearwaters (*Calonectris leucomelas*) during the nonbreeding period. *Auk* 127, 871–881. doi:10.1525/auk.2010.10029

Yee, T. (2025). VGAM: Vector Generalized Linear and Additive Models. *R Package Version 1.1-11*. doi:10.32614/CRAN.package.VGAM

Yoda, K., Shiomi, K., and Sato, K. (2014). Foraging spots of streaked shearwaters in relation to ocean surface currents as identified using their drift movements. *Prog. Oceanogr.* 122, 54–64. doi:10.1016/j.pocean.2013.12.002

Yoda, K., Tomita, N., Mizutani, Y., Narita, A., and Niizuma, Y. (2012). Spatio-temporal responses of black-tailed gulls to natural and anthropogenic food resources. *Mar. Ecol. Prog. Ser.* 466, 249–259. doi:10.3354/meps09939

Yun, H. R., Jo, Y. H., Kim, J., Shin, Y., Kim, S. S., and Choi, T. G. (2020). Roles of autophagy in oxidative stress. *Int. J. Mol. Sci.* 21, 3289. doi:10.3390/ijms21093289

Zuur, A. F., Ieno, E. N., and Elphick, C. S. (2010). A protocol for data exploration to avoid common statistical problems. *Methods Ecol. Evol.* 1, 3–14. doi:10.1111/j.2041-210x.2009.00001.x

frontiers | Frontiers in Physiology

TYPE Original Research
PUBLISHED 29 May 2025
DOI 10.3389/fphys.2025.1511476

OPEN ACCESS

EDITED BY
J. Chris McKnight,
University of St Andrews, United Kingdom

REVIEWED BY
Lene H. Petersen,
Texas A&M University at Galveston, United States
Kazuyoshi Komeyama,
Hokkaido University, Japan

*CORRESPONDENCE
Yuya Makiguchi,
yuya.makiguchi@gmail.com

RECEIVED 15 October 2024
ACCEPTED 16 May 2025
PUBLISHED 29 May 2025

CITATION
Makiguchi Y, Abe TK and Ichimura M (2025) Novel insights into sex-specific differences in heart rate variability and autonomic nervous system regulation during spawning behavior in chum salmon (*Oncorhynchus keta*) revealed by re-analysis of ECG logger data. *Front. Physiol.* 16:1511476. doi: 10.3389/fphys.2025.1511476

Novel insights into sex-specific differences in heart rate variability and autonomic nervous system regulation during spawning behavior in chum salmon (*Oncorhynchus keta*) revealed by re-analysis of ECG logger data

Yuya Makiguchi[1]*, Takaaki K. Abe[1] and Masaki Ichimura[2]

[1]College of Bioresource Sciences, Nihon University, Fujisawa, Kanagawa, Japan, [2]Shibetsu Salmon Museum, Shibetsu, Japan

This study reanalysed electrocardiogram (ECG) data collected in a previous study on chum salmon to explore sex-specific differences in heart rate variability (HRV) and autonomic nervous system regulation during spawning. The prior research included six female and five male salmon with implanted ECG loggers, observed during spawning, and ten additional females for pharmacological experiments on autonomic nervous system effects. The analysis uncovered distinct HRV patterns between sexes. Females exhibited an increase in heart rate from 82.27 to 86.16 bpm post-spawning, while males decreased from 74.71 to 67.78 bpm. Breakpoint analysis identified four change points in female HRV and five in male HRV. Females displayed a heart rate decrease 21 min before spawning, while males maintained stable rates until spawning. Both sexes experienced cardiac arrest at spawning, consistent with the previous study. HRV changes did not always correspond directly with spawning behaviors, indicating autonomic nervous system involvement beyond physical exertion. Pharmacological experiments showed that atropine, a parasympathetic blocker, suppressed HRV and prevented cardiac arrest, emphasizing the key role of the parasympathetic system in regulating spawning-related HRV. The study suggests that HRV during salmon spawning is regulated by physical activity and autonomic nervous system control, with an important role in parasympathetic activation. This activation begins 20 min before spawning in females, serving as a preparatory mechanism for the physiological demands of spawning. These findings improve our understanding of salmonid reproductive physiology and may inform conservation strategies. Future research should investigate direct measurements of autonomic activity, environmental influences on HRV, and the relationship between HRV patterns and reproductive success. Combining HRV data with other physiological measurements could offer a more comprehensive

understanding of the regulatory mechanisms underlying spawning behavior and the energetic costs associated with reproduction in salmonids.

KEYWORDS

salmonid reproduction, cardiovascular physiology, parasympathetic regulation, behavioral ecology, physiological adaptation, biologging, stress response

Introduction

The spawning period is a critical life event for salmonids, profoundly influencing individual survival and reproductive success. During migration from marine to freshwater habitats, salmon undergo complex physiological changes using considerable energy for swimming, sexual maturation, and spawning behaviors (Crossin et al., 2004; Quinn, 2018). For example, Chinook salmon reallocate a significant portion of their energy, with females dedicating approximately 14% to gonadal development and 78% to metabolism, whereas males allocate only 2% to gonadal development and 80% to metabolism (Bowerman et al., 2017). These adaptations are crucial for reproduction and are accompanied by significant shifts in gene expression to cope with environmental stressors such as changes in salinity and temperature (Evans et al., 2011; Miller et al., 2011).

Spawning behavior in salmonids reflects local adaptations, with traits like swimming performance are not necessarily directly linked to reproductive success (Quinn et al., 2001). The ability to optimize energy consumption and cardiovascular function during migration is necessary for Pacific salmon to meet the physical demands of upstream travel and prepare for spawning (Flores et al., 2012; Eliason and Farrell, 2016). However, salmon with limited energy reserves and high-stress indicators, such as elevated blood lactate, glucose, and cortisol levels, are at risk of premature mortality during migration (Cooke et al., 2006). Thus, understanding the physiological responses and behaviors during spawning is essential for understanding salmon's reproductive ecology and population dynamics.

Heart rate variability (HRV) analysis has emerged as a valuable non-invasive tool to assess the interplay between fish's sympathetic and parasympathetic branches of the autonomic nervous system (Vera and Priede, 1991; Altimiras et al., 1995). HRV measurements reveal how environmental factors such as water temperature influence cardiac function, reflecting physiological adjustments that maintain homeostasis. Notably, distinct HRV patterns during spawning have been observed; for example, male Atlantic salmon display higher activity levels and metabolic rates than females (Altimiras et al., 1996).

The autonomic nervous system is central to regulating HRV in fish by balancing sympathetic and parasympathetic inputs, with each branch contributing differently according to the physiological state (Cameron, 1979; Iversen et al., 2010). Pharmacological studies employing blockers such as atropine and propranolol have demonstrated that vagal (parasympathetic) regulation is critical for modulating heart rate and stroke volume, especially during rest, exercise, and stress. Sex-specific differences in autonomic regulation have been observed in spawning salmonids—males often exhibit higher heart rates and distinct low-frequency spectral peaks compared to females (Altimiras et al., 1996). Additionally, research on sockeye salmon suggests that females maintain higher resting heart rates due to lower cholinergic tone, implicating autonomic balance differences in spawning behavior and reproductive success (Sandblom et al., 2009). Despite these advances, the precise interactions between the sympathetic and parasympathetic systems under varying environmental stresses remain incomplete, highlighting the need for further investigation.

This study aims to clarify the relationship between heart rate variability (HRV) and spawning behavior in male and female chum salmon (*Oncorhynchus keta*), building on previous work by Makiguchi et al. (2009). Our primary objectives are to clarify the correlation between heart rate and specific spawning behaviors and to investigate the role of the autonomic nervous system during this critical life stage. By employing continuous HRV recordings via ECG loggers and pharmacological interventions, we seek to provide a detailed characterization of cardiac control under both physiological and environmental influences. Ultimately, our findings are expected to enhance understanding of reproductive physiology in salmonids and inform conservation and management strategies to improve salmon survival and reproductive success.

These studies emphasize the importance of high-resolution HRV analysis in elucidating the physiological mechanisms underlying salmon spawning. Our work provides insight regarding autonomic regulation during this critical life stage by integrating continuous ECG monitoring, detailed behavioral observations, and targeted pharmacological interventions. This comprehensive approach deepens our understanding of the interplay between cardiac function and spawning behavior. It lays the foundation for future research that may inform conservation and resource management strategies for sustainable salmon populations.

Materials and methods

Attachment procedure of ECG data logger

This study examined the dataset used by Makiguchi et al. (2009), which involved six female (mean ± s.d. fork length = 618 ± 22 mm; mean ± s.d. mass = 2648 ± 119 g) and five male (mean ± s.d. fork length = 655 ± 24 mm; mean ± s.d. mass = 3,028 ± 285 g) chum salmon (*Oncorhynchus keta*) implanted with ECG loggers (W400L-ECG, Little Leonard Co., Tokyo, Japan; 21 mm diameter, 110 mm length, 57 g mass in air). In addition to the ECG logger-implanted individuals, we used ten female chum salmon for pharmacological experiments. Specifically, three fish (mean ± s.d. fork length = 649

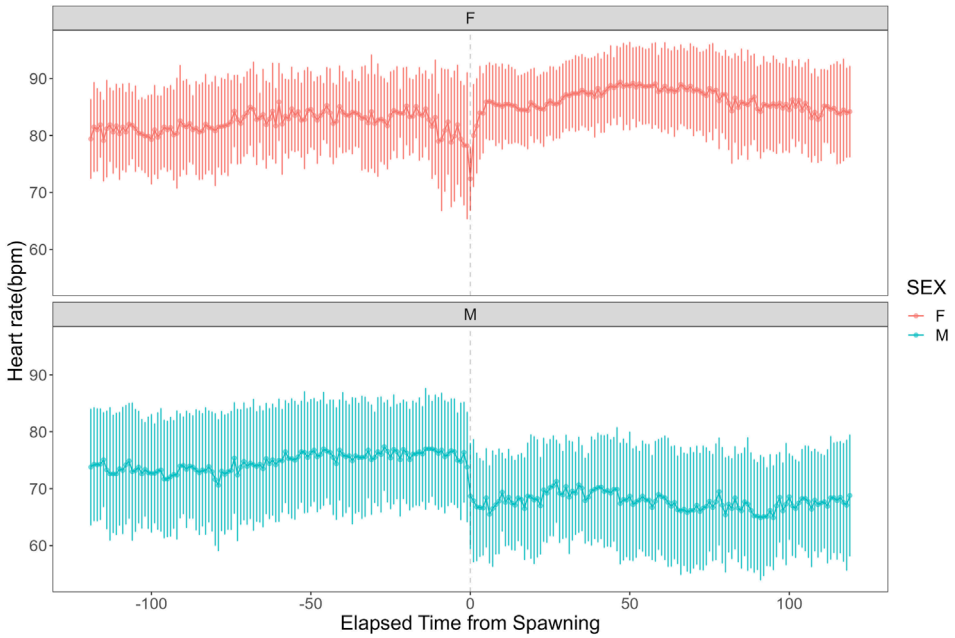

FIGURE 1
Heart rate time series data for female and male chum salmon (*Oncorhynchus keta*) during the 2 h before and after spawning. The x-axis represents time relative to spawning (in minutes), with 0 indicating the moment of spawning. Negative values denote time before spawning, while positive values indicate time after spawning. The y-axis shows the heart rate in beats per minute (bpm). The upper panel (pink) displays data for females (n = 6), while the lower panel (blue) shows data for males (n = 5). Each data point represents the mean heart rate; error bars indicate the standard deviation.

± 32 mm; mean ± s.d. mass = 3,045 ± 65 g) were administered physiological saline as a control, three fish (mean ± s.d. fork length = 665 ± 50 mm; mean ± s.d. mass = 3,157 ± 82 g) were administered atropine, a parasympathetic nervous system inhibitor, and four fish (mean ± s.d. fork length = 624 ± 13 mm; mean ± s.d. mass = 2771 ± 20 g) were administered sotalol, a sympathetic nervous system inhibitor. The drugs were administered via a cannula inserted into the dorsal aorta of the individuals equipped with ECG loggers. For detailed information on the drug administration methods, please refer to Makiguchi et al. (2009). We anesthetized the fish and surgically sutured a copper disc bipolar electrode to the ventral side of each fish. The ECG loggers were attached to the dorsal side, anterior to the dorsal fin, and programmed to record at a sampling rate of 200 Hz. After a 24-hour recovery period, we placed the implanted fish in a spawning channel (3.8 m × 2.9 m × 1.1 m) at the Shibetsu Salmon Museum, Hokkaido, Japan. The channel was supplied with 16.8°C spring water and had a silt-free gravel bottom (Groot, 1996). We recorded the spawning behavior of the fish with a digital video camera and synchronized it with the ECG signals. Among the experimental data, we observed four pairs of male and female salmon for spawning behavior, with both individuals in each pair equipped with ECG loggers. Each of these four pairs exhibited two spawning events. Additionally, we paired two females with males without ECG loggers and obtained data only from the females in these pairs. These two pairs also exhibited two spawning events each. Furthermore, we paired one male with a female with no ECG logger attached and obtained data only from the male in this pair, with two spawning events observed. We observed 14 spawning events and collected electrocardiogram data associated with 22 spawning events from both males and females combined.

Behavioral definitions

In this study, we defined two key spawning behaviors: redd digging and covering. Redd digging refers to the behavior where a female salmon uses her caudal fin to excavate gravel from the riverbed, creating a spawning nest. During this behavior, the female tilts her body and moves her caudal fin from side to side to displace gravel and form a depression for egg deposition. Covering behavior was defined as the action where a female uses her caudal fin to cover the deposited eggs with the excavated gravel. This action helps protect the eggs from predators and ensures a safe environment for hatching. Both behaviors were identified and analyzed using digital video recordings of the spawning events. We quantified the frequency of these behaviors by counting the number of instances per 10-minute interval.

Data analysis

To examine the relationship between spawning behavior and heart rate, we set 2 h before and after the observed spawning time as the analysis interval. The 2-hour period before spawning corresponds to the timing when females determine the approximate location of the spawning bed and engage in digging behavior. We determined R-R intervals using ECGtoHR (Sakamoto et al.,

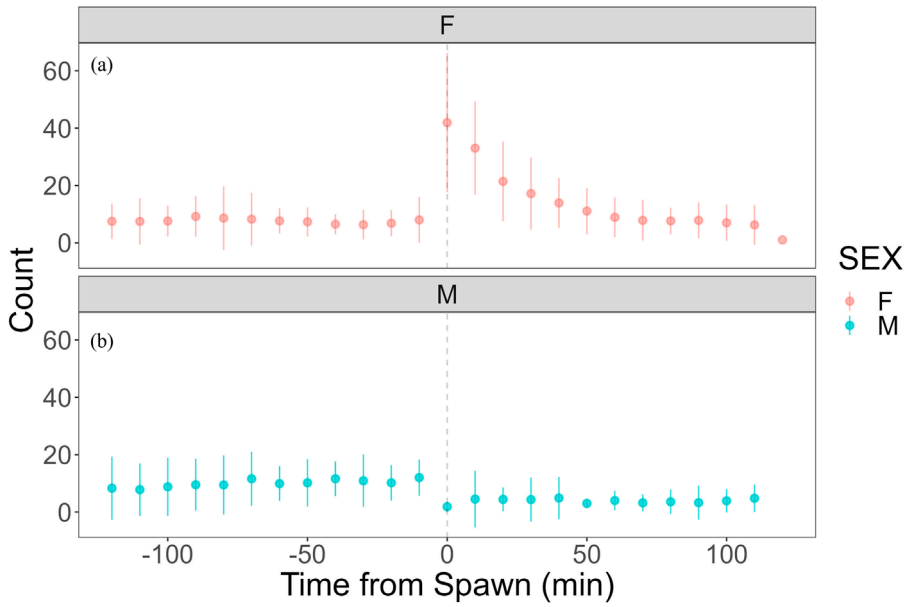

FIGURE 2
Time series data of female covering behavior and male quivering behavior in chum salmon (*Oncorhynchus keta*) during the 2 h before and after spawning. The x-axis represents time relative to spawning (in minutes), with 0 indicating the moment of spawning. Negative values denote time before spawning, while positive values indicate time after spawning. The y-axis shows the frequency of behaviors as counts per 10-minute interval. The upper panel (pink) displays covering behavior data for females (n = 6), while the lower panel (blue) shows quivering behavior data for males (n = 5). Each data point represents the mean count of behaviors per 10-minute interval, and error bars indicate standard deviation. Note the contrasting patterns between sexes: females show increased covering behavior immediately after spawning, while males exhibit peak quivering behavior just before spawning, followed by a sharp decline post-spawning. **(a)** Heart rate time series with identified change points. The x-axis represents time relative to spawning (in minutes), with 0 indicating the moment of spawning. The y-axis shows the heart rate in beats per minute (bpm). Vertical dashed lines indicate detected change points, with the numbers above showing the time (in minutes) relative to spawning when each change point occurred. Note the decrease in heart rate and increase in variability starting 21 min before spawning, followed by cardiac arrest at spawning (0 min), and subsequent increase until 46 min post-spawning. **(b)** Frequency of digging and covering behaviors with identified change points. The x-axis represents time relative to spawning (in minutes), with 0 indicating the moment of spawning. The y-axis shows the frequency of behaviors as counts per 10-minute interval. Vertical dashed lines indicate detected change points, with the numbers above showing the time (in minutes) relative to spawning when each change point occurred. Observe the decline in digging behavior until spawning, followed by a rapid increase in covering behavior immediately after spawning, with a slower rate of decrease starting 40 min post-spawning. These graphs illustrate the complex interplay between physiological and behavioral changes during the spawning process in female chum salmon.

2021), a computer program that calculates heart rate from electrocardiograms, running on IGOR Pro ver9.05 (WaveMetrics Inc., Lake Oswego, OR, United States). We used R software ver. 3.62 (Team, 2022) for the analysis. We set the significance level at 5%. When comparing heart rates before and after spawning in males and females separately, we used the lme4 library, specifying a Poisson distribution since the response variable, heart rate, is a count. Individual ID was treated as a random effect. Values are presented as mean ± standard deviation (s.d.). Heart rate is expressed as beats per minute (b.p.m.).

We also used the 'strucchange' library (Zeileis et al., 2003) in R software to investigate whether there were any breakpoints in the heart rate trends for both males and females during the period from 2 h before spawning to 2 h after spawning. The 'strucchange' library uses a function that detects structural changes in regression models, identifying potential breakpoints where the heart rate change significantly shifts along the time gradient. To determine the optimal number of breakpoints, we calculated the Bayesian Information Criterion (BIC) for each potential number of breakpoints. We selected the number of breakpoints resulting in the lowest BIC as the final number of change points (Zeileis et al., 2003). This method allows the most parsimonious model to be chosen, balancing the goodness of fit with the complexity of the model. This approach allows for identifying significant changes in heart rate trends over the spawning period, providing insights into the physiological responses of male and female salmon during this critical life stage.

Results

Heart rate increased in females from 82.27 ± 7.59 bpm (n = 1,190) before spawning to 86.16 ± 7.18 bpm (n = 1,200) after spawning ($p < 0.05$). Conversely, heart rate in males significantly decreased from 74.71 ± 9.46 bpm (n = 1,190) before spawning to 67.78 ± 9.09 bpm (n = 1,200) after spawning ($p < 0.05$). Additionally, females exhibited significantly higher heart rates than males before and after spawning ($p < 0.05$). Figure 1 shows the heart rate time series data for both sexes during the 2 h before and after spawning. Figure 2 displays the time series data of male courtship behavior and female digging and covering behavior. Breakpoint analysis using the 'strucchange' library (Zeileis et al., 2003) in R software identified

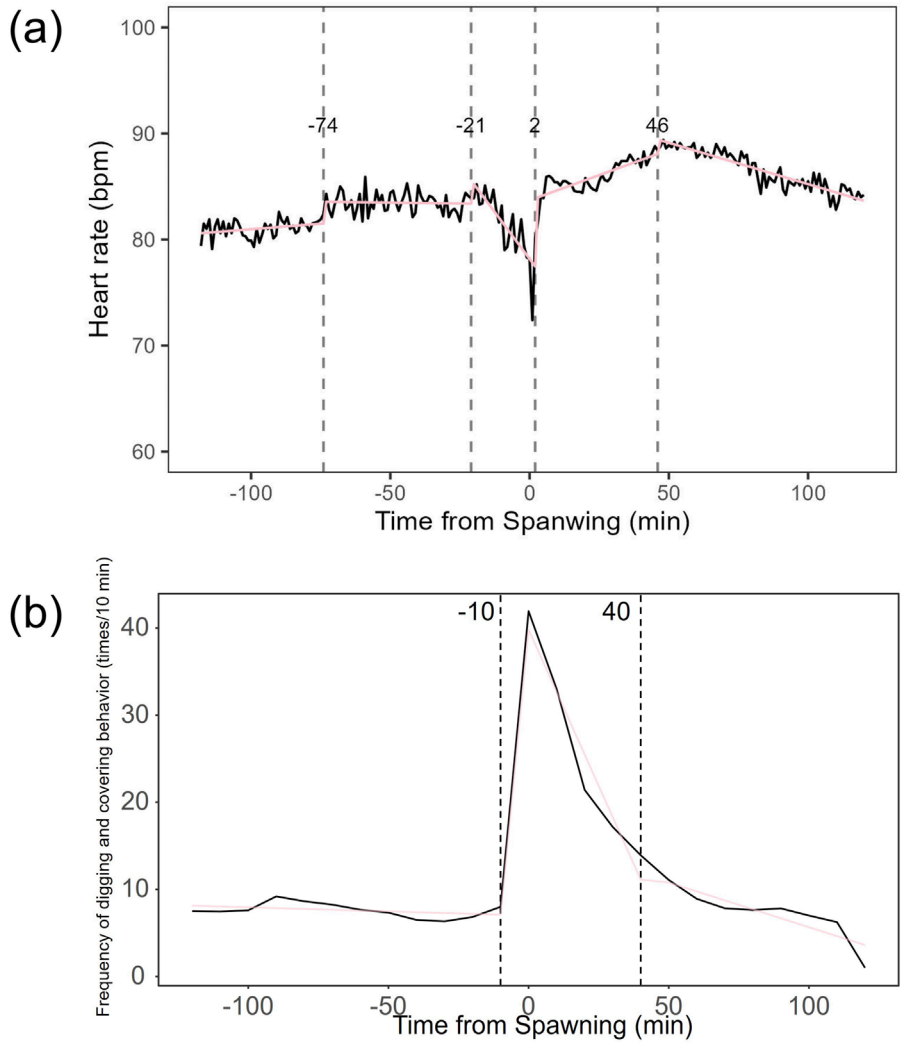

FIGURE 3
Breakpoint analysis of heart rate variability and behavioral changes in female chum salmon (Oncorhynchus keta) during spawning. **(a)** Heart rate time series with identified change points. The x-axis represents time relative to spawning (in minutes), with 0 indicating the moment of spawning. The y-axis shows the heart rate in beats per minute (bpm). Vertical dashed lines indicate detected change points, with the numbers above showing the time (in minutes) relative to spawning when each change point occurred. Note the decrease in heart rate and increase in variability starting 21 minutes before spawning, followed by cardiac arrest at spawning (0 minutes), and subsequent increase until 46 minutes post-spawning. **(b)** Frequency of digging and covering behaviors with identified change points. The x-axis represents time relative to spawning (in minutes), with 0 indicating the moment of spawning. The y-axis shows the frequency of behaviors as counts per 10-minute interval. Vertical dashed lines indicate detected change points, with the numbers above showing the time (in minutes) relative to spawning when each change point occurred. Observe the decline in digging behavior until spawning, followed by a rapid increase in covering behavior immediately after spawning, with a slower rate of decrease starting 40 minutes post-spawning. These graphs illustrate the complex interplay between physiological and behavioral changes during the spawning process in female chum salmon.

four change points in heart rate variability during spawning behavior in females (Figure 3a). Heart rate increased from 2 to 1.5 h before spawning and remained relatively stable until 21 min before spawning. At 21 min before spawning, heart rate decreased while heart rate variability increased, with a drop in heart rate observed at spawning due to cardiac arrest (Makiguchi et al., 2009). After spawning, the heart rate increased until 46 min post-spawning and then decreased until 2 h after spawning. The breakpoint analysis identified two change points in the frequency of female digging and covering behavior during spawning (Figure 3b). Female digging behavior declined until 2 h before spawning. Covering behavior occurred at spawning, increasing rapidly before decreasing. The rate of decrease slowed at 40 min after spawning, followed by a gradual decline. Changes in digging behavior frequency and heart rate did not clearly coincide before or after spawning. Female digging behavior occurred 6.3–9.2 times/10 min until spawning, with frequent covering behavior immediately after. Covering behavior frequency decreased after spawning, falling below 9 times/10 min 1–2 h post-spawning. In males, breakpoint analysis identified five change points for heart rate variability during spawning behavior (Figure 4a). Heart rate decreased from 2 h to 1.5 h before spawning, then increased until 43 min before spawning,

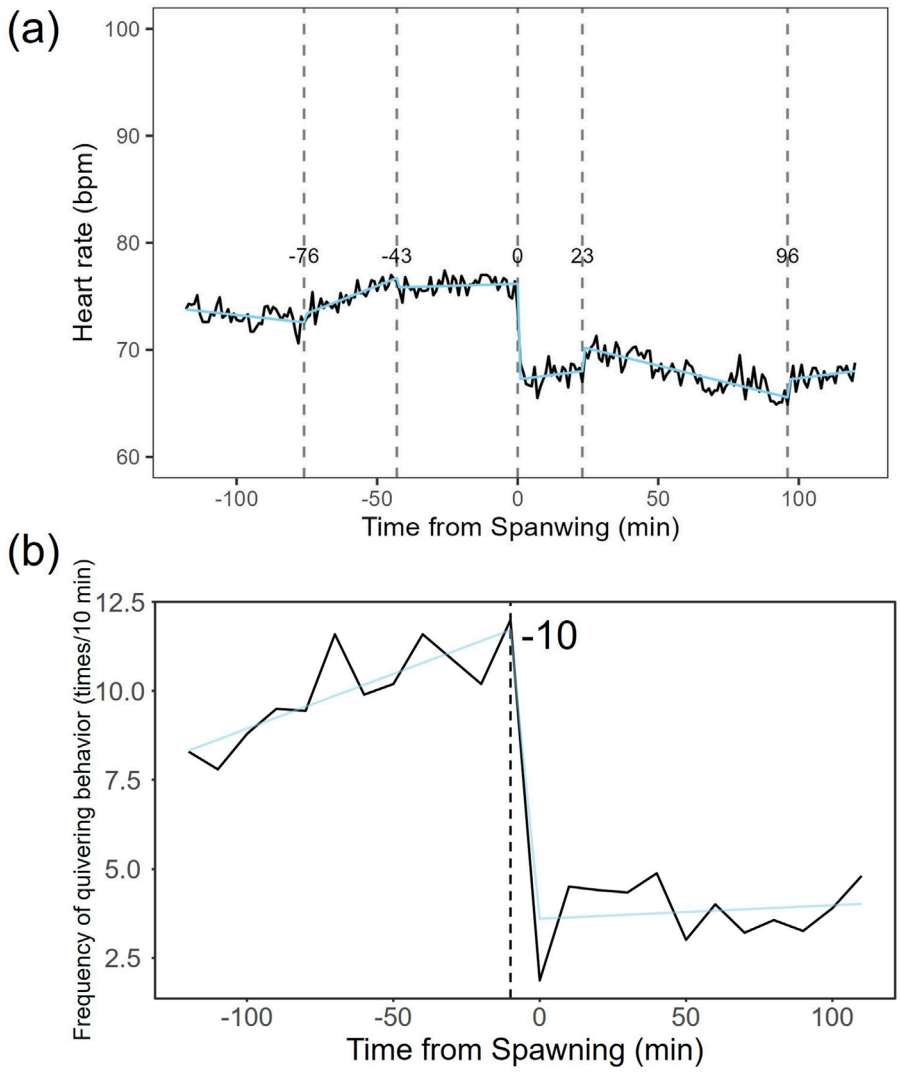

FIGURE 4
Breakpoint analysis of heart rate variability and courtship behavior changes in male chum salmon (*Oncorhynchus keta*) during spawning. **(a)** Heart rate time series with identified change points. The x-axis represents time relative to spawning (in minutes), with 0 indicating the moment of spawning. The y-axis shows the heart rate in beats per minute (bpm). Vertical dashed lines indicate detected change points, with the numbers above showing the time (in minutes) relative to spawning when each change point occurred. Note the initial decrease in heart rate from −120 to −90 min, followed by an increase until −43 min, stability until spawning, a sudden drop to 67 bpm at spawning (0 min) due to cardiac arrest, and sustained low heart rate with minor fluctuations post-spawning. **(b)** Frequency of quivering behavior with identified change point. The x-axis represents time relative to spawning (in minutes), with 0 indicating the moment of spawning. The y-axis shows the frequency of quivering behavior as counts per 10-minute interval. The vertical dashed line indicates the detected change point, with the number above showing the time (in minutes) relative to spawning when the change point occurred. Observe the increase in quivering behavior frequency from 2 h before spawning until spawning (ranging from 1.86 to 4.87 times/10 min), followed by a sharp decrease and sustained low levels post-spawning. These graphs illustrate the distinct patterns of physiological and behavioral changes in male chum salmon during spawning, highlighting the rapid shifts in both heart rate and courtship behavior around spawning.

after which it remained stable. During spawning, the heart rate drops to around 67 bpm due to cardiac arrest (Makiguchi et al., 2009). Heart rate remained low until 2 h after spawning, with only minor fluctuations. Breakpoint analysis detected one change point in male courtship behavior (Figure 4b). Courtship behavior frequency increased from 2 h before spawning until spawning, ranging between 1.86–4.87 times/10 min. After spawning, courtship behavior frequency decreased sharply and remained lower than pre-spawning levels, indicating that males rarely engage in courtship behavior after spawning.

To investigate the autonomic nervous system's regulation of heart rate during spawning, we administered atropine and sotalol to females and compared their heart rate and variability with that of a sham control group. In the atropine-treated group, heart rate did not change from 93.5 ± 4.07 bpm (n = 579) before spawning to 93.9 ± 3.41 bpm (n = 595) after spawning. However, the sotalol-treated group showed an increase in heart rate from 87.2 ± 5.84 bpm (n = 828) before spawning to 89.8 ± 5.16 bpm (n = 825) after spawning ($p < 0.05$). The sham control group did not show changes in heart rate, with 92.0 ± 4.78 bpm (n = 592)

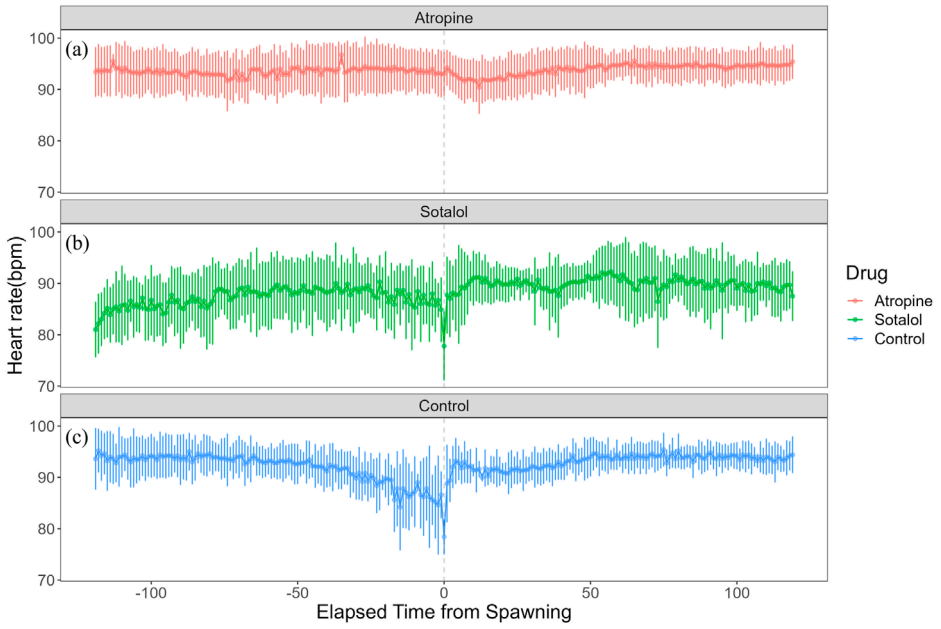

FIGURE 5
Effects of autonomic nervous system blockers on heart rate variability in female chum salmon (*Oncorhynchus keta*) during spawning. The x-axis represents time relative to spawning (in minutes), with 0 indicating the moment of spawning. The y-axis shows the heart rate in beats per minute (bpm). Each panel displays the heart rate time series for a different treatment group: Top panel (red line **(a)**): Atropine-treated group (parasympathetic blocker), Middle panel (green line **(b)**): Sotalol-treated group (sympathetic blocker), Bottom panel (blue line **(c)**): Sham control group.

before spawning and 93.0 ± 3.22 bpm (n = 599) after spawning. No significant differences in heart rate were found among the treatment groups before or after spawning. Figure 5 shows the heart rate time series for each treatment group. The atropine-treated group did not experience cardiac arrest, characterized by prolonged RR intervals, and showed decreased heart rate variability (Figure 5a). Conversely, the sotalol-treated group showed larger fluctuations in heart rate around spawning (Figure 5b). In contrast, the control group showed a sharp change in heart rate before and after spawning (Figure 5c).

Breakpoint analysis of heart rate variability revealed multiple change points in each treatment group (Figure 6). In the atropine-treated group, change points were identified at 66 min before, 31 min before, 5 min before, and 66 min after spawning (Figure 6a). The sotalol-treated group showed change points 48 min before spawning, 6 min after, and 42 min after spawning (Figure 6b). The sham control group had change points 42 min before spawning, 1 min after spawning, and 42 min after spawning (Figure 6c). No clear distinctions in change point patterns were apparent among the groups.

Figure 7 shows each group's coefficient of variation (CV) of heart rate during spawning. The atropine-treated group maintained a lower CV than the other two groups (Figure 7a). This suggests that atropine suppressed heart rate variability during the spawning process. The sotalol-treated group had a larger CV around spawning and maintained high variability during the observation period, except post-spawning (Figure 7b). This indicates a broader range of heart rate changes in the sotalol group. The control group showed a sharp increase in CV 24 min before spawning, suggesting that anticipating spawning significantly affected heart rate variability (Figure 7c). Post-spawning, the CV in the control group decreased from the large fluctuations observed pre-spawning.

Discussion

Sex-specific differences in heart rate variability patterns before and after spawning and their significance

This study analyzed the heart rate variability of salmon during spawning behavior in detail. A temporary increase in heart rate was observed immediately before spawning, followed by a rapid decrease in heart rate, or cardiac arrest, at the moment of spawning (Makiguchi et al., 2009). This cardiac arrest is suggested to be caused by increased parasympathetic nervous system activity (Taylor et al., 1999; Makiguchi et al., 2009). After recovery from cardiac arrest, the heart rate slowly recovers, but does not return to the pre-spawning level. This heart rate fluctuation is thought to reflect the energy expenditure and autonomic nervous system regulation during salmon spawning behavior. The increase in heart rate before spawning suggests increased sympathetic nervous system activity corresponding to the increased energy demand required for spawning (Altimiras et al., 1997; Taylor et al., 1999). On the other hand, the rapid decrease in heart rate during spawning is thought to be due to a rapid increase in parasympathetic nervous system activity to facilitate the release of eggs and sperm (Makiguchi et al., 2009). Such dynamic regulation of the autonomic nervous system is considered a physiological adaptation

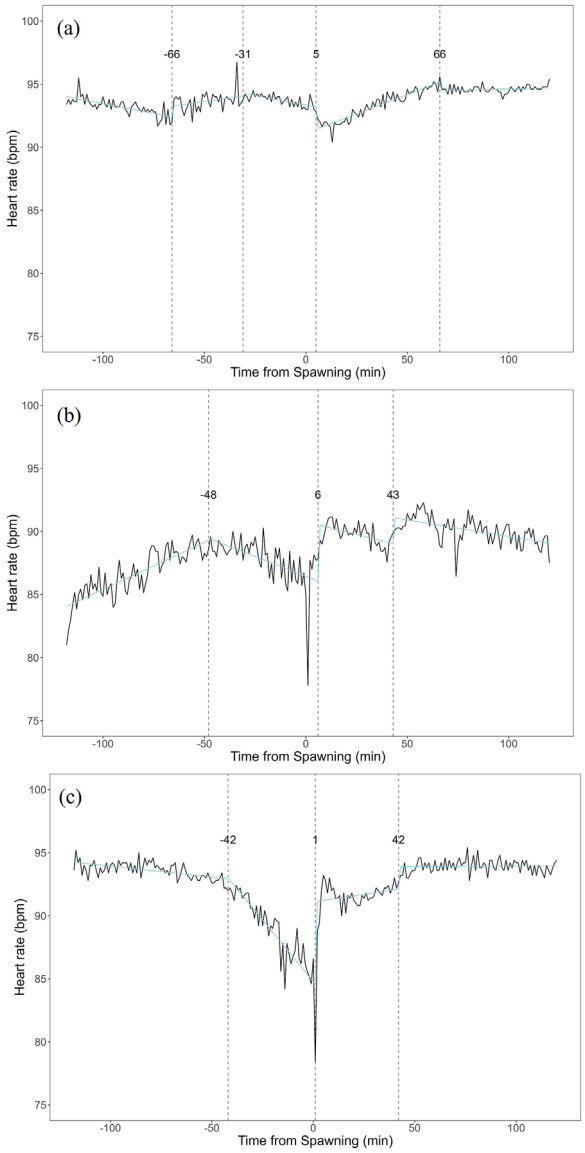

FIGURE 6
Breakpoint analysis of heart rate variability in female chum salmon (*Oncorhynchus keta*) under different autonomic nervous system blocker treatments during spawning. The x-axis represents time relative to spawning (in minutes), with 0 indicating the moment of spawning. The y-axis shows the heart rate in beats per minute (bpm). Vertical dashed lines indicate detected change points, with the numbers above showing the time (in minutes) relative to spawning when each change point occurred. **(a)** Atropine-treated group (parasympathetic blocker). Change points were detected at −66, −31, −5, and +66 min relative to spawning. **(b)** Sotalol-treated group (sympathetic blocker). Change points were identified at −48, +6, and +42 min relative to spawningc). **(c)** Sham control group. Change points were observed at −42, +1, and +42 min relative to spawning. Note that despite the different treatments, no clear distinctions in change point patterns were apparent among the groups. This suggests that factors beyond direct autonomic nervous system control may influence the overall temporal dynamics of heart rate variability during spawning.

for fish to efficiently perform reproductive behavior (Nilsson, 1983). Furthermore, analysis of heart rate variability (HRV) suggested the possibility of changes in the autonomic balance of salmon during the spawning period. HRV is a method of evaluating autonomic nervous system activity using the variability of heart beat intervals as an index, reflecting the balance between the sympathetic and parasympathetic nervous systems (Akselrod et al., 1981; Altimiras, 1999). Changes in HRV during the spawning period may reflect the regulation of the autonomic nervous system in response to stress and changes in energy consumption associated with reproductive behavior (Campbell et al., 2004, 2006). However, in this study, specific HRV indicators (e.g., LF/HF ratio by frequency analysis) were not analyzed, and further investigation is needed to quantitatively evaluate changes in autonomic balance. In future studies, a more detailed analysis of HRV will allow a more detailed understanding of the dynamics of the autonomic nervous system in salmon during spawning behavior. In addition, it is necessary to observe heart rate variability in more detail under natural conditions by utilizing bio-logging technology to better understand the relationship between spawning behavior and heart rate variability (Warren-Myers et al., 2021).

Relationship between heart rate variability and spawning behavior before and after spawning

The observed cardiac arrest during spawning suggests a potential adaptive strategy aimed at conserving energy and enhancing spawning efficiency. This phenomenon, also reported by Makiguchi et al. (2009) in chum salmon, may be common among salmonids. However, we did not observe a direct correspondence between the frequency of spawning behavior and HRV patterns. This discrepancy may be attributed to the complex nature of spawning, where HRV is also influenced by other environmental and individual factors. Additionally, sex differences in heart rate during the spawning period suggest potential variations in autonomic nervous system activity between males and females. Studies by Sandblom et al. (2009) indicate that the autonomic innervation of the heart differs between sexes in salmonids. The increase in heart rate after spawning in females compared to the decrease in males may reflect differences in the balance of sympathetic and parasympathetic activity. The results of the pharmacological experiments provide further support for these interpretations. The increase in heart rate after atropine administration suggests that parasympathetic activity is crucial for maintaining a lower heart rate during spawning. Furthermore, as Steele et al. (2011) have shown, β-adrenergic receptors play an important role in the autonomic control of the heart and these receptors may influence the changes observed in heart rate during spawning. These findings suggest that heart rate fluctuations in spawning salmon are controlled not by a single factor, but by a complex interaction of several autonomic and physiological factors.

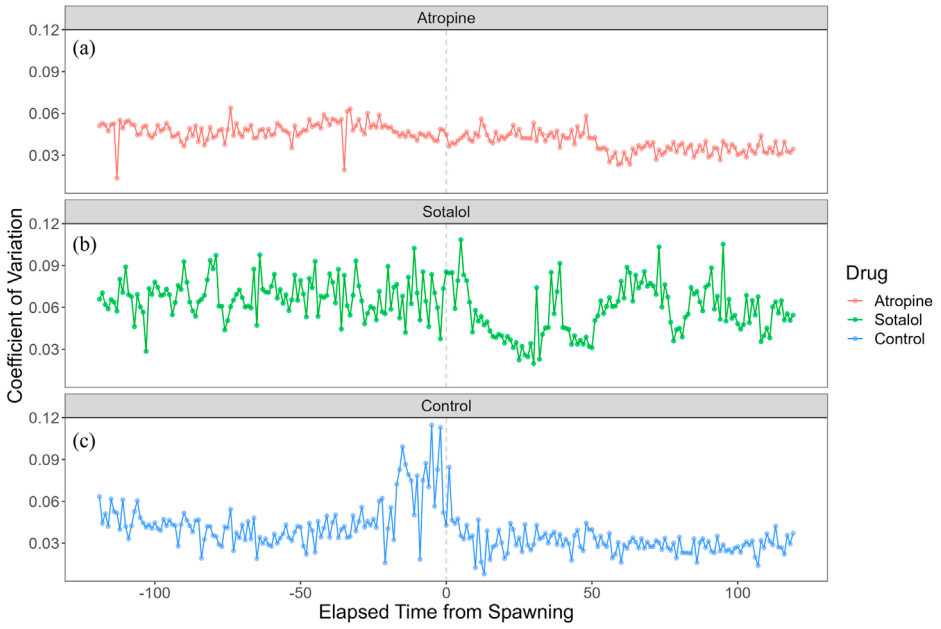

FIGURE 7
Coefficient of variation (CV) of heart rate in female chum salmon (*Oncorhynchus keta*) under different autonomic nervous system blocker treatments during spawning. The x-axis represents time relative to spawning (in minutes), with 0 indicating the moment of spawning. The y-axis shows the coefficient of heart rate variation (beats/minute). Each panel displays the CV time series for a different treatment group: **(a)** Atropine-treated group (red line): Note the consistently lower CV than other groups, indicating suppressed heart rate variability throughout spawning. **(b)** Sotalol-treated group (green line): Observe the more extensive CV around spawning and maintained high variability during most of the observation period, suggesting a more comprehensive range of heart rate changes. **(c)** Sham control group (blue line): Notice the sharp increase in CV 24 min before spawning, indicating that anticipation of spawning significantly affected heart rate variability. Post-spawning, the CV decreases from the large fluctuations observed pre-spawning. These graphs illustrate the differential effects of autonomic nervous system blockers on heart rate variability during the spawning process in female chum salmon.

The role of the autonomic nervous system in heart rate variability during spawning

Pharmacological experiments using atropine and sotalol have provided key insights into the autonomic regulation of heart rate in salmon during spawning (Campbell et al., 2009; Bazmi and Escobar, 2022). Atropine, a muscarinic cholinergic receptor antagonist, increases heart rate by blocking the parasympathetic nervous system's effects on the heart, removing inhibitory tone. Sotalol, a β-adrenergic receptor blocker, mainly antagonizes the sympathetic nervous system, reducing heart rate and contractility (Steele et al., 2011). These drugs are widely used in fish cardiac function studies to dissect the relative contributions of the parasympathetic and sympathetic systems. The use of atropine in particular highlights the strong vagal tone that suppresses heart rate in many fish species. For example, in Antarctic fish, pharmacological blockade of muscarinic receptors with atropine increased heart rate, demonstrating a significant cholinergic influence on resting heart rate (Campbell et al., 2009). Furthermore, the use of adrenergic antagonists, such as sotalol, allows the study of adrenergic contributions to cardiac function. Combining these pharmacological tools allows identification of the intrinsic heart rate of the cardiac pacemaker in the absence of autonomic input, providing a detailed understanding of the autonomic control of heart rate (Sandblom and Axelsson, 2011; Sandblom et al., 2016). In the study by Makiguchi et al., 2009, atropine administration did not prevent cardiac arrest, while sotalol administration did, and heart rate variability was similar to the control group. This suggests a key role for the parasympathetic nervous system in cardiac arrest during spawning. However, analysis of the coefficient of variation (CV) revealed that heart rate variability increased in the control group immediately before and after spawning, while this increase was blunted in the atropine and sotalol-administered groups (Watanabe-Asaka et al., 2022). This indicates that not only the parasympathetic, but also the sympathetic nervous system significantly affects heart rate variability during spawning. While the parasympathetic system appears to play a central role in the cardiac arrest itself, the sympathetic system also appears to be involved in the dynamic modulation of heart rate during the period from immediately before to immediately after spawning. These findings highlight the complex interplay of the autonomic nervous system in the control of heart rate during spawning, supporting previous knowledge about the importance of the parasympathetic nervous system, and suggesting a role for the sympathetic nervous system in regulating heart rate variability during spawning. This discussion emphasizes the importance of analyzing not only average heart rate but also the CV of heart rate variability to understand the dynamic regulatory actions of the autonomic nervous system.

ECG loggers and future research

Advances in data logger technology have significantly improved our ability to monitor physiological parameters in fish over extended periods, enabling detailed studies of cardiac function during critical life stages. In our study, high-resolution ECG loggers allowed the identification of precise change points in heart rate variability (HRV) that correlate with distinct spawning behaviors in chum salmon. Rather than simply reiterating our results, our findings suggest that the pre-spawning decrease in HRV observed 21 min before spawning in females may represent a preparatory autonomic adjustment, likely mediated by increased parasympathetic activity. This anticipatory response, similar to what has been observed in other salmonids (Sandblom et al., 2009), appears to optimize cardiac performance in anticipation of the high energetic demands of spawning. Similarly, the rapid post-spawning drop in heart rate in males, coinciding with a decline in courtship behavior, indicates a swift autonomic modulation that may serve to conserve energy following intense activity. This rapid change highlights the dynamic nature of autonomic control during spawning (Makiguchi et al., 2009). Furthermore, our findings are consistent with the understanding that heart rate variability is not solely governed by physical exertion, suggesting complex autonomic nervous system responses during this critical life history event (Warren-Myers et al., 2021).

Importantly, our pharmacological experiments further support the role of parasympathetic control in these processes; the suppression of HRV by atropine treatment confirms that the autonomic nervous system is actively involved in regulating cardiac function during spawning (Makiguchi et al., 2009). In contrast, sotalol treatment did not prevent the occurrence of cardiac arrest, suggesting a more complex interplay between sympathetic and parasympathetic influences that merits further investigation. This finding aligns with other studies indicating that parasympathetic mechanisms are dominant in mediating cardiac arrest during spawning (Makiguchi et al., 2009) while also highlighting that the specific roles of sympathetic and parasympathetic systems can vary significantly across different physiological responses (Mann et al., 2010; Steele et al., 2011).

Looking ahead, future research should integrate ECG logging with additional physiological and environmental measurements—such as hormonal profiles, gastrointestinal blood flow, and energy expenditure—to elucidate the multi-faceted regulation of spawning behavior. This approach would allow for a deeper understanding of the interplay between internal physiological changes and behavioral responses during spawning (Brownscombe et al., 2019; Prystay et al., 2019). Comparative studies across salmonid species will also be essential to determine whether these autonomic responses represent a conserved adaptive mechanism or if they vary with ecological context. Such comparative research will help to assess the generality of the findings across different salmonid species and their ecological contexts (Campbell et al., 2009; Sandblom et al., 2009). Ultimately, a deeper understanding of these mechanisms will not only advance basic reproductive physiology in fish but may also inform conservation strategies and aquaculture practices by highlighting sex-specific responses to environmental stressors. Understanding sex-specific differences and responses is crucial for effective conservation efforts, as these differences can significantly impact mortality rates and reproductive success (Cooke, 2004; Sandblom et al., 2009). By focusing on the interpretation of our data and its implications, we aim to provide a comprehensive framework for future studies that bridges the gap between high-resolution physiological monitoring and practical applications in fish management and conservation. This interdisciplinary approach is crucial for developing effective strategies for sustainable fisheries management (Cooke et al., 2012; Sandblom et al., 2016).

Data availability statement

The raw data supporting the conclusions of this article will be made available by the authors, without undue reservation.

Ethics statement

Ethical approval was not required for the studies on animals in accordance with the local legislation and institutional requirements.

Author contributions

YM: Conceptualization, Data curation, Formal Analysis, Funding acquisition, Investigation, Methodology, Project administration, Resources, Software, Supervision, Validation, Visualization, Writing – original draft, Writing – review and editing. TA: Methodology, Writing – review and editing. MI: Conceptualization, Writing – review and editing.

Funding

The author(s) declare that financial support was received for the research and/or publication of this article. This work was supported by Grant-in-Aid for Transformative Research Areas 21H05296.

Acknowledgments

We want to thank the Shibetsu Salmon Science Museum staff for their support in conducting the experiments.

Conflict of interest

The authors declare that the research was conducted in the absence of any commercial or financial relationships that could be construed as a potential conflict of interest.

Generative AI statement

The authors declare that no Generative AI was used in the creation of this manuscript.

Publisher's note

References

Akselrod, S., Gordon, D., Ubel, F. A., Shannon, D. C., Barger, A. C., and Chohen, R. J. (1981). Power spectrum analysis of heart rate fluctuation: a quantitative probe of beat-to-beat cardiovascular control. *Science* 213, 220–222. doi:10.1126/science.6166045

Altimiras, J. (1999). Understanding autonomic sympathovagal balance from short-term heart rate variations. Are we analyzing noise? *Comp. Biochem. Physiology a-Molecular and Integr. Physiology* 124, 447–460. doi:10.1016/s1095-6433(99)00137-3

Altimiras, J., Aissaoui, A., and Tort, L. (1995). Is the short-term modulation of heart rate in teleost fish physiologically significant? Assessment by spectral analysis techniques. *Braz. J. Med. Biol. Res.* 28, 1197–1206.

Altimiras, J., Aissaoui, A., Tort, L., and Axelsson, M. (1997). Cholinergic and adrenergic tones in the control of heart rate in teleosts. How should they be calculated? *Comp. Biochem. Physiology a-Physiology* 118, 131–139. doi:10.1016/s0300-9629(96)00402-1

Altimiras, J., Johnstone, A. D. F., Lucas, M. C., and Priede, I. G. (1996). Sex differences in the heart rate variability spectrum of free-swimming Atlantic salmon (*Salmo salar* L) during the spawning season. *Physiol. Zool.* 69, 770–784. doi:10.1086/physzool.69.4.30164229

Bazmi, M., and Escobar, A. L. (2022). Autonomic regulation of the Goldfish intact heart. *Front. Physiol.* 13, 793305. doi:10.3389/fphys.2022.793305

Bowerman, T. E., Pinson-Dumm, A., Peery, C. A., and Caudill, C. C. (2017). Reproductive energy expenditure and changes in body morphology for a population of Chinook salmon *Oncorhynchus tshawytscha* with a long distance migration. *J. Fish. Biol.* 90, 1960–1979. doi:10.1111/jfb.13274

Brownscombe, J. W., Lédée, E. J. I., Raby, G. D., Struthers, D. P., Gutowsky, L. F. G., Nguyen, V. M., et al. (2019). Conducting and interpreting fish telemetry studies: considerations for researchers and resource managers. *Rev. Fish. Biol. Fish.* 29, 369–400. doi:10.1007/s11160-019-09560-4

Cameron, J. S. (1979). Autonomic nervous tone and regulation of heart rate in the goldfish, *Carassius auratus*. *Comp. Biochem. Physiol. C* 63C, 341–349. doi:10.1016/0306-4492(79)90084-4

Campbell, H., Davison, W., Fraser, K. P. P., Peck, L. S., and Egginton, S. (2009). Heart rate and ventilation in Antarctic fishes are largely determined by ecotype. *J. Fish. Biol.* 74, 535–552. doi:10.1111/j.1095-8649.2008.02141.x

Campbell, H. A., Klepacki, J. Z., and Egginton, S. (2006). A new method in applying power spectral statistics to examine cardio-respiratory interactions in fish. *J. Theor. Biol.* 241, 410–419. doi:10.1016/j.jtbi.2005.12.005

Campbell, H. A., Taylor, E. W., and Egginton, S. (2004). The use of power spectral analysis to determine cardiorespiratory control in the short-horned sculpin *Myoxocephalus scorpius*. *J. Exp. Biol.* 207, 1969–1976. doi:10.1242/jeb.00972

Cooke, S. J. (2004). Sex-specific differences in cardiovascular performance of a centrarchid fish are only evident during the reproductive period. *Funct. Ecol.* 18, 398–403. doi:10.1111/j.0269-8463.2004.00878.x

Cooke, S. J., Hinch, S. G., Crossin, G. T., Patterson, D. A., English, K. K., Healey, M. C., et al. (2006). Mechanistic basis of individual mortality in Pacific salmon during spawning migrations. *Ecology* 87, 1575–1586. doi:10.1890/0012-9658(2006)87[1575:mboimi]2.0.co;2

Cooke, S. J., Hinch, S. G., Donaldson, M. R., Clark, T. D., Eliason, E. J., Crossin, G. T., et al. (2012). Conservation physiology in practice: how physiological knowledge has improved our ability to sustainably manage Pacific salmon during up-river migration. *Philos. Trans. R. Soc. Lond. B Biol. Sci.* 367, 1757–1769. doi:10.1098/rstb.2012.0022

Crossin, G. T., Hinch, S. G., Farrell, A. P., Higgs, D. A., Lotto, A. G., Oakes, J. D., et al. (2004). Energetics and morphology of sockeye salmon: effects of upriver migratory distance and elevation. *J. Fish. Biol.* 65, 788–810. doi:10.1111/j.0022-1112.2004.00486.x

Eliason, E. J., and Farrell, A. P. (2016). Oxygen uptake in Pacific salmon *Oncorhynchus* spp.: when ecology and physiology meet. *J. Fish. Biol.* 88, 359–388. doi:10.1111/jfb.12790

Evans, T. G., Hammill, E., Kaukinen, K., Schulze, A. D., Patterson, D. A., English, K. K., et al. (2011). Transcriptomics of environmental acclimatization and survival in wild adult Pacific sockeye salmon (*Oncorhynchus nerka*) during spawning migration. *Mol. Ecol.* 20, 4472–4489. doi:10.1111/j.1365-294X.2011.05276.x

Flores, A. M., Shrimpton, J. M., Patterson, D. A., Hills, J. A., Cooke, S. J., Yada, T., et al. (2012). Physiological and molecular endocrine changes in maturing wild sockeye salmon, *Oncorhynchus nerka*, during ocean and river migration. *J. Comp. Physiol. B* 182, 77–90. doi:10.1007/s00360-011-0600-4

Groot, C. (1996). "Salmonid life histories," in *Principles of salmonid culture*. Editors W. Pennell, and A. Bruce (Amsterdam: Elsevier), 97–230.

Iversen, N. K., Dupont-Prinet, A., Findorf, I., McKenzie, D. J., and Wang, T. (2010). Autonomic regulation of the heart during digestion and aerobic swimming in the European sea bass (*Dicentrarchus labrax*). *Comp. Biochem. Physiol. A Mol. Integr. Physiol.* 156, 463–468. doi:10.1016/j.cbpa.2010.03.026

Makiguchi, Y., Nagata, S., Kojima, T., Ichimura, M., Konno, Y., Murata, H., et al. (2009). Cardiac arrest during gamete release in chum salmon regulated by the parasympathetic nerve system. *PLoS One* 4, e5993. doi:10.1371/journal.pone.0005993

Mann, K. D., Hoyt, C., Feldman, S., Blunt, L., Raymond, A., and Page-McCaw, P. S. (2010). Cardiac response to startle stimuli in larval zebrafish: sympathetic and parasympathetic components. *Am. J. Physiol. Regul. Integr. Comp. Physiol.* 298, R1288–R1297. doi:10.1152/ajpregu.00302.2009

Miller, K. M., Li, S., Kaukinen, K. H., Ginther, N., Hammill, E., Curtis, J. M. R., et al. (2011). Genomic signatures predict migration and spawning failure in wild Canadian salmon. *Science* 331, 214–217. doi:10.1126/science.1196901

Nilsson, S. (1983). *Autonomic nerve function in the vertebrates*. Berlin and New York: Springer.

Prystay, T. S., de Bruijn, R., Peiman, K. S., Hinch, S. G., Patterson, D. A., Farrell, A. P., et al. (2019). Cardiac performance of free-swimming wild sockeye salmon during the reproductive period. *Integr. Org. Biol.* 2, obz031. doi:10.1093/iob/obz031

Quinn, T. P. (2018). *The behavior and ecology of pacific salmon and trout*. Second Edition. Vancouver: University of British Columbia Press.

Quinn, T. P., Kinnison, M. T., and Unwin, M. J. (2001). Evolution of chinook salmon (*Oncorhynchus tshawytscha*) populations in New Zealand: pattern, rate, and process. *Genetica* 112–113, 493–513. doi:10.1007/978-94-010-0585-2_30

Sakamoto, K. Q., Miyayama, M., Kinoshita, C., Fukuoka, T., Ishihara, T., and Sato, K. (2021). A non-invasive system to measure heart rate in hard-shelled sea turtles: potential for field applications. *Philos. Trans. R. Soc. Lond. B Biol. Sci.* 376, 20200222. doi:10.1098/rstb.2020.0222

Sandblom, E., and Axelsson, M. (2011). Autonomic control of circulation in fish: a comparative view. *Auton. Neurosci.* 165, 127–139. doi:10.1016/j.autneu.2011.08.006

Sandblom, E., Clark, T. D., Hinch, S. G., and Farrell, A. P. (2009). Sex-specific differences in cardiac control and hematology of sockeye salmon (*Oncorhynchus nerka*) approaching their spawning grounds. *Am. J. Physiology-Regulatory Integr. Comp. Physiology* 297, R1136–R1143. doi:10.1152/ajpregu.00363.2009

Sandblom, E., Ekström, A., Brijs, J., Sundström, L. F., Jutfelt, F., Clark, T. D., et al. (2016). Cardiac reflexes in a warming world: thermal plasticity of barostatic control and autonomic tones in a temperate fish. *J. Exp. Biol.* 219, 2880–2887. doi:10.1242/jeb.140319

Steele, S. L., Yang, X., Debiais-Thibaud, M., Schwerte, T., Pelster, B., Ekker, M., et al. (2011). *In vivo* and *in vitro* assessment of cardiac beta-adrenergic receptors in larval zebrafish (*Danio rerio*). *J. Exp. Biol.* 214, 1445–1457. doi:10.1242/jeb.052803

Taylor, E. W., Jordan, D., and Coote, J. H. (1999). Central control of the cardiovascular and respiratory systems and their interactions in vertebrates. *Physiol. Rev.* 79, 855–916. doi:10.1152/physrev.1999.79.3.855

Team, R. C. (2022). *R: a language and environment for statistical computing*. Vienna, Austria: R Foundation for Statistical Computing. Available online at: https://www.R-project.org/.

Vera, L. D., and Priede, I. (1991). Short communication: the heart rate variability signal in rainbow trout (*Oncorhynchus mykiss*). *J. Exp. Biol.* 156, 611–617. doi:10.1242/jeb.156.1.611

Warren-Myers, F., Hvas, M., Vågseth, T., Dempster, T., and Oppedal, F. (2021). Sentinels in salmon aquaculture: heart rates across seasons and during crowding events. *Front. Physiol.* 12, 755659. doi:10.3389/fphys.2021.755659

Watanabe-Asaka, T., Niihori, M., Sonobe, H., Igarashi, K., Oda, S., Iwasaki, K.-I., et al. (2022). Acquirement of the autonomic nervous system modulation evaluated by heart rate variability in medaka (*Oryzias latipes*). *PLoS One* 17, e0273064. doi:10.1371/journal.pone.0273064

Zeileis, A., Kleiber, C., Krämer, W., and Hornik, K. (2003). Testing and dating of structural changes in practice. *Comput. Stat. Data Anal.* 44, 109–123. doi:10.1016/s0167-9473(03)00030-6

frontiers | Frontiers in Physiology

TYPE Original Research
PUBLISHED 29 May 2025
DOI 10.3389/fphys.2025.1512043

OPEN ACCESS

EDITED BY
Christel Lefrancois,
UMR7266 Littoral, Environnement et Sociétés (LIENSs), France

REVIEWED BY
Lene H. Petersen,
Texas A&M University at Galveston, United States
Anthony (Tony) John Hickey,
The University of Auckland, New Zealand

*CORRESPONDENCE
Takaaki K. Abe,
t.abe.hpa@gmail.com

RECEIVED 16 October 2024
ACCEPTED 06 May 2025
PUBLISHED 29 May 2025

CITATION
Abe TK, Fuke M, Fujioka K, Noda T, Irino H, Kitadani Y, Fukuda H, Svendsen MBS, Steffensen JF and Kitagawa T (2025) Juvenile-specific high heat production contributes to the initial step of endothermic development in Pacific bluefin tuna. *Front. Physiol.* 16:1512043. doi: 10.3389/fphys.2025.1512043

Juvenile-specific high heat production contributes to the initial step of endothermic development in Pacific bluefin tuna

Takaaki K. Abe[1,2]*, Maho Fuke[1], Ko Fujioka[3,4], Takuji Noda[5], Hiroyuki Irino[6], Yoshikazu Kitadani[6], Hiromu Fukuda[4], Morten Bo Søndergaard Svendsen[7], John Fleng Steffensen[7] and Takashi Kitagawa[1,8]

[1]Atmosphere and Ocean Research Institute, The University of Tokyo, Chiba, Japan, [2]College of Bioresource Science, Nihon University, Fujisawa, Kanagawa, Japan, [3]Fisheries Resources Institute, Japan Fisheries Research and Education Agency, Yokohama, Kanagawa, Japan, [4]Department of Fisheries, School of Marine Science and Technology, Tokai University, Shizuoka, Japan, [5]Field Science Education and Research Center, Kyoto University, Kyoto, Japan, [6]Osaka Aquarium Kaiyukan, Osaka, Japan, [7]Marine Biological Section, University of Copenhagen, Helsingør, Denmark, [8]Graduate School of Frontier Sciences, The University of Tokyo, Chiba, Japan

Pacific bluefin tuna (*Thynnus orientalis*; PBT) can maintain their body temperature above ambient water (i.e., thermal excess) through high heat production and heat retention. The endothermic ability develops at 20–40 cm fork length (L_f), which has been attributed to improved heat retention. Meanwhile, the contribution of heat-production capacity to the development of thermal excess is insufficiently understood. This study aimed to elucidate the ontogenetic pattern of heat production and its contribution to endothermic capacity in juvenile PBT using a heat-budget model (HBM) and swim-tunnel respirometry. The HBM was applied to 2–4 months of biologging data from juveniles (23–50 cm L_f; 200–4 kg) to estimate heat production rates ($\dot{T}_m$), revealing that these rates remained high up to approximately 700 g and declined thereafter. Moreover, the comparison of the development of endothermic capacity with the HBM-estimated parameters suggests that in the early juvenile stages, when PBT rapidly develop the thermal excess, the high $\dot{T}_m$ contributes to the thermal excess. The high $\dot{T}_m$ in this stage implied the juvenile-specific development of aerobic capacity; therefore, metabolic rate and aerobic capacity-related tissues (red muscle and ventricle) were measured, and the scaling exponents were calculated in this stage (16–28 cm L_f; 50–420 g). Swim-tunnel respirometry was conducted on juvenile PBT in Japan (August–September 2022 and 2023), and the collected samples were used to measure red muscle and ventricular masses. The scaling exponents of tunas throughout life history are generally in the range of 0.6–0.9, while those for these traits were 1.0 or greater in this size range, supporting the juvenile-specific aerobic capacity development. In conclusion, this study reveals the ontogenetic characteristics of heat production-related traits in PBT and provides new

insights into the developmental process of endothermic ability, beyond heat retention capacity.

KEYWORDS

biologging, heat-budget model, metabolic rate, respirometry, red muscle development

1 Introduction

Animal body temperature is determined by internal heat production and heat exchange with the external environment (Schmidt-Nielsen, 1997; Butler et al., 2021). Each species possesses an optimal body temperature range and employs various strategies to maintain body temperature within this range (Butler et al., 2021). Based on their thermoregulation strategies, animals are classified as either endotherm or ectotherm. Endotherms sustain body temperatures above the surrounding environment through elevated metabolic heat production (Schmidt-Nielsen, 1997; Butler et al., 2021). In contrast, ectotherms do not retain their body temperature with their heat production; instead, they primarily rely on external heat sources, exploiting environmental thermal gradients to regulate body temperatures (Angilletta, 2009; Butler et al., 2021). Most fish are ectotherms: this is because the aquatic habitat is a challenging environment to maintain body temperature due to the high heat capacity of water, and the metabolic heat they produce is further lost through the gills and the skin. Nevertheless, among fish, a few species can maintain their body temperatures above ambient water, known as endothermic fish (Bernal et al., 2012; Wegner et al., 2015; Bernal et al., 2017). The endothermic ability is restricted to specific tissues/organs; therefore, it is referred to as "regional endothermy" to distinguish it from the "endothermy" observed in mammals and birds (Carey and Teal, 1969; Carey et al., 1971).

Tunas (tribe *Thunnini*) are notable examples of endothermic fish and have long been explored for their ability to maintain body temperatures (Kishinouye, 1923). Tuna species achieve their endothermic ability through both high heat production and retention capacity, and exhibit unique morphological traits associated with them. They possess a unique vascular arrangement around specific tissues/organs (e.g., red muscle, liver), where arteries and veins alternate (Kishinouye, 1923; Carey et al., 1971; Dickson and Graham, 2004). The vascular pattern, referred to as *rete mirabile*, functions as the counter-current heat exchangers to retain metabolic heat, and heat from venous blood returning to the heart is passed to arterial blood, thereby reducing heat loss at the gills.

Tuna species also exhibit high metabolic rates, generally measured by oxygen consumption rate ($\dot{M}_{O_2}$), compared with ectothermic fish, reflecting their high metabolic heat production (Blank et al., 2007a). Moreover, they exhibit developed features conducive to aerobic metabolism, such as greater proportions of the ventricle and red muscle (Dickson et al., 2000; Graham and Dickson, 2001; Kubo et al., 2008). The red muscle serves as a major source of metabolic heat, and the ventricle allows the high oxygen demand of tunas. The red muscle arrangement along the body's medial axis further reduces heat dissipation. The physio-morphological features of tuna are shared in endothermic sharks (lamnid sharks), demonstrating that these traits represent one valid solution to acquiring the endothermic ability for fish. However, the endothermic ability of tuna is not innate, which is statued throughout their ontogeny (Dickson, 1994; Dickson et al., 2000; Kubo et al., 2008; Malik et al., 2020; Kitagawa et al., 2022). Typically, the endothermic capability of tuna starts to represent the ability to maintain their body temperature from early juvenile (>20 cm fork length, L_f) (Dickson, 1994; Dickson et al., 2000). The developmental process of the endothermic ability has been well described in Pacific bluefin tuna (*Thynnus orientalis*; PBT).

Pacific bluefin tuna and other bluefin tuna species, including Atlantic bluefin tuna (*Thunnus thynnus*) and southern bluefin tuna (*Thynnus maccoyii*), have well developed *retia mirabilia* among tuna species, and the adults generally show high heat retention capacity exceeding 10°C of thermal excess (T_X) between body and water (ambient) temperatures ($T_b - T_a$) when in relatively cold water. They can elevate the temperature of their locomotor muscle, viscera, brain, and eye tissues above that of water (Carey and Teal, 1966; 1969; Carey et al., 1971; Graham, 1995; Altringham and Block, 1997). With the prominent endothermic ability, these fish species have expanded their niches to low-temperature waters and improved their ability to sustain high-speed swimming due to their high aerobic metabolism and warm muscles (Stevens and Carey, 1981; Block and Finnerty, 1994; Brill, 1996; Dickson and Graham, 2004; Bernal et al., 2017). Pacific bluefin tuna are widely distributed across the Pacific Ocean, whereas their spawning areas are limited to Asian waters (Figure 1A). One main stock of PBT breeds in the waters of the western North Pacific Ocean between the Philippines and the Nansei Islands of Japan from April to June (Yabe et al., 1966; Chen et al., 2006), and another stock breeds in the Sea of Japan in August (Okiyama, 1974; Tanaka et al., 2007) (Figure 1A). The larvae spawned in the western North Pacific Ocean are transported by ocean currents (e.g., Kuroshio Current) to the coastal waters of Japan in the summer 2–3 months after hatching (Chen et al., 2006; Tanaka et al., 2006; 2006; Satoh et al., 2008; Kitagawa et al., 2010; Satoh, 2010) (Figure 1A). While some PBT remain in the coastal waters around Japan, others migrate from the Kuroshio–Oyashio transition region to the eastern Pacific in what is referred to as the trans-Pacific migration (Orange and Fink, 1963; Clemens and Fittner, 1969; Bayliff et al., 1991; Itoh et al., 2003; Kitagawa et al., 2009; Fujioka et al., 2018).

It has long been known that PBT juveniles with a fork length of 30 cm or more exhibit a thermal excess of 3°C–4°C post-capture compared to the ambient water (Funakoshi et al., 1985), indicating that PBT of this size and larger already have developed the endothermic ability. The long-term measurements of T_b, T_a, and swimming depth using biologging devices, have demonstrated that they have developed ability to maintain T_b when more than 45 cm L_f fish (Kitagawa et al., 2000; 2001; Kitagawa and Kimura, 2006; Kitagawa et al., 2007a; 2007b; Fujioka et al., 2018). Kubo et al. (2008) measured the 'steady-state' T_b in PBT across a size range of 16.5–55.5 cm L_f and reported that the thermal excess increased

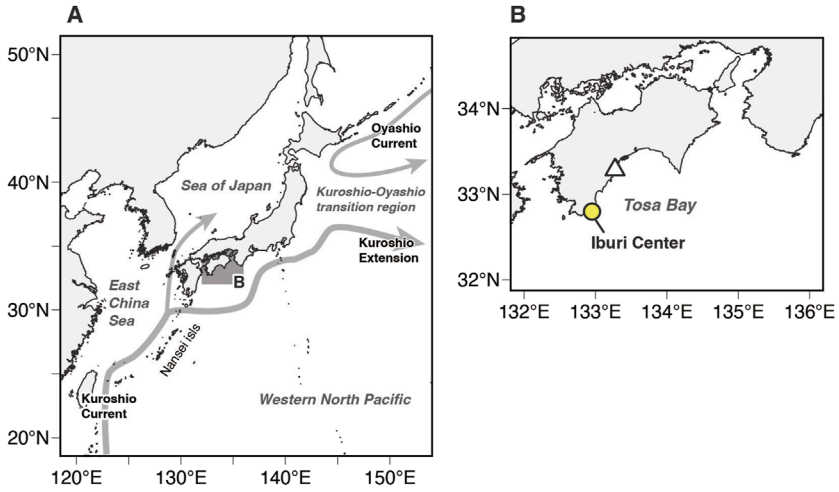

FIGURE 1
(A) Map of the western North Pacific Ocean, showing the study area (shaded area). Schematic of near-surface currents around Japan: Kuroshio Current, Kuroshio Extension, and Oyashio Current (gray arrows) **(B)** Enlarged map of the study area. The white triangle represents the release location of tagged Pacific bluefin tuna juveniles. The yellow-filled circle indicate the location of the Iburi Center, Osaka Kaiyukan Marine Biological Research Institute.

from 0.1°C to 1.5°C in individuals measuring 16.5–34.9 cm L_f to 2.6°C–4.4°C in those measuring 54.5–55.5 cm L_f, consistent with earlier observations in *Euthynnus* tunas (Dickson, 1994).

The mechanistic basis of thermal excess enhancement has mainly been attributed to the heat retention capacity, the development of *retia mirabilia*, because PBT develop the vascular structure rapidly during the juvenile stage (Funakoshi et al., 1985; Malik et al., 2020). Moreover, a biologging study has also shown that the heat retention capacity considerably improves with growth, while that of the heat-production rate decreases after >45 cm L_f (Kitagawa et al., 2007b). Meanwhile, the ontogenetic progression of heat production capacity and its role in the development of their endothermy remains less comprehensively understood. Achieving a body temperature above the ambient level necessitates not only heat retention but also substantial heat production. The total heat production capacity increases with body size due to the growth of red muscle mass (Malik et al., 2020), especially during the early juvenile stage (<30 cm L_f) (Kubo et al., 2008), implying an ontogenetic increase in heat production capacity.

Recent technological advancements have enabled the miniaturization of biologging devices and the *in situ* measurement of body temperature in small-sized tuna (<30 cm L_f), providing new insights into the dynamic developmental process of PBT's endothermic ability (Kitagawa et al., 2022). However, our previous study focused on the developmental process of heat retention capacity but did not discuss heat production capacity (Kitagawa et al., 2022). Therefore, the present study aimed to elucidate the ontogenic development of metabolic heat production capacity in PBT and its contribution to endothermic ability through reanalysis of the dataset in the previous study. In the present study, we (1) estimated the heat-production rate in juvenile PBT *via* heat-budget model and its scaling exponents in the juvenile as an index for developmental state, (2) discussed the relationship between the parameters estimated *via* heat-budget model and the contribution of heat production to the development of endothermic ability in PBT, and (3) evaluated aerobic capacity-related traits, including metabolic rate, total red muscle mass, and ventricular mass, and estimated scaling exponents of these traits.

2 Material and methods

2.1 Analysis of biologging data

2.1.1 Summary of analyzed data and electronic devices

In this study, we analyzed time-series temperature data of body (T_b) and ambient water (T_a) from nine juvenile Pacific bluefin tuna for a heat-budget model (Table 1). The data were originally obtained from tagging survey conducted on PBT by the National Institutions of Far Seas Fisheries, Fisheries Research Agency (present name: Japan Fisheries Research and Education Agency Fisheries Resources Institute) in Tosa Bay, Kochi Prefecture (Furukawa et al., 2017; Fujioka et al., 2018; Kitagawa et al., 2022) from July to August in 2012–2015.

Over the 4-year tagging survey, a total of 3,281 PBT juveniles were captured by trawling in the coastal area of Tosa Bay (2012–2015: n = 1,044, 1,725, 236, 276), and 2,518 fish were released with dart tags (2012–2015: n = 923, 1,147, 201, 247). Of the dart-tagged fish, 321 fish were surgically implanted with an archival tag (LAT2910; Lotek Wireless Inc. Ontario, Canada) into their peritoneal cavity and released from the coastal area (2012–2015: n = 75, 62, 77, 107). In total, 307 fish were recaptured off Tosa Bay, its adjacent waters, and in California, United States (2012–2015: n = 128, 60, 45, 74). Of these, 93 were archival-tagged individuals (2012–2015: n = 23, 8, 23, 39), but for about half of the fish, the archival tags themselves were not recovered, or the data were not retrieved due to the tag malfunction. As a result, 41 fish were used for the heat-budget model in our previous study (Kitagawa et al., 2022). In this study, we selected nine individuals with more than 2 months of time-series data for analysis (Table 1),

10.3389/fphys.2025.1512043

TABLE 1 Information on the individuals used for heat-budget model analysis. Fish size is expressed in fork length. The parentheses in size range analysis column indicate size estimated from growth rate due to the lack of size information at recapture.

Fish ID	Capture/Recapture date	Tagging/Recapture size (cm)	Size range for analysis (cm)	Growth rate (cm·day^{-1})	Data length (days)
2012-0925	July 28, 2012/August 25, 2014	24.0/n.a	24.0–(52.6)	0.24	120
2012-0932	July 29, 2012/December 19, 2012	28.0/53.5	28.9–47.1	0.18	102
2012-0948	July 29, 2012/October 21, 2012	24.5/50.0	28.9–42.8	0.18	78
2012-1,127	August 10, 2012/ July 28, 2013	26.5/n.a	26.5–(55.3)	0.24	120
2013-1766	August 15, 2013/September 19, 2014	23.0/n.a	23.0–(51.3)	0.24	120
2014-2,880	August 14, 2014/November 18, 2014	21.5/47.2	23.4–47.1	0.27	88
2014-2,922	August 18, 2014/November 13, 2014	23.0/49.0	23.0–49.0	0.30	87
2014-2,952	August 20, 2014/November 13, 2014	25.0/46.5	25.0–46.2	0.25	85
2015-3792	August 02, 2015/October 21, 2015	26.5/47.2	26.5–47.0	0.26	79

excluding 32 individuals with shorter data records, because this study aimed to evaluate the development of endothermic capacity from the 20 to >40 cm size range.

The archival tags consisted of a body ($\phi 8.5 \times 25$ mm) and stalk (154 mm), which weighed 3.3 g and 1.2 g in air and water, respectively. A temperature and pressure sensor were attached to the main body, and another temperature and illuminance sensor were attached to the tip of the stalk. The recorded temperatures at the main body were used as T_b in the peritoneal cavity (where the tag was placed in) and those at the stalk as T_a. The illuminance and pressure sensors were set to measure light level and depth, respectively. The sampling intervals of all sensors were set to 30 s (Furukawa et al., 2017; Fujioka et al., 2018; Kitagawa et al., 2022). The temperature sensors had a resolution of 0.02°C in the range of −5–45°C.

The tagging procedure was described in detail in previous studies (Furukawa et al., 2017; Fujioka et al., 2018). Briefly, a scalpel was used to make a 1 cm incision along the body approximately 0.5 cm from the midline and 1–2 cm anterior to the anus, through which the archival tag was inserted into the peritoneal cavity. At the tagging timing, the straight fork length of each fish (L_f, in cm) was measured. The implantation procedure was generally completed within 30 s.

2.1.2 Time-series data analysis

Igor Pro Ver 8.1 (WaveMetrics Inc., Portland, OR, United States) and its add-on package of Ethographer (Sakamoto et al., 2009) were used to analyze the T_a and T_b, recorded at 30s intervals by the archival tags. Temporary measurement abnormalities were corrected by taking a moving average of the values before and after the abnormal point (less than 0.01% of all data points). The diurnal pattern has been known in the PBT's body temperature (Kitagawa et al., 2022), where the temperatures in the daytime were higher than those in the nighttime, which generally reflects an increase in metabolic demand accompanied by activity and digestion in the daytime. In the present study, to reveal the developmental process of body temperature in the stable condition of early juvenile stages (20–40 cm L_f), the data during nighttime were focused on the analysis, assuming as a low-activity phase (10 p.m.–5 a.m.). Additionally, the data were limited to the first 120 days after release (Table 1), although our previous analysis had extended to the following year after the release (Kitagawa et al., 2022). This limitation was applied because estimating the increase in body size (fork length) during winter was difficult due to the reduced growth rate during this period.

2.1.3 Heat-budget model (HBM)

To analyze body temperature dynamics in juvenile PBT, we employed a heat-budget model to estimate changes in the whole-body heat-transfer coefficient (λ) and heat-production rate ($\dot{T}_m$) according to previous studies (Kitagawa and Kimura, 2006; Nakamura et al., 2015; Kitagawa et al., 2022). The heat-budget model follows the equation:

$$\frac{dT_b}{dt}(t) = \lambda\left(T_a(t) - T_b(t)\right) + \dot{T}_m, \tag{1}$$

where, $T_b(t)$ represents body temperature (in °C) as a function of time (t, in min), T_a is ambient water temperature (in °C)

as a function of t. The parameter λ indicates the whole-body heat-transfer coefficient (min^{-1}), which represents the rate of heat exchange between the body and ambient water. The term $\dot{T}_m$ represents the heat-production rate (°C $\cdot min^{-1}$), which indicates the rate of internal heat generation. Therefore, the heat-budget model shows that the time change in body temperature at a time t ($dT_b/dt(t)$, in °C min^{-1}) is determined by the rate of heat exchange (first term) and heat production (second term).

In our previous study (Kitagawa et al., 2022), we assumed that the ambient water temperature at a given time, $T_a(t)$, reflects the time change in T_b at the same time, $dT_b/dt(t)$ However, a time lag in heat transfer response was found. To account for this, the response time lag against $T_a(t)$ (τ, in min) was added to Equation 1:

$$\frac{dT_b}{dt}(t) = \lambda\left(T_a(t-\tau) - T_b(t)\right) + \dot{T}_m. \quad (2)$$

The parameters were estimated for each day using maximum likelihood method. We used the "lm" function in R [v.4.3.1, R Core Team (2023)] to estimate the parameters for models with different values of τ, and calculated the Bayesian information criterion (BIC) for each model according to previous studies (Nakamura et al., 2015; 2020) The model with the lowest BIC values was regarded as the more parsimonious model, and the parameters estimated by the lowest BIC model were used as parameters for the day.

2.1.4 Allometry of HBM parameters

To clarify the development of the heat-production rate in PBT, the heat-production rate was compared to body mass. The relationship between body mass (M_b) and a trait (I) is generally described by a power-law equation (Schmidt-Nielsen, 1984), known as the allometric equation, as follows:

$$I = \alpha M_b^{\beta}, \quad (3)$$

where, α is the scaling coefficient, and β is the scaling exponent or slope of the log-log plot of I vs M_b (Glazier, 2005; Killen et al., 2010). The scaling exponent indicates the rate of increase of a trait relative to the increase in body mass. In this study, we evaluated the development of the heat-production rate using the allometric equation. To apply linear models, both body mass (M_b) and heat-production rate ($\dot{T}_m$) were $\log_{10}$-transformed. Estimation was first conducted on a linear model using the lm function in R. To explore whether there is a change point in the allometric relationship of heat-production rate during ontogeny, segmented regression analysis was performed on the linear model, comparing the Akaike information criterion (AIC) and BIC to determine if breakpoints should be included. The segmented function in the "segmented" package of R was used for this analysis (Muggeo, 2008).

2.1.5 Body size estimation of the tagged PBT

To estimate the scaling exponent of the heat-production rate, the body mass of PBT juveniles on each day was estimated based on a calculation in a previous study (Kitagawa et al., 2022). Briefly, the estimation was conducted through two processes: (1) estimating the fork length on each day using the growth rate, and (2) estimating the body mass from the estimated fork length. The growth rate of PBT's fork length is rapid and linear in 0-age fish, for example, at 0.45 cm $\cdot$ day^{-1} at 30–120 days of age (Jusup et al., 2011). Even after 4 months of age, the rapid growth of 0-age fish is known to continue until the onset of their first winter (Fukuda et al., 2015b). PBT juvenile do not fit the von Bertalanffy growth function (Von Bertalanffy, 1938) otherwise widely used as a growth formula (Fukuda et al., 2015a), where the fork length during ontogeny is described by a sigmoid curve. Therefore, the increase in fork length during the analysis period (0–120 days after release) was estimated by linear regression between fork length and the days after release. For fish without fork length data at the time of recapture ($n = 3$; Table 1), fork length was estimated from the average growth rate (0.24 cm $\cdot$ day^{-1}) number based on linear regression of other fish ($n = 24$) in a previous study (Kitagawa et al., 2022). Body mass (M_b) during the analysis period was estimated from fork length (L_f) using the allometric formula (Equation 3), $M_b = \alpha_L L_f^{\beta_L}$ [$\alpha_L = 4.85 \cdot 10^{-3}$, $\beta_L = 3.39$, the values of the constant from Malik et al. (2020)].

2.2 Metabolic rate measurement

2.2.1 Fish collection and maintenance

Swimming respirometry was conducted at the Iburi Center (IC) of Osaka Kaiyukan Marine Biological Research Institute (Figure 1B) from August 9 to 26, 2022, and from August 15 to 9 September 2023. Juvenile Pacific bluefin tuna, ranging from 16.6 to 28.2 cm in fork length, were captured by hook-and-line trolling over a period of 2–3 days (August 11–13, 2022, August 18–19, 2023) off the waters of Tosa Bay, Japan. The captured fish were transported to IC on the final day of fishing each year. Upon arrival, the fish were transferred from the transport tank to 5-ton holding tanks (diameter 2.6 m, depth 0.94 m) with a custom-made dip-net, where the lower part was made of vinyl sheet and thus filled with water during fish handling. A total of 97 fish (2022: $n = 67$, 2023: $n = 30$) were collected and 31 fish (2022: $n = 16$, 2023: $n = 15$) were used for swimming respirometry. The holding tanks were aerated and supplied with filtered seawater. The holding tank water was maintained at the sea surface temperature at the location where the fish were caught (mean ± s.d.: 25.8°C ± 0.5°C). The PBT were fed larvae of Japanese anchovy (*Engraulis japonica*), to saturation twice daily, with the total daily feeding amounting to approximately 5%–10% of their body mass. They were not fed at least 12 h prior to the start of the swimming experiment. After the swimming experiment, the remaining fish not used for the experiment were euthanized with an overdose of FA100 (4-allyl-2-methoxyphenol, known as eugenol, 107 mg $\cdot$ mL^{-1}; Tanabe Seiyaku Co. Ltd., Osaka, Japan). The euthanized PBT juveniles were dissected for sampling, including ventricular mass measurement, or whole body frozen for red muscle mass measurement. The samples were then stored in a freezer at −20°C.

2.2.2 Swimming respirometry

A Steffensen-type swim tunnel respirometer (SW10210, Loligo Systems, Viborg, Denmark) situated at the IC was used to measure the oxygen consumption rate ($\dot{M}_{O_2}$, in mg$O_2 \cdot h^{-1}$) of the fish as a function of swimming speed (Svendsen et al., 2016). The tank in the swimming section of the respirometer held 90 L of water; water flow was generated using a voltage-controlled motor and propeller, where the voltage was calibrated against the water velocity. The swim

tunnel was connected to an optical O_2 sensor instrument (Firesting O_2; PyroScience GmbH, Aachen, Germany) using the dipping probe oxygen minisensor included in the instrument. The external water bath of the swim tunnel was connected to a plastic supply tank containing 200 L of air-saturated water. The water temperature of the supply tank was maintained in 25.6°C–26.4°C during the $\dot{M}_{O_2}$ measurement. The respirometer was darkened on the outside using a black curtain to prevent external disturbances.

The fish were transferred from the holding tank to the swim tunnel using a nylon sling. The fish were first given 0.5–3 h to acclimate to the swim tunnel at a water speed of 45–60 cm · s^{-1} (approx. 1.5–2.1 $L_f \cdot s^{-1}$), at which speed they swim regularly. Conversely, under a certain low flow speed (<25–35 cm · s^{-1}), they could not maintain their posture horizontally and opened their mouths, and eventually started to show active ventilation, resulting in increased $\dot{M}_{O_2}$ compared to $\dot{M}_{O_2}$ at a speed of 45–60 cm · s^{-1}. Some fish failed to maintain position in the swim tunnel, or repeatedly charged the upstream screen of the swim tunnel by 1 h after placing them in the swim chamber. In such a case, the fish was immediately removed from the swim tunnel and a new trial with a new fish started. During the acclimation period, the oxygen consumption rate was monitored, and confirmed that the $\dot{M}_{O_2}$ for all individuals were almost stabilized (defined by Iino et al. (2024) as an estimated $\dot{M}_{O_2}$ that did not vary by more than 10% from the mean over three consecutive measurement cycles). Each experimental run consisted of a 3–8 min period at each of the designated speeds up to 90 cm · s^{-1}. After each measurement, the seawater was exchanged with fresh seawater.

After each 15 min period, the water flow was increased by an additional 0.3 $L_f \cdot s^{-1}$ and was maintained at the new velocity for 15 min or until the fish were unable to swim against the current and were pushed to the downstream screen, and remained there for more than 10 s. After each trial, the fish were euthanized by overdose of anesthesia (FA100), and the fork length and body mass were measured. Some fish were dissected soon after euthanasia for sampling, while others were frozen whole bodies for later quantification of red muscle mass.

The oxygen consumption rate ($\dot{M}_{O_2}$, in $mgO_2 \cdot min^{-1}$) was determined during the measurement period (Δt, in min) as the decline in dissloved oxygen (ΔC_{O_2}, in mgO_2) in the swim tunnel. $\dot{M}_{O_2}$ was calculated as:

$$\dot{M}_{O_2} = \frac{\Delta C_{O_2}}{\Delta t}(V_{ch} - V_b), \tag{4}$$

where V_{ch} is the volume of the swim chamber (in l), V_b is the volume of the fish (in l, which was calculated from body mass assuming the density of the fish was 1 kg · l^{-1}). Background changes in dissolved oxygen concentration, measured when there were no fish in the swim chamber, were negligible. The swim speed was corrected for blocking effects, as recommended by Bell and Terhune (1970), when the cross-sectional area of the fish exceeded 2% of the swimming chamber area (Iino et al., 2024).

2.2.3 Scaling of metabolic rate

In this study, the standard metabolic rate (SMR) was determined to calculate the scaling exponent of a metabolic trait. The SMR is defined as the metabolic rate when swimming speed is zero, and for tunas, it is typically derived from the relationship between metabolic rate and swimming speed, known as the "swimming curve" (Dewar and Graham, 1994; Sepulveda and Dickson, 2000). Previous studies have reported a linear relationship between metabolic rate and swimming speed in tunas, and this study also identified a similar linear relationship (Dewar and Graham, 1994; Sepulveda and Dickson, 2000). Consequently, a linear model was employed for the estimation, where the oxygen consumption rate at a given speed ($\dot{M}_{O_2}(U)$) can be expressed as follows:

$$\dot{M}_{O_2}(U) = \gamma U + \dot{M}_{O_2,SMR}, \tag{5}$$

where U denotes swimming speed (cm · s^{-1}, and γ represents the slope of the linear function. The intercept indicates the oxygen consumption rate when the swimming speed is zero, thus providing an estimate of the SMR. For each individual, the swimming curve was estimated using a linear model, and the metabolic rate at a swimming speed of zero was defined as the SMR. However, since the metabolic rate estimated from the swimming curve is obtained through extrapolation, some concerns have been raised regarding the accuracy of such estimates (Chabot et al., 2016). To address this issue, we also determined the metabolic rate at the minimum (sustained) swimming speed ($\dot{M}_{O_2,U_{min}}$), defined as the lowest speed at which tunas can maintain their swimming, and used $\dot{M}_{O_2,U_{min}}$ for the metabolic trait scaling exponent calculation.

The minimum swimming speed (U_{min}) was determined for six individuals in 2023 by gradually reducing the flow speed after the measurement phase. Specifically, after the measurements, the flow speed was decreased incrementally at a speed of 5 cm · s^{-1}, and the U_{min} was defined as the speed just before the metabolic rate began to increase. Within the size range examined in this study, no significant correlation was observed between the U_{min} and body mass, so the average U_{min} of 44.3 cm · s^{-1} was used. By substituting the U_{min} into the swimming curve for each individual, we calculated $\dot{M}_{O_2,U_{min}}$.

2.2.4 Calculating red muscle and ventricle masses

Metabolic heat produced through aerobic metabolism in red muscles (RM) is a major source of body temperature, and the ventricle is closely related to aerobic capacity (Graham and Dickson, 2001). To evaluate the development of red muscle and ventricle in the early juvenile stage, a portion of PBT juveniles captured for swimming respirometry were measured for the masses of red muscle (M_{RM}) and ventricle (M_v).

Twenty-one fish (mean ± s.d. fork length: 20.6 ± 3.2 cm, body mass: 142.4 ± 80.6 g) were used to quantify total red muscle mass (M_{RM}, in g). The method was based on a previously described protocol (Bernal et al., 2003; Malik et al., 2020). For each fish, the total red muscle mass was calculated as the sum of the mass in the cross-sections. Before analysis, the fish were stored in −20 °C freezer and they were sectioned using a bandsaw while still frozen. Measurable quantities of RM did not occur in the anterior 20%–25% L_f. Thus, beginning at this position, whole frozen PBT juveniles were cut into 0.6–1.4-cm thick (approx. 4%–6% L_f) cross-section until 70%–90% L_f, where little to no red muscle remained visible. The anterior sides of each cross-section were photographed alongside a scale bar. For each of the cross-sections, the red muscle's cross-sectional area was measured using ImageJ. The cross-sectional area was multiplied by the thickness of section (0.6–1.4 cm) to give the

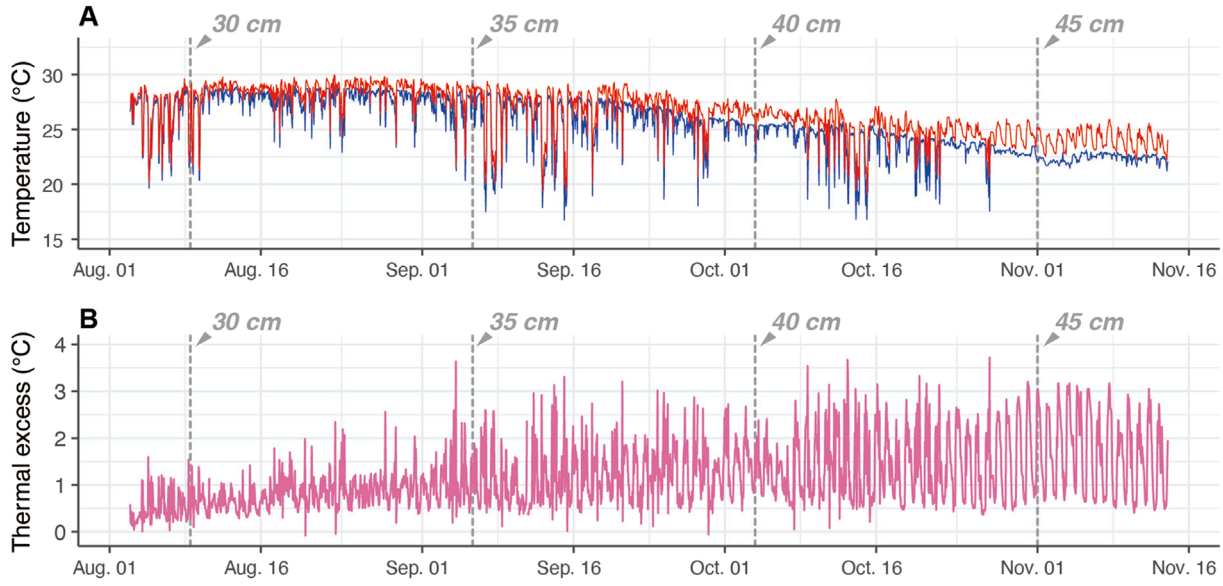

FIGURE 2
Example of time-series data of electronically tagged Pacific bluefin tuna (ID 2012-0932). The vertical dashed lines depict the estimated fork length at the time. **(A)** Body temperature (T_b, red) and ambient water temperature (T_a, blue). **(B)** The temperature difference between body and water (thermal excess).

volume value, and it was then multiplied by the published density [1.05 g · cm^{-3}; Bernal et al. (2003)] for the tuna muscle to give the mass value.

The ventricular masses (M_v, in g) were measured in 37 juveniles (mean ± s.d. fork length: 22.7 ± 3.4 cm, body mass: 207.0 ± 107.0 g). Each fish was dissected soon after euthanasia by anesthesia overdose. The ventricles were blotted and weighed to assess the ventricular mass. For each fish, the ventricular mass was divided by the body mass to give relative ventricular mass.

3 Results

3.1 Heat-production rate

Time-series data of the T_b, T_a, and T_X retrieved from one individual (ID 2012-0932) are shown by a representative example (Figure 2). During this period, it is estimated that its fork length increased from 29 to 47 cm (approx. 500 g to 2 kg; Table 1; Figure 2). The T_X exhibited a diurnal pattern; the daytime T_X was higher than the nighttime T_X. At small sizes (<30 cm L_f), the T_X ranged from 0.25°C to 1.5°C, but the T_X increased with growth, and at larger sizes (>45 cm L_f), the T_X range increased to 0.5°C–3°C (Figure 2).

For the fish, the heat-production rate ($\dot{T}_m$) and whole-body heat-transfer coefficient (λ) were estimated using the heat-budget model (Equation 2). The response time lag τ minimizing BIC of the heat-budget models on each day increased, accompanied by their growth. The minimizing τ ranged 0.5–1 min at the length of 30–35 cm L_f (approx. 500–1,000 g; Figures 3A,B), while the heat-budget model incorporating a τ of more than 2 min showed the lowest BIC over 40 cm L_f (approx. > 1.5 kg; Figures 3C,D). The calculated BIC values of the heat-budget models were at their minimum at a response time lag (τ) 0–3 min in the fork length range of 25–50 cm.

The heat-production rate ($\dot{T}_m$) was estimated for individuals with fork lengths ranging from 23.0 to 55.3 cm (body weight 200–3,900 g) (Figure 4). A decreasing trend in $\dot{T}_m$ was observed with body size, but when $\dot{T}_m$ was plotted against body weight on both logarithms, $\dot{T}_m$ tended to remain constant up to a certain body mass (Figure 4). The segmented regression model exhibited lower AIC and BIC values than the linear model (segmented model: AIC = 85.1; BIC = 108.9, linear model: AIC = 153.5; BIC = 167.7), which indicated a change in the slope of $\dot{T}_m$ at the breakpoint (714 g, 95%CI: 641.7–794.5).The slope of $\dot{T}_m$ remained close to 0 before the breakpoint (i.e., below 714 g), with no significant slope detected (estimate: 0.121, 95%CI: −0.082–0.324, $p = 0.74$) (Figure 4). In contrast, beyond the breakpoint (i.e., above 714 g), $\dot{T}_m$ decreased with increasing body weight (Estimate: −1.299, 95%CI: −1.421–−1.176, $p < 0.01$).

3.2 Relationship between the development of heat-production rate and endothermic ability

In the case of T_b is an equilibrium state—meaning the state where the left side of the heat-budget model is 0 (Equation 1)—the temperature difference between body and ambient water ($T_b - T_a$), or thermal excess (T_X), can be described by the following:

$$\dot{T}_m = \lambda T_X, \tag{6}$$

where the T_X is determined by the values of $\dot{T}_m$ and λ. For example, if $\dot{T}_m$ is twice λ, T_X is calculated as 2°C. Furthermore, if this equation

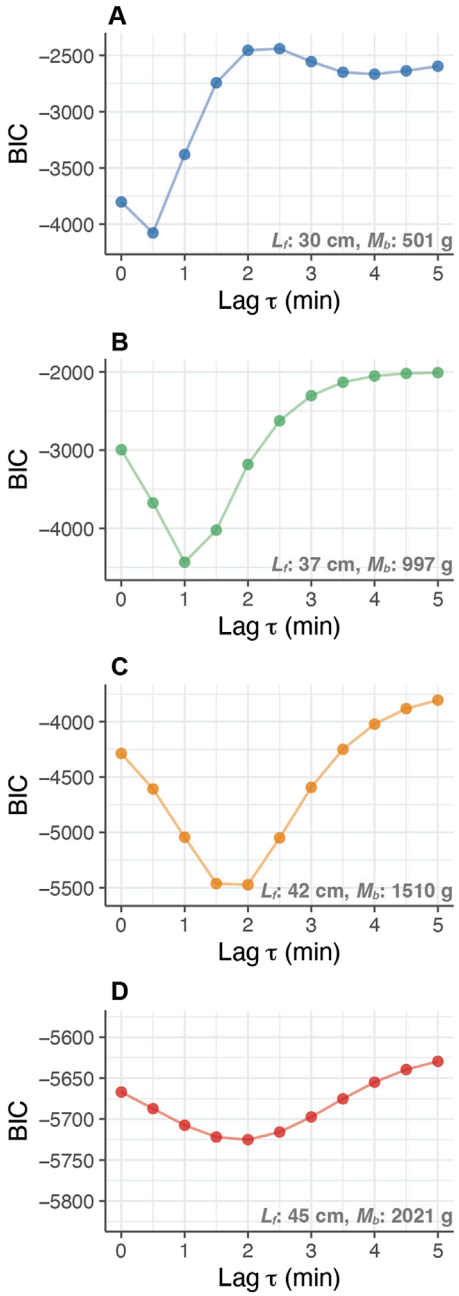

FIGURE 3
Relationship between the response time-lag (Lag τ in minutes) and the Bayesian Information Criterion (BIC) of heat-budget models with growth of PBT. The comparison of BIC values for different models with different time-lags was conducted for an individual (ID 2012-0932) at different body masses: **(A)** 0.5 kg (30 cm L_f), **(B)** 1.0 kg (37 cm L_f), **(C)** 1.5 kg (42 cm L_f), and **(D)** 2.0 kg (45 cm L_f).

is converted into logarithmic form, Equation 6 becomes:

$$\log \dot{T}_m = \log \lambda + \log T_X. \quad (7)$$

In this equation, the relationship between $\log \dot{T}_m$ and $\log \lambda$ is expressed as a linear function with slope 1 and the $\log T_X$ as the intercept of the linear function. The estimated T_X using the HBM parameters was consistent with the mean thermal excess on each

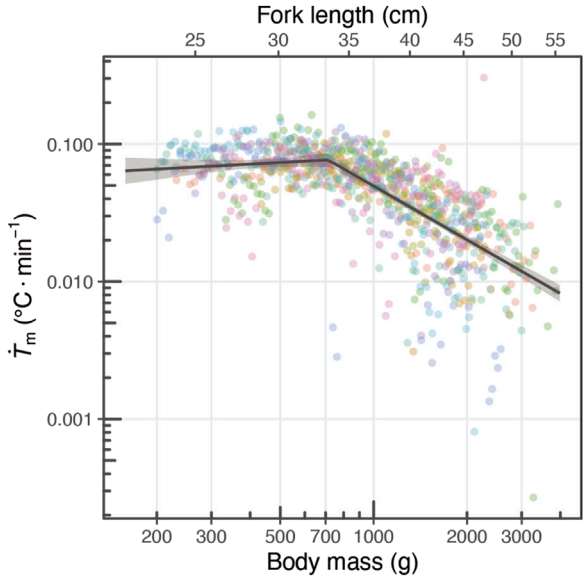

FIGURE 4
Changing relationship of $\dot{T}_m$ with their growth. The relationship between body mass and $\dot{T}_m$ is depicted, where the circles represent parameters estimated by the heat-budget model for each individual for each day. The colors of the circles correspond to different individuals. The dark gray line and shaded area represent the segment regression line and its 95% confidence interval area.

day, calculated as the difference between the mean T_b and the mean T_a (Figure 5A).

The HBM parameters estimated for each day were plotted on a log-log graph, revealing that the thermal excess increased as λ decreases with growth (Figure 5B). Focusing on the fork length range of 25–35 cm, thermal excess rised from 0.25°C to 1°C (Figure 5), and within this range, the distribution of the plots shifted horizontally from right to left (Figure 5B). The moving pattern of the plots suggests that, in addition to the decrease in λ, the maintenance of a high $\dot{T}_m$ is essential for the increase in thermal excess between 25 and 35 cm (Figure 5B). In contrast, beyond this size range, although the values of $\dot{T}_m$ decrease, thermal excess continues to increase due to the more pronounced decline in λ (Figure 5B).

3.3 Swimming respirometry

The oxygen consumption rate was linearly correlated with the swim speed (Figure 6A) (Equation 5). The minimum swim speed was evaluated for six fish (mean ± s.d. fork length: 23.0 ± 3.5 cm, body mass: 193 ± 90 g) by decreasing the flow speed. The average speed was 44.3 ± 1.51 (±s.d.) cm · s^{-1}. The minimum swim speed did not significantly correlate with body mass within the size range (p = 0.62). Therefore, the minimum swim speed in the $\dot{M}_{O_2,U_{min}}$ estimate was set to the average of 44.3 cm · s^{-1}.

$\dot{M}_{O_2,U_{min}}$ and $\dot{M}_{O_2,SMR}$ ranged 115.2–593.3 mgO_2 · h^{-1} and 64.6–466.3 mgO_2 · h^{-1}, respectively (Figure 6B). The both of $\dot{M}_{O_2,U_{min}}$ and $\dot{M}_{O_2,SMR}$ increased with body mass (Figure 6B). The scaling exponent of $\dot{M}_{O_2,U_{min}}$ was 0.95 (s.e.: 0.24) and that of $\dot{M}_{O_2,SMR}$ was 1.01 (s.e.: 0.33) (Table 3).

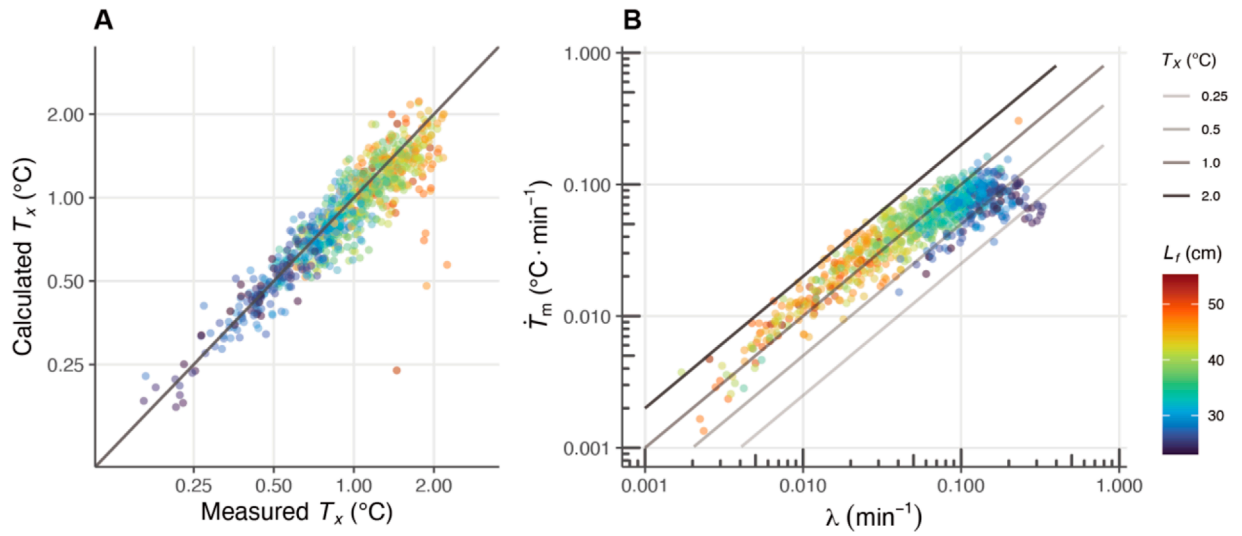

FIGURE 5
The effects of heat-production rate ($\dot{T}_m$) and whole-body heat-transfer coefficient (λ) on the difference between body and ambient (water) temperatures (thermal excess: $T_X = T_b - T_a$, °C). **(A)** The comparison of the estimated T_X with the measured T_X. The estimated T_X indicates the T_X calculated by $\dot{T}_m$ and λ, and the measured T_X shows the mean thermal excess on each day. **(B)** The relationships between $\dot{T}_m$ and λ are shown on a log-log plot, the T_X is expressed as the intercept. Each circular marker represents an individual fish, and the marker colors correspond to the fork length (L_f, in cm), as indicated by the color bar on the right. The solid lines represent different temperature differentials between body and water temperatures (T_X), with thicker lines indicating larger differentials.

The mean (±s.d.) value of mass-specific $\dot{M}_{O_2,U_{min}}$ was 719.7 (±303.5) $mgO_2 \cdot h^{-1}$ and that of mass-specific $\dot{M}_{O_2,SMR}$ was 1,198.3 (±366.1) $mgO_2 \cdot h^{-1}$ (Table 2; Figure 6C). The scaling exponent of the mass-specific $\dot{M}_{O_2,U_{min}}$ was −0.05 (s.e.: 0.24) and that of the mass-specific $\dot{M}_{O_2,SMR}$ was 0.33 (s.e. 0.33), but both exponents were not significantly different from zero (Table 3).

3.4 Development of red muscle and ventricular masses

Total red muscle mass was evaluated using the fish's cross-sectional area [$n = 21$, mean ± s.d. (min–max range) fork length: 20.6 ± 3.2 (16.3–27.9) cm, body mass: 142.4 ± 80.6 (48–362) g]. The red muscle mass increased with body mass (Figure 7A) and it spanned 2.8–38.7 g in 48–362 g fish. The red muscle mass significantly increased with body mass in the log-log transformed regression model, and the scaling exponent was estimated at 1.20 (s.e.: 0.11) (Figure 7A). The ventricular mass was measured in 37 individuals [mean ± s.d. (min–max range) fork length: 22.4 ± 3.4 (17.1–28.2) cm; body mass: 199.0 ± 109.4 (73–423) g]. The ventricular masses significantly increased with body mass in the log-log transformed regression model, and the scaling exponent was estimated as 1.15 (s.e.: 0.05) (Figure 7B).

The relative value of red muscle mass to body mass ranged 3.77%–10.69% (mean ± s.d.: 6.07% ± 1.79%) (Table 2; Figure 7C), but the scaling exponent of the relative red muscle mass was not significantly larger than 0 ($p = 0.09$; Table 2). The relative ventricular mass ranged 0.132%–0.279% (Table 2; Figure 7D). The scaling exponent of the relative ventricular mass was 0.15 (s.e.: 0.054), which was significantly larger than 0 ($p = 0.009$; Table 2).

4 Discussion

Endothermic fish, such as tuna and lamnid sharks, can maintain the temperatures of certain tissues/organs higher than the surrounding water, if in cold water, by retaining high levels of heat production. In the early juvenile stage, a strong correlation has been observed between red muscle mass and thermal excess (Dickson et al., 2000; Kubo et al., 2008), suggesting that heat production plays an important role in thermal excess. However, thermal excess is influenced not only by heat production, but also by heat retention capacity. Since the development of the *rete mirabile* occurs around the same time as the red muscle (Funakoshi et al., 1985; Malik et al., 2020), the ontogenetic pattern of heat production capacity and the extent to which heat production specifically contributes to thermal excess remain insufficiently understood compared to the heat retention capacity. Therefore, in this study, we aimed to explore the ontogenetic pattern of heat production capacity and to discuss the extent to which heat production contributes to the thermal excess between the inside and outside of the body. The thermal excess of juvenile PBT increased with growth as shown in our previous study [Figure 2; Kitagawa et al. (2022)]. By estimating parameters using a heat-budget model, we found that heat production is maintained at a high level in the early juvenile stage. Through comparison of the parameters of the heat-budget model, we found that a high heat-production rate is important for the early formation of thermal excess. To reinforce the mechanistic basis for highly maintained heat production in early juveniles, scaling exponents were estimated for physiological and/or morphological traits related to aerobic metabolic capacity, such as metabolic rate, red muscle mass, and ventricular mass.

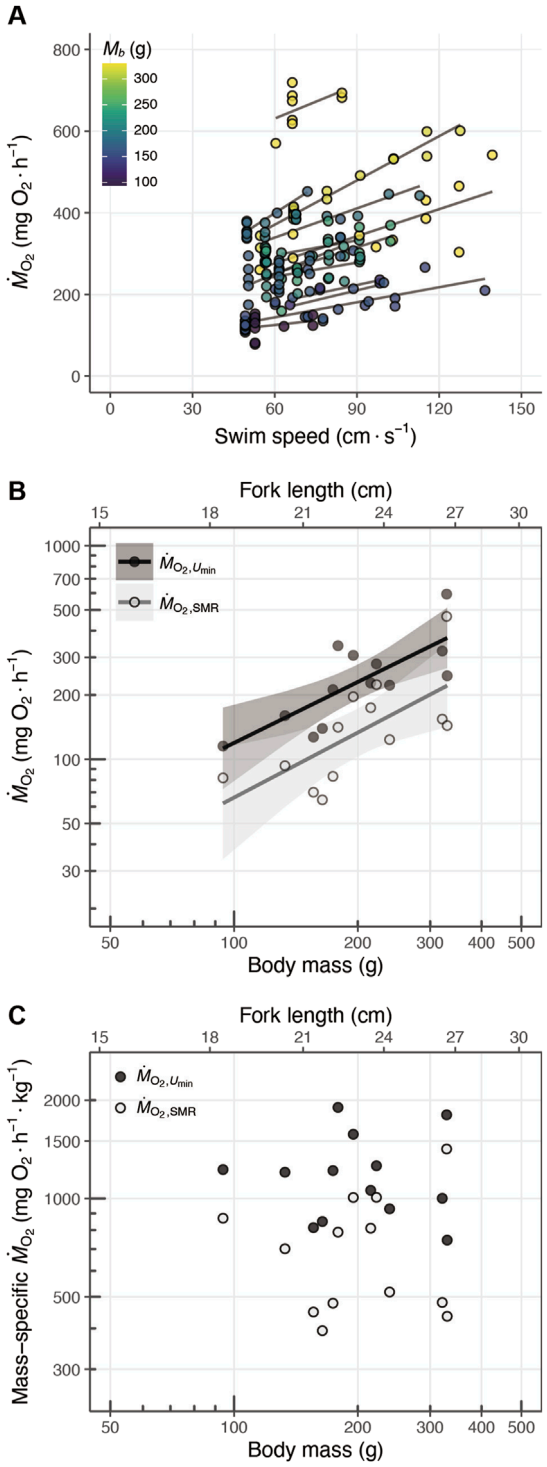

FIGURE 6
(A) Relationship between the swim speed (cm $\cdot s^{-1}$) and oxygen consumption rate (mg$O_2 \cdot h^{-1}$), where point color represents body mass (M_b, in g). The solid lines represent the fitting results for each individual fish. **(B)** Scaling of and standard metabolic rate ($\dot{M}_{O_2,SMR}$, pale color; scaling exponent: 0.95) and metabolic rate at minimum swim speed ($\dot{M}_{O_2,U_{min}}$, dark color; scaling exponent: 1.01) with body mass. **(C)** Scaling of and mass-specific standard metabolic rate ($\dot{M}_{O_2,SMR}$, pale color) and mass-specific metabolic rate at minimum swim speed ($\dot{M}_{O_2,U_{min}}$, dark color) with body mass. The solid lines indicate the linear regression fits, and the shaded areas show the 95% confidence intervals.

4.1 Ontogenetic patterns of heat production in PBT

The heat production rate ($\dot{T}_m$) estimated by the heat-budget model decreases with growth for fish after 45 cm L_f (Kitagawa et al., 2007b), which is natural given the scaling law of metabolic rate. Since heat production depends on metabolic heat, the internal heat production is closely related to the metabolic rate (Carey and Teal, 1969; Dewar and Graham, 1994; Blank et al., 2007a; 2007b). The heat-production rate ($\dot{T}_m$, in °C $\cdot$min^{-1}) reflects the heating rate for a fish body (in °C min^{-1} $\cdot$ind.$^{-1}$). Therefore, $\dot{T}_m$ can be interpreted as the mass-specific heating rate (i.e., °C min^{-1} $\cdot$ kg^{-1}) and the ontogenetic trend is expected to be similar to the mass-specific metabolic rate (in mg$O_2 \cdot h^{-1} \cdot kg^{-1}$). Metabolic rate (in mg$O_2 \cdot h^{-1}$) is proportional to body mass to the power of 0.5–0.9 according to the scaling laws of metabolic rate (Glazier, 2005; Killen et al., 2010), which means that the mass-specific metabolic rate (in mg$O_2 \cdot h^{-1} \cdot kg^{-1}$) decreases in proportion to the −0.5 to the −0.1 power of body mass. The scaling exponent of metabolic rate throughout life history depends on the species, and species with higher metabolic rates exhibit lower scaling exponents (Killen et al., 2010). The scaling exponents of metabolic rates in tuna species estimated using >40 cm L_f fish ranged from 0.5 to 0.6 (Killen et al., 2010), which is consistent with the decline in $\dot{T}_m$ with growth in PBT larger than a certain size (>45 cm L_f in Kitagawa et al. (2007b); > approx. 35 cm L_f in Figure 4). In contrast to the decline in $\dot{T}_m$ after 45 cm L_f (Kitagawa et al., 2007b), in the present study, we observed that $\dot{T}_m$ did not decrease in the early juvenile stages (approx. < 35 cm, Figure 4). These results might seem to contradict the scaling laws; however, it is known that the allometry of traits, particularly metabolic rate, is not constant throughout life history but varies depending on the life history stage (Glazier, 2005; Killen et al., 2010). Previous studies have reported that the scaling exponent of the metabolic rate tends to be higher during early life stages in fish (Glazier, 2005).

4.2 Contribution of juvenile-specific high heat production into endothermic ability in juvenile PBT

We aimed to discuss the extent to which heat production contributes to the rise in thermal excess by comparing parameters estimated using a heat-budget model (Figure 5). The heat-budget model estimates parameters for heat production and heat retention capacity, denoted as $\dot{T}_m$ and λ, respectively. Assuming the body temperature is in a steady state, the ratio of these parameters is considered to determine the thermal excess (T_X) (Equations 6 and 7). The thermal excess in juvenile PBT reaches approximately 2°C by the time they grow to approximately 45 cm L_f (Figure 5A), which corresponds with the average nighttime body temperature. The distribution of plots before reaching 45 cm L_f shifts to the left between 25 and 35 cm L_f, indicating an increase in thermal excess from approximately 0.25°C–1°C (Figure 5B). Based on the pattern of this shift, it can be inferred that, as suggested by previous studies (Kitagawa et al., 2007b; Kitagawa et al., 2022), the decrease in λ plays an important role in the increase in thermal excess. Additionally, it was found that the maintenance of high heat production levels

TABLE 2 Summarized information on fish body size and measurements of physiological traits. Each physiological trait is represented as a value relative to body mass. Mean ± s.d., and min-max range (in parentheses) are presented.

Trait	*n*	Fork length (cm)	Body mass (g)	Relative values to body mass	Units
$\dot{M}_{O_2,SMR}$	13	23.3 ± 2.5 (19.4–27.5)	211.6 ± 75.7 (94.0–330.0)	719.7 ± 303.5 (393.6–1,417.4)	mg $O_2 \cdot h^{-1} \cdot kg^{-1}$
$\dot{M}_{O_2,U_{min}}$	13	23.3 ± 2.5 (19.4–27.5)	211.6 ± 75.7 (94.0–330.0)	1,198.3 ± 366.1 (745.4–1900.0)	mg $O_2 \cdot h^{-1} \cdot kg^{-1}$
Red muscle	21	20.6 ± 3.2 (16.4–27.9)	142.4 ± 80.6 (48.0–362.0)	6.07 ± 1.79 (3.77–10.69)	%
Ventricle	39	22.4 ± 3.6 (16.2–28.2)	199.0 ± 109.4 (53.0–423.0)	0.21 ± 0.06 (0.08–0.48)	%

TABLE 3 Scaling exponents for physiological traits. Each row represents a physiological trait and its corresponding scaling exponent values, including absolute values and values relative to body mass (or mass-specific, ms). Scaling exponent values with a $p < 0.05$ are highlighted in bold.

Abs./Rel	Trait	Units of trait	Scaling exponent estimate	*P*
Absolute	$\dot{M}_{O_2,U_{min}}$	mg $O_2 \cdot h^{-1}$	**0.95 (0.42–1.48)**	**0.002**
	$\dot{M}_{O_2,SMR}$	mg $O_2 \cdot h^{-1}$	**1.01 (0.29–1.73)**	**0.011**
	Red muscle	g	**1.12 (0.96–1.43)**	**< 0.001**
	Ventricular mass	g	**1.15 (1.04–1.26)**	**< 0.001**
Relative to M_b	ms-$\dot{M}_{O_2,U_{min}}$	mg $O_2 \cdot h^{-1} \cdot kg^{-1}$	−0.05 (−0.58–0.475)	0.831
	ms-$\dot{M}_{O_2,SMR}$	mg $O_2 \cdot h^{-1} \cdot kg^{-1}$	0.01 (−0.71–0.73)	0.974
	Rel. red muscle mass	%	0.45 (−0.09–1.00)	0.096
	Rel. ventricular mass	%	**0.15 (0.04–0.26)**	**0.009**

also contributed to the rapid increase in thermal excess during the early juvenile stage. Although heat production began to decline after 35 cm L_f, it is likely that the improvement in heat retention capacity exceeded the rate of decrease in heat production, resulting in a continued enhancement in thermal excess (Figure 5B). One possible ecological reason that prevents the increase of the thermal excess due to high heat production from occurring after 35 cm L_f is the energetic cost. Tunas require an enormous amount of food to maintain their elevated body temperatures (Estess et al., 2014). According to model estimates, the cost of heat production is substantial, with more than 80% of assimilated energy being lost after reaching 35 cm L_f (Jusup and Matsuda, 2015), suggesting that reliance on high heat production to maintain body temperature may impose excessive energy costs.

Figure 5B also provides insights into the challenges small-sized fish face in maintaining thermal excess. For example, the plots of $\dot{T}_m$ and λ for individuals smaller than 25 cm L_f were mainly distributed 0.05°C–0.1°C · min −1 and 0.2–0.4 min −1, respectively. Juvenile PBT of this size exhibited a T_X of 0.25°C; however, assuming that the T_X increase up to 1°C, the fish would require a 2- to 8-fold increase in $\dot{T}_m$ (i.e., 0.2°C–0.4°C · min −1). Meanwhile, the juveniles around 40 cm L_f showed a T_X of 1°C, with the $\dot{T}_m$ of 0.04°C–0.1°C · min −1 and the λ of 0.05–0.1 min −1, and a 1- to 5-fold $\dot{T}_m$ (i.e., 0.1°C–0.2°C · min −1) would be needed to increase T_X to 2°C. Therefore, it is considered difficult for the small-sized fish to produce a T_X of more than 1°C due to low heat retention ability, which also implies the limitation of body size to produce a certain level of T_X.

4.3 Mechanistic basis of juvenile-specific high heat production

To examine the juvenile-stage-specific development of aerobic capacity, metabolic rate, red muscle mass, and ventricular mass, we measured and evaluated their scaling exponents (Table 3). The mass-specific $\dot{M}_{O_2,SMR}$ and $\dot{M}_{O_2,U_{min}}$ of PBT juveniles were 719.7 ± 303.5 $mgO_2 \cdot h^{-1} \cdot kg^{-1}$ and 1,198.3 ± 366.1 $mgO_2 \cdot h^{-1} \cdot kg^{-1}$ (mean ± s.d.), respectively (Table 2; Figure 6). The mass-specific SMR of PBT was significantly higher than that of other ectothermic fish species. Although measurements of the early juvenile stages of tuna are limited, kawakawa tuna (*E. affinis*) is the only species for which a swimming curve has been provided at 24°C (Sepulveda and Dickson, 2000). The mean ± s.d. of mass-specific $\dot{M}_{O_2,SMR}$ and the mass-specific $\dot{M}_{O_2,U_{min}}$ (calculated at 44.3 $cm \cdot s^{-1}$) of kawakawa tuna ($n = 8$, L_f range: 18.2–25.5 cm, M_b range: 59–265 g) derived from the swimming curve were 616.9 ± 289.9 $mgO_2 \cdot h^{-1} \cdot kg^{-1}$ and 1,052.5 ± 257.5 $mgO_2 \cdot h^{-1} \cdot kg^{-1}$, respectively (Sepulveda and Dickson, 2000), which were generally consistent with the values estimated in this study. The ventricle, which is an organ critical for blood circulation, had a relative mass of 0.21% ± 0.04% (mean ± s.d.) (Table 2). The relative ventricular mass of tunas (M_b range:

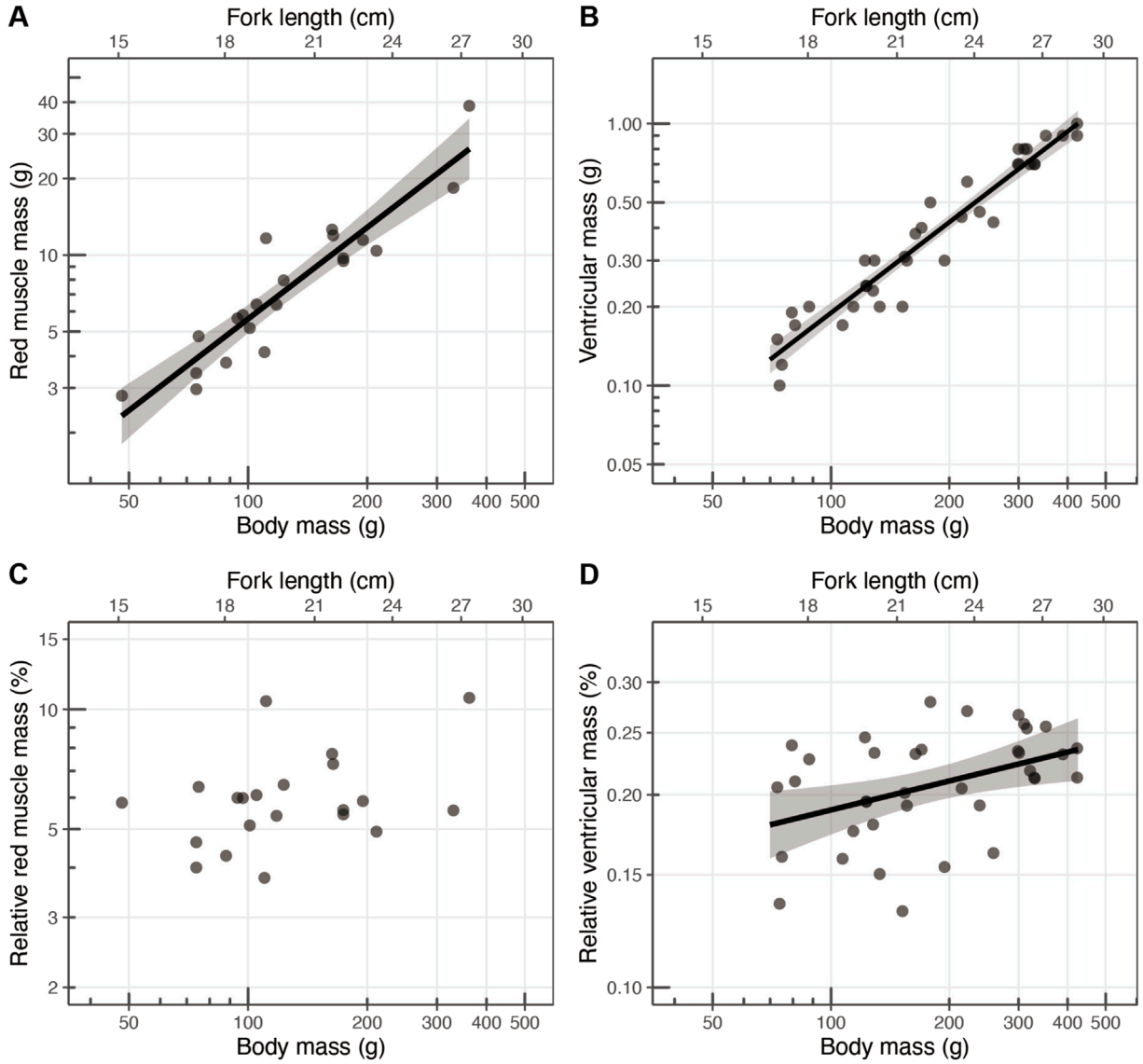

FIGURE 7
Scaling relationships between body mass (g) and **(A)** red muscle mass (g; scaling exponent: 1.12), **(B)** ventricular mass (g; scaling exponent: 1.15), **(C)** relative red muscle mass (%), and **(D)** relative ventricular mass (%; scaling exponent: 0.15). Each point represents an individual, with the solid black lines indicating the linear regression fits, and the shaded areas representing the 95% confidence intervals.

280 g–37 kg) ranges from 0.2% to 0.4% (Poupa et al., 1981; Brill and Bushnell, 1991; Graham and Dickson, 2001; Blank et al., 2004), in agreement with our results and notably higher than that of ectothermic fish species (2–2000 g), which ranges from 0.07% to 0.17% (Driedzic and Stewart, 1982; Santer et al., 1983; Sidell and Driedzic, 1985; Farrell et al., 1988). Additionally, the proportion of red muscle mass was 6.07% ± 1.79% (mean ± s.d.) (Table 2), which was also higher than that of other ectothermic fish species (Graham and Dickson, 2001).

In the early juvenile stage (15–35 cm L_f), the scaling exponents of these physiological traits were close to or greater than 1.0, and those of the mass-specific values (or values relative to body mass) were also close to or greater than 0 (Table 3), indicating that the traits increased isometrically or more. Although the scaling exponents of metabolic rate have not been reported not only for PBT but also for other bluefin tuna species, as it is known that scaling exponents tend to be similar among species that are phylogenetically related and have a comparative lifestyle (Killen et al., 2010). Therefore, it is reasonable to expect that bluefin tuna would have similar scaling exponents to other tuna species. The scaling exponents of other tuna species ranged from 0.5 to 0.6 [e.g., *Thynnus albacares*: 0.57, *Katsuwonus pelamis*: 0.56, *E. affinis*: 0.50, as reported by Killen et al. (2010)]. The scaling exponents for both $\dot{M}_{O_2,SMR}$ and $\dot{M}_{O_2,U_{min}}$ were close to 1.0, and tended to be high compared to the previous study. The confidence intervals for the scaling exponents in $\dot{M}_{O_2,SMR}$ and $\dot{M}_{O_2,U_{min}}$ were wider because of the large variations in metabolic rates between individuals and the narrow size range measured. Because metabolic rates are generally known to vary 2- to 3-fold among

individuals (Burton et al., 2011), it is necessary not only to increase the sample size but also to measure a wider range of sizes in order to more accurately determine and discuss the juvenile-specific scaling exponents; however, the scaling exponents of red muscle mass and ventricular mass would corroborate the juvenile-specific scaling exponent of metabolic traits.

For red muscle, it has been reported that the scaling exponent for PBT 20–60 cm L_f was 0.9, and the relative mass of red muscle to body decreased from approximately 7%–4% within this size range (Malik et al., 2020). In the 15–30 cm L_f range, the scaling exponent was close to 1.0, suggesting that in this size range, the red muscle is expected to grow isometrically and to decrease after this size range. Little is known about the scaling of ventricular mass in tunas, but the ventricular mass is expected to increase beyond the 30 cm L_f as the scaling exponent exceeded 1.0, and the relative ventricular mass also increased in this study (Table 3). Although it is not known to what extent the PBT's ventricle relatively increases, the relative ventricular mass has been reported to be 0.32% in approximately 65 cm L_f fish (6.0–7.5 kg) (Blank et al., 2004). This study observed that the high scaling exponents in the ventricular mass, but the interpretation of ventricular mass and its high scaling exponent should be noted. The ventricle is composed of two layers, an inner spongy layer and an outer dense layer (Poupa and Lindström, 1983). The dense layer is called the compact layer, and the compact layer plays an important role in the pumping of blood. The high scaling exponents could be attributed to an increased ratio of the compact layer to the spongy layer, not simply an increase in ventricular volume. Further histological study is required for the interpretation of the high scaling exponent in ventricular mass. In addition, the development of other tissues/organs could also contribute to that of endothermic ability. For example, the study on bigeye tuna (*Thunnus obesus*) showed the importance of white muscle on thermogenesis and thermoconservation ability (Boye et al., 2009). The present study observed that the high scaling exponents for certain physiological traits—metabolic rate, red muscle mass, and ventricular mass—during the early juvenile stages in PBT, which supports the ontogenetic pattern of heat production capacity at this stage, although other traits could also contribute to the development of endothermic ability. These results align with recent findings of higher scaling exponents specific to early life history and the hypothesis that these patterns can be attributed to relative increases in tissues with higher oxygen demand (Oikawa and Itazawa, 1993; Glazier, 2005).

4.4 Ecological implications of high metabolic rate

Although high heat production should be associated with high energetic costs, the ontogenetic pattern of $\dot{T}_m$ suggest that juvenile PBT maintains a high heat-production rate during the early juvenile stage, contributing to an increase in thermal excess. The elevated body temperature of tunas is thought to allow them to maintain a high metabolic rate, conferring advantages for growth and swimming performance (Brill, 1996). The rapid development of aerobic metabolic capacity observed during this period is consistent with the ecological characteristics of juvenile PBT. The juveniles exhibit rapid growth up to 1 year of age, with the cohorts born in the Pacific Ocean between April and July reaching a body size of 20–30 cm L_f by August–September upon their migration to the Tosa Bay. The growth rate during this stage is particularly high compared to the later stage (Jusup et al., 2011), and the juveniles reach 40 cm L_f by October. Concurrently, their diet shifts from zooplankton to more energy-rich prey, such as small fish (Shimose et al., 2013; Kitagawa and Fujioka, 2017), and their caudal fins undergo morphological changes, increasing aspect ratios to optimize for high-speed sustained swimming (Kitagawa and Fujioka, 2017). Given that high growth rates during the early stages play a crucial role in determining juvenile survival (Tanaka et al., 2006), the juvenile-specific development of aerobic capacity in the PBT during this stage likely plays a key functional role in the early ecology of PBT.

A recent study has provided ecological insights into the high scaling exponents of metabolic rate during the early life stages of fish (Norin, 2022). The relationship between metabolic rate and growth rate has long been recognized (Altringham and Block, 1997; Sogard, 1997), with species or individuals exhibiting higher metabolic rates often showing faster growth rates, provided they meet their dietary demands (Auer et al., 2015a; 2015b; 2015c). Since mortality rates are highest during the early life stages of fish, rapid growth is believed to enhance survival rate (Sogard, 1997; Norin, 2022). Therefore, the study hypothesized that the ontogenetic scaling of the metabolic rate in fish is a result of selective pressures associated with high mortality in early life stages (Norin, 2022). The eco-physiological features of PBT juveniles are considered to coincide with this concept.

4.5 Conclusions and perspectives

It has been known that tunas begin to exhibit higher body temperature than ambient water at fork lengths of 20–40 cm, but the development of heat production capacity and its contribution to the difference between body and water temperature at this stage has not been fully understood. By examining multiple traits related to heat-producing capacity in PBT juveniles, this study provides new insights into the ontogenetic patterns of heat production capacity and its physiological basis underlying the development of endothermic ability in PBT juveniles. Our findings demonstrate that the juvenile-specific high heat-production rate is critical during the early stages of endothermic development. The observed high heat-production rates during this stage contrast with the subsequent decline as the fish grow larger. This study elucidates the ontogenetic development of metabolic heat production in juvenile PBT and its role in the acquisition of endothermic capability.

However, although the results of the present study implied a developmental shift in the physiological state, further studies are needed to explore internal changes, particularly energetic dynamics through ontogeny, in natural environments. Pioneering studies have proposed the measurement of heart rate in bluefin tunas (Clark et al., 2008; Clark et al., 2010), and recent technological advances in data loggers enable the measurement of long-term heart rate in bluefin tuna (Rouyer et al., 2023). It is hoped that an increasing number of physiological traits measured using biologging techniques will clarify the developmental process from exothermic to endothermic attributes in tuna species.

Data availability statement

The original contributions presented in the study are included in the article/supplementary material, further inquiries can be directed to the corresponding author.

Ethics statement

The animal study was approved by Animal Ethics Committee of the University of Tokyo. The study was conducted in accordance with the local legislation and institutional requirements.

Author contributions

TA: Conceptualization, Data curation, Formal Analysis, Funding acquisition, Investigation, Methodology, Project administration, Software, Validation, Visualization, Writing – original draft, Writing – review and editing. MF: Conceptualization, Data curation, Funding acquisition, Investigation, Methodology, Software, Validation, Writing – original draft, Writing – review and editing. KF: Writing – review and editing, Funding acquisition, Resources, Supervision. TN: Writing – review and editing, Investigation, Methodology, Supervision. HI: Writing – review and editing, Investigation, Resources. YK: Writing – review and editing, Resources. HF: Resources, Writing – review and editing. MS: Writing – review and editing, Methodology, Supervision. JS: Writing – review and editing, Methodology, Supervision. TK: Writing – review and editing, Conceptualization, Funding acquisition, Project administration, Resources, Supervision.

Funding

The author(s) declare that financial support was received for the research and/or publication of this article. This study was financially supported by the Research and Assessment Program for Fisheries Resources, the Fisheries Agency of Japan, the Japan Society for the Promotion of Science (JSPS) [grant number 23K14004], the Core Research for Evolutional Science and Technology (CREST) program of the Japan Science and Technology (JST) Agency [grant number JPMJCR23P2 to ST], and a Sasakawa Scientific Research Grant from the Japan Science Society [grant number 2023-4027].

Acknowledgments

We extend our sincere gratitude to the fishermen who supported the collection of specimens for this study. This research was supported by the Cooperative Program [number JURCAOSKAV23-49] of Atmosphere and Ocean Research Institute, the University of Tokyo. We are also deeply grateful to the staff of the Osaka Aquarium Kaiyukan, Iburi Center, for their invaluable assistance in rearing Pacific bluefin tuna. Additionally, we would like to thank Taiyo Komatsubara from Nihon University for his significant contribution to the quantification of red muscle. Their support and collaboration were crucial to the success of this research.

Conflict of interest

The authors declare that the research was conducted in the absence of any commercial or financial relationships that could be construed as a potential conflict of interest.

Generative AI statement

The author(s) declare that Generative AI was used in the creation of this manuscript. During the preparation of this study, we used Trinka AI and ChatGPT to correct grammar.

Publisher's note

All claims expressed in this article are solely those of the authors and do not necessarily represent those of their affiliated organizations, or those of the publisher, the editors and the reviewers. Any product that may be evaluated in this article, or claim that may be made by its manufacturer, is not guaranteed or endorsed by the publisher.

References

Altringham, J. D., and Block, B. A. (1997). Why do tuna maintain elevated slow muscle temperatures? Power output of muscle isolated from endothermic and ectothermic fish. *J. Exp. Biol.* 200, 2617–2627. doi:10.1242/jeb.200.20.2617

Angilletta, M. J. (2009). "Thermal heterogeneity," in *Thermal adaptation: a theoretical and empirical synthesis*, (New York: Oxford University Press), 19–34.

Auer, S. K., Salin, K., Anderson, G. J., and Metcalfe, N. B. (2015a). Aerobic scope explains individual variation in feeding capacity. *Biol. Lett.* 11, 20150793. doi:10.1098/rsbl.2015.0793

Auer, S. K., Salin, K., Rudolf, A. M., Anderson, G. J., and Metcalfe, N. B. (2015b). Flexibility in metabolic rate confers a growth advantage under changing food availability. *J. Anim. Ecol.* 84, 1405–1411. doi:10.1111/1365-2656.12384

Auer, S. K., Salin, K., Rudolf, A. M., Anderson, G. J., and Metcalfe, N. B. (2015c). The optimal combination of standard metabolic rate and aerobic scope for somatic growth depends on food availability. *Funct. Ecol.* 29, 479–486. doi:10.1111/1365-2435.12396

Bayliff, W. H., Ishizuki, Y., and Deriso, R. B. (1991). Growth, movement, and attrition of northern bluefin tuna, *Thunnus thynnus*, in the Pacific Ocean, as determined by tagging. *Inter-American Trop. Tuna Comm. Bull.* 20, 1–94.

Bell, W. H., and Terhune, L. D. B. (1970). Water tunnel design for fisheries research. *Fish. Res. Board Can. Tech. Rep.* 195, 1–69.

Bernal, D., Brill, R. W., Dickson, K. A., and Shiels, H. A. (2017). Sharing the water column: physiological mechanisms underlying species-specific habitat use in tunas. *Rev. Fish. Biol. Fish.* 27, 843–880. doi:10.1007/s11160-017-9497-7

Bernal, D., Carlson, J. K., Goldman, K. J., and Lowe, C. G. (2012). "Energetics, metabolism, and endothermy in sharks and rays," in *Biology of sharks and their relatives* (London: CRC Press), 28.

Bernal, D., Sepulveda, C., Mathieu-Costello, O., and Graham, J. B. (2003). Comparative studies of high performance swimming in sharks I. Red muscle morphometrics, vascularization and ultrastructure. *J. Exp. Biol.* 206, 2831–2843. doi:10.1242/jeb.00481

Blank, J. M., Farwell, C. J., Morrissette, J. M., Schallert, R. J., and Block, B. A. (2007a). Influence of swimming speed on metabolic rates of juvenile Pacific bluefin tuna and yellowfin tuna. *Physiol. Biochem. Zool.* 80, 167–177. doi:10.1086/510637

Blank, J. M., Morrissette, J. M., Farwell, C. J., Price, M., Schallert, R. J., and Block, B. A. (2007b). Temperature effects on metabolic rate of juvenile Pacific bluefin tuna *Thunnus orientalis*. *J. Exp. Biol.* 210, 4254–4261. doi:10.1242/jeb.005835

Blank, J. M., Morrissette, J. M., Landeira-Fernandez, A. M., Blackwell, S. B., Williams, T. D., and Block, B. A. (2004). *In situ* cardiac performance of Pacific bluefin tuna hearts in response to acute temperature change. *J. Exp. Biol.* 207, 881–890. doi:10.1242/jeb.00820

Block, B. A., and Finnerty, J. R. (1994). Endothermy in fishes: a phylogenetic analysis of constraints, predispositions, and selection pressures. *Environ. Biol. Fish.* 40, 283–302. doi:10.1007/BF00002518

Boye, J., Musyl, M., Brill, R., and Malte, H. (2009). Transectional heat transfer in thermoregulating bigeye tuna (*Thunnus obesus*) – a 2D heat flux model. *J. Exp. Biol.* 212, 3708–3718. doi:10.1242/jeb.031427

Brill, R. W. (1996). Selective advantages conferred by the high performance physiology of tunas, billfishes, and dolphin fish. *Comp. Biochem. Physiol. A Mol. Integr. Physiol.* 113, 3–15. doi:10.1016/0300-9629(95)02064-0

Brill, R. W., and Bushnell, P. G. (1991). Metabolic and cardiac scope of high energy demand teleosts, the tunas. *Can. J. Zool.* 69, 2002–2009. doi:10.1139/z91-279

Burton, T., Killen, S. S., Armstrong, J. D., and Metcalfe, N. B. (2011). What causes intraspecific variation in resting metabolic rate and what are its ecological consequences? *Proc. R. Soc. B* 278, 3465–3473. doi:10.1098/rspb.2011.1778

Butler, P. J., Brown, J. A., Stephenson, D. G., and Speakman, J. R. (2021). *Animal pysiology: an environmental perspective*. New York: Oxford University Press.

Carey, F. G., and Teal, J. M. (1966). Heat conservation in tuna fish muscle. *Proc. Natl. Acad. Sci. U. S. A.* 56, 1464–1469. doi:10.1073/pnas.56.5.1464

Carey, F. G., and Teal, J. M. (1969). Regulation of body temperature by the bluefin tuna. *Comp. Biochem. Physiol.* 28, 205–213. doi:10.1016/0010-406X(69)91336-X

Carey, F. G., Teal, J. M., Kanwisher, J. W., Lawson, K. D., and Beckett, J. S. (1971). Warm-bodied fish. *Am. Zool.* 11, 137–143. doi:10.1093/icb/11.1.137

Chabot, D., Steffensen, J. F., and Farrell, A. P. (2016). The determination of standard metabolic rate in fishes. *J. Fish Biol.* 88, 81–121. doi:10.1111/jfb.12845

Chen, K.-S., Crone, P., and Hsu, C.-C. (2006). Reproductive biology of female Pacific bluefin tuna *Thunnus orientalis* from south-western North Pacific Ocean. *Fish. Sci.* 72, 985–994. doi:10.1111/j.1444-2906.2006.01247.x

Clark, T. D., Brandt, W. T., Nogueira, J., Rodriguez, L. E., Price, M., Farwell, C. J., et al. (2010). Postprandial metabolism of Pacific bluefin tuna (*Thunnus orientalis*). *J. Exp. Biol.* 213, 2379–2385. doi:10.1242/jeb.043455

Clark, T. D., Taylor, B. D., Seymour, R. S., Ellis, D., Buchanan, J., Fitzgibbon, Q. P., et al. (2008). Moving with the beat: heart rate and visceral temperature of free-swimming and feeding bluefin tuna. *Proc. R. Soc. B.* 275, 2841–2850. doi:10.1098/rspb.2008.0743

Clemens, A., and Fittner, G. (1969). Bluefin tuna migrate across the Pacific Ocean. *Calf. Fish. Game* 55, 132–135.

Dewar, H., and Graham, J. B. (1994). Studies of tropical tuna swimming performance in a large water tunnel:I. Energetics. *J. Exp. Biol.* 192, 13–31. doi:10.1242/jeb.192.1.13

Dickson, K. A. (1994). Tunas as small as 207mm fork length can elevate muscle temperatures significantly above ambient water temperature. *J. Exp. Biol.* 190, 79–93. doi:10.1242/jeb.190.1.79

Dickson, K. A., and Graham, J. B. (2004). Evolution and consequences of endothermy in fishes. *Physiol. Biochem. Zool.* 77, 998–1018. doi:10.1086/423743

Dickson, K. A., Johnson, N. M., Donley, J. M., Hoskinson, J. A., Hansen, M. W., and D'souza Tessier, J. (2000). Ontogenetic changes in characteristics required for endothermy in juvenile black skipjack tuna (*Euthynnus lineatus*). *J. Exp. Biol.* 203, 3077–3087. doi:10.1242/jeb.203.20.3077

Driedzic, W. R., and Stewart, J. M. (1982). Myoglobin content and the activities of enzymes of energy metabolism in red and white fish hearts. *J. Comp. Physiol. B* 149, 67–73. doi:10.1007/BF00735716

Estess, E. E., Coffey, D. M., Shimose, T., Seitz, A. C., Rodriguez, L., Norton, A., et al. (2014). Bioenergetics of captive Pacific bluefin tuna (*Thunnus orientalis*). *Aquaculture* 434, 137–144. doi:10.1016/j.aquaculture.2014.08.002

Farrell, A. P., Hammons, A. M., Graham, M. S., and Tibbits, G. F. (1988). Cardiac growth in rainbow trout, *Salmo gairdneri*. *Can. J. Zool.* 66, 2368–2373. doi:10.1139/z88-351

Fujioka, K., Fukuda, H., Furukawa, S., Tei, Y., Okamoto, S., and Ohshimo, S. (2018). Habitat use and movement patterns of small (age-0) juvenile Pacific bluefin tuna (*Thunnus orientalis*) relative to the Kuroshio. *Fish. Oceanogr.* 27, 185–198. doi:10.1111/fog.12244

Fukuda, H., Uyama, H., and Oshima, K. (2015a). *A minor change in the estimation of length composition data of Japanese troll fisheries. Kaohsiung.* Taiwan: International Scientific Committee for Tuna and Tuna-Like Species in the North Pacific Ocean (ISC). ISC/15/PBFWG-2/03.

Fukuda, H., Yamasaki, I., Takeuchi, Y., Kitakado, T., Himose, T., Ishihara, T., et al. (2015b). *Estimates of growth function from length-at-age data based on otolith annual rings and daily rings for Pacific bluefin tuna.* Kaohsiung, Taiwan: International Scientific Committee for Tuna and Tuna-Like Species in the North Pacific Ocean (ISC). ISC/15/PBFWG-2/11.

Funakoshi, S., Wada, K., and Suzuki, T. (1985). Development of the rete mirabile with growth and muscle temperature in the young bluefin tuna. *Nippon. Suisan Gakkaishi* 51, 1971–1975. doi:10.2331/suisan.51.1971

Furukawa, S., Fujioka, K., Fukuda, H., Suzuki, N., Tei, Y., and Ohshimo, S. (2017). Archival tagging reveals swimming depth and ambient and peritoneal cavity temperature in age-0 Pacific bluefin tuna, *Thunnus orientalis*, off the southern coast of Japan. *Environ. Biol. Fish.* 100, 35–48. doi:10.1007/s10641-016-0552-3

Glazier, D. S. (2005). Beyond the "3/4-power law": variation in the intra- and interspecific scaling of metabolic rate in animals. *Biol. Rev.* 80, 611–662. doi:10.1017/S1464793105006834

Graham, J. B. (1995). Heat exchange in the yellowfin tuna, *Thunnus albacares*, and skipjack tuna, *Katsuwonus pelamis*, and the adaptive significance of elevated body temperatures in scombrid fishes. *Fish. Bull.* 73, 219–229.

Graham, J. B., and Dickson, K. A. (2001). Anatomical and physiological specializations for endothermy. *Fish. Physiol.*, 121–165. doi:10.1016/S1546-5098(01)19005-9

Iino, Y., Abe, T. K., Shimizu, Y., Nagasaka, T., and Kitagawa, T. (2024). Body size- and temperature-related metabolic traits of juvenile chum salmon during northward migration. *Can. J. Fish. Aquat. Sci.* 81, 1514–1527. doi:10.1139/cjfas-2023-0334

Itoh, T., Tsuji, S., and Nitta, A. (2003). Migration of tagged bluefin tuna across the Pacific Ocean. *Fish. Bull.* 101, 514–534.

Jusup, M., Klanjscek, T., Matsuda, H., and Kooijman, S. A. L. M. (2011). A full lifecycle bioenergetic model for bluefin tuna. *PLoS One* 6, e21903. doi:10.1371/journal.pone.0021903

Jusup, M., and Matsuda, H. (2015). "Mathematical modeling of bluefin tuna growth, maturation, and reproduction based on physiological energetics," in *Biology and ecology of bluefin tuna* (Boca Raton, FL: CRC Press), 369–399.

Killen, S. S., Atkinson, D., and Glazier, D. S. (2010). The intraspecific scaling of metabolic rate with body mass in fishes depends on lifestyle and temperature. *Ecol. Let.* 13, 184–193. doi:10.1111/j.1461-0248.2009.01415.x

Kishinouye, K. (1923). Contributions to the comparative study of the so-called scombroid fishes. *J. Coll. Agric.*, 293–475.

Kitagawa, T., Abe, T. K., Kubo, K., Fujioka, K., Fukuda, H., and Tanaka, Y. (2022). Rapid endothermal development of juvenile Pacific bluefin tuna. *Front. Physiol.* 13, 968468. doi:10.3389/fphys.2022.968468

Kitagawa, T., Boustany, A. M., Farwell, C. J., Williams, T. D., Castleton, M. R., and Block, B. A. (2007a). Horizontal and vertical movements of juvenile bluefin tuna (*Thunnus orientalis*) in relation to seasons and oceanographic conditions in the eastern Pacific Ocean. *Fish. Oceanogr.* 16, 409–421. doi:10.1111/j.1365-2419.2007.00441.x

Kitagawa, T., and Fujioka, K. (2017). Rapid ontogenetic shift in juvenile Pacific bluefin tuna diet. *Mar. Ecol. Prog. Ser.* 571, 253–257. doi:10.3354/meps12129

Kitagawa, T., Kato, Y., Miller, M. J., Sasai, Y., Sasaki, H., and Kimura, S. (2010). The restricted spawning area and season of Pacific bluefin tuna facilitate use of nursery areas: a modeling approach to larval and juvenile dispersal processes. *J. Exp. Mar. Biol. Ecol.* 393, 23–31. doi:10.1016/j.jembe.2010.06.016

Kitagawa, T., and Kimura, S. (2006). An alternative heat-budget model relevant to heat transfer in fishes and its practical use for detecting their physiological thermoregulation. *Zool. Sci.* 23, 1065–1071. doi:10.2108/zsj.23.1065

Kitagawa, T., Kimura, S., Nakata, H., and Yamada, H. (2007b). Why do young Pacific bluefin tuna repeatedly dive to depths through the thermocline? *Fish. Sci.* 73, 98–106. doi:10.1111/j.1444-2906.2007.01307.x

Kitagawa, T., Kimura, S., Nakata, H., Yamada, H., Nitta, A., Sasai, Y., et al. (2009). Immature Pacific bluefin tuna, *Thunnus orientalis*, utilizes cold waters in the Subarctic Frontal Zone for trans-Pacific migration. *Environ. Biol. Fish.* 84, 193–196. doi:10.1007/s10641-008-9409-8

Kitagawa, T., Nakata, H., Kimura, S., Itoh, T., Tsuji, S., and Nitta, A. (2000). Effect of ambient temperature on the vertical distribution and movement of Pacific bluefin tuna *Thunnus thynnus orientalis*. *Mar. Ecol. Prog. Ser.* 206, 251–260. doi:10.3354/meps206251

Kitagawa, T., Nakata, H., Kimura, S., and Tsuji, S. (2001). Thermoconservation mechanisms inferred from peritoneal cavity temperature in free-swimming Pacific bluefin tuna *Thunnus thynnus orientalis*. *Mar. Ecol. Prog. Ser.* 220, 253–263. doi:10.3354/meps220253

Kubo, T., Sakamoto, W., Murata, O., and Kumai, H. (2008). Whole-body heat transfer coefficient and body temperature change of juvenile Pacific bluefin tuna *Thunnus orientalis* according to growth. *Fish. Sci.* 74, 995–1004. doi:10.1111/j.1444-2906.2008.01617.x

Malik, A., Dickson, K. A., Kitagawa, T., Fujioka, K., Estess, E. E., Farwell, C., et al. (2020). Ontogeny of regional endothermy in Pacific bluefin tuna (*Thunnus orientalis*). *Mar. Biol.* 167, 133. doi:10.1007/s00227-020-03753-3

Muggeo, V. M. R. (2008). Segmented: an R package to fit regression models with broken-line relationships. *R. News* 8, 20–25.

Nakamura, I., Goto, Y., and Sato, K. (2015). Ocean sunfish rewarm at the surface after deep excursions to forage for siphonophores. *J. Anim. Ecol.* 84, 590–603. doi:10.1111/1365-2656.12346

Nakamura, I., Matsumoto, R., and Sato, K. (2020). Body temperature stability in the whale shark, the world's largest fish. *J. Exp. Biol.* 223, 210286. doi:10.1242/jeb.210286

Norin, T. (2022). Growth and mortality as causes of variation in metabolic scaling among taxa and taxonomic levels. *Integr. Comp. Biol.* 62, 1448–1459. doi:10.1093/icb/icac038

Oikawa, S., and Itazawa, Y. (1993). Tissue respiration and relative growth of parts of body of a marine teleost, porgy *Pagrus major*, during early life stages with special reference to the metabolism-size relationship. *Comp. Biochem. Physiol. A Physiol.* 105, 741–744. doi:10.1016/0300-9629(93)90277-B

Okiyama, M. (1974). Occurrence of the postlarvae of bluefin tuna, *Thunnus thynnus*, in the Japan Sea. *Sea Reg. Fish. Res. Lab. Bull* 25, 89–97.

Orange, C. J., and Fink, B. D. (1963). Migration of tagged bluefin tuna across the Pacific Ocean. *Calf. Fish. Game* 49, 307–309.

Poupa, O., and Lindström, L. (1983). Comparative and scaling aspects of heart and body weights with reference to blood supply of cardiac fibers. *Comp. Biochem. Physiol. A Mol. Integr. Physiol.* 76, 413–421. doi:10.1016/0300-9629(83)90441-3

Poupa, O., Lindström, L., Maresca, A., and Tota, B. (1981). Cardiac growth, myoglobin, proteins and DNA in developing tuna (*Thunnus thynnus thynnus* L.). *Comp. Biochem. Physiol. A Mol. Integr. Physiol.* 70, 217–222. doi:10.1016/0300-9629(81)91448-1

R Core Team (2023). *R: a language and environment for statistical computing*. Vienna, Austria: R Foundation for Statistical Computing.

Rouyer, T., Bonhommeau, S., Bernard, S., Kerzerho, V., Derridj, O., Bjarnason, Á., et al. (2023). A novel protocol for rapid deployment of heart rate data storage tags in Atlantic bluefin tuna *Thunnus Thynnus* reveals cardiac responses to temperature and feeding. *J. Fish. Biol.* 15507. doi:10.1111/jfb.15507

Sakamoto, K. Q., Sato, K., Ishizuka, M., Watanuki, Y., Takahashi, A., Daunt, F., et al. (2009). Can ethograms be automatically generated using body acceleration data from free-ranging birds? *PLoS One* 4, e5379. doi:10.1371/journal.pone.0005379

Santer, R. M., Walker, M. G., Emerson, L., and Witthames, P. R. (1983). On the morphology of the heart ventricle in marine teleost fish (teleostei). *Comp. Biochem. Physiol. A Mol. Integr. Physiol.* 76, 453–457. doi:10.1016/0300-9629(83)90445-0

Satoh, K. (2010). Horizontal and vertical distribution of larvae of Pacific bluefin tuna *Thunnus orientalis* in patches entrained in mesoscale eddies. *Mar. Ecol. Prog. Ser.* 404, 227–240. doi:10.3354/meps08431

Satoh, K., Tanaka, Y., and Iwahashi, M. (2008). Variations in the instantaneous mortality rate between larval patches of Pacific bluefin tuna *Thunnus orientalis* in the northwestern Pacific Ocean. *Fish. Res.* 89, 248–256. doi:10.1016/j.fishres.2007.09.003

Schmidt-Nielsen, K. (1984). *Scaling: Why is animal size so important ?* Cambridge: Cambridge University Press.

Schmidt-Nielsen, K. (1997). "Temperature regulation," in *Animal physiology: adaptation and environment* (Cambridge: Cambridge University Press), 241–300.

Sepulveda, C., and Dickson, K. A. (2000). Maximum sustainable speeds and cost of swimming in juvenile kawakawa tuna (*Euthynnus affinis*) and chub mackerel (*Scomber japonicus*). *J. Exp. Biol.* 203, 3089–3101. doi:10.1242/jeb.203.20.3089

Shimose, T., Watanabe, H., Tanabe, T., and Kubodera, T. (2013). Ontogenetic diet shift of age-0 year Pacific bluefin tuna *Thunnus orientalis*. *J. Fish. Biol.* 82, 263–276. doi:10.1111/j.1095-8649.2012.03483.x

Sidell, B. D., and Driedzic, W. R. (1985). "Relationship between cardiac energy metabolism and cardiac work demand in fishes," in *Circulation, respiration, and metabolism*. Editor R. Gilles (Heidelberg: Springer), 386–401. doi:10.1007/978-3-642-70610-3_31

Sogard, S. M. (1997). Size-selective mortality in the juvenile stage of teleost fishes: a review. *Bull. Mar. Sci.* 60, 1129–1157.

Stevens, E. D., and Carey, F. G. (1981). One why of the warmth of warm-bodied fish. *Am. J. Physiol. Regul. Integr. Comp. Physiol.* 240, R151–R155. doi:10.1152/ajpregu.1981.240.3.R151

Svendsen, M. B. S., Bushnell, P. G., and Steffensen, J. F. (2016). Design and setup of intermittent-flow respirometry system for aquatic organisms. *J. Fish. Biol.* 88, 26–50. doi:10.1111/jfb.12797

Tanaka, Y., Mohri, M., and Yamada, H. (2007). Distribution, growth and hatch date of juvenile Pacific bluefin tuna *Thunnus orientalis* in the coastal area of the Sea of Japan. *Fish. Sci.* 73, 534–542. doi:10.1111/j.1444-2906.2007.01365.x

Tanaka, Y., Satoh, K., Iwahashi, M., and Yamada, H. (2006). Growth-dependent recruitment of Pacific bluefin tuna *Thunnus orientalis* in the northwestern Pacific Ocean. *Mar. Ecol. Prog. Ser.* 319, 225–235. doi:10.3354/meps319225

Von Bertalanffy, L. (1938). A quantitative theory of organic growth (inquiries on growth laws. II). *Hum. Biol.* 10, 181–213.

Wegner, N. C., Snodgrass, O. E., Dewar, H., and Hyde, J. R. (2015). Whole-body endothermy in a mesopelagic fish, the opah, *Lampris guttatus*. *Science* 348, 786–789. doi:10.1126/science.aaa8902

Yabe, H., Ueyanai, S., and Watanabe, H. (1966). Studies on the early life history of bluefin tuna *Thunnus thynnus* and on the larvae of the southern bluefin tuna *T. maccoyii*. *Rep. Nankai Reg. Fish. Res. Lab.* 23, 95–129.

frontiers | Frontiers in Physiology

TYPE Brief Research Report
PUBLISHED 02 July 2025
DOI 10.3389/fphys.2025.1540252

OPEN ACCESS

EDITED BY
Takashi Kitagawa,
The University of Tokyo, Japan

REVIEWED BY
Yukiko Himeno,
Ritsumeikan University, Japan
Ippei Suzuki,
Hokkaido University, Japan

*CORRESPONDENCE
Tomoko Narazaki,
narazaki@meijo-u.ac.jp

RECEIVED 05 December 2024
ACCEPTED 13 June 2025
PUBLISHED 02 July 2025

CITATION
Narazaki T, Mori M, Matsuzawa Y, Saito A, Kinoshita C, Kurita M, Matsumiya K, Okada H and Sakamoto KQ (2025) Apparent reduction in heart rate during oviposition revealed by non-invasive heart rate monitoring of gravid loggerhead turtles.
Front. Physiol. 16:1540252.
doi: 10.3389/fphys.2025.1540252

Apparent reduction in heart rate during oviposition revealed by non-invasive heart rate monitoring of gravid loggerhead turtles

Tomoko Narazaki[1]*, Masanori Mori[2], Yoshimasa Matsuzawa[3], Ayaka Saito[4], Chihiro Kinoshita[1], Masanori Kurita[2], Kensuke Matsumiya[3], Hikari Okada[1] and Kentaro Q. Sakamoto[4]

[1]Faculty of Agriculture, Meijo University, Aichi, Japan, [2]Port of Nagoya Public Aquarium, Nagoya Port Foundation, Aichi, Japan, [3]Sea Turtle Association of Japan, Osaka, Japan, [4]Atmosphere and Ocean Research Institute, The University of Tokyo, Chiba, Japan

Reproductive processes place significant physiological demands on animals, often accompanied by hormonal and neural changes. In this study, we examined changes in heart rate of gravid loggerhead turtles (*Caretta caretta*) during nesting activities on the beach, especially during egg-laying phase. To examine heart rate throughout the nesting activities, non-invasive electrocardiogram (ECG) loggers and accelerometers were deployed on five gravid females. Heart rate increased markedly upon beach landing and remained elevated during most nesting phases. However, a significant decrease in heart rate, often accompanied by increased RMSSD, was observed during egg-laying, suggesting parasympathetic nervous system dominance during this phase. This pattern is similar to observation reported in other species (e.g., horses and chum salmon), where bradycardia during reproductive events is associated with elevated parasympathetic tone. Our study reported an apparent reduction in heart rate during oviposition, which reflects the physiological mechanisms underlying nesting activities in sea turtles, and suggest that external stressors disrupting parasympathetic activity may reduce egg-laying success.

KEYWORDS

heart rate, bradycardia, *Caretta caretta*, nesting, bio-logging

1 Introduction

Heart rate, an important physiological parameter reflecting an animal's internal state, is widely used in studies to estimate energy expenditure (Butler et al., 2002; Weimerskirch et al., 2002), evaluate stress and health conditions (Ellenberg et al., 2006; von Borell et al., 2007), and understand adaptations to physiologically challenging environments such as hypoxia during breath-hold diving and high-altitude flights (Ponganis et al., 1997; Wright et al., 2014; Meir et al., 2019; Saito et al., 2024). Reproductive processes (e.g., egg-laying, parturition) are essential biological processes for species survival. However, these processes place significant physiological demands on the reproductive animal, often accompanied by hormonal changes and physical exertion.

Monitoring heart rate and heart rate variability, which serve as indicators of autonomic nervous system activity, has become an important tool for studying the drastic changes in maternal condition during reproductive processes of livestock (Nagel et al., 2014; Kovács et al., 2015). For example, in horses, parturition is associated with a decrease in heart rate, and the occurrence of arrhythmia was observed during the 15 min prior to and 45 min following delivery (Nagel et al., 2014). Analysis of heart rate variability and plasma catecholamine concentration patterns suggest that high parasympathetic activity is a prerequisite for the onset of parturition, with horses giving birth in a state of marked relaxation and elevated parasympathetic tone (Nagel et al., 2014). Similarly, in cows, an increase in the high-frequency component of heart rate variability, which reflects parasympathetic activity, is observed following the onset of behavioral signs of parturition (Kovács et al., 2015). Heart rate and heart rate variability indicators are also used to improve the prediction of the time of calving, which is crucial for maintaining efficient and profitable daily farming (Kishi et al., 2024). In contrast, studies on heart rate during reproductive process in non-livestock animals are scarce, particularly for marine animals (but see Wells, 1979 for octopus; Makiguchi et al., 2009 for chum salmon).

Sea turtles spend most of their lives in the ocean; however, they emerge onto beaches to nest. The nesting process typically involves crawling up the beach, digging a body pit and egg chamber, laying eggs, covering the nest, and returning to the sea (Miller et al., 1997). These terrestrial nesting activities place significant physical and physiological demands on turtles (Jackson and Prange, 1979). For example, green turtles are shown to experience a tenfold increase in metabolic rate compared to resting levels during nesting activities (Jackson and Prange, 1979). Numerous hormonal studies have provided valuable insights into general hormone patterns (Owens, 1997; Jessop and Hamann, 2004); however, little is known about the changes in heart rate and neural activity associated with nesting behaviors.

Nesting turtles on the beach are known to be sensitive and often halt their nesting behavior in response to external disturbances. However, once egg-laying begins, the turtle generally continues laying eggs, even in the presence of disturbances (Miller et al., 1997). Based on this observation, we hypothesized that high parasympathetic nervous system activity may play a role in sea turtle egg-laying, as has been reported in horse parturition (Nagel et al., 2014). Parasympathetic activity is typically dominant during relaxed states and helps lower heart rate through the vagus nerve. To test this hypothesis, we monitored the temporal changes in heart rate of minimally disturbed loggerhead turtles (*Caretta caretta*) throughout their nesting activities using a non-invasive electrocardiogram data logger (Sakamoto et al., 2021). If supported, the hypothesis predicts a decrease in heart rate during egg-laying.

2 Materials and methods

2.1 Animals and study sites

All experimental procedures were covered by the guidelines of the Animal Ethics Committee of Meijo University, and the protocol of the study was approved by this committee (2021A13, 2022A17, 2023A14, 2023A15, 2024A23). Electrocardiogram (ECG) data from gravid female loggerhead turtles were collected throughout their nesting activities using animal-borne ECG loggers at two locations in Japan: Port of Nagoya Public Aquarium (35°5'N, 136°52'E) and Senri beach in Minabe, Wakayama (33°46'N, 135°18'E). At the aquarium, the measurements were conducted in 2021 and 2023 on captive turtles whose follicle development had been confirmed via ultrasound examination. The turtles equipped with loggers were kept in a tank connected to an artificial beach, allowing them to move freely between the tank and the beach. Nesting behavior was monitored with three night-vision cameras installed at the artificial beach. Once oviposition was confirmed, the data loggers were retrieved from the turtles the following morning. The field study in Minabe was conducted during the 2022, 2023 and 2024 nesting seasons. Once the turtles emerged onto the nesting beach, the turtles were promptly captured, fitted with data loggers, and released at the same site. When the turtles were returned on the beach, their nesting behavior was observed from a distance to avoid disturbance. After oviposition was confirmed, the turtles were recaptured just before they return to the sea to retrieve the data loggers.

2.2 Data loggers

The ECG was recorded at 250 Hz (ECG400-DT; Little Leonardo, Tokyo, Japan; 21 mm width, 64 mm length, 23 mm height, 60 g mass in air) using a non-invasive method by attaching two electrode pads to the turtles' carapace, following Sakamoto et al. (2021) with some modifications (Kinoshita et al., 2022). A step-by-step instruction with detailed illustrations for attaching the electrodes and loggers is provided in Kinoshita et al. (2022). While electrode pads on the plastron provide stronger ECG signals (Kinoshita et al., 2022), the pads were attached to the carapace due to the high risk of detachment while the turtles crawl on the beach. The activity of the turtles was recorded using a behavioral logger: a M190L-D2GT (Little Leonardo; cylindrical shape; 15 mm diameter, 53 mm length, 18 g mass in air) recording 2-axis acceleration, depth and temperature, or a W2000-3MPD3GT (Little Leonardo; cylindrical shape; 26 mm diameter, 175 mm length, 140 g mass in air) recording 3-axis acceleration and the Earth's magnetic field, depth, and temperature. Acceleration was recorded at either 16 Hz (CcW19 and M3) or 32 Hz (CcW06, M4 and M7). Depth, temperature and the Earth's magnetic field were recorded at 1 Hz.

2.3 Data analysis

Nesting activities were categorized into 5 phases based on visual observation of the captive turtles and acceleration-magnetometer recordings of wild turtles: 1) crawling and body-pitting, 2) digging an egg chamber, 3) laying eggs, 4) covering the egg chamber, and 5) camouflaging the site (Figure 1; Supplementary Figure S1). While crawling and body-pitting are typically classified separately, they were grouped into the same category in this study due to difficulty in distinguish between them based on acceleration-magnetometer recordings. The definitions of classifications are provided in Supplementary Material.

Time-series biologging data were analyzed using IGOR Pro version 8.04 (Wavemetrics, Portland, OR, United States). To remove

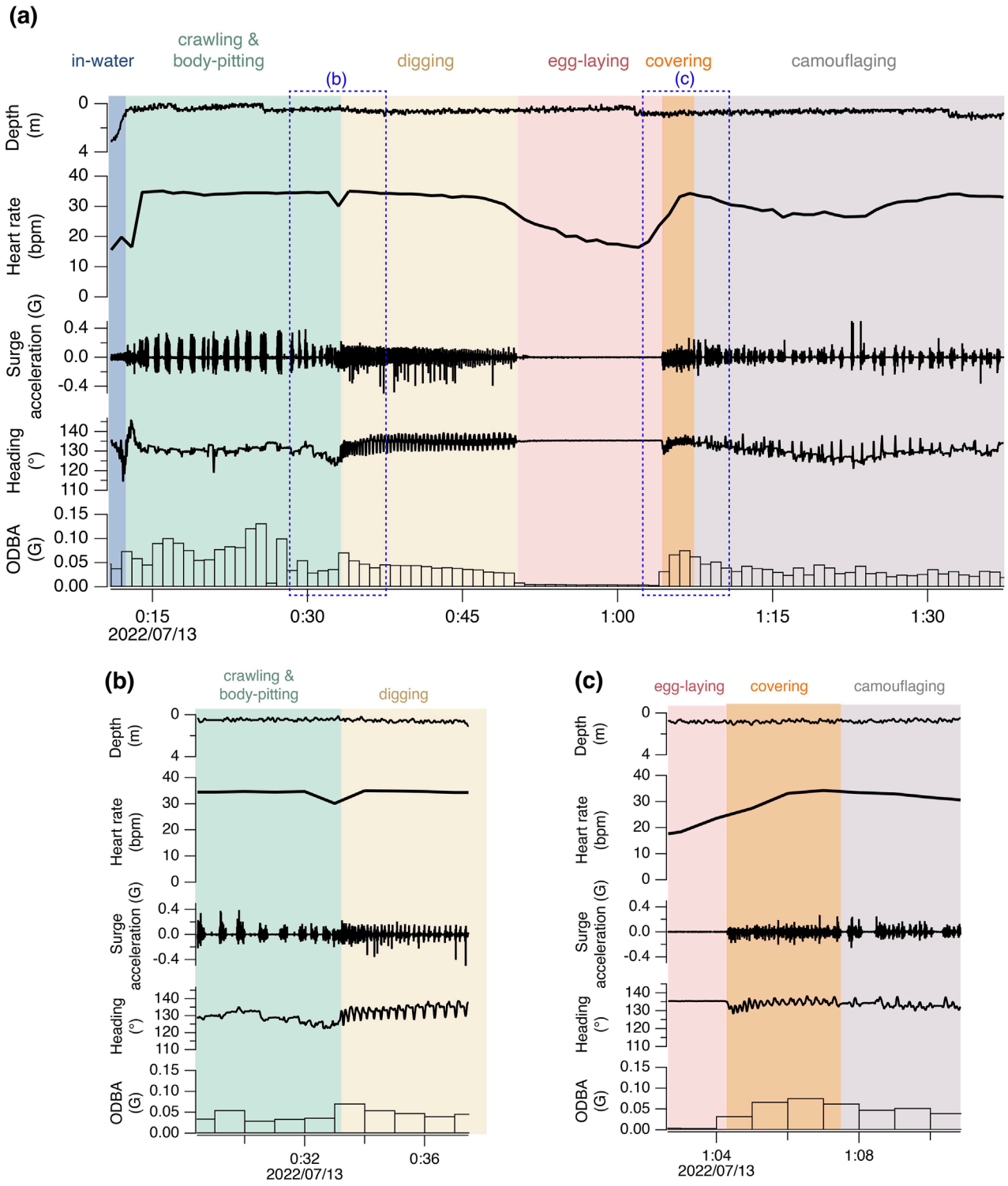

FIGURE 1
Time-series data of heart rate, depth, and high-frequency surge acceleration, heading, and 1-minute mean ODBA during the nesting activity of turtle M3. The areas enclosed by the blue dashed lines in **(a)** are magnified in **(b, c)**.

noise primarily caused by turtles' movements, the ECG recordings were processed using the ECGtoHR program, which employs an FIR filter with a Hanning window to isolate the QRS complex and detect R peaks (Sakamoto et al., 2021). The parameters of the ECGtoHR program were visually adjusted to set a QRS frequency of 10–12 Hz and maximum heart rate of 60–80 bpm for each deployment (Sakamoto et al., 2021). The instantaneous heart rate was then calculated as the reciprocal of the time interval

between consecutive R waves (RR interval). The heart rate was calculated as the median of instantaneous heart rate per minute. In addition, the root mean square of successive differences in consecutive RR intervals (RMSSD) was quantified every minute. RMSSD is a widely used time-domain measure of heart rate variability, with higher values indicating greater parasympathetic nervous system activity (Shaffer et al., 2014).

The acceleration data recorded by behavioral loggers was separated into two components using a frequency-based filter: a high-frequency dynamic body acceleration component (i.e., flipper movements) and a low-frequency gravity-based acceleration component (Shiomi et al., 2010). As a proxy for activity level, overall dynamic body acceleration (ODBA) in G was calculated by summing the absolute values of dynamic acceleration at 16 or 32 Hz across the three axes of the W2000-3MPD3GT (Wilson et al., 2006). ODBA was not calculated for the turtle (i.e., CcW06) equipped with the M190L-D2GT. The orientation of turtles (pitch, roll and heading) was calculated every second using 3-axis magnetism and low-frequency acceleration data using the macro ThreeD_path, which is compatible with IGOR Pro (Shiomi et al., 2010; https://japan-biologgingsci.org/home/macro/threed_path/).

Variations in heart rate throughout the nesting activities were examined using a linear mixed model (LMM). As data obtained from the same nesting event was not independent, 'nesting ID' was included as random effect. Explanatory variables were the behavioral modes (i.e., crawling, digging, egg-laying, covering the egg chamber, camouflaging) and ODBA. The most parsimonious model was selected based on AIC, followed by the Tukey-Kramer *post hoc* test for the behavioral modes. All statistical analysis was performed using R (The R project for Statistical Computing, http://www.r-project.org).

3 Results

ECG and behavioral data were collected from a total of five gravid sea turtles over seven nesting events, including a pseudo-nesting event by turtle M7 (Table 1). The wild turtles equipped with loggers returned to nest the following night (M3, 4) or the second night after release (M7). M7 exhibited behavior consistent with normal nesting: it created a body pit, dug an egg chamber, and displayed typical egg-laying behaviors, such as letting its tail hang into the egg chamber and remained motionless for a while. However, the only difference from normal nesting was that no eggs were actually laid. After completing this pseudo-egg-laying, M7 filled the chamber and camouflaged the site.

For the six true nesting events, the heart rate during the 10 min preceding beach landing was 19.7 ± 7.0 bpm (mean ± s.d.), but it rapidly increased to 29.3 ± 5.5 bpm during the 10 min immediately after landing (Figure 1; Supplementary Figure S1). There was substantial variability in heart rate during nesting events, with a weak positive relationship observed with ODBA ($P < 0.05$, $F(1, 576.69) = 20.4$, Supplementary Figure S2). The heart rate during egg-laying was significantly lower than during any other behavioral modes ($P < 0.05$, $F(4, 576.91) = 138.6$; 16.9 ± 5.0 bpm, Figure 2), showing a 54% decrease compared to the heart rate during the preceding digging the egg chamber (31.2 ± 2.4 bpm). With the onset of egg-laying, the heart rate gradually decreased, accompanied by increased variability (Figure 3). This decrease in heart rate was not only due to the increase in RR intervals but also associated with greater variability in the RR intervals: the mean RR intervals during the 5 min prior to egg-laying were 2.0 ± 0.5 s, increasing to 3.5 ± 1.5 s during egg-laying. A general trend of increase in RMSSD was also observed during egg-laying (Figure 3). After the completion of egg-laying, the heart rate rapidly returned to levels comparable to those measured prior to egg-laying (Figure 3).

During pseudo-egg-laying observed in M7, a decrease in heart rate was noted at the onset of the pseudo-egg-laying. However, the return of heart rate after the completion of pseudo-egg-laying was more gradual to the return observed after true egg-laying (Figure 3).

4 Discussion

By using non-invasive ECG monitoring method, we were able to measure heart rate in loggerhead turtles throughout nesting activities. In all turtles, a marked increase in heart rate was recorded upon landing on the beach. Loggerhead turtles have been reported to exhibit diving bradycardia as an adaptation to reduce oxygen consumption during breath-holding dives (Saito et al., 2024). It is likely that a similar bradycardic response occurred until their bodies were fully out of the water, although apnea occurs both in water and on land. Once on the beach, the heart rate generally remained elevated at 24.2–30.4 bpm, although it varied depending on the behavioral modes (Table 1; Figure 1). In diving sea turtles, an increase in heart rate corresponding to underwater activity intensity has been reported in captive turtles (Williams et al., 2019; Okuyama et al., 2020), as oxygen must be transported from their primary oxygen store in the lungs to the muscles (Lutcavage et al., 1997). In nesting turtles on the beach, a positive relationship between heart rate and activity intensity was also observed, with the relationship being weak (Supplementary Figure S2). Nesting activities on the beach are considered physically and physiologically demanding (Jackson and Prange, 1979). Furthermore, the lower specific heat capacity of air compared to water facilitates an increase in body temperature, which in turn raises metabolic rate, although the effect of temperature may be small in this study due to relatively low air temperature (Table 1). One possible reason for the weak relationship between heart rate and activity intensity is that the heart rate while on the beach may already be at very high level for sea turtles, leaving little capacity for significant increase in response to high exercise intensity. In fact, the heart rates recorded in this study represent the highest levels reported for loggerhead turtles, even exceeding those observed during inter-dive surface intervals when heart rate typically increases (Saito et al., 2022; 2024; Williams et al., 2019). Another possibility could be that turtles may be exposed to other factors (e.g., external stimuli, internal condition associated with egg-laying) that influence heart rate aside from activity intensity. Similarly, the relationship between heart rate and activity observed in turtles freely diving in their natural environment was weaker than that reported during voluntary diving in a simpler captive environment (Saito et al., 2024).

Our results showed a significant decrease in heart rate associated with egg-laying, as predicted by the hypothesis that egg-laying is

10.3389/fphys.2025.1540252

TABLE 1 Descriptive statistics during nesting activity and egg-laying phase.

Turtle ID	Study site[a]	Accelerometer type	Time of landing	Water temperature (°C)	Temperature at the beach (°C)	Whole period on the beach[b]		Egg-laying phase	
						Duration (min)	Heart rate (bpm)	Duration (min)	Heart rate (bpm)
CcW06	PNPA	D2GT[c]	2021/05/16 21:37	26.7 ± 0.04	24.5 ± 0.5	211	27.6 ± 5.6	15.7	17.7 ± 5.2
		D2GT	2021/06/09 22:56	27.9 ± 0.03	26.7 ± 0.3	174	29.1 ± 5.2	10.6	21.6 ± 6.1
CcW19	PNPA	3MPD3GT	2023/04/30 02:26	25.7 ± 0.1	23.9 ± 0.2	162	28.2 ± 5.2	29.1	19.2 ± 4.5
		3MPD3GT	2023/05/12 21:57	26.7 ± 0.1	25.8 ± 0.5	226	24.2 ± 4.5	30.9	16.0 ± 2.9
M3	M	3MPD3GT	2022/07/13 00:12	27.2 ± 0.3	25.8 ± 0.5	94	30.4 ± 5.3	14.1	20.7 ± 3.6
M4	M	3MPD3GT	2023/07/07 22:31	24.3 ± 0.6	26.1 ± 0.2	103	27.2 ± 9.6	25.0	12.5 ± 5.7
M7[d]	M	3MPD3GT	2024/06/24 22:33	24.2 ± 0.09	23.7 ± 0.1	75	24.3 ± 7.6	11.8	11.6 ± 3.5

Mean heart rate, temperature and heart rate are provided with standard deviation. Water temperatures during the 90 min before landing are presented.

[a]The abbreviations of the study sites are PNPA for Port of Nagoya Public Aquarium and M for Minabe.

[b]From beach landing to return to the pool for PNPA turtles; from beach landing to logger retrieval during camouflage phase for Minabe turtles.

[c]No data due to logger failure.

[d]The duration and heart rate during a pseudo-nesting behavior are presented for M7.

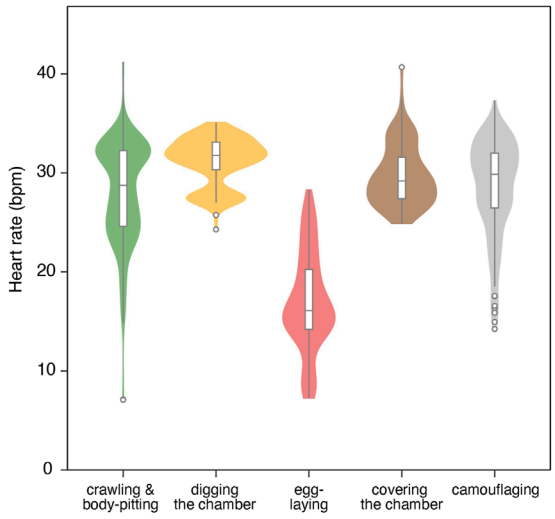

FIGURE 2
Violin/box plot for heart rate across different behavioral modes of four turtles during six nesting events. The box represents the interquartile range (IQR), with outliers (beyond 1.5 x IQR) shown as points beyond the whiskers.

linked to parasympathetic nervous system activity. Upon the onset of egg-laying, a gradual decrease in heart rate was observed, resulting from an increased RR interval and its variability, suggesting the potential occurrence of arrhythmia (Figures 1, 3). This pattern in heart rate is similar to that observed during horse parturition, which occurs under elevated parasympathetic tone (Nagel et al., 2014). Similar phenomena have also been reported in non-mammalian species: transient cardiac arrest, considered an extreme case of bradycardia, was observed at the moment of gamete transfer and release in octopus (*Octopus vulgaris*) and chum salmon (*Oncorhynchus keta*), respectively (Wells, 1979; Makiguchi et al., 2009). The decrease in heart rate can result from increased parasympathetic nervous activity and/or decreased sympathetic activity. However, the low norepinephrine levels observed during arrhythmia events in horses (Nagel et al., 2014) and the abolition of cardiac arrest following administration of anticholinergic drugs in chum salmon (Makiguchi et al., 2009) indicate that these reproductive processes occurred under a high parasympathetic tone. In this study, a general trend of increased RMSSD was observed in association with bradycardia during egg-laying, suggesting that parasympathetic nervous activity may play a dominant role in this process. In contrast to the gradual decrease in heart rate at the onset of egg-laying, the sharp return to baseline levels after the completion of egg-laying suggests that different mechanisms may be involved in controlling heart rate (Figure 3). Interestingly, a similar decrease in heart rate was observed in M7 during pseudo-egg-laying, although the temporal pattern of RMSSD was different, remaining relatively low. Additionally, the recovery of heart rate to the baseline was more gradual toward the end of pseudo-egg-laying. The only observed difference between pseudo- and true egg-laying was the absence of actual oviposition. It is possible that the rapid recovery of heart rate may be triggered by physiological changes, such as hormonal shifts and neural activity, associated

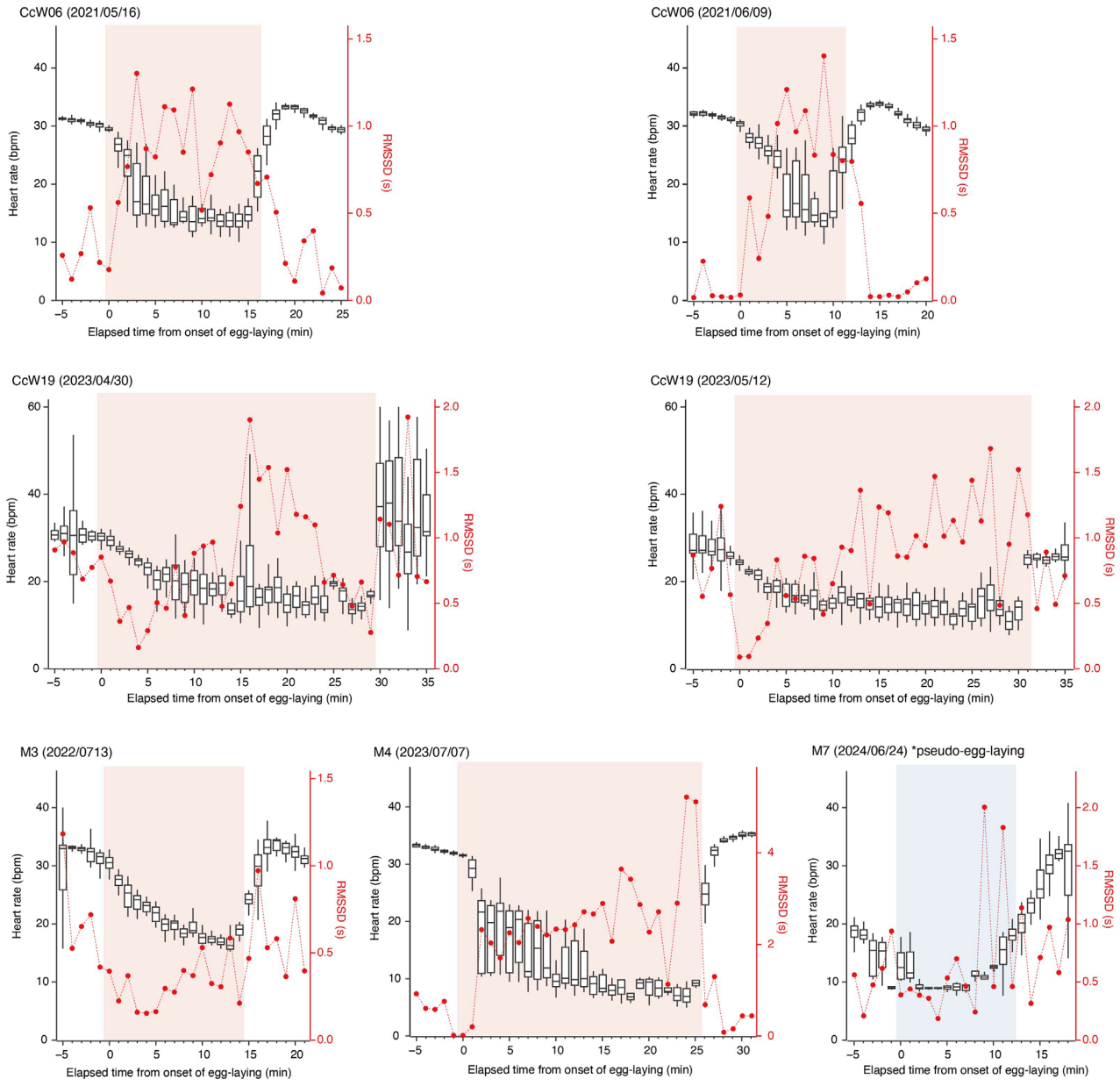

FIGURE 3
Temporal changes in heart rate (box plots) and RMSSD (red dots) before, during, and after the egg-laying periods. RMSSD and the median heart rate are shown for each minute. The upper and lower edges of the box represent the third and first quartiles, respectively. Time zero corresponds to the onset of the egg-laying period. The egg-laying and pseudo-egg-laying periods are highlighted in pink and blue, respectively.

with the successful completion of egg-laying. Further studies, including hormonal and/or pharmacological researches, to examine autonomic nervous system control, are important for elucidating physiological mechanism underlying nesting activities.

This study represents the first heart rate monitoring of sea turtles during nesting activities, demonstrating that heart rate remained elevated throughout most of the nesting activities, except during egg-laying. This indicates that nesting turtles have high metabolic rate, likely driven by physical demands, such as supporting their body weight, and increased body temperature. Considering that nesting activities on the beach typically last for over an hour, these results suggest high physiological strain associated with the activity. Furthermore, our data suggest that egg-laying in sea turtles occurs under parasympathetic tone, although further investigation into hormonal patterns and heart rate variability is necessary for validation. The parasympathetic nervous system is in an antagonistic relationship with the stress-activated sympathetic nervous system. If high parasympathetic activity is a prerequisite for initiating egg-laying, external stressors, such as disturbance from tourists or strong light, may significantly reduce egg-laying success. Further studies uncovering the physiological mechanisms underlying nesting activities with ecological perspectives could

provide valuable insights for the effective conservation and management of endangered sea turtles.

Data availability statement

The original contributions presented in the study are included in the article/Supplementary Material, further inquiries can be directed to the corresponding author.

Ethics statement

The animal studies were approved by Animal Ethics Committee of Meijo University. The studies were conducted in accordance with the local legislation and institutional requirements. Written informed consent was obtained from the owners for the participation of their animals in this study.

Author contributions

TN: Conceptualization, Formal Analysis, Investigation, Writing – original draft, Writing – review and editing. MM: Investigation, Writing – review and editing. YM: Investigation, Project administration, Writing – review and editing. AS: Investigation, Writing – review and editing. CK: Investigation, Writing – review and editing. MK: Project administration, Writing – review and editing. KM: Investigation, Project administration, Writing – review and editing. HO: Formal Analysis, Investigation, Writing – review and editing. KS: Investigation, Writing – review and editing.

Funding

The author(s) declare that financial support was received for the research and/or publication of this article. This study was supported by the Interdisciplinary Collaborative Research Program of the Atmosphere and Ocean Research Institute, the University of Tokyo.

Acknowledgments

We are grateful to the staff of Port of Nagoya Public Aquarium for their support during the experiments conducted at the aquarium. We thank the numerous volunteers for their assistance with the nightly patrols on the nesting beach during the fieldwork in Minabe. Acknowledgement is given to K. Maeda and Y. Konishi from the Minabe Town Board of Education for their support in facilitating our fieldwork. We also thank S. Sato, M. Kawamoto, A. Mizuno, T. Kagaya, Y. Hattori, K. Matsumoto, N. Motohira, S. Yamaguchi, for their works in the fieldwork and data analysis. Special thanks go to K. Sato for lending the data loggers.

Conflict of interest

The authors declare that the research was conducted in the absence of any commercial or financial relationships that could be construed as a potential conflict of interest.

The handling editor TK declared a shared affiliation with the author(s) AS, KQS at the time of review.

Generative AI statement

The author(s) declare that Generative AI was used in the creation of this manuscript. We acknowledge the use of generative AI (OpenAI's ChatGPT, GPT-4, via OpenAI's platform) only for assistance with English language refinement and proofreading of the manuscript.

Publisher's note

All claims expressed in this article are solely those of the authors and do not necessarily represent those of their affiliated organizations, or those of the publisher, the editors and the reviewers. Any product that may be evaluated in this article, or claim that may be made by its manufacturer, is not guaranteed or endorsed by the publisher.

Supplementary material

The Supplementary Material for this article can be found online at: https://www.frontiersin.org/articles/10.3389/fphys.2025.1540252/full#supplementary-material

References

Butler, P. J., Frappell, P. B., Wang, T., and Wikelski, M. (2002). The relationship between heart rate of oxygen consumption in Galapagos marine iguanas (*Amblyrhynchus cristatus*) at two different temperatures. *J. Exp. Biol.* 205, 1917–1924. doi:10.1242/jeb.205.13.1917

Ellenberg, U., Mattern, T., Seddon, P. J., and Jorquera, G. L. (2006). Physiological and reproductive consequences of human disturbance in humboldt penguins: the need for species-specific visitor management. *Biol. Conserv.* 133, 95–106. doi:10.1016/j.biocon.2006.05.019

Jackson, D. C., and Prange, H. D. (1979). Ventilation and gas exchange during rest and exercise in adult green sea turtles. *J. Comp. Physiol.* 134, 315–319. doi:10.1007/bf00709998

Jessop, T. S., and Hamann, M. (2004). Hormonal and metabolic responses to nesting activities in the green turtle, *Chelonia mydas*. *J. Exp. Mar. Biol. Ecol.* 308, 253–267. doi:10.1016/j.jembe.2004.03.005

Kinoshita, C., Saito, A., Kawai, M., Sato, K., and Sakamoto, K. Q. (2022). A non-invasive heart rate measurement method is improved by placing the electrodes on the ventral side rather than the dorsal in loggerhead turtles. *Front. Physiol.* 13, 811947. doi:10.3389/fphys.2022.811947

Kishi, S., Kojima, T., Huang, C., Yayou, K., and Fujioka, K. (2024). A feasibility study on predicting cow calving time over 40h in advance using heart rate and financial technical indicators. *Sci. Rep.* 14, 21748. doi:10.1038/s41598-024-72521-w

Kovács, L., Tőzsér, J., Kézér, F. L., Ruff, R., Aubin-Wodala, M., Albert, E., et al. (2015). Heart rate and heart rate variability in multiparous dairy cows with unassisted calvings in the periparturient period. *Physiol. Behav.* 129, 281–289. doi:10.1016/j.physbeh.2014.11.039

Lutcavage, M. E., and Lutz, P. L. (1997). "Diving physiology," in *The biology of sea turtles* (Boca Raton, FL: CRC Press), 277–296.

Makiguchi, Y., Nagata, S., Kojima, T., Ichimura, M., Konno, Y., Murata, H., et al. (2009). Cardiac arrest during gamete release in chum salmon regulated by the parasympathetic nerve system. *PLoS ONE* 4 (6), e5993. doi:10.1371/journal.pone.0005993

Meir, J. U., York, J. M., Chua, B. A., Jardine, W., Hawkes, L. A., and Milsom, W. K. (2019). Reduced metabolism supports hypoxic flight in the high-flying bar-headed goose (*Anser indicus*). *eLife* 8, e44986. doi:10.7554/eLife.44986

Miller, J. D. (1997). "Reproduction in sea turtles," in *The biology of sea turtles* (Boca Raton, FL: CRC Press), 51–81.

Nagel, C., Erber, R., Ille, N., von Lewinski, M., Aurich, J., Mo¨stl, E., et al. (2014). Parturition in horses is dominated by parasympathetic activity of the autonomous nervous system. *Theriogenology* 82, 160–168. doi:10.1016/j.theriogenology.2014.03.015

Okuyama, J., Shiozawa, M., and Shioide, D. (2020). Heart rate and cardiac response to exercise during voluntary dives in captive sea turtles (cheloniidae). *Biol. Open* 9, bio049247. doi:10.1242/bio.049247

Owens, D. W. (1997). "Hormones in the life history of sea turtles," in *The biology of sea turtles*. Editors P. L. Lutz, and J. A. Musick (Boca Raton, FL: CRC Press), 315–342.

Ponganis, P. J., Kooyman, G. L., Winter, L. M., and Starke, L. N. (1997). Heart rate and plasma lactate responses during submerged swimming and trained diving in California sea lions, *Zalophus californianus*. *J. Comp. Physiol. B* 167, 9–16. doi:10.1007/s003600050042

Saito, A., Kinoshita, C., Kawai, M., Fukuka, T., Sato, K., and Sakamoto, K. Q. (2022). Effects of a parasympathetic blocker on the heart rate of loggerhead sea turtles during voluntary diving. *J. Exp. Biol.* 225, jeb243922. doi:10.1242/jeb243922

Saito, A., Kinoshita, C., Sakai, K., Sato, K., and Sakamoto, K. Q. (2024). Heart rate reduction during voluntary deep diving in free-ranging loggerhead sea turtles. *J. Exp. Biol.* 227, jeb246334. doi:10.1242/jeb.246334

Sakamoto, K. Q., Miyayama, M., Kinoshita, C., Fukuoka, T., Ishihara, T., and Sato, K. (2021). A non-invasive system to measure heart rate in hard-shelled sea turtles: potential for field applications. *Phil. Trans. R. Soc. B* 376, 20200222. doi:10.1098/rstb.2020.0222

Shaffer, F., McCraty, R., and Zerr, C. L. (2014). A healthy heart is not a metronome: an integrative review of the heart's anatomy and heart rate variability. *Front. Psychol.* 5, 1040. doi:10.3389/fpsyg.2014.01040

Shiomi, K., Narazaki, T., Sato, K., Shimatani, K., Arai, N., Ponganis, P. J., et al. (2010). Data-processing artefacts in three-dimensional dive path reconstruction from geomagnetic and acceleration data. *Aquat. Biol.* 8, 289–294. doi:10.3354/ab00239

von Borell, E., Langbein, J., Després, G., Hansen, S., Leterrier, C., Marchant, J., et al. (2007). Heart rate variability as a measure of autonomic regulation of cardiac activity for assessing stress and welfare in farm animals - a review. *Physiol. Behav.* 92 (3), 293–316. doi:10.1016/j.physbeh.2007.01.007

Weimerskirch, H., Shaffer, S. A., Mabille, G., Martin, J., Boutard, O., and Rouanet, J. L. (2002). Heart rate and energy expenditure of incubating wandering albatrosses: basal levels, natural variation, and the effects of human disturbance. *J. Exp. Biol.* 205, 475–483. doi:10.1242/jeb.205.4.475

Wells, M. J. (1979). The heartbeat of *Octopus vulgaris*. *J. Exp. Biol.* 78, 87–104. doi:10.1242/jeb.78.1.87

Williams, C. L., Sato, K., and Ponganis, P. J. (2019). Activity, not submergence, explains diving heart rates of captive loggerhead sea turtles. *J. Exp. Biol.* 222, jeb200824. doi:10.1242/jeb.200824

Wilson, R., White, C., Quintana, F., Halsey, L., Liebsch, N., Martin, G., et al. (2006). Moving towards acceleration for estimates of activity-specific metabolic rate in free-living animals: the case of the cormorant. *J. Anim. Ecol.* 75, 1081–1090. doi:10.1111/j.1365-2656.2006.01127.x

Wright, A. K., Ponganis, K. V., McDonald, B. I., and Ponganis, P. J. (2014). Heart rates of emperor penguins diving at sea: implications for oxygen Store management. *Mar. Ecol. Prog. Ser.* 496, 85–98. doi:10.3354/meps10592

Frontiers in Physiology

Understanding how an organism's components work together to maintain a healthy state

The second most-cited physiology journal, promoting a multidisciplinary approach to the physiology of living systems - from the subcellular and molecular domains to the intact organism and its interaction with the environment.

Discover the latest Research Topics

See more →

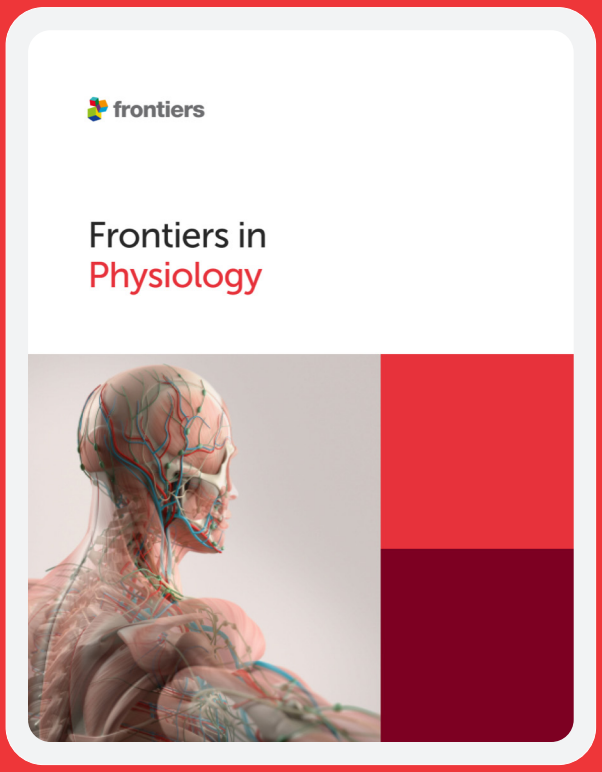

Frontiers

Avenue du Tribunal-Fédéral 34
1005 Lausanne, Switzerland
frontiersin.org

Contact us

+41 (0)21 510 17 00
frontiersin.org/about/contact